EFFECTS OF A NOVEL METABOLITE OF PENTOXIFYLLINE *IN VITRO* AND *IN VIVO* IN MODELS OF FIBROSIS AND INFLAMMATION

by

Jennifer M. Raoul

Submitted in partial fulfillment of the requirements
for the degree of Doctor of Philosophy

at

Dalhousie University
Halifax, Nova Scotia
September, 2004

Your file Votre référence
ISBN: 0-612-94050-0
Our file Notre référence
ISBN: 0-612-94050-0

DALHOUSIE UNIVERSITY

To comply with the Canadian Privacy Act the National Library of Canada has requested that the following pages be removed from this copy of the thesis:

Preliminary Pages

Examiners Signature Page (pii)

Dalhousie Library Copyright Agreement (piii)

Appendices

Copyright Releases (if applicable)

This thesis is dedicated to my fiancé Geoff and to my family, for their undying support and encouragement, and for giving me a place to vent my excitements and frustrations over the past four years.....

TABLE OF CONTENTS

LIST OF FIGURES

LIST OF TABLES

ABSTRACT

Crohn's disease (CD) is a chronic relapsing and remitting inflammatory bowel disease characterized by transmural granulomatous inflammation and ulceration with development of intestinal fibrosis and strictures. Current treatments for CD target acute symptoms but do little to prevent fibrotic complications of the disease. Our lab has been investigating the antifibrogenic effects of pentoxifylline (PTX), a methylxanthine derivative with known anti-inflammatory actions. We have previously shown that PTX inhibits fibrogenic events *in vitro* and in a swine model of hepatic fibrosis. The combined antifibrogenic and anti-inflammatory effects of PTX make it an attractive candidate for the treatment of human CD. We have developed a method to produce a racemic mixture of the chiral metabolite-1 (M-1) of PTX and this thesis work was an examination of the antifibrogenic and anti-inflammatory effects of M-1 *in vitro* and in an animal model of CD. M-1 was more potent than PTX *in vitro* at inhibiting platelet-derived growth factor (PDGF)-stimulated fibroblast proliferation and collagen synthesis, hallmark events in fibrosis. Kinetics of M-1 showed that higher levels of total active drug were achieved *in vivo* following M-1 administration compared to PTX. A pharmacologic interaction between M-1 and the antibiotic ciprofloxacin was demonstrated that may enhance the biological effects of M-1 *in vivo*. Both PTX and M-1 attenuated inflammation and colon damage in the TNBS rat model of colitis when administered intracolonically. Anti-inflammatory actions of PTX and M-1 *in vivo* are likely due to inhibition of NF-κB, which was significantly elevated in colitis. Intestinal fibrosis in the model was characterized by elevated levels of collagen types I and III and PDGF in colon tissue. Only M-1 prevented intestinal fibrosis in this model of colitis. These results suggest that PTX and M-1 could have therapeutic potential in the treatment of inflammation and ulceration associated with human CD. M-1 may also inhibit inflammation-induced intestinal fibrosis in CD, for which there is currently no treatment. This is the first study to examine the effects of M-1 *in vivo* and one of the only studies to examine the effects of pharmacological agents on fibrosis in an experimental model of IBD.

LIST OF ABBREVIATIONS

α1(I)	alpha-1 chain of collagen type I
α2(I)	alpha-2 chain of collagen type I
α1(III)	alpha-1 chain of collagen type III
A/A	antibiotic/antimycotic
AEC	aminoethylcarbazole
ANOVA	analysis of variance
AP-1	activator protein-1
ATCC	American Type Culture Collection
ATF-2	activator of transcription factor-2
BSA	bovine serum albumin
°C	degrees Celcius
C57BL/6	strain of mouse
cAMP	cyclic adenosine monophosphate
CD	Crohn's disease
CD1	strain of mouse
CH_2Cl_2	dichloromethane
Cipro	ciprofloxacin
CO_2	carbon dioxide
cpm	counts per minute
CYP450	cytochrome P450 enzyme
CYP1A2	cytochrome P450 isoform 1A2

CYP3A4	cytochrome P450 isoform 3A4
COL1A1	gene for α1 chain of collagen type I
COL1A2	gene for α2 chain of collagen type I
DAB	diaminobenzidine
dH_2O	distilled water
DMEM	Dulbecco's Modified Eagle's Medium
ECL	enhanced chemiluminescence
ECM	extracellular matrix
EDTA	ethylenediaminetetraacetic acid
ELISA	enzyme linked immunosorbent assay
ERK	extracellular signal-regulated kinase
EtOH	ethanol
F8	normal human dermal fibroblast cell line
FBS	fetal bovine serum
^{1}H-NMR	proton nuclear magnetic resonance spectroscopy
H_2O_2	hydrogen peroxide
H&E	hematoxylin and eosin
HEPES	hydroxyethyl-piperizine-2-ethanesulfonic acid
HETAB	hexadecyltrimethylammonium bromide
HPLC	high performance liquid chromatography
HRP	horseradish peroxidase
HSC	hepatic stellate cells
ICC	immunocytochemistry

I.D.	internal diameter
IEC-6	normal rat intestinal epithelial cell line
IHC	immunohistochemistry
IL	interleukin
IL-1β	inteluekin-1 beta
IL-18	interleukin-18
IL-18R	IL-18 receptor
i.c.	intracolonic
IgG	immunoglobulin G
i.p.	intraperitoneal
JNK	c-jun N-terminal kinase
LN_2	liquid nitrogen
mH_2O	Millipore water
M-1	metabolite-1 of pentoxifylline
M-1R	R-enantiomer of metabolite-1 of pentoxifylline
M-1S	S-enantiomer of metabolite-1 of pentoxifylline
MAPK	mitogen activated protein kinase
MeOH	methanol
MPO	myeloperoxidase
$NaBH_4$	sodium borohydride (reducing agent)
NaOH	sodium hydroxide
Na_2SO_4	sodium sulfate (drying agent)
NF-1	nuclear factor-1

NF-κB	nuclear factor kappa B
NF-κBp65	p65 subunit of NF-κB also called RelA
NT	neutrophil
O^-	oxygen free radical
O_2	oxygen
p	phosphorylated
p38	p38 mitogen activated protein kinase
PA	phosphatidic acid
PBS	phosphate buffered saline
PDE	phosphodiesterase
PDGF	platelet derived growth factor
PFA	paraformaldehyde
PKA	protein kinase A
PLP	periodate-lysine paraformaldehyde
PMSF	phenylmethanesulfonylfluoride
PTX	pentoxifylline
PVDF	polyvinylidene difluoride
RT	room temperature
SAPK	stress-activated protein kinase
SDS	sodium dodecyl sulfate
SDS-PAGE	sodium dodecyl sulfate-polyacrylamide gel electrophoreisis
SEM	standard error of the mean
Ser73	c-jun phosphorylation site – serine residue number 73

SR/FG	Sirius red/Fast green dyes
TBS	Tris-buffered saline
TBS-T	Tris-buffered saline + 0.1% Tween
TCA	trichloroacetic acid
TGF-β	transforming growth factor beta
TNBS	2,4,6-trinitrobenzenesulfonic acid
TNF-α	tumor necrosis factor alpha
UV	ultraviolet
v/v	volume/volume
VSMC	vascular smooth muscle cells

ACKNOWLEDGEMENTS

I would like to thank my supervisor Dr. Theresa Peterson for introducing me to research as an undergraduate, and for taking a chance on me when I decided to try my hand at it. She always encouraged independence and lateral thinking, yet was there to remind me to "focus" when I was going off on a tangent. I would also like to thank the Nova Scotia Health Research Foundation for three years of funding. I have thoroughly enjoyed my PhD experience and have learned so much...like how fast four years flies by when you're dedicated to something and how long a day can drag on when you're giving rat enemas! I have learned to think critically and independently, to learn from my mistakes, to appreciate the "ups" (they'll get you through the downs), and to work out multiple dilution factors *only* after I've had my morning coffee.

I would like to thank Jacquie, the best technician in the world, for being there alongside me for the past two years. Without her, I wouldn't have accomplished as much as I did. She was always a step ahead of me to ensure everything was prepared, and we were never lacking in good conversation during those long experiments. It made the days so enjoyable! I would like to thank Monica and Susan for being great friends and for making me laugh even in the face of pure frustration! I would like to thank Marc P. for all his help and for putting up with me as an office-mate. I still don't know whose desk was messier! I would like to thank Luisa, Janet, and Sandi for all their help over the years, and for being patient with me even though they had to show me how to use the fax machine "every" time. I would also like to thank Mark Nachtigal for his support and encouragement over the years, and for always having an open-door policy even if I just wanted to chat. This PhD was a ton of work....but I had a blast!!

Chapter 1

INTRODUCTION

1.1 INFLAMMATION

1.1.1 Introduction to the Inflammatory Response

Inflammation can be defined in simple terms as "the protective response of body tissues to irritation or injury" (Anderson *et al.*, 1998). It is a common response initiated as the body protects itself from harmful agents in its environment, but the inflammatory response is by no means simple. Inflammation entails the concerted actions of multiple immune and non-immune cell-types, and is mediated through direct cell-cell interactions, release of soluble mediators (e.g. cytokines, enzymes and reactive oxygen species), altered protein and lipid mediator synthesis, changes in receptor and adhesion molecule expression, and increased vascular permeability (Closa and Folch-Puy, 2004; Kuby, 2000; Tortora and Grabowski, 1996). An effector cell can trigger a host of downstream effects in multiple target cells resulting in rapid amplification of the inflammatory response. The response generally targets an antigenic stimulus, such as a virus or invading bacteria, and is tightly regulated so that inflammation subsides once the invading pathogen has been destroyed. Negative regulation of inflammation is as complex as the inflammatory response itself (Hanada and Yoshimura 2002; Inagaki-Ohara *et al.*, 2003; Mantovani and Garlanda, 1999; Walsh and Sata, 1999; Wisniewski and Vilcek, 1997). The hallmark symptoms of inflammation are redness, swelling, heat, and pain, often accompanied by loss of tissue function in the affected area (Tortora and Grabowski, 1996). The study of inflammation is an enormous field and the following discussions will focus on aspects relevant to this thesis.

1.1.2 T Cell Subtypes and Inflammation

T lymphocytes derive their name from their site of maturation in the body, the thymus. Mature T cells leave the thymus and populate peripheral lymphoid tissues including the lymph nodes, spleen, and mucosa-associated lymphoid tissue (MALT) (Savino *et al.*, 2004). T cells participate in cell-mediated immunity and recognize foreign antigen when it is processed and displayed on the surface of antigen-presenting cells (APCs) bound to a self-molecule encoded by the genes of the major histocompatibility complex (HMC) (Kuby, 2000). There are different subtypes of T cells that have distinct immune functions and can be distinguished according to specific molecules (ex. co-stimulatory molecules and chemokines) expressed on their surface (Adams *et al.*, 2004). Cells that express the dimeric membrane glycoprotein CD8 (CD8+) are described as cytotoxic T cells (T_C). They are activated in response to altered self-cells (e.g. virus infected or cancerous) expressing MHC class I and function to destroy those cells. CD4-expressing cells (CD4+) generally function as helper T cells (T_H). They are activated by recognition of antigen-MHC class II complexes displayed on APCs. Once activated, they undergo clonal expansion and secrete various cytokines that influence the type of response that occurs in surrounding leukocytes (O'Garra and Arai, 2000; Kuby, 2000).

Depending on the cytokine environment, antigen-primed helper T cells may develop into T_H1 or T_H2 subsets, which differ in the cytokines they secrete and the biological functions they induce (O'Garra, 1998; Abbas *et al.*, 1996; Mosman and Coffman, 1989). T cell receptor (TCR)-antigen-MHCII interactions in the presence of interleukin (IL)-12 secreted by activated macrophages and dendritic cells, induce T_H1

development with subsequent secretion of interferon-gamma (IFN-γ), tumor necrosis factor-α (TNF-α) and IL-2 (Lederer *et al.*, 1996; O'Garra and Arai, 2000). IFN-γ, the hallmark cytokine of T_H1 responses, activates macrophages and stimulates further secretion of IL-12 by these cells thereby initiating a positive loop. This T_H1 activation loop is enhanced by upregulation of IL-12 receptor (IL-12R) on activated T cells and suppression of T_H2 expansion by T_H1 cytokines (Storkus *et al.*, 1998). Activation of downstream targets, including macrophages and cytotoxic T cells, induces further inflammatory cytokine secretion and release of cytotoxic mediators. Cytokines associated with a T_H1 response, often referred to as type I cytokines, are IFN-γ, TNF-α, IL-1, IL-2, IL-6, IL-8, IL-12, and IL-18 (Rogler and Andus, 1998). T_H1 responses are often associated with promotion of excessive inflammation and tissue injury (Kuby, 2000).

TCR-ligation in the presence of IL-4 secreted by activated T_H2 cells, natural killer cells (NK) and mast cells, encourages development of the T_H2 subtype of helper T cells (Abbas *et al.*, 1996; Lederer *et al.* 1996). T_H2 cells promote activation of eosinophils, B cells, and mast cells through the secretion of type II cytokines such as IL-4, IL-5, IL-10 and IL-13 (Rogler and Andus, 1998). T_H2 responses can suppress T_H1 expansion and are generally associated with allergic inflammation (Kuby, 2000). A third subset of regulatory T cells (suppressor T cells) secretes transforming growth factor-β (TGF-β), an immunomodulatory cytokine that can suppress development of both T_H1 and T_H2 responses, and aids in the induction of tolerance to self-derived antigens and oral tolerance to mucosal antigens (Weiner, 1997; Miller *et al.*, 1992). A recent article suggests the existence of two distinct subsets of innate and adaptive regulatory T cells (Bluestone and Abbas, 2003).

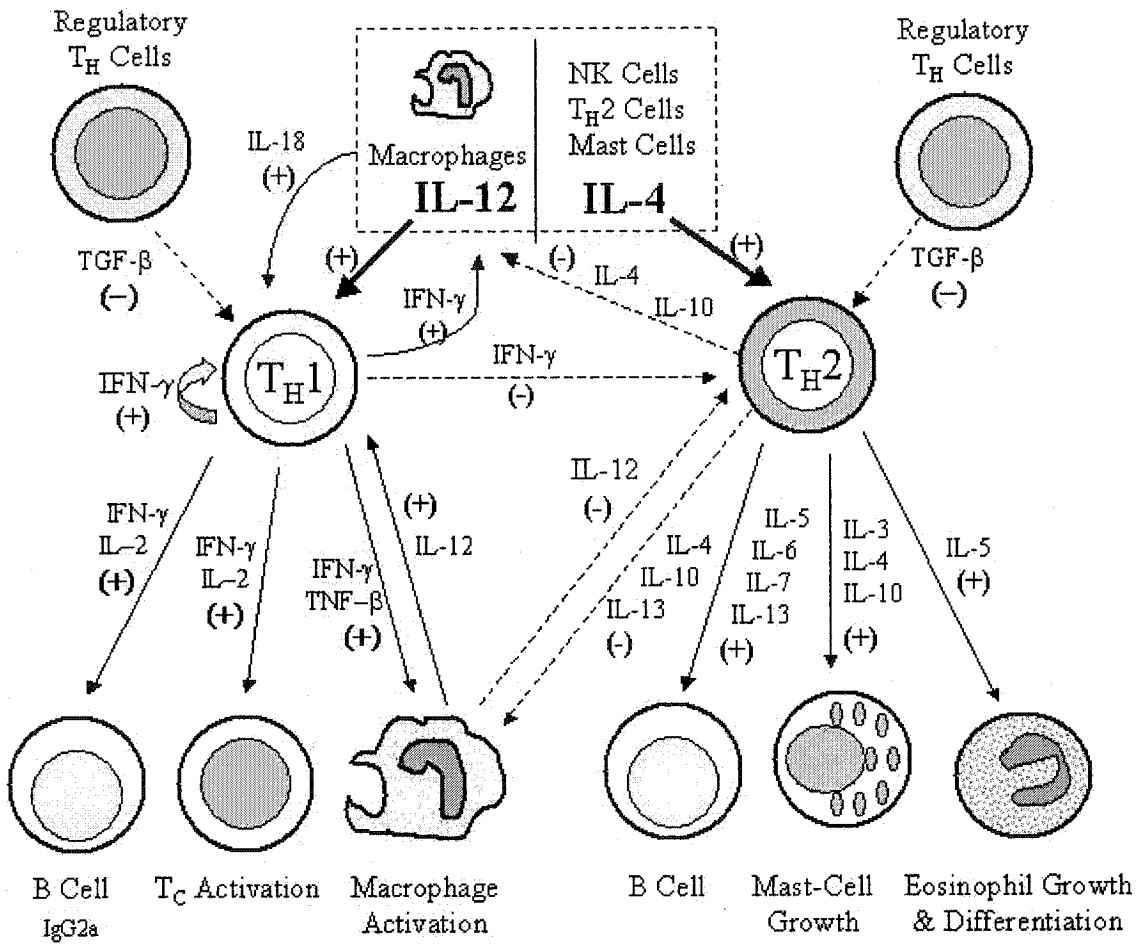

Figure 1-1. T cell differentiation into T_H1 and T_H2 subsets. Factors affecting T cell differentiation into T_H1 and T_H2 subsets and the downstream effects of type I and type II cytokines (adapted from Kuby, 2000).

1.1.3 T_H1/T_H2 Responses and Chronic Inflammation

The balance between T_H1 and T_H2 responses, and the negative cross-regulation of these responses, is very important in maintaining homeostasis following an inflammatory or allergic insult. When the balance is tipped and there is excessive production of type I or type II cytokines, the response is prolonged (O'Neil and Steidler, 2003). If the balance is not corrected, chronic inflammation persists leading to tissue destruction, tissue remodeling, fibrosis development and eventual loss of tissue function (Whitte and Barbul, 1997). Chronic inflammation is at the root of many human disorders. Chronic inflammatory diseases may be characterized by a predominance of type I or type II cytokines, although there is no clear division and cytokines of one type are often overexpressed in an attempt to counterregulate the dominant actions of opposing cytokines.

T_H1-mediated inflammatory disorders include rheumatoid arthritis (Vervoordeldonk and Tak, 2002; Fiersten, 1996), sarcoidosis (Sugiyama and Oshikawa, 2002), psoriasis (Nickoloff and Nestle, 2004; Ghoreschi and Rocken, 2004), preeclampsia (Saito and Sakai, 2003) and Crohn's Disease (Monteleone *et al.*, 2002). Conditions associated with T_H2 responses include asthma (Filosso *et al.*, 2003; Prescott, 2003), atopic dermatitis (Esche *et al.*, 2004; Leung *et al.*, 2004), Still's disease (Saiki *et al.*, 2004), chronic rhinosinusitis (Hamilos and Lund, 2004; Kennedy, 2004), progressive systemic sclerosis (Romagnani, 1999), and ulcerative colitis (Monteleone *et al.*, 2002).

1.2 THE INTESTINE AND "PHYSIOLOGICAL INFLAMMATION"

1.2.1 Anatomy and Physiology of the Intestine

Food contains a variety of nutrients required for repair and maintenance of body tissues and is the primary source of energy driving chemical reactions that take place in every cell of the body. Through the processes of digestion and absorption, the gastrointestinal (GI) system is responsible for converting food into small molecules that can be utilized by cells (Tortora and Grabowski, 1996). Organs composing the GI tract include the mouth, pharynx, esophagus, stomach, small intestine, and large intestine (or colon). The intestines are the primary sites of absorption of nutrients, electrolytes, and fluid. While anatomy and physiology of the small and large intestine are somewhat distinct, both tissues are divided into four general layers (Fig 1-2).

The innermost layer, in contact with the gut lumen, is the *mucosa* and it consists of the epithelium, lamina propria, and muscularis mucosa. The epithelial lining of the human intestine spans a surface area of about $200m^2$ and is only a single layer thick (Neish, 2002). It is a dynamic layer involved in secretion of digestive enzymes and mucous, bidirectional trafficking of fluids, and regulated transport of nutrients and ions (Madara, 1990). It acts as a protective barrier between the host and a constant flood of microorganisms that can reach a density of up to 10^{11} organisms/ml of lumenal contents in the colon (Neish, 2002). Beneath the epithelial layer is the lamina propria, a supportive layer of areolar connective tissue scattered with blood vessels and lymphatic vessels. The lamina propria contains most of the cells of the mucosa-associated lymphoid tissue

(MALT), which consists of various immune cell-types involved in host defense against invading pathogens (Tortora and Grabowski, 1996). The GI tract is estimated to contain as many immune cells as the rest of the entire body, which makes sense since the gut is continually exposed to pathogens from the outside environment. The lamina propria connects the epithelium to the muscularis mucosa, which is comprised of two thin bands of circular and longitudinal smooth muscle.

The *submucosa* is a connective tissue layer that connects the mucosa with the thicker muscle layers below. This layer contains a large amount of collagen type I (68%) and collagen type III (20%) and provides tensile strength to the intestine (Thornton *et al.*, 1997). The submucosa is highly vascular and contains a portion of the autonomic nervous system (plexus of Meissner) that innervates the muscularis mucosa, blood vessels, and secretory cells of mucosal glands (Tortora and Grabowski, 1996). The submucosa also contains its own glands and lymphatic tissue. The *muscularis* consists of smooth muscle arranged into an inner layer of circular muscle fibers and an outer layer of longitudinal fibers. This layer is much thicker than the muscularis mucosa. Contractions of the muscularis are important for peristalsis, or propulsion of contents through the intestinal lumen. Innervation of this layer comes from the myenteric plexus, the major nerve supply to the GI tract. It is embedded within the muscularis and contains fibers from both autonomic divisions (Tortora and Grabowski, 1996). The most superficial layer of the intestine is the *serosa*, or visceral peritoneum, a serous membrane composed of connective tissue and simple squamous epithelium that supports the intestine and helps suspend it in the abdominopelvic cavity.

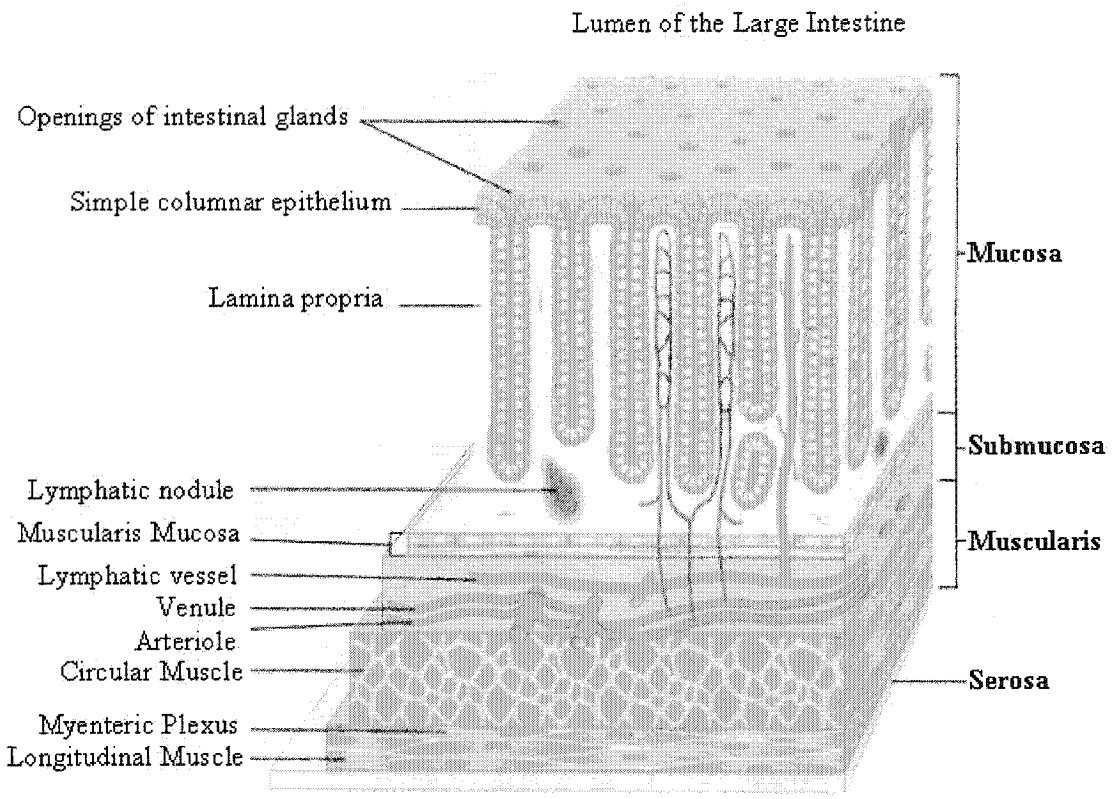

Figure 1-2. Schematic illustrating the major components of the large intestine (adapted from Tortora and Grabowski, 1996). The large intestine consists of four major layers: the mucosa, submucosa, muscularis and serosa.

1.2.2 "Physiological" Intestinal Inflammation:

The gut is continually exposed to factors from the external environment and therefore must remain on guard for attack at all times. It is no small feat that the healthy gut exhibits tolerance toward beneficial and innocuous antigens derived from food and commensal flora, yet mounts powerful and efficient immune responses against harmful antigens associated with invading pathogens (Sherman and Kalman, 2004). The mechanisms controlling the balance between tolerance and active immunity are critical to gut homeostasis but these mechanisms are not well understood (Bilsborough and Viney, 2002; Dasgupta *et al.*, 2001; Gotsman *et al.*, 2001). Chronic exposure to microbial antigens keeps the gut in a state of low-grade "physiological inflammation", manifested by an abundant presence of leukocytes in the intraepithelial and subepithelial layers of the mucosa (Fiocci, 1997). During encounters with invading pathogens, the mucosal immune system launches a true inflammatory response, or "pathophysiological inflammation", comprised of both innate and antigen-specific immune responses.

1.2.2.1 Immune Cells

T and B cells are involved in receptor-mediated antigen-specific recognition in the intestine. These cells migrate from their respective sites of maturation and populate peripheral sites including the gut-associated lymphoid tissues (GALT) comprised of Peyer's immune patches, intraepithelial compartments, and the loosely organized lamina

propria (Rothenberg *et al.*, 2001). In addition to the thymus, evidence now demonstrates that the intestinal epithelium supports the development of an extra-thymic population of T cells (Lefrancois and Paddington, 1995; Lynch *et al.*, 1995). T cells, primarily CD4+ T helper cells, constitute about one-third of the cells in the lamina propria (Monteleone *et al.*, 2002). A variety of cells in the intestine function as antigen-presenting cells for T cells, including B cells, macrophages, dendritic cells, and epithelial cells (Pavli et al., 1993; Pavli *et al.*, 1996; Panja *et al.*, 1993). Activated T cells regulate the functions of surrounding lymphocytes and leukocytes by direct cell-to-cell contact and cytokine secretion.

Neutrophils, or polymorphonuclear leukocytes (PMN), account for 50-60% of circulating leukocytes and act as a first line of defense against foreign invasion (Elliott and Wallace, 1998). Neutrophil infiltration is a hallmark of acute and chronic inflammation of the GI tract. Neutrophils play an important role in the attack against microbial invasion via synthesis and secretion of inflammatory mediators, along with release of pre-formed mediators including destructive enzymes and reactive molecules, that have potent effects on surrounding cells (Fiocci, 1997). During an inflammatory response in the gut, activated immune cells, primarily neutrophils, macrophages, and cytotoxic T cells play the role of aggressors that attack, destroy, and engulf nearby cells. Unfortunately, mediators released by these activated cells can also cause damage to host tissues. Other immune cells, such as mast cells (Santos *et al.*, 2001; Soderholm et al., 2002), eosinophils (Jeziorska et al., 2001), and dendritic cells (Stagg *et al.*, 2003), are involved in immune responses in the gut but will not be discussed here (Fiocci, 1997 provides a review).

1.2.2.2 Non-immune cells

Non-immune cells in the intestine were traditionally thought of as passive bystanders during an inflammatory response; however, it is now clear that virtually all cell-types in the inflamed mucosa play an active role in gut immunity and inflammation (Fiocci, 1997). Intestinal epithelial cells (IECs) respond to a wide variety of stimuli including adherent and invasive bacteria, bacterial products, cytokines, and short-chain fatty acids (Berin *et al.*, 1999; Hecht and Savkovic, 1997), and they exert their immune functions by processing and presenting antigens to T cells, secreting inflammatory cytokines and chemokines, expressing adhesion molecules, and releasing eicosanoids and other inflammatory mediators (Jobin and Sartor, 2000). Mesenchymal cells, which include fibroblasts, myofibroblasts, and smooth muscle cells, were originally described in terms of their structural roles, particularly providing support for surrounding cells and synthesizing collagen for the extracellular matrix. More recent investigations show that mesenchymal cells from normal and inflamed intestine produce various cytokines, express cytokine receptors and physically interact with immune cells including activated T cells (Fiocci, 1997). Crosstalk between immune and nonimmune cells is complex and occurs directly, through cell-to-cell contact, and indirectly, through the release of cytokines and destructive molecules (e.g. enzymes and reactive molecules) that influence neighboring cells and damage surrounding tissue.

The normal intestine is in a steady-state of physiologic inflammation represented by a balance between factors that activate the host immune system (microbes, antigens,

inflammatory mediators) and host mechanisms that maintain mucosal integrity and down-regulate the inflammatory response (MacDermott, 1994). When strict regulation of physiological inflammation is lost, the perpetuating loops of cell activation and cytokine secretion continue unopposed resulting in a state of chronic inflammation.

1.3 INFLAMMATORY BOWEL DISEASE

1.3.1 Subtypes of Inflammatory Bowel Disease

Inflammatory bowel disease (IBD) is an umbrella term describing a group of chronic relapsing and remitting conditions generally characterized by inflammation, ulceration, and fibrosis of the GI tract (Cotran *et al.*, 1999). Common symptoms include abdominal pain, diarrhea, rectal bleeding, low-grade fever, and weight loss. The two most prevalent forms of IBD are Crohn's disease (CD) and ulcerative colitis (UC) that together affect up to 200 people per 100,000 worldwide, with the highest incidence in white populations of Europe and North America (Fedorak and Thomson, 2000). Clinical diagnosis is made by radiology, endoscopy, and biopsy of affected regions (Hommes and van Deventer, 2004; Lo, 2004). Collagenous colitis and lymphocytic (microscopic) colitis are rarer forms of IBD that cannot be diagnosed by endoscopy (Zeroogian and Chopra, 1994).

1.3.2 Crohn's Disease

CD predominantly attacks the terminal ileum and colon although it can affect any segment of the GI tract from the mouth to the anus. It is characterized by transmural granulomatous inflammation, ulceration, bowel wall thickening, and intestinal fibrosis (Cotran *et al.*, 1999; Pucilowska *et al.*, 2000). Inflammation is discontinuous with normal bowel separating segments of diseased bowel. This is referred to as "skip-lesioning" and it is a hallmark of CD versus other forms of IBD (Fedorak and Thompson, 2000). Since inflammation in CD is transmural (meaning that all layers of the intestine are affected), involved segments of bowel may become adhered to each other, and to other organs, via the inflamed serosa and mesentery that become sticky and edematous (Fedorak and Thompson, 2000). Ulceration in CD is also transmural and can manifest as ulcers, fissures and fistulas. Fissures are narrow ulcers that may penetrate deep into the intestinal wall. Fistulas are sinus tracts that begin as ulcers and burrow down through the bowel wall, penetrating through the serosa and into adhered tissue, which may include intestine, bladder, and perineum, or they may form open-ended abscesses in the peritoneum. Fibrosis involving the submucosa, muscularis, and mucosa can lead to stricture formation, a complication of CD requiring surgical resection (Cotran *et al.*, 1999). In contrast to CD, inflammation and ulceration in UC is restricted to the mucosa of the large intestine, thus involvement of deeper layers of the intestine does not occur.

1.3.3 Etiology of Inflammatory Bowel Disease

The etiology of CD remains unclear but there is evidence supporting both environmental and genetic components (Fiocci, 1998). Familial studies have shown that the frequency of IBD in first-degree relatives may be as high as 40% (Farmer and Michener, 1986) with a higher concordance in monozygotic twins than dizygotic twins, suggesting a genetic component (Tysk *et al.*, 1988). While investigators have begun to map genetic predisposition to specific chromosomes (Hugot *et al.*, 1994; Hugot *et al.* 1996; Satsangi *et al.*, 1996) there are significant discrepancies between studies, which is likely due to genetic variations in the populations being tested. This reinforces the idea that IBD is a heterogeneous disorder and environmental factors play an important role in disease development (Fiocci, 1998). In addition to environmental factors such as diet, toxins, and exposure to microbes, other suspected risk factors for CD are smoking (Somerville *et al.*, 1984) and increased intestinal permeability (Hollander *et al.*, 1986).

Whatever the underlying trigger, it is presumed that chronic intestinal inflammation is caused by an excessive immune response to an unidentified mucosal antigen (which may be a previously innocuous microbe) that is inappropriately controlled by the normal counterregulatory mechanisms (Fiocci, 1998). Chronic activation of the intestinal immune system in CD results in prolonged T_H1-type inflammation characterized by elevated production of inflammatory mediators including cytokines, growth factors, chemokines, and adhesion molecules (O'Neil and Steidler, 2003; Rogler and Andus, 1998). Figure 1-3 outlines factors contributing to IBD development.

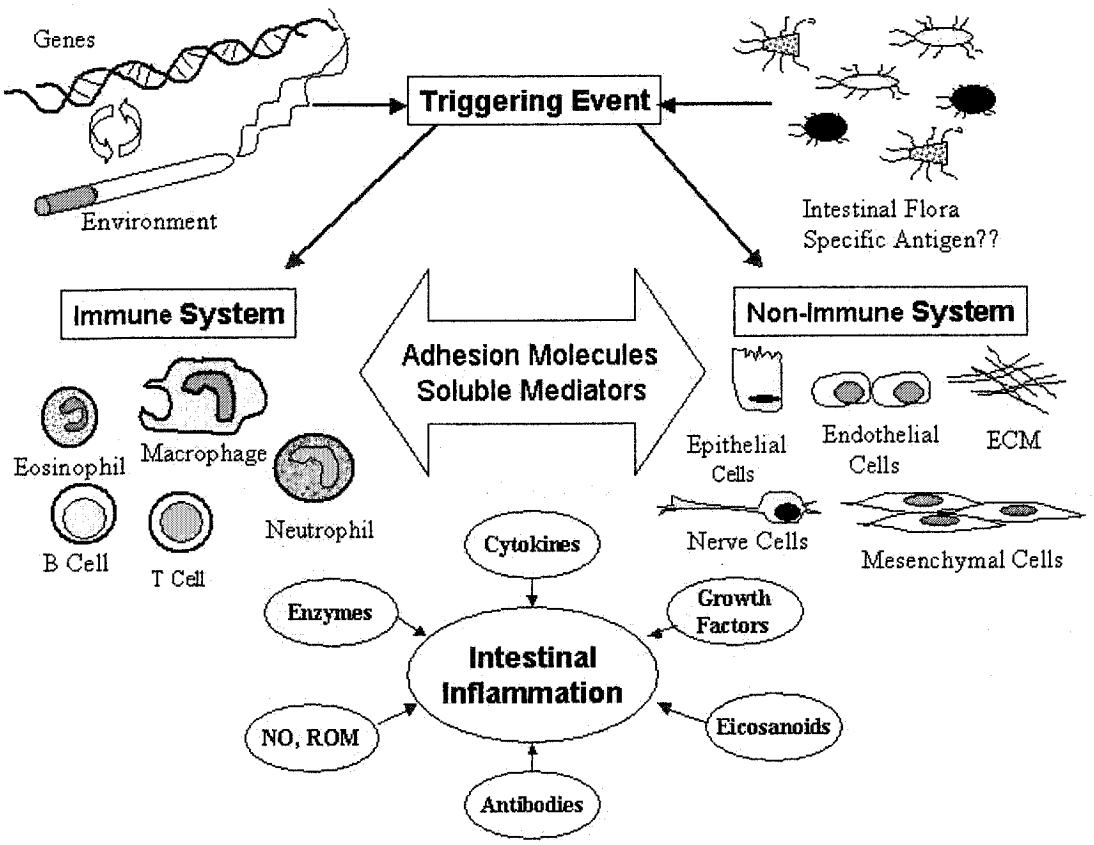

Figure 1-3. Factors influencing the development of IBD (adapted from Fiocci, 1998). Triggering events may involve intestinal bacteria as well as genetic and environmental risk factors. Complex interaction between various immune and non-immune cells leads to sustained inflammation characterized by elevated production of cytokines, growth factors, adhesion molecules, and various other mediators that drive the inflammatory response in the intestine. NO = nitric oxide, ROM = reactive oxygen metabolites

1.4 CYTOKINES AND SIGNALING PATHWAYS IN IBD

1.4.1 Type I cytokines and Crohn's Disease

Evidence suggests that there is an "imbalance" between pro-inflammatory and anti-inflammatory cytokine production in CD, with traditional type I pro-inflammatory mediators such as IFN-γ, IL-1β, TNF-α, IL-6, and IL-8 predominating (O'Neil and Steidler, 2003; McCormack *et al*, 2001). Although there is often a compensatory increase in negative regulatory cytokines including IL-10 and TGF-β, this is not enough restore homeostasis (Li and He, 2004). The role of traditional type I cytokines in CD has been studied extensively (see O'Neil and Steidler, 2003 for review). Much recent attention has been paid to the role of more novel cytokines, such as IL-12 (Camoglio *et al*, 2002; Bouma *et al*., 2002; Neurath *et al*., 2000), IL-15 (Liu *et al*., 2000) and IL-18 (Maerten *et al*., 2004; Pages *et al*; 2001; Pizarro *et al*; 1999) in the pathology of CD. In the inflamed intestine, cytokines are secreted by invading macrophages, neutrophils, and activated lymphocytes, as well as resident non-immune cells such as endothelial cells, fibroblasts, smooth muscle cells, and epithelial cells (Fiocci, 1997). Inflammatory cytokines induce the synthesis and secretion of adhesion molecules that aid in migration of inflammatory cells into the tissue, as well as other mediators such as reactive oxygen metabolites (ROM) and lipid mediators that propagate the inflammatory response and also lead to tissue destruction (Rogler and Andus, 1998).

Synthesis of many pro-inflammatory cytokines is induced by the activation of nuclear factor-κB (NF-κB), a transcription factor produced in virtually all cell types (Rogler and Andus, 1998). NF-κB activation and nuclear translocation is an important

step in the signaling pathways of several inflammatory cytokines elevated in CD, including TNF-α, IL-1β, and IL-18 (O'Neil and Steidler, 2003). These cytokines and their role in IBD pathology are discussed below, with emphasis on recent data implicating NF-κB and the novel IL-18 in Crohn's Disease.

1.4.2 Tumor Necrosis Factor-α

1.4.2.1 Tumor Necrosis Factor-α Signaling

TNF-α is a pleiotropic cytokine produced by activated macrophages, monocytes, and T_H1 cells (Wallach *et al.*, 1999). The cytokine itself is synthesized as a membrane protein that is proteolytically cleaved by TNF-α-converting enzyme (TACE) to its mature soluble form. TNF-α is a potent inflammatory factor and a key regulator of apoptotic cell death. The distinct signaling endpoints are achieved by TNF-α binding, in trimeric form, to one of two distinct TNF receptors, TNFR-1 (55kDa) and TNFR-2 (75kDa). Ligation of TNFR-2 leads to NF-kB activation via recruitment of TNFR-associated factor-2 (TRAF-2), thereby promoting cell survival and inflammation (O'Neil and Steidler, 2003). Ligation of TNFR-1 can lead to activation of NF-κB or induction of apoptosis depending on which signaling intermediates are recruited to the intracellular death domain (DD) of TNFR-1. In the absence of apoptotic stimuli, NF-κB activation occurs when TRAF-2 associates with TNFR-1 via an accessory molecule, TNFR-associated DD (TRADD). If apoptotic stimuli are present, Fas-associated death domain (FADD) associates with TRADD and an apoptotic signaling cascade involving caspase activation ensues (Wallach

et al., 1999). Soluble TNF receptors act as inhibitors of TNF signaling (O'Neil and Steidler, 2003).

In addition to NF-κB and caspases, TNF-α can activate members of the mitogen activated protein kinase (MAPK) family, which includes the stress-activated protein kinase (SAPK), c-Jun N-terminal kinase (JNK) (Liu and Han, 2001). Recent studies of TNF-α-induced activation of JNK have revealed important mechanisms in regulating life or death responses to this cytokine. Activation of JNK seems to be required for TNF-α-induced apoptosis (Deng *et al.*, 2003; Varfolomeev and Ashkenazi, 2004), while activation of specific NF-κB target genes inhibits JNK activation and prevents apoptosis (Tang *et al.*, 2001). In support of this, absence of NF-κB-mediated inhibition of JNK activation leads to enhanced TNF-α-induced apoptosis (Tang *et al.*, 2002). These recent investigations have shed light on the cross-regulation of TNF-α-induced signals regulating survival and apoptosis.

1.4.2.2 Tumor Necrosis Factor-α in Crohn's Disease

Although a central role for TNF-α in CD is well-established, reported data regarding the expression of TNF-α in IBD has been somewhat contradictory. Some studies have been able to demonstrate increased mucosal, serum, and stool levels of TNF-α (Maeda *et al.*, 1992; Braeggar *et al.*, 1992; Andus *et al.*, 1993), while others were unable to detect increased mucosal expression of TNF-α in IBD patients compared to controls (Isaacs *et al.*, 1992; Stevens *et al.*, 1992). Regardless of conflicting reports in measuring TNF-α levels, the importance of TNF-α in the pathology of human CD is

clearly exemplified by the potent therapeutic effects of the anti-TNF-α therapy, Infliximab, observed in clinical trials of patients with refractory or fistulizing CD (Hanauer *et al.*, 2002; Sandborn and Hanauer, 2002). Improvements in anti-TNF-α therapy aimed at reducing immunogenicity and side effects are underway (Lim *et al.*, 2004). The lamina propria macrophage and monocyte populations are the major source of local TNF-α production contributing to intestinal manifestations of CD (O'Neil and Steidler, 2003). TNF-α is thought to mediate some of the systemic effects of CD as well, such as fever, lethargy, loss of appetite, growth suppression and chronic anemia (Murch, 1998).

1.4.3 Interleukin-1β

1.4.3.1 Interleukin-1β Signaling

IL-1 is one of the most pleiotropic inflammatory cytokines, affecting virtually every cell type, and its endogenous expression exhibits a very narrow margin between biological benefit and toxicity (O'Neil and Steidler, 2003). Thus, expression of IL-1, its receptors, and the naturally occurring receptor antagonist (IL-1Ra), are tightly regulated at multiple levels in order to minimize IL-1 toxicity during an inflammatory response (Dinarello, 1998). IL-1β is produced as an inactive precursor molecule that must be cleaved by caspase-1, also called interleukin-1 converting enzyme (ICE), to its mature active form. Biologically active IL-1β associates with the IL-1RI signaling complex consisting of the IL-1R type I and the IL-1R accessory protein (IL-1RAcP). Upon

ligation of IL-1RI signaling complex, intracellular IL-1R-activating kinases (IRAKs) are recruited followed by activation of TRAF-6, an important signaling intermediate (Dinarello, 1998). The major pathway activated by IL-1β is the NF-κB pathway, which leads to transcription of many genes involved in the inflammatory response (Kuno and Matsushima, 1994).

1.4.3.2 Interleukin-1β in Crohn's Disease

IL-1β expression is increased in inflammatory lesions of patients with IBD (Mahida *et al.*, 1989; Ligumsky *et al.*, 1990). IL-1Ra is also increased in IBD (Kuboyama, 1998) indicating an attempt to counteract IL-1β, although the increase in IL-1β outweighs its antagonist (Casini-Raggi *et al.*, 1995). Macrophages are considered to be the primary source of IL-1β in the inflamed mucosa whereas intestinal epithelial cells are the primary source of IL-1Ra (Rogler and Andus, 1998). IL-1Ra administration has been beneficial in modulating intestinal inflammation in animal models of IBD (Kuboyama, 1998). Levels of IL-1β secreted into culture supernatants from inflamed IBD tissue correlate with disease severity in the mucosa from which biopsies were removed, further supporting a direct role for IL-1β in the pathology of IBD (Dionne *et al.*, 1998). Levels of mature ICE are also elevated in inflamed colonic mucosa from IBD patients, indicating increased processing of pro-IL-1β in the disease. Colonic macrophages isolated from CD patients express active ICE and thus secrete mature IL-1β in a manner similar to circulating monocytes (O'Neil and Steidler, 2003). Although a role for IL-1β in

CD has been clearly established, biological therapies targeting IL-1β have not been attempted in human trials.

1.4.4 Interleukin-18

1.4.4.1 Interleukin-18 Signaling

IL-18 was originally described as "IFN-γ-inducing factor" (IGIF) since it augments IFN-γ secretion by T_H1 cells (Gracie *et al.*, 2003). It also enhances T cell activation in the presence of IL-12 and stimulates T cell proliferation (Kohno *et al.*, 1997). IL-18 is a member of the IL-1 family of cytokines and shares common structural and signaling features with IL-1 (Gillespie and Horwood, 1998; Azam *et al.*, 2003). It is constitutively expressed as a 24 kDa precursor molecule and is cleaved to its 18 kDa mature form by both caspase-1-dependent mechanisms (Ghayur *et al.*, 1997; Gu *et al.*, 1997; Fantuzzi *et al.*, 1999) and caspase-1-independent mechanisms (Tsutsui *et al.*, 1999), one of which is activation by protinase-3, an enzyme derived from activated neutrophils (Sugawara *et al.*, 2001). Consistent with its proposed role in T_H1 inflammatory responses, IL-18 expression has been identified in macrophages (Gillespie and Horwood, 1998), Kuppfer cells (Matsui *et al.*, 1997), dendritic cells (Stoll *et al.*, 1998), and microglial cells (Prinz *et al.* 1999). IL-18 is also produced by certain non-hemopoietic cells including keratinocytes (Stoll *et al.*, 1997), osteoblasts (Udagawa *et al*, 1997), oral epithelial cells (Sugawara *et al.*, 2001) and intestinal epithelial cells (Tekeuchi *et al.*, 1997; Muneta *et al.*, 2002). IL-18-binding protein (IL-18BP) is a natural

inhibitor of IL-18 (Im *et al.*, 2002) that is induced by IFN-γ (Paulukat *et al.*, 2001; Hurgin *et al.*, 2002) and IFN-α (Kaser *et al.*, 2002), illustrating a negative feedback loop that decreases IL-18-induced IFN-γ production. A positive loop also exists however, since IFN-γ increases IL-18 gene expression in macrophages (Kim *et al.*, 2000).

There are two known IL-18 receptors that form a functional complex resembling the IL-1RI receptor complex. The IL-18Rα is related to IL-1RI and is responsible for extracellular binding of IL-18, while the non-binding signal-transducing IL-18Rβ resembles the IL-1RAcP (Gracie *et al.*, 2003). Both chains are required for functional IL-18 signaling (Born *et al.*, 1998). IL-18R are expressed on neutrophils, macrophages, natural killer cells, endothelial cells, and smooth muscle cells (Leung *et al.*, 2001; Hyodo *et al*, 1999; Gerdes *et al.*, 2002) and the IL-18R complex can be upregulated on naïve T cells, T_H1 cells, and B cells by IL-12 (Yoshimoto *et al.*, 1998; Xu *et al.*, 1998; Sareneva *et al.*, 2000). IL-18R complex-ligation leads to recruitment of IRAK and activation of TRAF-6, as does activation of the IL-1RI signaling complex. Activated TRAF-6 phosphorylates NF-κB-inducing kinase (NIK) leading to subsequent activation and nuclear translocation of NF-κB (O'Neil and Steildler, 2003). While the major signaling pathway activated by IL-18 is the NF-κB pathway (Robinson *et al.*, 1997; Matsumoto *et al.*, 1997; Kojima *et al.*, 1999), IL-18 also activates MAPK cascades (Wyman *et al.*, 2002; Gracie *et al.*, 2003).

In addition to its synergism with IL-12 in enhancing T cell functions, it was recently discovered that IL-18 is a direct chemoattractant for human CD4+ T_H1 cells (Komai-Koma *et al.*, 2003). IL-18 also induces neutrophil (NT) activation (Leung *et al.*, 2001), likely via a p38 MAPK-dependent mechanism (Wyman *et al.*, 2002), and was

reported to play a role in NT chemotaxis by inducing TNF-α and leukotriene-B_4 production, a potent NT chemoattractant (Cannetti *et al.*, 2003). IL-18 increased TNF-α and IL-1β production by monocytes in contact with activated T cells, and upregulated expression of TNFR, intercellular adhesion molecule-1 (ICAM-1) and vascular cell adhesion molecule-1 (VCAM-1) on monocytes (Dai *et al.*, 2004), indicating additional important roles of IL-18 in the T_H1-mediated inflammatory response.

1.4.4.2 Interleukin-18 and Crohn's Disease

IL-18 mRNA levels are increased in intestinal epithelial cells and lamina propria mononuclear cells (LPMN) from patients with CD compared to UC and healthy controls (Pizarro *et al.*, 1999). Bioactive IL-18 in colonic mucosal samples (Monteleone *et al.*, 1999), and serum IL-18 levels (Furuya *et al.*, 2002), were also elevated in CD patients but not UC patients, suggesting that IL-18 is involved in T_H1-mediated diseases like CD. An abundance of IL-18-producing macrophages can be detected in the lamina propria of inflamed CD mucosal biopsy samples (Kanai *et al.*, 2000). Intestinal mucosal lymphocytes from CD biopsies proliferate readily in response to IL-18 whereas normal control lymphocytes do not, indicating that IL-18R expression is up-regulated in active CD (Kanai *et al.*, 2000). Mature IL-18 (18.3 kDa) was detected by Western immunoblotting of inflamed intestinal CD samples, whereas only the inactive precursor form (24 kDa) was detected in control and UC samples (Monteleone *et al.*, 1999; Pizarro *et al.*, 1999). Thus it appears that processing of IL-18 rather than *de novo* synthesis may

play an important role in CD, consistent with the finding of elevated bioactive caspase-1 (ICE p20) in inflamed tissue form CD patients (Monteleone *et al.*, 1999).

Up-regulation of macrophage-derived IL-18 in intestinal mucosa was detected in a murine trinitrobenzenesulfonic acid (TNBS) model of CD, and treatment with anti-IL-18 antibody attenuated colonic inflammation (Kanai *et al.*, 2001). Importantly, no significant colitis was induced in IL-18-deficient mice in this study, illustrating the importance of IL-18 in the development of TNBS-induced murine colitis. Treatment of mice with recombinant human IL-18 binding protein attenuated colitis in the same model by decreasing local production of TNF-α (Ten Hove *et al.*, 2001). Treatment with an adenovirus expressing IL-18 antisense mRNA blocked colitis in a T cell dependent model of IBD in SCID (severe-combined immunodeficiency) mice (Wirtz *et al.*, 2002). In dextran sulphate sodium (DSS)-induced colitis, neutralization of IL-18 corresponded with decreased intestinal IFN-γ and TNF-α levels and attenuation of colitis (Siegmund *et al.*, 2001a; Sivakumar *et al.*, 2002). Interestingly, IL-18-deficient and IL-18R-deficient mice were recently shown to develop worse DSS-induced colitis than control mice (Takagi *et al.*, 2003), suggesting that IL-18 may actually serve some protective function in this model. The ICE-inhibitor, pralnacasan, reduced DSS-induced murine colitis and decreased colonic expression of mature IL-18 (Loher *et al.*, 2004). The beneficial effects of pralnacasan were due decreased mature IL-18 and IL-1β with subsequent reduction of IFN-γ production. DSS-colitis was also attenuated in ICE-deficient mice compared to controls (Seigmund *et al.*, 2001b). A monoclonal antibody to human IL-18 has been developed and human trials are awaited (Holmes *et al.*, 2000).

1.4.5 – Nuclear Factor *kappa* B

1.4.5.1 NF-κB Activation and Regulation of Gene Transcription

The NF-κB/Rel family of transcription factors form dimers that regulate the expression of a large number of genes containing *cis*-acting κB binding motifs (GGGRNNYYCC, where R is a purine, Y is a pyrimidine, and N is any base), particularly genes involved in inflammation and immunity (Martone *et al.*, 2003; Neurath *et al.*, 1998). The different dimers exhibit varied affinities for κB-binding sequences. Binding sites for NF-κB have been described in the promoters of various pro-inflammatory cytokines including IL-1, IL-6, IL-8, IL-18 and TNF-α, suggesting that NF-κB plays a central role in the pathogenesis of chronic T_H1-mediated inflammatory disorders such as CD (Barnes and Karin, 1997). Classical NF-κB activation (Fig 1-4) involves phosphorylation of the cytoplasmic inhibitor of NF-κB (IκB) by activated IκB kinases (IKK) (Ghosh and Baltimore, 1990; Finco and Baldwin, 1995). IKK can be phosphorylated by NF-κB-inducing kinase (NIK), which is phosphorylated by upstream signaling molecules in the IL-1β (O'Neil and Greene, 1998), IL-18 (Matsumoto *et al.*, 1997), and TNF-α (Wallach *et al.*, 1999) pathways, including TRAF-2 and TRAF-6. Following phosphorylation, the inhibitory IκB is targeted to the 26S proteosome for degradation (Ciechanover, 1994), allowing free NF-κB dimers (particularly p50/p65 heterodimers) to be phosphorylated by various upstream kinases and enter the nucleus to stimulate gene transcription (Naumann and Scheidereit, 1994). Reversible acetylation of NF-κB (at various lysine residues) in the nucleus has recently been reported as a

mechanism of regulating the strength, specificity, and duration of NF-κB responses, by affecting transcriptional activation, DNA binding affinity, IκBα assembly, and subcellular localization (Green and Chen, 2004b). Deacetylation of NF-κB p65 by histone deacetylase-3 (HDAC3) in the nucleus promotes IκBα-binding and nuclear export of NF-κB, thereby terminating gene transcription (Green and Chen 2004a).

1.4.5.2 NF-κB in Crohn's Disease

NFκB is a pivotal transcription factor in chronic inflammatory diseases. Its activation induces the expression of many inflammatory genes including cytokines, enzymes, and adhesion molecules (Neurath *et al.*, 1998a; Barnes and Karin, 1997). Rectal administration of NF-κB antisense phosphorothioate oligonucleotides to the p65 subunit abrogated colitis in two murine models (Neurath *et al.*, 1996b; Murano *et al.*, 2000). Overexpression of NF-κB was demonstrated in colonic macrophages from patients with CD, and targeted down-regulation of NF-κB p65 by antisense oligonucleotide administration, considerably reduced pro-inflammatory cytokine production by these cells suggesting therapeutic potential of down-regulating NF-κB in CD (Neurath *et al.*, 1998b). A small pilot study recently showed that 71% of patients with distal colonic IBD received therapeutic benefit from one topical administration of NF-κB p65 antisense oligonucleotide, compared to only 25% in the placebo group (Lofburg *et al.*, 2002). Further human trials are needed to confirm the results.

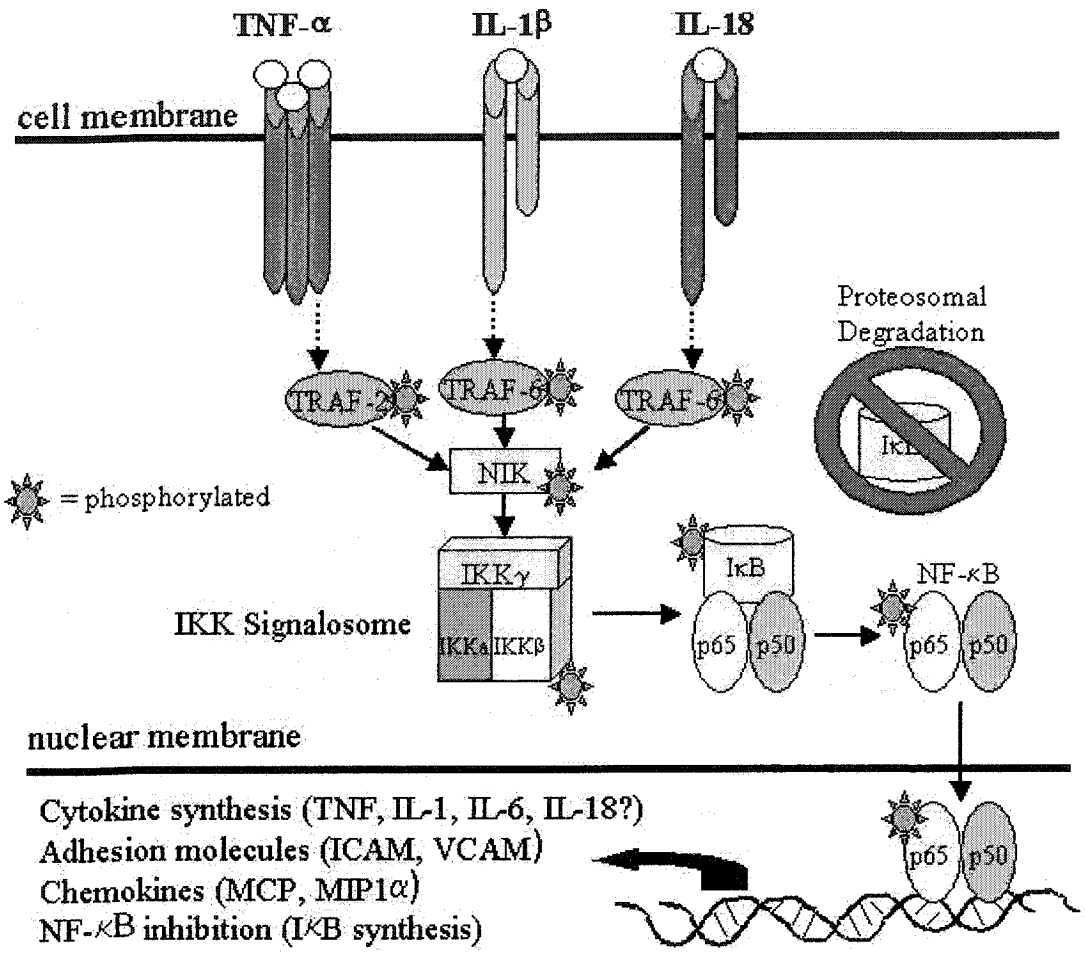

Figure 1-4. Activation of NF-κB by TNF-α, IL-1β, and IL-18. Activation leads to nuclear translocation of the p65/p50 heterodimer and initiation of gene transcription. TRAF = TNF receptor associated factor, NIK = NF-κB inducing kinase, IκB = inhibitor of NF-κB, IKK = IκB kinase, ICAM = intercellular adhesion molecule, VCAM = vascular cell adhesion molecule, MCP = monocyte chemoattractant protein, MIP1α = macrophage inflammatory protein-1α

1.5 FIBROSIS

1.5.1 Collagen

Collagens are a structurally and functionally heterogeneous group of extracellular matrix proteins encoded by a family of genes that share common evolutionary history (Raghow and Thopmson, 1989). Nineteen distinct types of collagen have been described that vary in their structure as well as the function they serve in various tissues (Bateman *et al.*, 1999). Fibrillar collagens (e.g. collagens type I and III) form fiber-like bundles that provide tensile strength to tissues, while non-fibrillar collagens (e.g. collagen type IV) form mesh-like bundles such as that seen in basement membrane, that provide scaffolding for other collagenous and non-collagenous ECM components (Rojkind and Greenwel, 1994) A common structural feature of all collagens is a triple helix region within the molecule, which is made up of 3 polypeptide α-chains folded in a ropelike coil. Each α-chain is composed of repeating sequences of amino acids ("glycine-X-Y") that is very important for proper helical formation, with X often being proline and Y often being hydroxyproline (Linsenmayer, 1991; Kielty *et al.*, 1993; Witte and Barbul, 1997).

Specific types of collagen are formed from different combinations of α-chains. The helical complex is further strengthened through intermolecular bond formation between the α-chains of adjacent molecules (Oryan, 1995). The terminals of the collagen molecules are non-helical and are important for formation of collagen fibrils and interactions with other extracellular components. The α-chains of the principal collagens

are synthesized with long extremities at their terminals and are secreted from the cell after formation of the triple helix (this is called pro-collagen). The non-helical ends are enzymatically cleaved in the extracellular space, allowing the "tropocollagen" molecules to associate with each other and form fibrils, which then aggregate to form large fibers that are visible by light microscopy (Burgeson, 1992). See figure 1-5 for an overview of collagen synthesis and assembly.

The fibrillar collagens (e.g. types I, II and III) account for over 70% of the total collagen found in the body (Kielty *et al.*, 1993). Collagen type I is the most abundant collagen and is present in many tissues including bone, tendon, ligaments and joint capsules (Burgeson, 1992). Collagen type III plays a role in tissue extensibility and is found in tissues such as arteries, skin, and soft organs. Collagen type III is prominent in the initial stages of wound healing and scar-tissue formation where it provides mechanical strength to newly formed matrix (Burgeson, 1992). As healing tissue gains strength, collagen type III is replaced by stronger type I fibers. Thus, elevated levels of collagens type III and type I are detected during normal wound healing. They are also characteristic of disease-related fibrosis, including intestinal fibrosis seen in Crohn's Disease (Geboes *et al.*, 2000; Gonzalez *et al.*, 2004; Kershenobich Stalnikowitz and Weissbrod, 2003). The cleaved collagen type III amino-terminal pro-peptide (PIIINP) has become a standard serological indicator of new collagen synthesis in human fibrotic disorders such as alcoholic liver disease and hepatitis C (Peterson, 1988; Peterson *et al*,. 2003a; Niemela, 1994; Plebani and Burlina, 1991), has recently been shown to correlate with disease activity in IBD (Peterson *et al.*, 2003b), and may serve as a prognostic indicator of scar tissue formation following severe burns (Ulrich *et al.*, 2002).

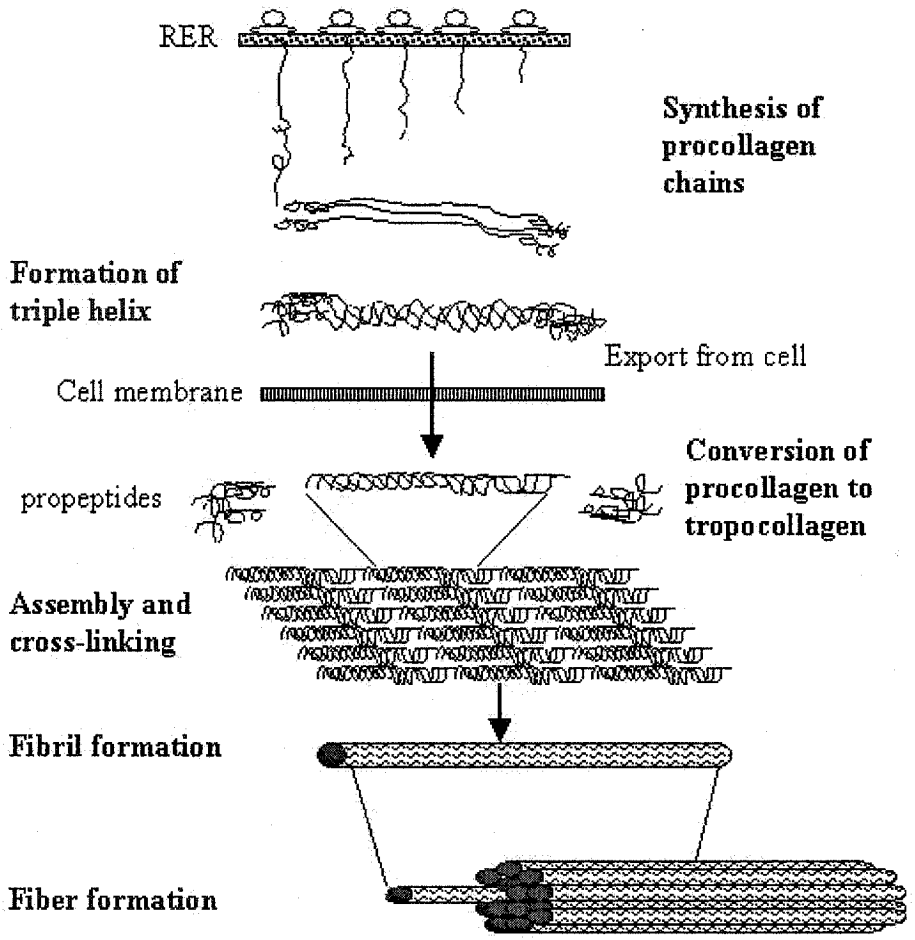

Figure 1-5. Schematic illustrating the process of collagen synthesis and fiber formation. Three procollagen α-chains assemble to form a procollagen molecule containing a triple helix region. Procollagen is then secreted from the cell where enzymatic processing occurs to form tropocollagen. Tropocollagen is assembled and cross-linked to form collagen fibrils, which then associate to form larger collagen fibers (adapted from Culav *et al.*, 1999).

1.5.2 Wound Healing and Fibrosis

1.5.2.1 Normal Wound Healing

Normal wound-healing is a highly ordered and efficient process characterized by distinct but overlapping phases of homeostasis, followed by inflammation, cell proliferation, and finally tissue remodeling (Diegelmann and Evans, 2004). In the inflammatory phase, neutrophils are the first wave of leukocytes to penetrate the wound, followed by macrophages and finally lymphocytes (Witte and Barbul, 1997). An abundance of inflammatory cytokines (e.g. IL-1β and TNF-α) are produced during this phase that prolong the response. The purpose of this initial invasion of activated leukocytes is to rid the area of invading microbes, to activate surrounding cell-types (e.g. via cytokine and growth factor secretion), and to stimulate wound healing. In the proliferative stage, fibroblasts are attracted to the wound by potent chemotactic signals (e.g. PDGF) released at the site, and are stimulated to produce collagen and ECM proteins that aid in closing the wound. Transforming growth factor-β (TGF-β) is important at this stage since it stimulates collagen synthesis by fibroblasts and also dampens the inflammatory response. Epithelial cells and endothelial cells also proliferate during this stage to re-establish a protective barrier and circulation, respectively. In the final stage of wound healing, a wave of apoptosis kills off the collagen-producing fibroblastic cells and the wound healing response is terminated, often leaving permanent scar tissue behind (Gabbiani, 2003).

1.5.2.2 Fibrosis

Fibrosis is a complication of chronic inflammation and develops from an aberrant wound-healing response in the presence of chronic stimuli (Atamas, 2002). Hallmark events in fibrosis are sustained hyper-proliferation of fibroblasts and fibroblast-like cells (e.g. myofibroblasts, smooth muscle cells) with excessive synthesis of collagen by these cells (Atamas, 2002). The result is massive tissue collagen deposition over time, with permanent remodeling of tissue architecture and loss of tissue function (Gabbiani, 2003).

1.6 FIBROSIS IN CROHN'S DISEASE

Fibrosis in CD results from excessive collagen deposition that can occur in any layer of the intestine from the lamina propria to the serosa, in contrast to UC where fibrosis is restricted to the mucosa (Pucilowska *et al.* 2000). The cells responsible for collagen deposition in the inflamed intestine are smooth muscle cells (SMC) and various populations of fibroblasts and myofibroblasts (Lawrance *et al.*, 2001; Powell *et al.*, 1999). Regulation of inflammation-induced fibrosis by cytokines and growth factors is complex. It occurs both indirectly, via attraction and activation of inflammatory cells that sustain the pro-fibrotic inflammatory response, and directly, through stimulation of proliferation and collagen synthesis by fibroblasts and smooth muscle cells (Atamas, 2002; Lawrence *et al.*, 2001). Fibrosis and muscularis overgrowth (due to excessive SMC proliferation) contribute to intestinal stricture formation, a serious complication of CD leading to surgical resection in the majority of CD patients (Farmer *et al.*, 1985; Harper *et*

al., 1987). Progressive loss of intestinal function due to fibrosis occurs in CD despite the use of immunosuppressive and anti-inflammatory agents (Schuppan *et al.*, 2000).

1.7 TNBS-INDUCED COLITIS: A MODEL OF IBD

2,4,6-Trinitrobenzenesulfonic acid (TNBS), shown in figure 1-6, is a hapten molecule that binds to tissue proteins and is capable of stimulating a cell-mediated immune response (Fidler, 1985). When administered into the colon dissolved in ethanol, which deteriorates the protective mucosal barrier, TNBS penetrates the tissue and initiates a mucosal immune response that persists for at least 8 weeks (Morris *et al.*, 1989; Boughton-Smith *et al.*, 1988; Grisham *et al.*, 1991). TNBS-induced colitis is a well-established animal model of IBD that has been reproduced in several species including rat (Morris *et al.*, 1989; Tatsumi and Lichtenberger, 1996; Sykes *et al.*, 1999), rabbit (Homaidan *et al.*, 1999; Depoortere *et al.*, 2000; Depoortere *et al.*, 2001), mouse (Neurath *et al.*, 1995; Neurath *et al.*, 1996a; Maerton *et al.*, 2004), and recently in guinea-pig (Linden *et al.*, 2003; Linden *et al.*, 2004). TNBS elicits an IL-12-driven, T_H1-mediated colitis (Neurath *et al.*, 2000), with many characteristics resembling human Crohn's disease including transmural inflammation and fibrosis, similar ulcer morphology with skip-lesioning, granulomas, similar lymphoid infiltrates, and intestinal crypt distortion (Morris *et al*, 1989; Torres *et al.*, 1999). Colitis in this model has been shown to respond to drugs useful in the treatment of human IBD (Elson *et al.*, 1995).

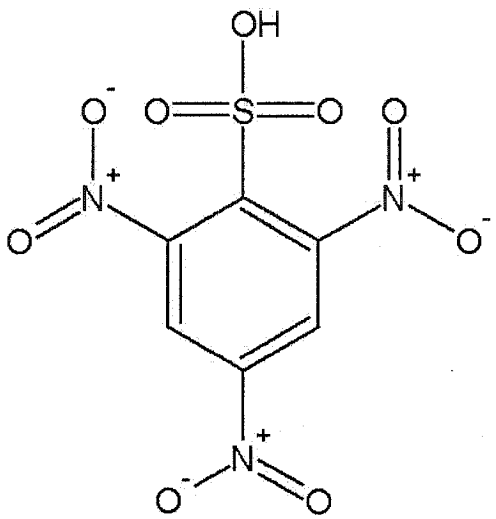

Figure 1-6. Structure of 2,4,6-trinitrobenzenesulfonic acid (TNBS).

1.8 CURRENT TREATMENT OF CROHN'S DISEASE

Treatments available for CD include anti-inflammatory, immunosuppressant, and anti-bacterial agents that target acute symptoms but do little to alter the natural course of the disease or prevent fibrotic complications such as stricture formation (Lawrance *et al.*, 2001). These agents include sulfasalazine and newer 5-aminosalicylic acid (5-ASA) derivatives that are often ineffective and have side effects including paradoxical worsening of colitis (Stein and Hanauer, 2000). Corticosteroids are used in moderate to severe CD but are not appropriate for long-term therapy due to unwanted side effects (Scribano and Prantera, 2003; Feagan, 2003). Immunomodulating agents such as azathioprine, 6-mercaptopurine, and methotrexate have some effect as maintenance therapies, although relapse still occurs, and they are associated with a host of adverse effects including nausea, headache, hypertension, and pancreatitis (Golstein *et al.*, 2004; Stein and Hanauer, 2000; Kim and Lichtenstein, 2004). Anti-bacterial agents such as metronidazole and ciprofloxacin are often used to treat or prevent bacterial overgrowth and invasion (Sartor, 2004; Castiglione *et al.*, 2003).

New biologic agents are now emerging for the treatment of CD and some results have been quite promising. The anti-TNF-α therapy, Infliximab, has shown considerable benefit in the treatment of acute exacerbations of CD in patients refractory to standard treatment, and has also prolonged remission in many cases (Akobeng and Zachos, 2004; D'Haens *et al.*, 2001; Hanauer *et al*, 2002). However, the extreme cost, risk of severe side effects, and unknown long-term effects of anti-TNF-α therapy, currently inhibit its

use in the general CD population. Other biologic therapies are currently being investigated (see Lim *et al.*, 2004 for a review). Recent reviews examining the efficacy and tolerability of treatments currently available for CD indicate that while some progress is being made, there is dire need for improved therapy (Feagan, 2003; Stein and Hanauer, 2000). For instance, there are currently no medicinal treatments aimed at preventing or reversing fibrosis in CD, a complication necessitating surgery in >50% of CD patients (van Assche *et al.*, 2004). An ideal therapy for CD would be effective, safe, inexpensive, and prevent long-term complications of the disease as well as treat acute symptoms.

1.10 PENTOXIFYLLINE

Pentoxifylline (PTX; 1-(5-oxyohexyl)-3,7-dimethylxanthine) is a well-known methylxanthine derivative and non-specific phosphodiesterase (PDE) inhibitor (Ward and Clissold, 1987; Samlaska and Winfield, 1994). It is widely prescribed for the treatment of certain vascular disorders such as intermittent claudication due to its ability to improve blood flow through narrow vessels (Tjon *et al*; 2001; Samlaska and Winfield, 1994). In addition to its effects on the microcirculation, PTX is known to have diverse anti-inflammatory actions, including *in vitro* and *in vivo* inhibition of T_H1 cytokine synthesis (e.g. TNF-α, IL-12, IL-2, and IFN-γ) by various immune cells (Rieneck *et al.*, 1993; Tilg *et al.*, 1993; Bienvenu *et al.*, 1995; Mytar *et al.*, 1995; Rieckmann *et al.*, 1996; Windmeier and Gressner, 1997; Reimund 1997; Wang *et al.*, 1997). A recent study reported that PTX inhibited IL-18 production by cultured splenocytes and macrophages (Samardzic *et al.*, 2001). PTX is reported to inhibit T cell activation, natural killer cell

activity, and neutrophil degranulation (Marks *et al.*, 2001). Many effects of PTX are attributed to elevation of cyclic adenosine monophosphate (cAMP) levels within the cell due to PDE inhibition (Streiter *et al.*, 1988). In general though, PTX is considered to be a weak PDE inhibitor (Ely, 1988; Muller and Lehrach, 1980). Another molecular target of PTX is the transcription factor NF-κB (Jimenez *et al.*, 2001; Chen *et al.*, 2003; Biswaz *et al.*, 1994). Inhibition of NF-κB activation has diverse anti-inflammatory effects including suppression of cytokine gene expression by T cells and other leukocytes.

In addition to its effects on the immune system, results from our lab and others have shown that PTX is a potent anti-fibrogenic compound. PTX inhibits proliferation and collagen synthesis by cultured fibroblasts, myofibroblasts, hepatic stellate cells, renal myofibroblasts, intestinal smooth muscle cells and vascular smooth muscle cells in the presence of various proliferative stimuli (Peterson *et al.*, 1994; Isbrucker and Peterson, 1998; Peterson and Tanton, 1996; Pinzani, 1995; Preaux *et al.*, 1997; Chen *et al.*, 1999; Hewitson *et al.*, 2000). PTX also attenuated fibrosis in animal models of glomerulonephritis (Lin *et al.*, 2002), Peyronie's disease (Valente *et al.*, 2003), and hepatic fibrosis (Peterson and Isbrucker, 1991; Peterson, 1993; Peterson and Neumeister, 1996; Isbrucker and Peterson, 1998). PDGF is a potent mitogen for fibroblasts and has been implicated in the pathology of many fibrotic diseases including liver fibrosis (Peterson and Isbrucker, 1990 and 1992; Gressner, 1992), scleroderma (Raoul *et al.*, 2004), interstitial lung disease (Uebelhoer *et al.*, 1995), and collagenous colitis (Peterson and Huet, 1996; Peterson and Tanton, 1996). PDGF may also play a role in fibrosis associated with CD (Kumagai *et al.*, 2000; Beck and Podolsky, 1999). PTX was recently reported to interrupt PDGF-stimulated fibroblast proliferation by inhibiting

phosphorylation of c-Jun, a component of the AP-1 transcription factor (Peterson *et al.*, 2002). While PDGF stimulated both *c-fos* and *c-jun* expression in this study, inhibitory effects of PTX were selective for *c-jun*.

The combined anti-inflammatory and anti-fibrotic effects of this drug, along with its safety and affordability, make PTX an attractive candidate for treatment of chronic inflammatory diseases like CD. PTX treatment was reported to attenuate intestinal inflammation and damage in experimental colitis (Peterson and Davey 1997; Murthy *et al*, 1999) and reduce intestinal collagen deposition in human collagenous colitis patients (Peterson and Tanton, 1996).

1.11 METABOLITE-1 OF PENTOXIFYLLINE

PTX is metabolized to 7 metabolites in mammals with metabolites 1 and 5 being the major products formed (Smith *et al.*, 1986). Metabolite-1 (M-1; 1-(5-hydroxyhexyl)-3,7-dimethylxanthine) is formed from PTX *in vivo* by the reduction of a single carboxyl group to a corresponding hydroxyl group, forming a chiral center in the molecule (Fig 2-1). The S-enantiomer of M-1 (M-1S) is selectively formed during PTX metabolism *in vivo* and is thought to have biological properties similar to PTX although few studies have examined this (Aviado and Dettlebach, 1984; Crouch and Fletcher, 1992; Ward and Clissold, 1987). We have been investigating the *in vitro* effects of racemic M-1 (R/S) and have shown that it is as effective as PTX in inhibition of PDGF-stimulated human skin fibroblast proliferation (Peterson, 1996) and is more potent than PTX in inhibiting collagen synthesis by PDGF-stimulated porcine hepatic myofibroblasts (Isbrucker and

Peterson, 1995; Isbrucker and Peterson, 1998). These results indicate that M-1 has potential as an anti-fibrogenic agent.

1.12 DRUG INTERACTION WITH CIPROFLOXACIN

An *in vivo* interaction between PTX and the antibiotic ciprofloxacin has been reported in humans that results in elevated serum levels of both PTX and M-1 and improved therapeutic effects of PTX administration (Thompson *et al.*, 1994). We have shown that this interaction can be reproduced in mice (Wornel and Peterson, 1997), and that elevated serum drug levels are not due to down-regulation of the *CYP1A2* gene, but rather to inhibition of the catalytic activity of CYP1A2, a liver enzyme involved in PTX metabolism (Peterson *et al.*, 2004). Since both PTX and M-1 are active compounds, elevated levels of these drugs in mice *in vivo* would likely improve the therapeutic effects of PTX administration, as was the case in humans. A direct interaction between M-1 and ciprofloxacin has not been examined.

1.13 HYPOTHESES AND OBJECTIVES

Proliferation and collagen synthesis by fibroblasts and fibroblast-like cells are hallmark events in fibrosis. We have previously demonstrated that PTX (1-(5-oxyohexyl)-3,7-dimethylxanthine) and its first metabolite, M-1 (1-(5-hydroxyhexyl)-3,7-dimethylxanthine) have potent anti-fibrogenic effects *in vitro* (Isbrucker and Peterson, 1998) and *in vivo* (Peterson, 1993). The first objective of this investigation was to synthesize a racemic M-1 (R/S) by modification of a chemical reduction reaction, and to confirm its anti-fibrogenic effects *in vitro* compared to PTX.

An interaction between PTX and the antibiotic ciprofloxacin has been demonstrated in humans that increases serum levels of PTX and M-1 *in vivo* thereby enhancing the therapeutic effects of PTX (Thompson *et al.*, 1994). We have shown that this interaction can be reproduced in mice (Wornel and Peterson, 1997). A direct interaction between M-1 and ciprofloxacin has not been examined. **HYPOTHESIS 1**: Since M-1 is a methylxanthine derivative, similar in structure to PTX, we predicted that a drug interaction would occur between ciprofloxacin and M-1 *in vivo* resulting in increased serum levels of M-1 and PTX. Since M-1 has never been administered *in vivo*, a preliminary objective was to examine toxicity and kinetics following M-1 injection in mice compared to PTX. Following this preliminary investigation, mice would be pretreated with ciprofloxacin, followed by injection of M-1, and serum drug levels would be analyzed by high performance liquid chromatography (HPLC).

Since PTX and M-1 have both anti-fibrogenic and anti-inflammatory properties, they are attractive candidates for treatment of Crohn's disease (CD). Current treatments

for CD target acute inflammatory symptoms but do little to prevent intestinal fibrosis. A major objective of this investigation was to determine the effects of racemic M-1 on inflammation and fibrosis *in vivo*, compared to the parent drug PTX, using the well-established TNBS rat model of CD. **HYPOTHESIS 2:** Since PTX and M-1 have anti-fibrogenic and anti-inflammatory properties, these compounds will attenuate inflammation and fibrosis in the TNBS model of IBD.

Additional objectives of this investigation were to examine cytokines and signaling molecules in TNBS-induced colitis and fibrosis in order to identify potential therapeutic targets in CD and molecular mechanisms of M-1 effects. IL-18 is a novel pro-inflammatory cytokine recently implicated in human CD. PDGF is a profibrotic cytokine recently implicated in collagenous colitis. **HYPOTHESIS 3**: IL-18 and PDGF levels will be elevated in TNBS-colitis. ELISA and Western analysis, respectively, were performed on colon tissue lysates. In order to identify inflammatory signaling molecules involved in TNBS-colitis, several molecules were assessed by Westerns. **HYPOTHESIS 4:** NF-κB, JNK, and p38 levels will be elevated indicating a role in TNBS-colitis. Many cytokines elevated in human CD activate NF-κB (e.g. IL-18, TNF-α, IL-1β) and PTX is known to block activation of NF-κB *in vitro* and *in vivo*. We investigated the effect of M-1 on NF-κB activation *in vitro* since this has not been examined. An experimental M-1R compound was recently reported not to block NF-κB activation. **HYPOTHESIS 5**: Since the R-enantiomer of M-1 has previously been reported not to block NF-κB activation, we predicted that racemic M-1 would not block activation of NF-κB *in vitro*. However, the effects of M-1S on NF-κB activation have not been examined, making this a novel molecular investigation.

Chapter 2

MATERIALS AND METHODS

2.1 CHEMICALS AND REAGENTS

Sigma (Oakville, ON, Canada)

hexadecyltrimethylammonium bromide (HETAB), *o*-dianisidine, BSA, ascorbic acid, pentoxifylline, 1M TNBS, collagenase, Sigma blend collagenase, pronase, Triton X-100, HEPES, DTT, hematoxylin, eosin, pepsin, AEC, PMSF, aprotinin, sodium orthovanadate, phosphatase inhibitor cocktail I, EDTA, Tween-20, diaminobenzidine (DAB), Igepal CA 630, sodium deoxycholate, PLP, 2-mercaptoethanol, bovine insulin, bromophenol blue

BDH Inc. (Toronto, ON, Canada)

Sirius Red, Fast Green, HCl, methiolate, glycerol, NaOH, tannic acid, 2-propanolol, sodium bicarbonate, formaldehyde solution, diethyl ether, picric acid, sodium phosphate heptahydrate, sodium phosphate dihydrate (monobasic), potassium phosphate monobasic, glycine

Fisher (Ottawa, ON, Canada)

KCl, TCA, sodium acetate, paraformaldehyde, formaldehyde solution, HPLC-grade methanol, acetonitrile, sodium borohydride, dichloromethane

ICN Biomedicals Inc. (Montreal, QC, Canada)

Tris-HCl, Tris Base, phenacetin

Gibco/Invitrogen (Ontario, Canada)

FBS, bovine insulin, antibiotic/antimycotic (A/A), trypsin EDTA, goat serum, high glucose Dulbecco's Modified Eagle's Medium

BioRad (Hercules, CA, USA)

Pre-stained kaleidoscope molecular weight ladder, biotinylated molecular weight ladder, pre-cast (7.5%, 10%, 15%, 4-20%) polyacrylamide Tris-HCl gels, PVDF membrane

Miscellaneous Suppliers

Tritiated [^{3}H]-thymidine and Hyperfilm ECL (Amersham Biosciences, Baie d'Urfe, QC, Canada), tritiated [^{3}H]-proline (Perkin Elmer), somnotol (sodium pentobarbital, MTC Pharmaceuticals, Cambridge, ON, Canada), heparin (Leo Pharma Inc., Thornhill, ON, Canada), ciprofloxacin (Cipro IV®, Bayer), isofluorane (Aerrane, Baxter), rat IL-18 ELISA Kit (Medicorp, Biosource Int distributor, Toronto, ON), skim milk powder (Carnation), enhanced chemiluminescence kit (Cell Signaling Technology, Maine, USA)

2.2 CYTOKINES

Recombinant human platelet derived growth factor (rhPDGF), recombinant rat interleukin-18 (rrIL-18), recombinant rat inteleukin-1β (rrIL-1β), recombinant rat tumor necrosis factor-α (rrTNF-α) were purchased from Cedar Lane Laboratories (Hornby, ON, Canada).

2.3 ANTIBODIES

2.3.1 Primary Antibodies

The following primary antibodies were purchased from Santa Cruz Biotechnology (Santa Cruz, CA, USA): rabbit anti-NF-κBp65 polyclonal, mouse anti-phospho-ATF-2 polyclonal, mouse anti-JNK1 monoclonal, mouse anti-phospho-JNK monoclonal, rabbit anti-β-tubulin polyclonal, goat anti-collagen I (α1) polyclonal, and goat anti-collagen III (α1) polyclonal, rabbit anti-PDGF-B polyclonal, rabbit anti-TGF-β1 polyclonal. Rabbit anti-p38 polyclonal and rabbit anti-phospho-p38 polyclonal were purchased from Cell Signaling Technology (Maine, USA)

2.3.2 Secondary Antibodies

Secondary antibodies purchased from Sigma were rabbit anti-goat IgG peroxidase conjugate and goat anti-mouse IgG peroxidase conjugate. HRP-linked anti-rabbit IgG and HRP-linked anti-biotin antibody were purchased from Cell Signaling Technology. The anti-biotin antibody was used to visualize the biotinylated molecular weight marker (BioRad, Hercules, CA, USA). LSAB II kit containing biotinylated anti-mouse/anti-rabbit IgG solution and streptavidin-HRP solution was purchased from DAKO (Germany).

2.4 CELL CULTURES

Normal rat small intestinal epithelial cells (IEC-6) and mouse embryonic fibroblasts (3T3) were purchased from ATCC. Human dermal fibroblasts (F8s) are a normal skin fibroblast cell line that was established in our lab.

2.5 ANIMALS

Male CD1 mice (25 g), male C57BL/6 mice (25 g) and female Sprague-Dawley rats (125-150 g) were purchased from Charles River Laboratories, QC, Canada.

2.6 SYNTHESIS OF THE METABOLITE

2.6.1 Chemical Synthesis of Metabolite-1 from Pentoxifylline

Metabolite-1 is a chiral molecule derived from PTX by the reduction of a single ketone functional group to a hydroxyl group (Fig 2-1). A racemic mixture of metabolite-1 was synthesized from PTX in a chemical reduction reaction carried out in the Department of Chemistry at Dalhousie University with the assistance of Dr. Jim Pincock. PTX (10 g) was dissolved in HPLC-grade methanol (500 ml) and sodium borohydride ($NaBH_4$; 1.8 g) was slowly added as the reducing agent. The reaction proceeded for 1 hour at room temperature with constant stirring and the methanol was evaporated using a rotary evaporator. The crude product was dissolved in 150 mL of distilled water (dH_20) and was

extracted four times using dichloromethane (4 x 100 mL CH_2Cl_2). The original protocol developed in 1996 used only two extractions with a recovery of less than 50 %. Four extractions were employed here to increase recovery of product. A powdered drying agent (Na_2SO_4) was added to the organic phase to absorb water and the solution was gravity filtered. The remaining organic solvent (CH_2Cl_2) was evaporated leaving a powdered compound (M-1) behind. This product was recrystallized from 2-propanol overnight at 4 °C, dried by suction filtration the following day, and was allowed to air dry for several days before use. A yield greater than 80 % was consistently achieved with this method.

2.6.2 Identification of the Metabolite

The product was identified as M-1 by proton nuclear magnetic resonance spectroscopy (^{1}H-NMR). NMR spectrographs for PTX and M-1 were obtained and assessed by Dr. Jim Pincock in the department of chemistry (Figure 3-1).

PENTOXIFYLLINE

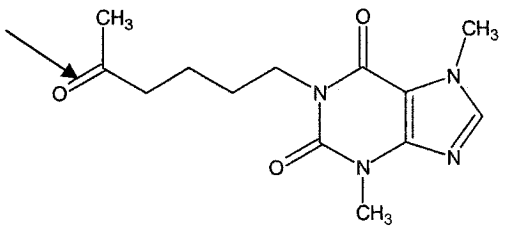

METABOLITE-1S

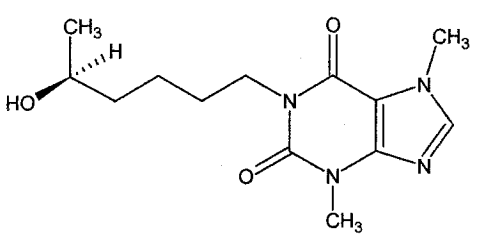

METABOLITE-1R

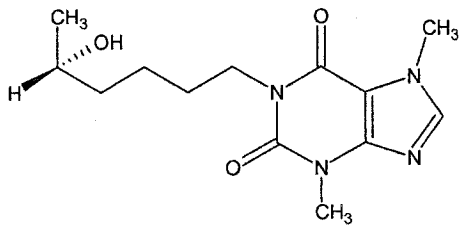

Figure 2-1. Structures of pentoxifylline and its major metabolite (M-1). M-1 is formed from the reduction of a carboxyl group (C=O) on the PTX molecule (arrow) to a corresponding hydroxyl group (-OH), forming a chiral center in the metabolite. The different spatial orientations of the hydroxyl group around the chiral carbon atom of M-1 give rise to the two enantiomers of the molecule (M-1S and M-1R). The S-enantiomer is the major metabolite formed *in vivo* during PTX metabolism.
[dark wedge = out of the plane of the page; dashed wedge = into the plane of the page]

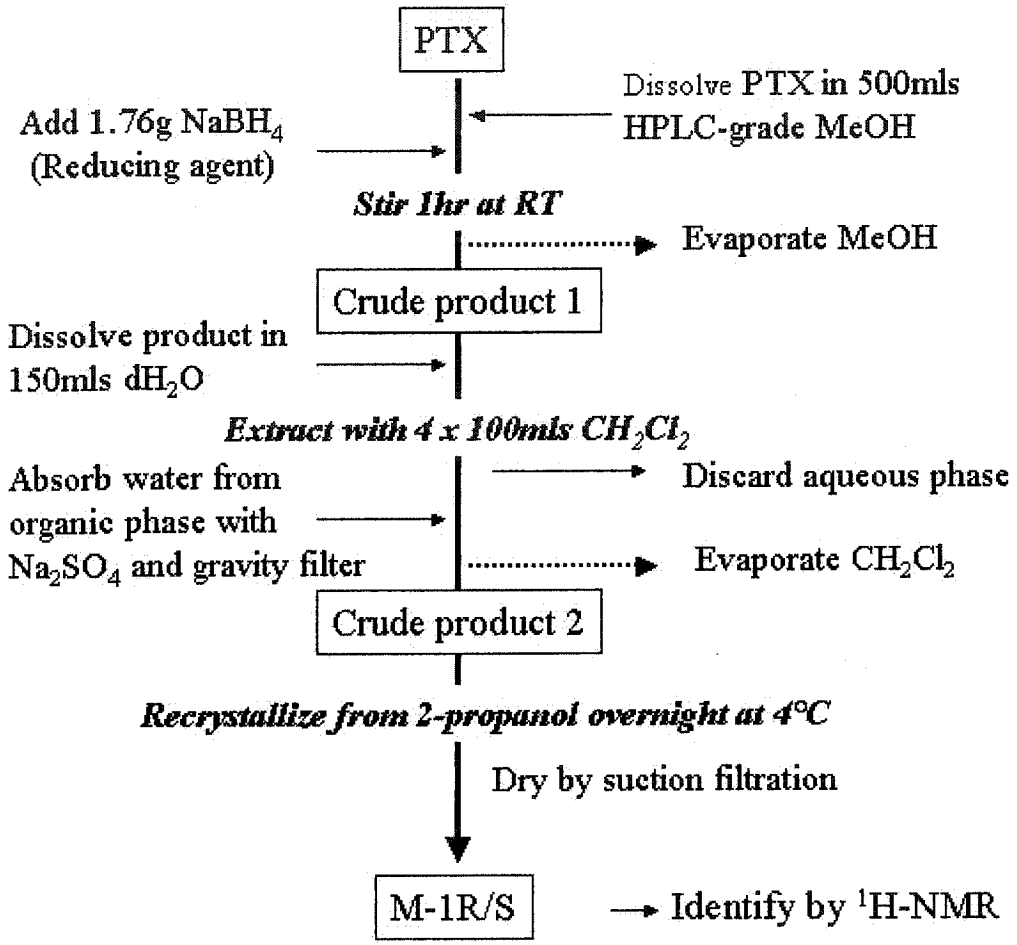

Figure 2-2. Flowchart illustrating the synthesis of M-1 from PTX. A racemic mixture of metabolite-1 (M-1R/S) was synthesized from pentoxifylline (PTX) using sodium borohydride as the reducing agent.

2.7 INITIAL CHARACTERIZATION OF M-1 IN VITRO

2.7.1 Maintenance of Cell Cultures

Human skin fibroblasts (F8) and mouse fibroblasts (3T3) were maintained in 75 mm^2 tissue culture flasks (VWR) in a humidified incubator (Sanyo CO_2 incubator) at 37 °C with 5%CO_2/ 95% O_2. Culture media was Dulbecco's Modified Eagle's Medium (DMEM) containing glucose (4.5 g/L), L-glutamine (4 mM), supplemented with 1% antibiotic/antimycotic (1 % A/A), 1-5 % FBS and sodium bicarbonate (1.75 g/L). Rat intestinal epithelial cell (IEC-6) media was DMEM supplemented with sodium bicarbonate (1.5 g/L), bovine insulin (0.1 units/mL), 10 % FBS, and 1 % A/A.

Culture media was replaced twice per week and cells were subcultured weekly using 0.5 % trypsin with 0.53 mM sodium EDTA (10 mls). Trypsinized cells were mixed with culture media containing 10 % FBS (10 mls) and cells were pelleted by centrifugation at 3100 rpm for 10 min at 4 °C. Trypsin and media were removed and cell pellet was resuspended in fresh media (10 mls). Cells were seeded into fresh 75 mm^2 flasks at a subculture ratio of approximately 1:6 (2 mls cell suspension plus 10 mls fresh culture media).

2.7.2 Assessment of *in vitro* cell proliferation

Since fibroblast proliferation is a key event in fibrosis, fibroproliferation in response to fibrogenic stimuli serves as an *in vitro* model of fibrosis. Proliferation of cultured fibroblasts was measured using a modification of the tritiated [^{3}H]-thymidine incorporation assay (Dohlman *et al.*, 1984; Peterson and Isbrucker, 1992). Fibroblasts were lifted with 0.5 % trypsin with 0.53 mM EDTA (10 mls) and the resulting cell suspension was combined with culture media containing 10 % FBS and 1 % A/A (15 mls). This cell suspension was centrifuged for 10 min at 3100 rpm at 4 °C. The supernatant was removed and the cell pellet was resuspended in culture media containing 5 % FBS. Cell density was counted using a hemocytometer and the suspension was diluted to 40,000 cells/ml in culture media. Cells were seeded into the inner 60 wells of a 96-well microtiter plate (VWR) in 200 µL aliquots (8000 cells/well). Plates were incubated for 24 hrs at 37 °C in a tissue culture incubator with 5 % CO_2/95 % O_2. The media was removed and replaced with 100 µL of media containing 1 % FBS and cells were incubated for 24 hrs.

Media was removed and replaced with 100 µL of fresh media supplemented with growth factors in the presence and absence of PTX and M-1 (section 2.7.3), and cells were incubated for 22 hrs. Tritiated [^{3}H]-thymidine (0.5 µCi; Amersham Biosciences) was added to each well and cells were incubated for 2 hrs. Proliferating cells uptake radioactive thymidine from the culture media that is incorporated into newly synthesized DNA. Following the 2 hr incubation, cells were briefly exposed to trypsin and harvested

by aspiration onto glass fiber filters using a Brandel Cell Harvester (Xymotech Biosystems). Radioactivity was measured using a scintillation counter and results were expressed in radioactive counts per minute (cpm) per 8000 cells plated. All treatments were tested in quadruplicate.

2.7.3 Assessment of M-1 and PTX Effects on Platelet-derived Growth Factor (PDGF)-stimulated Fibroproliferation

Human skin fibroblasts (F8s) were first treated with increasing concentrations of PDGF (4-64 ng/mL) in order to determine the optimal concentration of cytokine to use in further experiments. F8 cells were then treated with PDGF (8 ng/mL) in the presence of a range of concentrations of PTX and M-1 (240-1900 μM).

2.7.4 Assessment of Potency between Batches of M-1

A proliferation assay was performed to compare the potency of two batches of M-1 synthesized during the course of this project. Inhibition of PDGF-stimulated fibroproliferation was the parameter assessed. These batches of M-1 (synthesized in 2000 and 2003, respectively) were compared to the parent compound (PTX) and a batch of M-1 produced in 1996 by a previous student. F8 cells were exposed to treatment with PDGF (16 ng/ml) in the presence of three doses of PTX and M-1 (240, 950, 1900 μM).

2.7.5 Assessment of *in vitro* collagen synthesis by fibroblasts

Collagen synthesis by cultured fibroblasts was measured using a modification of the [^{3}H]-proline incorporation assay (Diegleman *et al.*, 1990). Cultured fibroblasts were briefly exposed to 0.5 % trypsin with 0.53 mM EDTA (10 mls) and the resulting cell suspension was added to DMEM containing 10 % FBS and 1 % A/A (15 mls). This cell suspension was centrifuged for 10 min at 3100 rpm at 4 °C. The supernatant was removed and the cell pellet was resuspended in DMEM + 10 % FBS + 1 % A/A. Cell number was counted using a hemocytometer and the suspension was diluted to 40,000 cells/ml and seeded into a 24-well plate in 1 mL aliquots (40,000 cells/well). Cell monolayers were grown to confluence to eliminate growth-related events. Confluent cells were treated with fibrogenic factors in the presence and absence of PTX and M-1 (section 2.7.6), supplemented with tritiated [^{3}H]-proline (1 μCi; Amersham Biosciences) and ascorbic acid (4 μg/well) in a total volume of 500 μL per well. Cells were incubated for 48 hrs in a tissue culture incubator with 5 % CO_2/ 95 % O_2. Collagen is a proline-rich molecule and cells incorporate tritiated [^{3}H]-proline from the culture media for new protein synthesis. Following this 48-hr incubation, EDTA (20 μL; 0.5 M; pH 8.0) was added to each well and the 24-well plate could be frozen at –20 °C until the continuation of the assay.

The plate was thawed and the contents of each well were sonicated for 20 seconds and transferred to 1.5 mL Eppendorf tubes. Cold 100 % TCA (50 μL) was added to each

tube to precipitate protein and tubes were incubated at 4 °C for 1 hr. Tubes were centrifuged at 2500 rpm for 10 minutes and supernatants were discarded. The pellet was resuspended in cold 10 % TCA (1 ml) and tubes were incubated at 4 °C for 1 hr. Tubes were centrifuged as above and supernatants were discarded. Pellets were resuspended in ice-cold ethanol/ether (3:1) (1ml) and incubated at –20 °C overnight. Tubes were centrifuged as above and supernatants were discarded. Pellets were resuspended in cold ethanol/ether (3:1) (1 ml) and placed in the freezer for 1 hr, after which tubes were centrifuged as above and supernatants were discarded. The ethanol/ether was allowed to evaporate in a fumehood.

Dry pellets were resuspended in collagenase solution (200 μL of 2 mg/ml Sigma blend collagenase in 50 mM Tris, 5 mM $CaCl_2$, pH 7.6) and incubated at 37 °C for 90 minutes in a shaking water bath to solubilize collagenous protein. Two hundred microliters of 10 % TCA/5 % Tannic Acid was added and tubes were incubated on ice for 1 hr to allow separation of collagenous and non-collagenous protein. Non-collagenous protein was pelleted by centrifugation and supernatant containing acid-soluble collagenous protein was transferred to scintillation vials. Pellets were resuspended in another 200 μL of TCA/Tannic Acid and tubes were incubated on ice for 10 min before centrifugation. Supernatants were added to the original scintillation vials. Non-collagenous protein pellets were dissolved in 1 N NaOH (200 μL) and transferred to a second set of scintillation vials. Tubes were washed with another 200 μL of NaOH and this was added to the second set of scintillation vials. Radioactivity in collagenous and non-collagenous fractions was determined using a scintillation counter and results were

expressed in radioactive counts per minute (cpm) per 40,000 cells plated. All treatments were tested in quadruplicate.

2.7.6 Assessment of M-1 and PTX Effects on PDGF-stimulated Collagen Synthesis

Confluent human skin fibroblasts (F8s) were treated with increasing concentrations of PDGF (4-64 ng/ml) in order to determine the optimal concentration of cytokine to use in further collagen assays. F8 cells were then treated with PDGF (32 ng/ml) in the presence of a low and high dose of PTX and M-1 (240 and 1900 μM).

2.8 INITIAL CHARACTERIZATION OF M-1 IN VIVO

2.8.1 Assessment of M-1 Toxicity *in vivo*

Five C57BL/6 mice were injected with M-1 (32 mg/kg i.p.) in 0.9 % saline and were monitored for signs of toxicity for 20 minutes. Signs of toxicity include lethargy, hypersalivation, and dizziness (rotating head motion). At 20 minutes post-injection, the animals were euthanized with 0.05 mL somnotol (i.p.) and blood was collected by cardiac puncture for serum analysis by HPLC. Serum analysis gave an initial indication of M-1 levels (μg/mL) in serum following administration by this route and conversion of M-1 to PTX *in vivo*. A second group of mice were then injected with M-1 (100 mg/kg i.p.) and the same procedure was followed.

2.8.2 Kinetics of M-1 and PTX *In Vivo*

Male CD1 mice (Charles River Laboratories) were injected with heparin (1000 units/kg i.p.) to prevent blood from clotting during the procedure. After 40 minutes, animals received an injection of either PTX or M-1 (100 mg/kg i.p.). Each animal was placed in a plastic 50 ml tube with the tail protruding from a hole in the cap of the tube. Tubes were perforated to allow airflow and cotton gauze was placed inside for comfort. Blood samples (~50 μL) were collected at 5, 10, 15, 25, 40, 60, and 120 minutes post-injection from small puncture at the tip of the tail. Animals did not appear bothered by this procedure. Animals were returned to their cages between the last two timepoints so each animal spent approximately 1 hour in the restraining apparatus. Blood was centrifuged and serum was collected for HPLC analysis (section 2.10).

2.9 INTERACTION OF M-1 AND PTX WITH CIPROFLOXACIN IN VIVO

2.9.1 Animal Maintenance and Ethical Approval

Male CD1 mice weighing approximately 25 g were obtained from Charles River Laboratories and maintained in the Carlton Animal Care Facility at Dalhousie University. Animals were housed 6 per cage with a 12-hour light/dark cycle and *ad libitum* access to water and standard chow. Animals were given one week to acclimatize to the facility

before experimentation began. The experimental protocol was approved by the University Committee on the use of Laboratory Animals at Dalhousie University.

2.9.2 *In Vivo* Interaction with Ciprofloxacin: Experimental Protocol

Combination of ciprofloxacin and PTX *in vivo* is reported to elevate serum levels of PTX in humans with increased formation of the rare R-enantiomer of M-1, which is not generally produced during PTX metabolism (Thompson et al., 1994). A direct interaction between ciprofloxacin and M-1 has never been investigated. In order to assess the interaction of ciprofloxacin with PTX and the novel M-1 in mice, animals were first divided into two groups of 15. One group received daily injections of the antibiotic ciprofloxacin (25 mg/kg i.p.) for 9 days while the control group received daily injections of sterile 0.9 % saline solution. On the ninth day, 5 animals from each group received an injection of PTX (100 mg/kg i.p.), 5 animals received an injection of M-1 (100 mg/kg i.p.), and the remaining animals received an equivalent volume of saline (~200 μL). Table 2-1 gives a summary of the treatment groups. Animals were sacrificed at 30-minutes post-injection, a time determined from the kinetics experiment to capture drug levels at a point in the α-elimination phase of the curve. This ensured that both drugs were beyond their peak in absorbance by the i.p. route. Blood was collected by cardiac puncture for serum analysis by HPLC (section 2.10).

A preliminary experiment was also performed in female Sprague-Dawley rats (125-150 g) examining the effect of ciprofloxacin pre-treatment (25 mg/kg i.p. 9 days) on serum levels of PTX following PTX injection (32 mg/kg i.p.) or enema (64 mg/kg i.c.).

Table 2-1. TREATMENT GROUPS IN CIPROFLOXACIN EXPERIMENT

DAY 1-9	*DAY 9*	*N (mice)*
Saline (i.p.)	Saline (i.p.)	5
Saline (i.p.)	PTX (100 mg/kg i.p.)	5
Saline (i.p.)	M-1 (100 mg/kg i.p.)	5
Cipro® (25 mg/kg i.p.)	Saline (i.p.)	5
Cipro® (25 mg/kg i.p.)	PTX (100 mg/kg i.p.)	5
Cipro® (25 mg/kg i.p.)	M-1 (100 mg/kg i.p.)	5

2.10 HIGH PERFORMANCE LIQUID CHROMATOGRAPHY (HPLC)

2.10.1 Preparation of Standards and Samples for HPLC Analysis

Serum drug levels were measured using routine reverse-phase HPLC methods (Hodgson and Peterson, 1995; Blanchard and Peterson, 1999) and comparing samples of unknown drug concentration to standard curves prepared using a range of known concentrations of PTX and M-1 (final concentration 1-15 μg/ml). A stock solution of each drug was made at a concentration of 1mg/ml in Millipore water (mH_20). Standards were prepared by dilution with mH_20 to 10 times (10X) the final concentration in a total of 1ml (range 10 – 150 μg/ml). Each 10X standard was then diluted to 1X by addition of 10 μL of standard to 90 μL of control serum from an untreated animal. For animals treated with PTX or M-1 *in vivo*, 10 μL of serum was used for HPLC sample preparation and the serum drug concentrations obtained were multiplied by a factor of 10. Phenacetin (30 μg/ml) was added to all standards and samples as an internal control. Phenacetin was used because it has a retention time similar to PTX and can be visualized on the same HPLC chromatogram.

Samples and standards were prepared for HPLC analysis by extraction through 1 ml C-18 Solid Phase Extraction cartridges (JT Baker) that were placed into 13mm x 100mm glass test tubes. Cartridges were washed twice with HLPC-grade methanol (1 ml) by pipetting the methanol into cartridges and centrifuging the test tubes at 3100 rpm for 2.5 min at 4 °C. During centrifugation, liquid passes through the C-18 extraction cartridge into the tube below. Cartridges were then washed twice with Millipore water (1

ml) by the same procedure. Cartridges were transferred to clean labeled tubes and 10 μL of sample or 100 μL of drug standard were added along with 100 μL of phenacetin (30 μg/ml), the internal standard. Tubes were centrifuged at 3100 rpm for 2.5 min at 4 °C. At this point, drugs are retained in the extraction cartridge while the liquid passes through. The cartridges were washed twice with Millipore water (1 ml) to remove impurities and cartridges were again transferred to clean labeled tubes. Products trapped in the cartridge were eluted three times with HPLC-grade methanol (1 ml) and the methanol was subsequently evaporated using a nitrogen evaporator. Dried samples can be stored for extended periods at 4 °C until HPLC analysis.

2.10.2 HPLC Analysis of Standards and Samples

Dried samples were dissolved in HPLC mobile phase (100μL; 75 % mH_20: 25 % acetonitrile) and 10 μL was injected into the HPLC injection port using a glass syringe. The HPLC instrument used was Beckman System Gold consisting of an Analogue Interface Module 406 coupled to a UV detector Module 166 and Programmable Solvent Module 126. The stationary phase used was a C-18 column (250 mm length, I.D. 4.6 mm; Econosource) and the flow rate was set at 1 ml/min with a run-time of 15 minutes. As samples are passed through the hydrophobic C-18 column, they are eluted based on size and charge where smaller charged compounds are retained for shorter periods than larger hydrophobic compounds. Retention times for PTX and M-1 were determined by analyzing samples of the pure compounds. HPLC printouts were obtained containing a chromatograph and relevant data for each sample, including retention times, peak height

and peak area. The ratio of the area under the drug peak to the area under the phenacetin peak (peak $area_{drug}$/peak $area_{phen}$) was used to construct a standard curve, with drug concentration (μg/ml) on the x-axis and peak area ratio (peak $area_{drug}$/peak $area_{phen}$) on the y-axis. Serum drug levels from treated animals were determined by calculating peak $area_{drug}$/peak $area_{phen}$ for each sample and comparing to the standard curves (x = y-b/m).

2.11 EFFECTS OF M-1 AND PTX IN TNBS-INDUCED COLITIS

2.11.1 Animal Model of Inflammatory Bowel Disease

TNBS (2,4,6-trinitrobenzenesulfonic acid) is a hapten molecule that penetrates the colonic mucosa and initiates a sustained immune response resulting in colitis with many features of human CD (Neurath *et al.,* 2000) (see section 1.7). TNBS-induced colitis is a well-established model of IBD that has been reproduced in several species including rabbit, rat, and mouse (Morris *et al.*, 1989). This model has been shown to respond to drugs useful in the treatment of human IBD (Elson *et al.*, 1995) and is therefore an appropriate model to examine the effects of PTX and M-1 in colitis.

2.11.2 Animal Maintenance and Ethical Approval

Virgin female Sprague-Dawley rats weighing 125-150 g upon arrival from Charles River Laboratories were maintained in the Carlton Animal Care Facility at Dalhousie University. Animals were housed 2-3 per cage with a 12-hour light/dark cycle

and access to food and water *ad libitum*. Animals were given one week to acclimatize to the facility before experimentation began. The experimental protocol was approved by the University Committee on the use of Laboratory Animals at Dalhousie University.

2.11.3 *In Vivo* Response to Various Doses of TNBS

An experiment was performed to determine a dose of TNBS that would result in sufficient reproducible colitis. TNBS was administered intracolonically (i.c.) at four different doses (15 - 25 mg/rat) dissolved in 50 % EtOH in a total volume of 250 μL per rat (Table 2-2). There were 4 animals in each group. One extra rat received an intermediate dose of 17.5 mg TNBS. A catheter was created using 7 cm of flexible polyethylene tubing (Intramedic® PE 205 O.D. 2.08 mm, VWR, Mississauga, ON, Canada) attached to a 16 gauge needle and 1 cc syringe. The catheter was inserted 6 cm into the lumen of the colon, to a point just distal to the splenic flexure, where the TNBS solution was ejected. This solution was retained in the colon for five minutes while the animal was maintained under light gas anesthetic with the hind end slightly raised. Animals were allowed to recover and were returned to their cages. Controls animals received 250 μL of sterile 0.9 % saline by the same procedure. Animals were to be sacrificed 14 days after TNBS administration. Colons were removed, weighed, and assessed for morphological damage according to a well-established scale (section 2.11.6).

Table 2-2. TREATMENT GROUPS IN TNBS DOSE-RESPONSE EXPERIMENT

TNBS Dose (mg/rat)	*Volume(μL)*	*n*	*Duration (days)*
0	250	4	14
15	250	4	14
17.5	250	1	14
20	250	4	14
25	250	4	14

2.11.4 TNBS-Induced Colitis Experiments: Series I - III

TNBS (90 mg/kg; ~12.5-15 mg/rat) was chosen based on the previous experiment (section 2.11.2). On Day 0, colitis was induced in female Sprague-Dawley rats via intracolonic administration of TNBS from a stock solution (60 mg/ml) in 50 % ethanol (v/v) for a total volume of ~250 μL/rat. Three separate series of experiments were performed to determine the effects of M-1 and PTX in TNBS-induced colitis.

In series I and II, treatment did not begin until 72 hours post-TNBS to ensure development of a strong response to the TNBS. Rats were randomly allocated into groups on Day 3 and treatments were administered twice daily (bid) from days 3-14. PTX and M-1 were dissolved in sterile 0.9 % saline and administered by injection (32 mg/kg i.p. bid) in the first series of experiments (Table 2-3). In the second series (Table 2-4), drugs or saline were administered by enema (64 mg/kg i.c. bid) using a 4 cm polyethylene catheter as described above for TNBS administration (section 2.11.3). Treatments given by enema were retained in the colon for five minutes while the animal was maintained under light anesthetic with the hind end slightly raised. Additional control groups assessing the effect of PTX and M-1 in non-colitic rats were also included in series II.

A third series of experiments using the same basic TNBS protocol examined the effects of M-1 and PTX when drug treatment by enema began 1-hour post-TNBS administration (Table 2-5). Treatments were administered from days 0-14 in these experiments.

Controls underwent the same procedures as experimental groups but received an equivalent volume of sterile 0.9 % saline instead of drug. The experiments were

terminated at day 14 post-TNBS. This treatment period was chosen because previous data indicated that microscopic and macroscopic injury was still present 14 days after TNBS while spontaneous healing was minimal (Peterson *et al.*, 2000).

Animals were euthanized on day 14 by intraperitoneal injection of 0.2-0.4 ml of somnotol. The chest cavity was opened and blood was collected by cardiac puncture for serum analysis. The abdominal cavity was then opened and the distal 6 cm of colon was carefully excised and opened longitudinally. Fecal matter was gently removed and the colon was weighed and scored for macroscopic damage (section 2.11.5). Two thin longitudinal strips were cut for myeloperoxidase assay (section 2.11.6): one at the site of damage and/or healing (generally between 2-4 cm from anus) and one from an adjacent site (usually 4-6 cm from anus). One strip (spanning 1-4 cm from anus) was cut for ELISA (section 2.14.1) and one strip (spanning 0.5-6 cm from anus) was cut for Western analysis (section 2.15.1). These tissue segments were stored in liquid nitrogen until further analysis. The remainder of the colon was rolled longitudinally with the distal end (anus) in the center of the roll. The roll was secured with suture thread and fixed in 4 % paraformaldehyde for histological processing (Figure 2-3).

Additional rats were administered TNBS (90 mg/kg) and were sacrificed at earlier timepoints (4 hrs, 12 hrs, 3 days, 7 days) in order to assess changes in IL-18, colon weight, MPO, and damage score, over time in TNBS-induced colitis. These values were then compared to values obtained at 14 days post-TNBS. Groups received saline enemas beginning either 1 or 72 hours after TNBS for comparison with series II and III.

Table 2-3. TREATMENT GROUPS IN TNBS-INDUCED COLITIS EXPERIMENTS: SERIES I

Treatment Groups	*Colitis induction (Day 0)*	*Treatment (Days 3-14)*
Control Group		
Saline/Saline (n=5)	Saline (i.c.)	Saline (i.p. bid)
Experimental Groups		
TNBS/Sal (n=5)	TNBS (i.c. 90 mg/kg)	Saline (i.p. bid)
TNBS/PTX (n=5)	TNBS (i.c. 90 mg/kg)	PTX (i.p. 32 mg/kg bid)
TNBS/M-1 (n=5)	TNBS (i.c. 90 mg/kg)	M-1 (i.p. 32 mg/kg bid)

Table 2-4. TREATMENT GROUPS IN TNBS-INDUCED COLITIS EXPERIMENTS: SERIES II

Treatment Groups	*Colitis induction (Day 0)*	*Treatments (Days 3-14)*
Control Groups		
Saline/Saline (n=4)	Saline (i.c.)	Saline (i.c. bid)
Saline/PTX (n=4)	Saline (i.c.)	PTX (i.c. 64 mg/kg bid)
Saline/M-1 (n=4)	Saline (i.c.)	M-1 (i.c. 64 mg/kg bid)
Experimental Groups		
TNBS/Sal (n=4)	TNBS (i.c. 90 mg.kg)	Saline (i.c. bid)
TNBS/PTX (n=4)	TNBS (i.c. 90 mg/kg)	PTX (i.c. 64 mg/kg bid)
TNBS/M-1 (n=4)	TNBS (i.c. 90 mg.kg)	M-1 (i.c. 64 mg/kg bid)

Table 2-5. TREATMENT GROUPS IN TNBS-INDUCED COLITIS EXPERIMENTS: SERIES III

Treatment Groups	*Colitis induction (Day 0)*	*Treatment (Days 0-14)*
Control Group		
Saline/Saline (n=4)	Saline (i.c.)	Saline (i.c. bid)
Experimental Groups		
TNBS/Sal (n=4)	TNBS (i.c. 90 mg/kg)	Saline (i.c. bid)
TNBS/PTX (n=4)	TNBS (i.c. 90 mg/kg)	PTX (i.c. 64 mg/kg bid)
TNBS/M-1 (n=4)	TNBS (i.c. 90 mg/kg)	M-1 (i.c. 64 mg/kg bid)

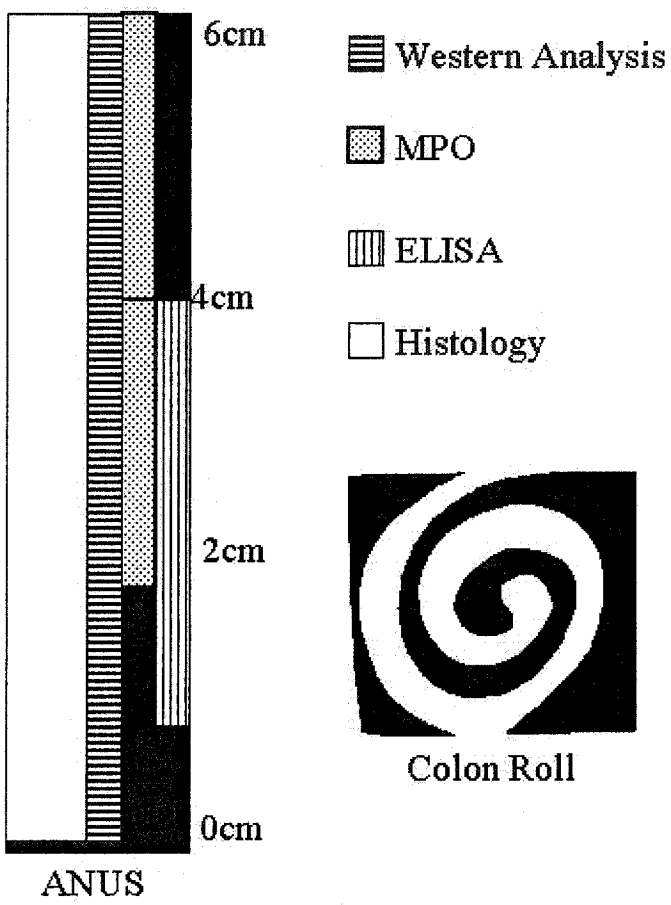

Figure 2-3. Schematic illustrating the preparation of rat colon tissue for analysis. One strip (0.5-6 cm) was frozen in LN_2 for Western analysis, two shorter strips (2-4 cm, 4-6 cm) were frozen for MPO analysis, one strip (1-4 cm) was frozen for ELISA, and the remainder of the colon (white rectangle) was rolled with the distal end in the center, as shown in the cartoon of the colon roll. This roll was secured with suture thread and fixed in 4 % PFA for histological processing.

2.11.5 Macroscopic Rating of Colon Damage

The mucosal surface of the distal 6 cm of rat colon was scored for macroscopic damage according to a scale developed by Wallace and colleagues (1992). The scale takes into account the presence or absence of hyperemia, ulceration, adhesions, and diarrhea (Fig 2- 4). This is a well-established scoring system that has previously been used to assess colon damage in our laboratory (Peterson *et al*, 2000).

2.11.6 Myeloperoxidase Enzyme Activity Assay

Myeloperoxidase (MPO) is an enzyme located predominantly in the intracellular primary granules of neutrophils. Assessing MPO activity in the colon gives an estimate of neutrophil infiltration into the tissue and can be used as a measure of inflammation. This assay was a modification of previously described methods (Bradley *et al.*, 1982; Wallace *et al.*, 1987). Longitudinal strips of colon tissue measuring approximately 2 cm in length were removed from liquid nitrogen storage and weighed using an analytical scale. These colon segments were cut from regions containing evidence of macroscopic damage, which generally occurs between 2-4 cm from the anus (Fig 2-3). In the event that the damage occurred at a site higher or lower than this region, a 2 cm strip was cut from the damaged region and used for MPO analysis. A second strip containing uninvolved tissue was often cut and could be used for comparison.

FEATURE	SCORE
Ulceration	
Normal appearance	1
Focal hyperemia, no ulcers	2
Ulceration without hyperemia or bowel wall thickening	3
Ulceration with inflammation at one site	4
>1 site of inflammation and ulceration	5
Major sites of damage extending >1cm along length of colon	***6***
When an area of damage extends >2cm along the length of the **colon**, the score is increased by 1 for each additional cm of involvement	7-11
	SCORE 6
Adhesions	
No adhesions	***0***
Minor adhesions (colon can be separated from other tissue with little effort)	1
Major Adhesions	2
	SCORE 0
Diarrhea	
No diarrhea over the course of treatment period	0
Diarrhea noted at least once during the treatment period	***1***
	SCORE 1
	TOTAL SCORE 7

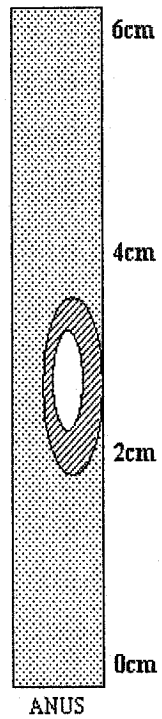

Figure 2-4. Schematic of a rat colon and the scoring system used to tabulate Damage Score for each animal in the TNBS experiments (adapted from Wallace *et al.*, 1992). Colon shows an ulcer (white oval) surrounded by thick inflamed tissue (striped oval). The damage extends from approximately 1.9 cm to 3.6 cm from the anus corresponding to a score of 6 for ulceration (bold italicized). Absence of adhesions of colon to surrounding tissue (score=0) and presence of diarrhea (score=1) gives rise to an overall damage score of 7 for this hypothetical animal.

Tissue was placed into 13 mm x 100 mm test tubes containing HETAB buffer (0.5 ml) on ice. This buffer contains 0.5 % hexadecyltrimethylammonium bromide in 50 mM phosphate buffer (pH 6.0). Tissue was homogenized for 45 seconds (Polytron PT 10-35). A second tube containing HETAB buffer (0.5 ml) was used to wash the homogenizer probe and this wash was added to the original tube for a total volume of 1 ml. Tissue homogenates were sonicated (Fisher Sonic Dismembrator 300) for 40 seconds and centrifuged for 10 minutes at 3100 rpm at 4 °C (Sorvall RT 6000D centrifuge). Supernatants were transferred to 1.5 ml Eppendorf tubes and centrifuged for an additional 5 minutes at 10,000 rpm (Eppendorf centrifuge 5415 D).

A 100 μL aliquot of supernatant was transferred to a plastic cuvette containing *o*-dianisidine reagent (1.9 ml) consisting of *o*-dianisidine (0.167 mg/ml) in 50 mM phosphate buffer (pH 6.0) with 0.0005 % H_2O_2. This reagent provides the basis for a colorimetric reaction whereby H_2O_2 is first converted to H_2O and an oxygen free radical (O^-) via the MPO enzyme. This oxygen radical then reacts with *o*-dianisidine to form H_2O and a colored product. The colorimetric reaction was measured at 450 nm using a spectrophotometer (Milton Roy Spectronic 1001 Plus) at 0 min, 1 min, and 2 min to determine the average change in absorbance per minute. All samples were run in duplicate. One unit of MPO activity is described as that needed to convert 1 micromole of H_2O_2, which corresponds to a change in absorbance of 1.13×10^{-2}. Data are expressed as units of MPO activity per milligram of tissue.

2.12 HISTOLOGICAL PROCESSING OF COLON TISSUE FOR STAINING AND IMMUNOHISTOCHEMISTRY

2.12.1 Fixation, Paraffin-Embedding, and Cutting of Colon Tissue

Colons were rolled longitudinally and stored in 4 % paraformaldehyde (PFA) as described above. PFA-fixed colon rolls were sliced in half longitudinally using a microtome blade. Half of the colon was processed in 4 % PFA and half was processed in buffered formalin prior to paraffin-embedding of all samples. Paraffin-embedded tissues were chilled on ice packs to harden the wax and cut into 8 μm sections using a microtome. Sections were then floated onto siliconized slides and slides were dried for 1 hr at 60 °C or overnight at 37 °C.

Formalin-fixed sections on slides were used for H&E staining (section 2.12.2) and Sirius Red/Fast Green staining (section 2.13.1). Formalin-fixed colon sections were also cut at 8 μm and placed into glass test tubes for Sirius Red/Fast Green staining (section 2.13.1). PFA-fixed colon sections on slides were cut at 8 μm and dried onto siliconized slides for immunohistochemistry (section 2.13.3).

2.12.2 Hematoxylin and Eosin Staining of Fixed Colon Sections

One formalin-fixed colon section (slide) from each animal was stained with hematoxylin and eosin (H&E) by a histologist in the Department of Oral Pathology for visualization of colon morphology. Hematoxylin is a nuclear stain (blue), while eosin stains cellular proteins giving the cells an overall pink appearance. While H&E staining

does not distinguish between different cell types, it allows the investigator to examine cellular structure, density, and changes in cell and tissue morphology.

2.13 ASSESSMENT OF FIBROSIS IN TNBS-INDUCED COLITIS

2.13.1 Sirius Red/Fast Green Method of Collagen Quantitation

Collagen levels in colon tissue were assessed by a modification of the Sirius Red/Fast Green staining method (Lopez de Leon and Rojkind, 1985; Gascon-Barre *et al.*, 1989). Paraffin-embedded tissues were deparaffinized by exposure to xylenes (2 x 15min), and rehydrated by incubation in 100 % ethanol (3 x 5 min), 95 % ethanol (2 x 5min), and 75 % ethanol (2 x 5min). Deparaffinized tissues were incubated in a solution of 0.04 % Fast Green in saturated picric acid for 20 minutes and then washed with mH_2O several times until the water was clear. Tissues were then incubated in 0.1 % Fast Green/0.04 % Sirius Red in saturated picric acid for 30 minutes and were again washed with mH_2O. Interaction of Sirius Red with collagen fibrils is dependent on the presence of picric acid (Lopez de Leon and Rojkind, 1985). Stain was eluted from tissues with 0.05 N NaOH (1 ml) in 50 % methanol.

The eluted stain was transferred to a cuvette and read in a spectrophotometer at 540 nm and 604 nm, corresponding to the peak absorbances of Sirius Red and Fast Green respectively. Since Fast Green has a small amount of absorbance at 540 nm, equations have been formulated to account for this contribution to the Sirius Red absorbance, as

well as color equivalences for both dyes determined by comparing colorimetric and chemical methods of collagen detection on the same tissue sections (Lopez-de Leon and Rojkind, 1985).

Non-collagenous protein was determined by formula 1:

(1) non-collagenous protein (mg) = absorbance @ 604 nm/ 2.08.

Collagen content was calculated from formula 2:

(2) collagen (μg) = absorbance @ 540 nm – 0.26 (absorbance @ 605 nm)/ 38.4.

Formula 3 was used to determine collagen levels in tissue relative to total protein:

$$\text{(3) collagen content (μg/mg total protein)} = \frac{\text{collagen (μg)}}{\text{collagen (μg) + non-collagenous protein (mg)}}$$

The ratio of collagen to total protein was then corrected to account for differences in colon weight between individual samples giving an estimate of colonic collagen level (mg collagen/g protein x g tissue/6 cm colon). This measure of colonic collagen level was then further corrected for the protein concentration in each colon to give an estimation of the collagen content for each colon segment. Protein determination (PD) was performed using the BCA QuantiPro Assay Kit (Sigma) according to the manufacturers instructions. The full calculation was: μg collagen/mg tissue (SR/FG) x mg protein/g tissue (PD) x g tissue/6 cm colon segment (colon weight).

2.13.2 Immunohistochemical Staining of Collagen III in Frozen Colon Tissue

Colon tissue was frozen in embedding media and 10 μm sections were cut using a cryostat and dried onto slides. Tissue was fixed in ice-cold acetone for 2 min followed by fixation in periodate-lysine-paraformaldehyde (PLP) for 10 min at room temperature (RT). An endogenous peroxidase block was performed by incubating slides in 2 % H_2O_2 for 15 min followed by a protein block in 5 % goat serum in PBS for 1 hr at RT. Slides were washed well (3 x 5 min) between steps but no wash was performed between the protein block and primary antibody incubation. Mouse anti-rat collagen type III (Sigma) and mouse anti-rat collagen type I (Sigma) were applied to slides (1:1000) in PBS overnight followed by incubation with goat anti-mouse-HRP secondary antibody for 1 hr at RT (1:100). Staining was visualized with AEC in the presences of 2 % H_2O_2 for 15 min at RT. Slides were counterstained with hematoxylin and mounted for viewing using a glycerol-gelatin mounting solution.

2.13.3 Western Blotting of Collagen Type I in Frozen Colon Tissue

Colon tissue lysates were prepared as described below (section 2.15.1) and proteins were separated on pre-cast 7.5 % and 4-20 % pre-cast gels by SDS-PAGE (section 2.15.1). Membranes were incubated overnight at 4 °C with goat anti-collagen type I or goat anti-collagen type III antibodies diluted 1:500 in TBS-T with 10 % BSA. Membranes were washed with TBS-T followed by incubation with rabbit anti-goat IgG peroxidase conjugate (1:25000) and rabbit anti-biotin-HRP antibody (1:1000), to

visualize the biotinylated molecular weight marker, in blocking buffer for 1 hr at RT (2.15.1). Bands were visualized by ECL.

2.14 ASSESSMENT OF INTERLEUKIN-18 BY ELISA

2.14.1 Enzyme-linked Immunosorbent Assay

2.14.1.1 Preparation of colon lysates for ELISA

Colon tissue was weighed and placed in a 13 mm x 100 mm test tube in PBS (pH 7.4) on ice. Tissue was homogenized for 45 seconds (Polytron PT 10-35). An aliquot of PBS (0.5 ml) was placed in a separate tube to rinse the homogenizer probe. This rinse was added to the original tube. The final ratio of tissue to PBS was 50 mg tissue/ml PBS. The tissue homogenate was sonicated for 40 seconds (Fisher Sonic Dismembrator 300) followed by centrifugation at 3100 rpm for 10 minutes at 4 °C (Sorval RT 6000D). Supernatants were transferred to 1.5 ml Eppendorf tubes and centrifuged for an additional 5 minutes at 10,000 rpm (Eppendorf centrifuge 5415 D). IL-18 levels in colon lysates were analyzed by ELISA.

2.14.1.2 ELISA Method

Enzyme-linked immunosorbent assay (ELISA) of rat IL-18 was carried out on supernatants and serum according to the manufacturer's instructions. Briefly, 100 μL of

supernatant or serum was added to individual wells of a strip-well plate coated with anti-rat IL-18 capture antibody, along with the supplied incubation buffer (50 µL/well). Biotinylated anti-rat IL-18 detection antibody was then applied followed by Streptavidin-HRP and chromogenic color development. Wells were washed thoroughly between each step. All samples were run in duplicate. The colorimetric response was measured at 450 nm (Multiscan Ascent; Thermo Labsystems) and analysis was carried out using the appropriate software (Ascent software version 2.6). The level of detection of the Biosource Rat IL-18 ELISA kit was 4 – 1200 pg/mL IL-18.

2.15 WESTERN ANALYSIS OF MOLECULAR EVENTS IN TNBS-INDUCED COLITIS

2.15.1 Western Immunoblotting Method

2.15.1.1 Preparation of Colon Lysates for Westerns

Colon tissue lysates were prepared by pulverizing frozen tissue with a LN_2-cooled mortar and pestle and transferring tissue to a cold 2 ml Eppendorf tube using a LN_2-cooled metal spatula. Ice-cold RIPA buffer (1 % Igepal CA 630, 0.5 % sodium deoxycholate, 0.1 % SDS in PBS, pH 7.4) containing protease inhibitors (PMSF, aprotinin, sodium orthovanadate) was added at a ratio of 3 µL RIPA/mg tissue. The suspension was homogenized for 10 sec with a handheld tissue tearer (Biospec Products, USA) followed by sonication for 10 sec (Fisher Sonic Dismembrator 300). Homogenates were incubated on ice for 30 minutes with additional PMSF (0.03 µl/mg tissue) before

being centrifuged for 10 minutes at 10,000 rpm at 4 °C (Eppendorf centrifuge 5415 D). Supernatants (lysates) were stored at –86 °C.

2.15.1.2 General Immunoblotting Method

Protein determination was performed using the QuantiPro BCA Assay Kit (Sigma) and SDS polyacrylamide gel electrophoresis (SDS-PAGE) was carried out by standard methods. Proteins (40-50 μg of tissue or whole-cell lysate; 10-20 μg of nuclear lysate) were separated on pre-cast polyacrylamide Tris-HCl gels with pore sizes appropriate for the molecular weights of particular proteins being assessed. Proteins were transferred to Immuno-Blot PVDF membrane at 25 V overnight or at 100 V for 1 hr. A biotinylated molecular weight ladder and a kaleidoscope pre-stained molecular weight ladder were run on the gels along with appropriate controls (section 2.15.3). Membranes were incubated in blocking buffer [Tris-buffered saline containing 0.1 % Tween-20 (TBS-T) and 5 % skim milk powder] for 1 hr at RT, followed by incubation overnight at 4 °C with primary antibody diluted in 10 mls of TBS containing 0.1 % Tween-20 and 10 % BSA. Membranes were washed well with TBS-T and incubated in blocking buffer for 1 hr at RT with the appropriate HRP-linked secondary antibody plus rabbit anti-biotin-HRP (1:1000) to visualize the biotinylated ladder. Membranes were washed and bands were visualized on film by enhanced chemiluminescence. Equal loading was determined by probing for β-tubulin or staining blots with amido black. Since β-tubulin levels were affected by TNBS-treatment, careful protein determination and amido black-staining were the methods of verifying equal loading for Westerns in the TNBS-studies.

2.15.2 Densitometric Analysis of Western Results

Western Blot films were scanned (UMAX AstraNETe3470) and saved in ".TIF" format using Adobe Photoshop Elements LE 5.0. Images were opened with Scion Image software and relevant bands were analyzed by densitometry. Background density for each lane was subtracted from the corresponding band density. Measurements are reported in relative density units (rdu).

2.15.3 Experiment Details

Western immunoblotting was performed on control and TNBS-exposed colon tissues at various timepoints following induction of colitis (0, 4 hrs, 3 days, 7 days, 14 days). Proteins assessed (and antibody dilutions) were NF-κB p65 (1:1000), JNK1 (1:500), phospho-JNK (1:500), p38 MAPK (1:1000), phospho-p38 MAPK (1:1000), phospho-ATF-2 (1:1000), TGF-β1 (1:1000), PDGF-B (1:1000). Molecular weight controls used were 3T3 whole-cell lysate (NF-κB), anicomycin-treated 3T3 cell lysate (p38, p-p38, p-ATF-2), UV-treated 3T3 cell lysate (JNK1, p-JNK), and recombinant cytokines (TGF-β and PDGF-B).

2-16 EFFECTS OF M-1 AND PTX ON NF-κB ACTIVATION IN VITRO

2.16.1 Immunocytochemistry

2.16.1.1 ICC Method

IECs were seeded into a 96-well-plate (section 2.7.2) at a density of 20,000 cells/ml in media with 10 % FBS (200 μL/well). Media was removed the following day and replaced with fresh media containing 1 % FBS (100 μL/well) for an additional 72 hrs. Cells were then exposed to various treatments for specified lengths of time (cytokines in the presence or absence of PTX and M-1). See below for details of specific experiments. At the end of the experiment, media was removed from all wells and replaced with 4 % PFA for 15 min at RT. After fixation, cells were washed well with PBS-T and rabbit NF-κB p65 polyclonal antibody was added diluted in PBS with 1 % goat serum (50 μL/well). Control wells were not exposed to primary antibody. IECs were incubated with primary antibody overnight at RT with gentle shaking. Cells were again washed with PBS-T before exposure to anti-rabbit anti-mouse secondary antibody followed by streptavidin-HRP for 1 hr each at RT (LSAB II Kit). After another wash with PBS-T the cells were exposed to the chromogen DAB. DAB reagent was prepared by adding one DAB pellet to 1X TBS (15 mls) with 12 μL of fresh 30 % H_2O_2, followed by filtration to remove undissolved DAB. DAB solution (50 μL) was added to each well. When adequate color development was seen, DAB was removed and cells were washed

well with PBS-T. PBS containing methiolate (100 μL/well) was added to the plate, which was then wrapped in plastic for storage at 4 °C. Staining was visualized by light microscopy and digital images were captured.

2.16.1.2 ICC Experiment Details

IECs were treated with rrIL-1β (50 ng/ml), rrTNF-α (50 ng/ml), and rrIL-18 (50 ng/ml) for various times ranging from 10 min to 2 hours and nuclear staining of NF-κB was assessed. IECs were treated with rrIL-1β (50 ng/ml) or rrTNF-α (50 ng/ml) in the presence and absence of PTX or M-1 (1 mg/ml). Drugs were added 10 minutes prior to cytokines and cells were fixed 1 hour after addition of the cytokines. Nuclear staining of NF-κB was assessed.

2.17 EFFECT OF IL-18 ON NF-κB ACTIVATION IN VITRO

2.17.1 General method for *in vitro* experiments

IEC-6 cells were seeded into sterile petri dishes at a density of 1,000,000 cells/dish in culture media with 10 % FBS (2 mls). On the following day, the media was removed and replaced with fresh media containing 1 % FBS for a further 24 hrs incubation. Cells were then exposed to cytokines for various timepoints. See below for experiment details. At the end of the experiment, media was removed and cells were washed with cold PBS before whole-cell or nuclear protein extraction. Extracted proteins

were analyzed by Western Immunoblotting (section 2.15.1) of 40-50 μg of whole-cell protein or 10-20 μg of nuclear protein per lane on pre-cast 10 %-15 % polyacrylamide Tris-HCl gels. Western blotting was followed by densitometric analysis using Scion Image software (section 2.15.2).

2.17.2 Extraction of nuclear protein for Western immunoblotting

Nuclear protein was extracted using a modification of the original method by Andrews and Faller (1991). Media was removed from petri dishes and cold PBS (500 μL) was added. Cells were scraped using a rubber policeman and the suspensions were transferred to 1.5 mL Eppendorf tubes on ice. Dishes were washed with cold PBS (0.5 mls) and this was added to the original suspensions. Tubes were centrifuged at 4,000 x g for 4 min at 4 °C to pellet the cells. Supernatants were discarded and pellets were resuspended in ice-cold Buffer A (200 μL) (see Table 2-6) by "flicking" the tubes. Tubes were incubated on ice for 10 min to allow cells to swell. Tubes were vortexed for 10 sec each and centrifuged at 4000 x g for 4 min at 4 °C. Supernatants (cytoplasmic fraction) were removed and pellets were resuspended in ice-cold Buffer B (200 μL) (Table 2-6) and incubated on ice for 30 min. Tubes were centrifuged at 16,000 x g for 15 min at 4 °C and supernatants containing nuclear protein were stored at –86 °C for Western Immunoblotting (section 2.15.1).

Table 2-6. BUFFERS USED FOR NUCLEAR PROTEIN EXTRACTION

Buffer A	*Buffer B*
10 mM HEPES (pH 7.9 with KOH)	20 mM HEPES (pH 7.9 with KOH)
1.5 mM $MgCl_2$	1.5 mM $MgCl_2$
10 mM KCl	420 mM NaCl
0.1 % Triton-X	25 % glycerol
0.5 mM DTT	0.2 M EDTA
0.2 mM PMSF	0.5 mM DTT
10 μg/mL Aprotinin	0.2 mM PMSF
	10 μg/mL Aprotinin

2.17.3 Experiment Details

IECs were treated with IL-18 (50 ng/ml and 100 ng/ml) for 1 and 2 hours. Nuclear extracts were prepared and assessed for NF-κB by Western immunoblotting.

2.18 STATISTICAL ANALYSIS

Data were analyzed by one-way ANOVA. Post-hoc analysis was carried out using the Student-Newman-Keuls method of multiple pairwise comparisons to analyze differences between groups. A t-test was used when only two groups were being compared. A Spearman correlation was performed between variables when at least one variable was non-linear. The level of type I error was set at 5 % thus p-values below 0.05 were considered statistically significant. Statistical software used was SigmaStat version 2.0. Data are expressed as mean ± SEM.

Chapter 3

RESULTS

3.1 SYNTHESIS OF METABOLITE-1 OF PENTOXIFYLLINE

3.1.1 Chemical Synthesis of Metabolite-1 from Pentoxifylline

The chemical reduction reaction described in section 2.6.1 was performed twice during the course of these studies resulting in two separate batches of M-1. The first batch produced in June of 2000 yielded M-1 (8.1 g) from PTX (10 g). A second batch produced in 2003 yielded M-1 (8.7 g) from PTX (10 g). The average percent recovery of M-1 from PTX by this method was 84 %. This is an improvement over the original method developed in 1996 (recovery <50 %) using only two CH_2Cl_2 extractions.

3.1.2 Identification of Metabolite-1

The success of the chemical reduction reaction was determined by analyzing samples of the starting compound (PTX) and the reaction product by ^{1}H-NMR. NMR spectrographs revealed that the reaction product was M-1 (Fig 3-1). A key feature identifying the conversion of PTX to M-1 was the disappearance of a sharp peak at 2.1 ppm in the PTX spectrograph (Fig 3-1a) corresponding to a carboxyl group (C=O) present on the alkyl chain of the PTX molecule (see Figure 2-1 for structures). This carboxyl group was reduced to a hydroxyl group (-OH) in the formation of M-1. The NMR spectrograph for M-1 (Fig 3-1b) shows the emergence of a broad peak at 3.7 ppm indicating proton coupling to a hydroxyl group. These and other features of the spectrographs confirmed that PTX was successfully converted to M-1.

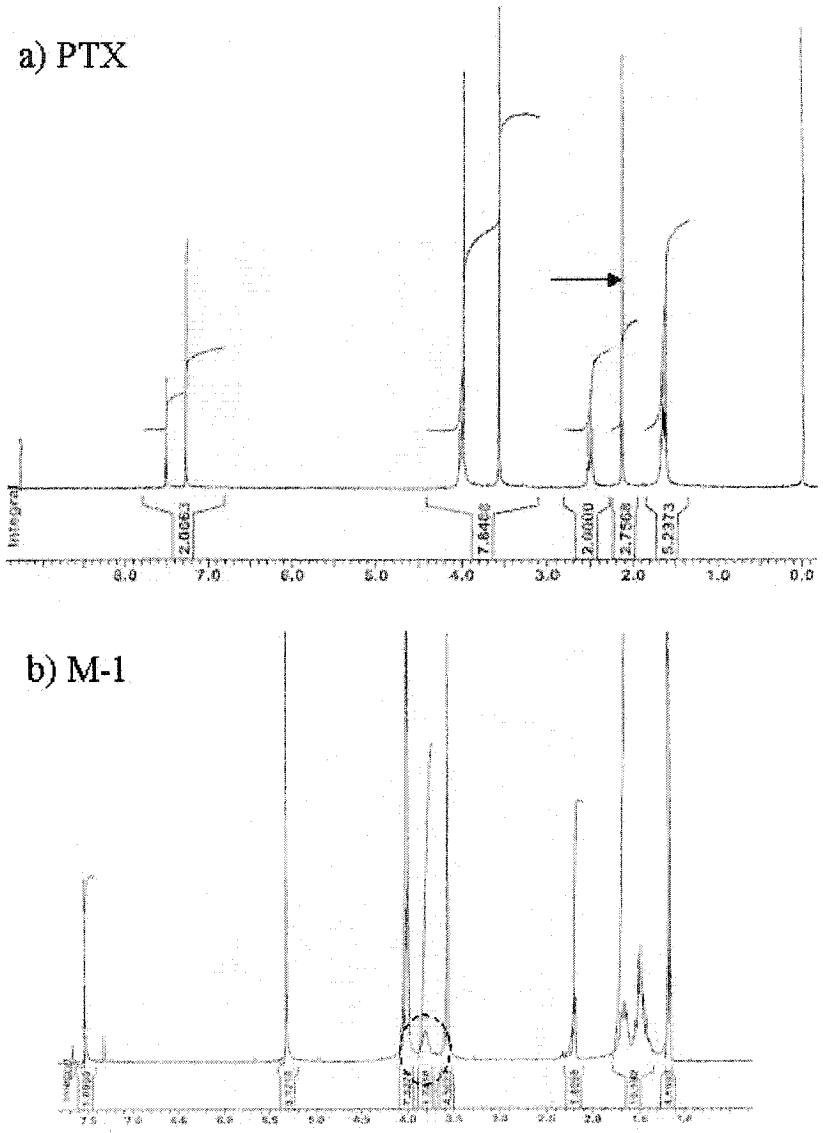

Figure 3-1. ^{1}H-NMR Spectrographs of PTX and M-1. The conversion of PTX to M-1 was confirmed by proton nuclear magnetic resonance (^{1}H-NMR) spectroscopy. The NMR spectrographs for PTX (a) and M-1 (b) are shown above. The broad peak at approximately 3.7 ppm in the M-1 plot (dashed circle) indicates proton coupling to a hydroxyl group (-OH), and corresponding loss of the sharp single peak at 2.1 ppm (arrow) indicates loss of the carboxyl group (C=O) present in the PTX molecule. These key events as well as other changes in the coupling patterns indicate that PTX was completely converted to M-1 in the reduction reaction.

3.2 INITIAL CHARACTERIZATION OF M-1 IN VITRO

3.2.1 Stimulation of Fibroblast Proliferation with PDGF

Fibroblast proliferation was measured using an established tritiated [^{3}H]-thymidine incorporation assay (section 2.7.2). Initial assays were conducted to determine the optimal concentration of PDGF to stimulate proliferation of human dermal fibroblasts (Fig 3-2). A significant increase in fibroproliferation over controls (culture media supplemented with 1 % FBS) was achieved with PDGF (2 ng/ml) (6836 ± 258 cpm compared to 3264 ± 66 cpm; $p<0.05$). PDGF-stimulated proliferation reached a peak at PDGF (8ng/ml) compared to controls (11950 ± 742 vs. 3264 ± 66 cpm; $p<0.05$) that was only slightly increased by doubling the concentration of PDGF (16 ng/ml) (12110 ± 419 cpm). Proliferation was sub-maximal at PDGF concentrations above 16 ng/ml. PDGF (8 ng/ml) was used to stimulate F8 proliferation in further experiments. Results are expressed as mean cpm/8000 cells plated ± SEM.

3.2.2 Effect of M-1 and PTX on PDGF-Stimulated Fibroblast Proliferation

Proliferation assays were performed to assess the inhibitory potential of M-1 synthesized by the modified method described above (section 2.6.1). Both M-1 and PTX (240-1900 μM) produced dose-dependent inhibition of PDGF-stimulated dermal fibroblast proliferation (Fig 3-3). A significant 41 % inhibition of PDGF-stimulated proliferation was achieved with M-1 (240 μM) compared to PDGF-stimulated cells not exposed to M-1 (5361 ± 613 cpm vs. 9145 ± 321 cpm; $p<0.05$). The concentration of

M-1 that inhibited PDGF-stimulated proliferation by 50 % (IC_{50}) compared to baseline proliferation was 190 μM.

A significant 26 % inhibition of PDGF-stimulated proliferation was achieved with PTX (240 μM) compared to PDGF-stimulated cells not exposed to PTX (6727 ± 71 cpm vs. 9145 ± 321 cpm; $p<0.05$) with an IC_{50} of approximately 290 μM. The IC_{50} for M-1 was approximately 44 % lower than for PTX. Significant differences were observed between equivalent concentrations of M-1 and PTX in the range of 240-950 μM indicating that M-1 was more potent than PTX in its inhibition of PDGF-stimulated fibroproliferation *in vitro* within this range ($p<0.05$).

3.2.3 Comparison of Potency between PTX and three separate batches of M-1

A proliferation assay was performed to ensure that the two batches of M-1 synthesized during the course of this thesis (2000 and 2003, respectively) were of equivalent potency. These two batches of M-1 were compared to PTX and a previous batch of M-1 (1996) for their ability to inhibit PDGF-stimulated proliferation of dermal fibroblasts. Results indicated that the three batches of M-1 were of equivalent potency since there were no significant differences between batches at any of the concentrations tested (Fig 3-4). All three batches of M-1 were significantly more potent than PTX within the range of 240-950 μM ($p<0.05$). Each drug significantly inhibited PDGF-stimulated fibroproliferation at all doses tested (240 μM to 1900 μM; $p<0.05$), consistent with previous experiments (Fig 3-3).

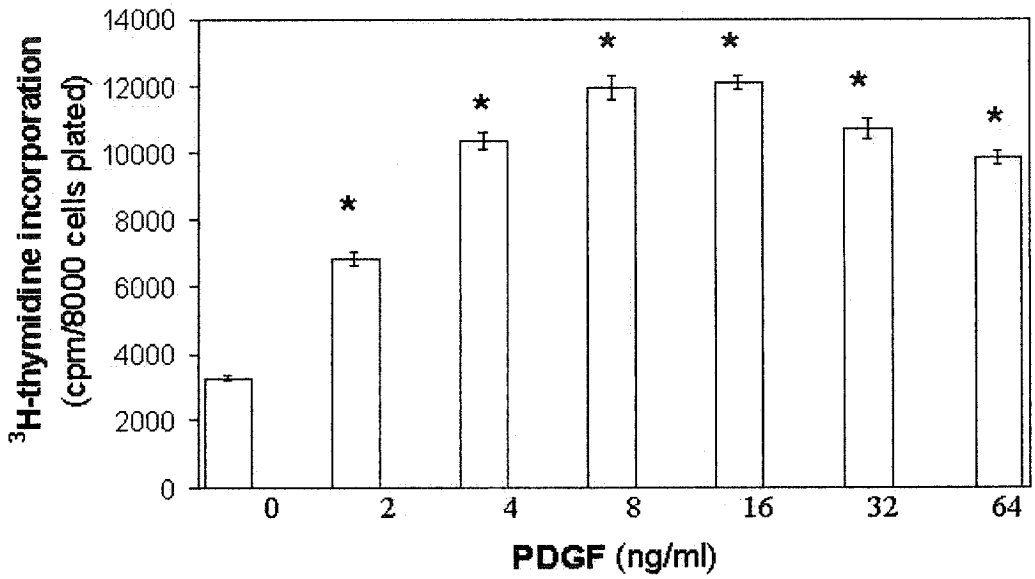

Figure 3-2. PDGF-stimulated proliferation of human skin fibroblasts (F8s). Fibroproliferation was measured using a tritiated [^{3}H]-thymidine incorporation assay. Results are reported as mean cpm/8000 cells plated ± SEM (n=4). Figure is representative of three individual experiments.
*=significant difference from control (culture media with 1% FBS and no PDGF); $p<0.05$

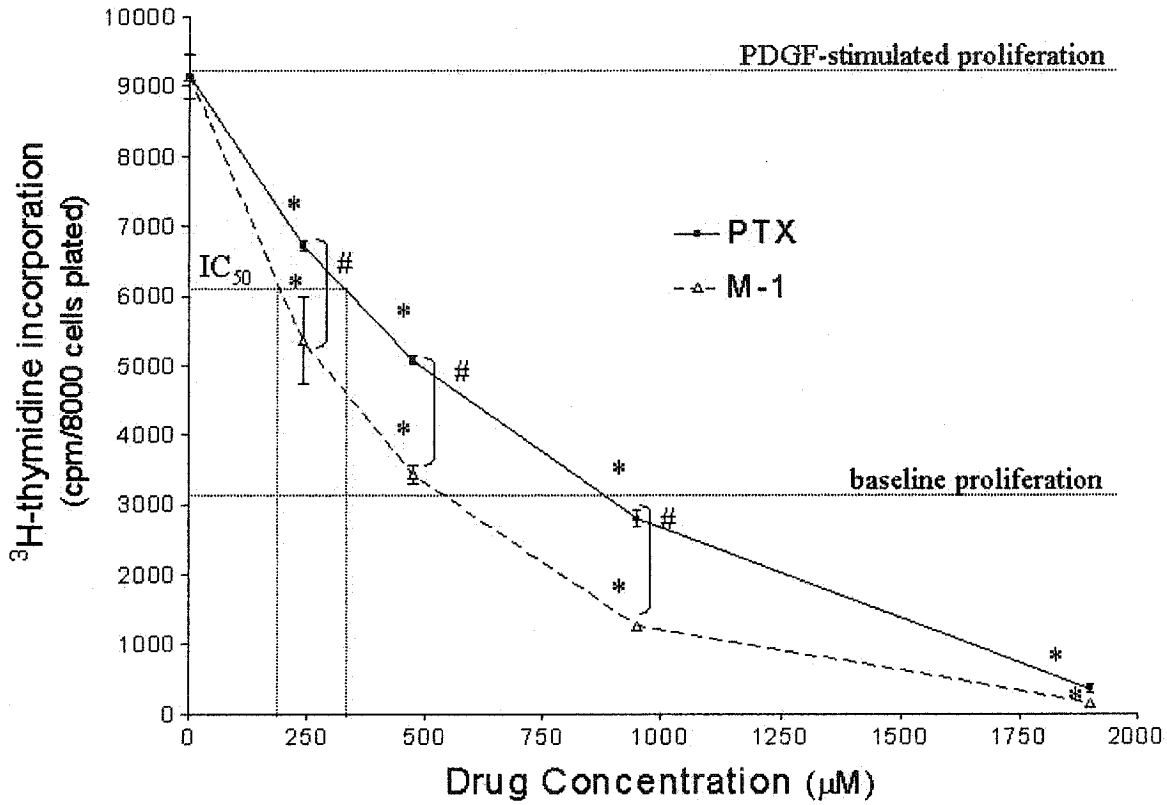

Figure 3-3. Effect of M-1 and PTX on PDGF-stimulated fibroblast proliferation. Subconfluent fibroblasts were stimulated with PDGF (8 ng/ml) in the absence and presence of PTX or M-1 (240-1900 μM) for 24 hours. Data are reported as mean cpm/8000 cells plated ± SEM (n=4). Figure is representative of two separate experiments.
* = significant difference from PDGF-stimulated fibroproliferation (0 μM drug); $p<0.05$
# = significant difference between groups indicated; $p<0.05$

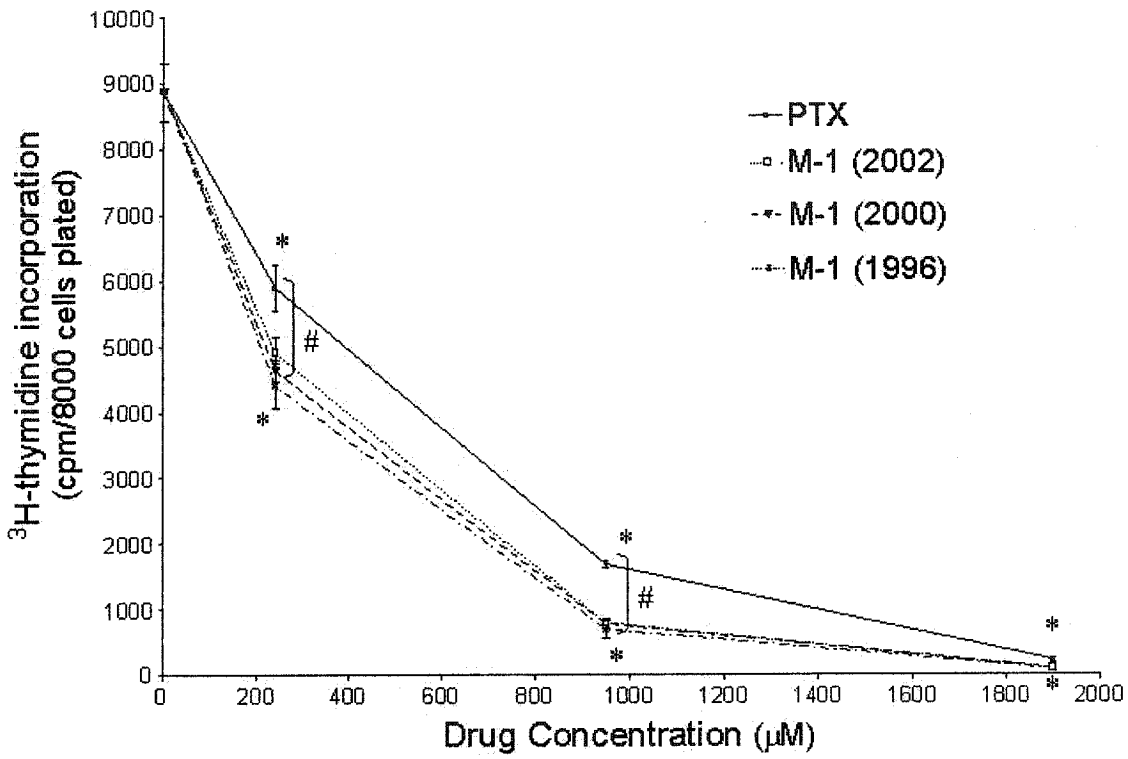

Figure 3-4. Comparison of potency between PTX and three separate batches of M-1. The two most recent batches of M-1 (2000 and 2003) were used throughout the experiments in this thesis. Inhibition of PDGF-stimulated fibroproliferation was assessed at three concentrations of each drug (240, 950, 1900 μM). Results shown are mean cpm/8000 cells plated ± SEM (n=4).
* = significant difference from PDGF-stimulated fibroproliferation (0 μM Drug); $p<0.05$
# = significant difference between groups indicated; $p<0.05$

3.2.4 Stimulation of Fibroblast Collagen Synthesis with PDGF

Collagen synthesis by confluent human skin fibroblasts was measured using a tritiated [^{3}H]-proline incorporation assay described above (section 2.7.1). PDGF produced a dose-dependent stimulation of collagen production (Fig 3-5) reaching statistical significance at PDGF (16 ng/ml) compared to controls (6828 ± 453 cpm vs. 4606 ± 677 cpm; $p<0.05$). A peak in PDGF-stimulated collagen synthesis was reached at PDGF (32 ng/ml) compared to controls (9166 ± 1233 vs. 4606 ± 677; $p<0.05$) and this was the concentration chosen to stimulate collagen synthesis in further experiments.

3.2.5 Effect of M-1 and PTX on PDGF-Stimulated Collagen Synthesis

Tritiated [^{3}H]-proline incorporation assays (section 2.7.5) were performed to assess the ability of M-1 to inhibit collagen production *in vitro* (Fig 3-6). PDGF (32 ng/ml) significantly increased collagen production by fibroblasts compared to controls (4100 ± 226 vs. 2682 ± 248 cpm; $p<0.05$). A significant 100 % inhibition of PDGF-stimulated collagen synthesis was achieved with M-1 (240 μM) (2614 ± 328 vs. 4100 ± 226 cpm; $p<0.05$). PTX (240μM) significantly inhibited PDGF-stimulated collagen synthesis by 50 % (3387 ± 168 vs. 4100 ± 226 cpm; $p<0.05$). There was a significant difference in the ability of M-1 and PTX to inhibit collagen synthesis at 240 μM ($p<0.05$). Both M-1 and PTX (1900 μM) significantly decreased PDGF-stimulated collagen synthesis ($p<0.05$) with no difference between M-1 and PTX.

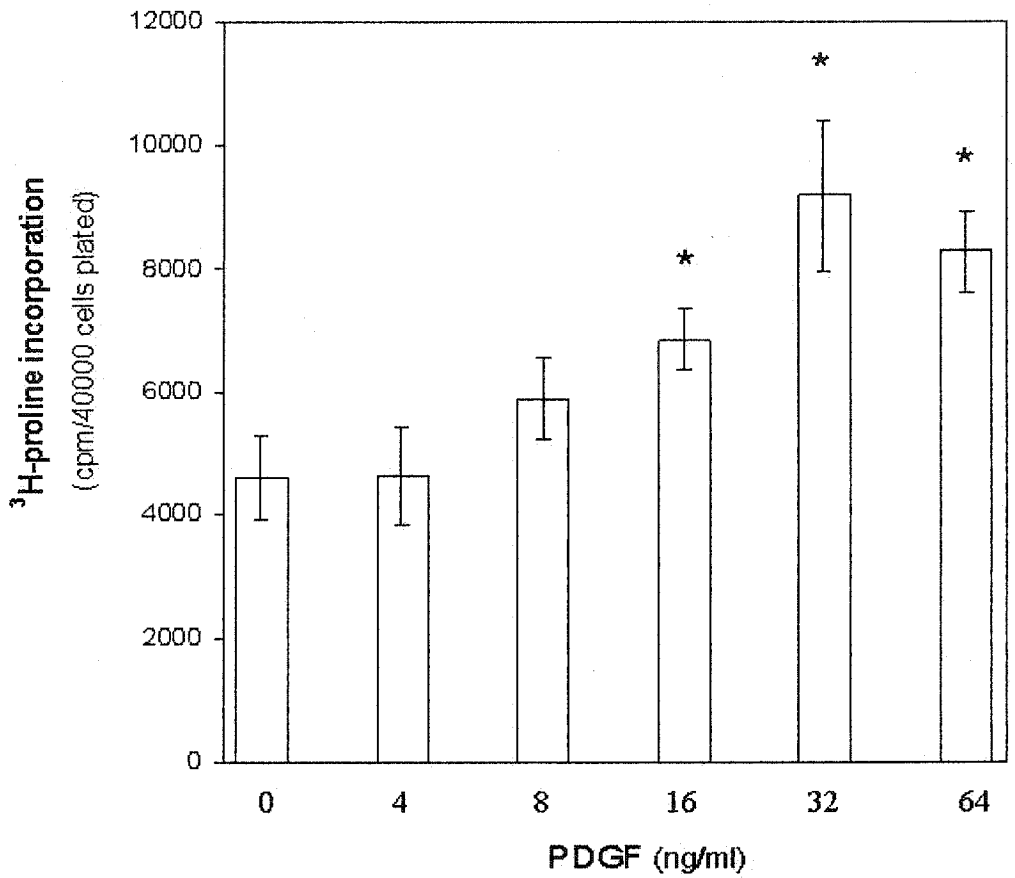

Figure 3-5. PDGF-stimulated collagen synthesis by human skin fibroblasts (F8s). Collagen synthesis by confluent F8s was measured using a tritiated [^{3}H]-proline incorporation assay. Results shown are mean cpm/40000 cells plated ± SEM (n=4). Figure is representative of two separate experiments.
* = significant difference from control (0 ng/ml PDGF); $p<0.05$

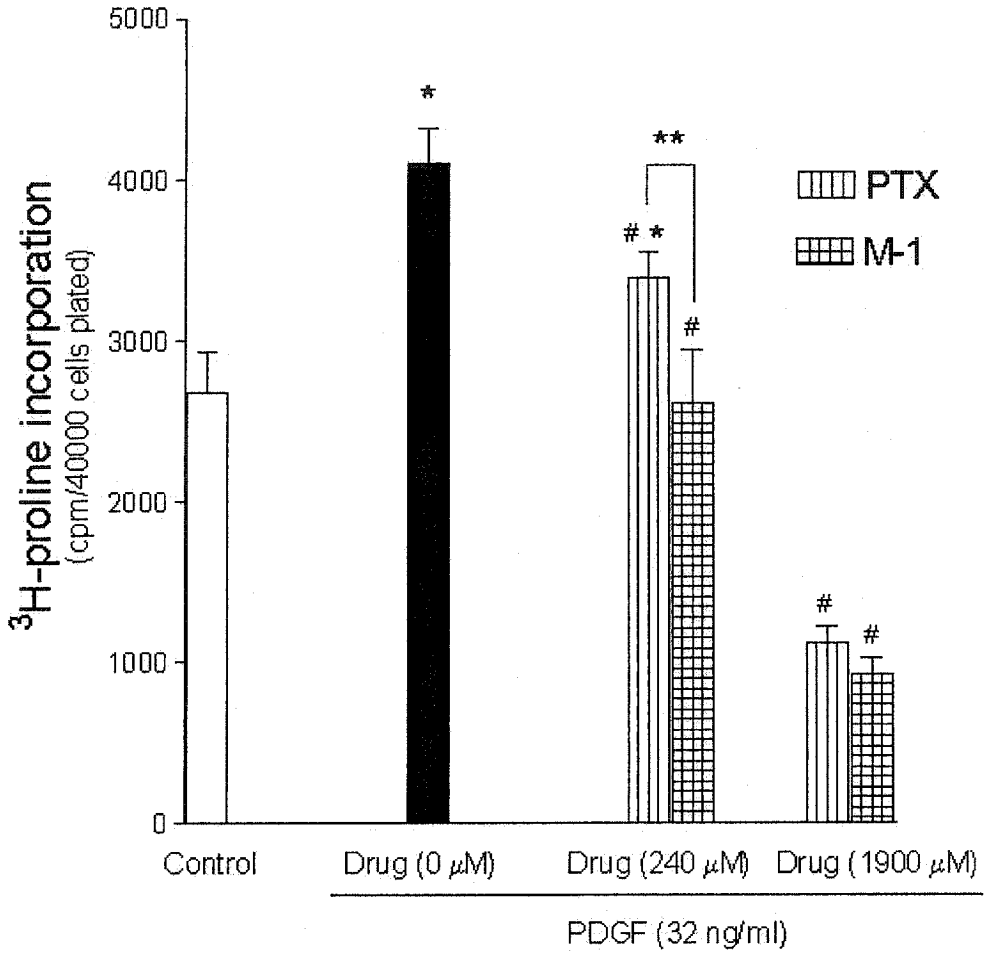

Figure 3-6. Inhibition of PDGF-stimulated collagen synthesis by M-1 and PTX in confluent human skin fibroblasts (F8s). Collagen synthesis was stimulated with PDGF (32 ng/ml) in the presence and absence of low-dose (240 μM) and high-dose (1900 μM) M-1 or PTX for 48 hours. Tritiated [^{3}H]-proline was incorporated into collagen and results are expressed as mean cpm/40000 cells plated ± SEM (n=4).
* = significant difference from control (culture media containing 1% FBS); $p<0.05$
# = significant difference from PDGF (32 ng/ml) alone; $p<0.05$
** = significant difference between groups indicated; $p<0.05$

3.3 INITIAL CHARACTERIZATION OF M-1 IN VIVO

3.3.1 Assessment of M-1 Toxicity *in vivo*

Five C57BL/6 mice were injected with M-1 (32 mg/kg i.p.) dissolved in sterile 0.9 % saline. The mice were monitored for 20 minutes with no signs of toxicity observed. Signs of toxicity include dizziness, lethargy, and hypersalivation. HPLC-analysis of mouse serum collected at 20 minutes post-injection revealed both PTX and M-1 in the serum (not shown). Side effects were also not observed when 5 mice were injected with M-1 (100 mg/kg i.p.).

3.3.2 Kinetics of M-1 and PTX *in vivo*

3.3.2.1 HPLC conditions and standard curve construction

HPLC conditions were optimized to provide complete separation of M-1, PTX, and phenacetin peaks. Figure 3-7 shows two typical HPLC chromatographs used in the construction of standard curves: top is M-1 (7.5 μg/ml) and bottom is PTX (10 μg/ml). M-1 chromatographs also confirmed that no PTX remained in the drug preparation following the M-1 synthesis reaction. Phenacetin (30 μg/ml) was used as an internal control for all standards and a ratio was calculated using the area under the drug peak (M-1 or PTX) divided by the area under the phenacetin peak (peak area ratio). A standard curve was then constructed for each drug by plotting known drug concentrations (x-axis) against peak area ratios (y-axis) (Fig 3-8).

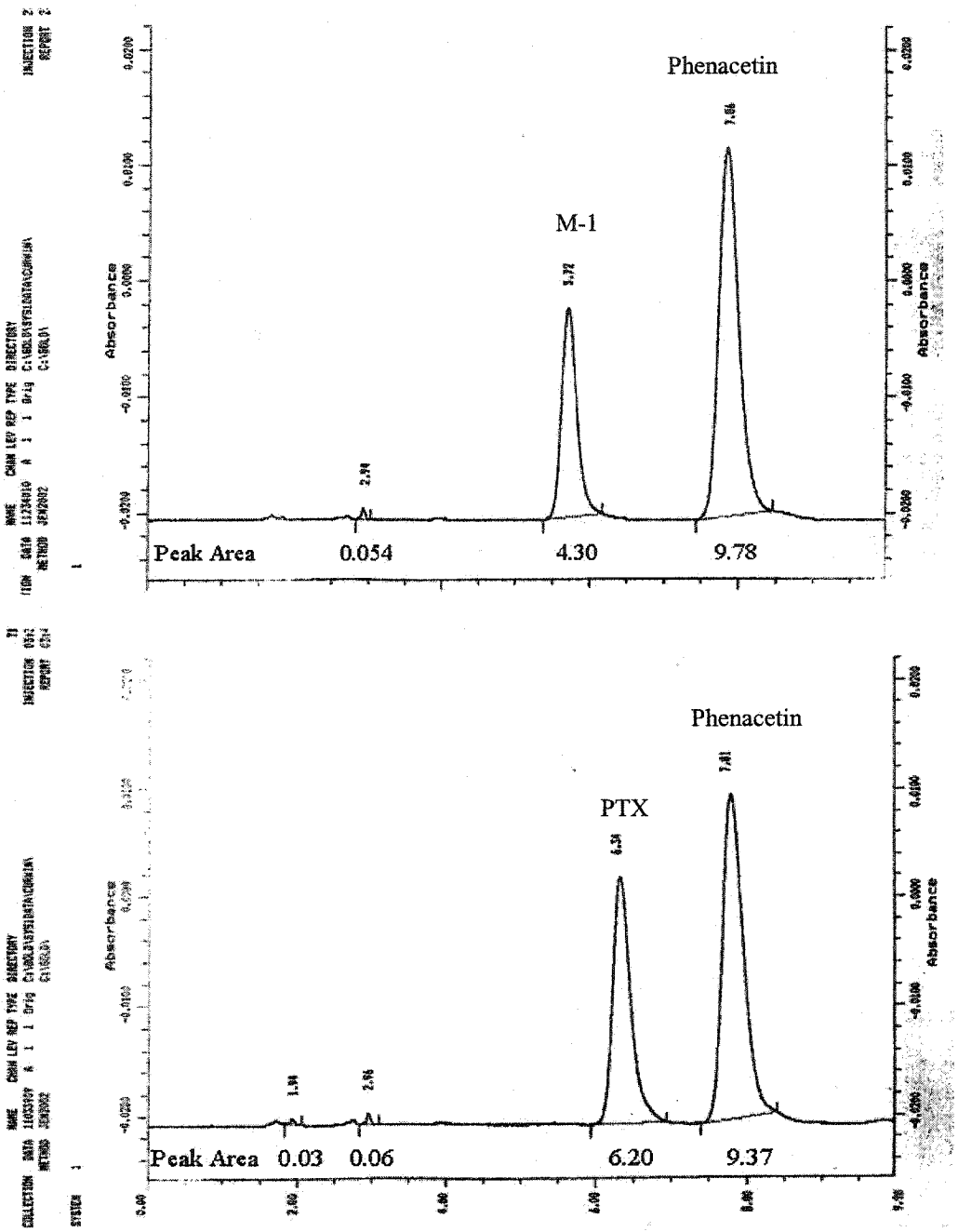

Figure 3-7. Typical HPLC chromatographs of M-1 and PTX standards along with the internal standard phenacetin. M-1 standard shown (top) is 7.5 μg/mL, PTX (bottom) is 10 μg/mL and phenacetin (top and bottom) is 30 μg/mL. Retention times: M-1 (5.7 min), PTX (6.3 min), and phenacetin (5.8 min). Peak area values from HPLC printouts and are shown below each peak. These values are used to construct the peak area ratio for the y-axis of the standard curves.

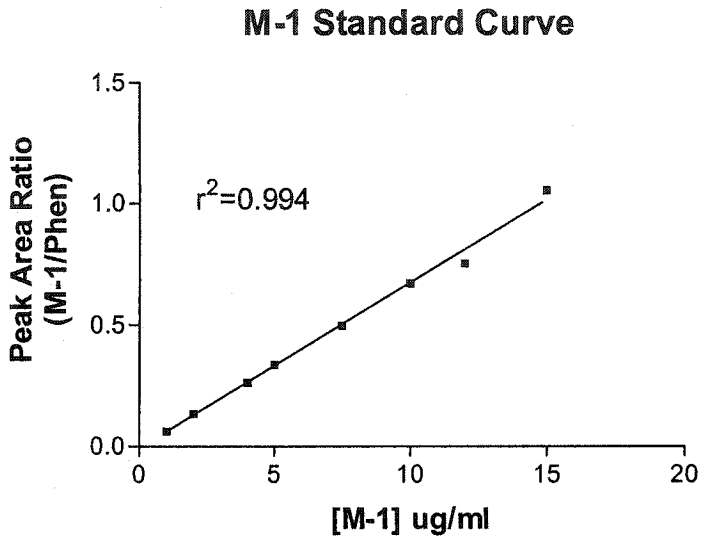

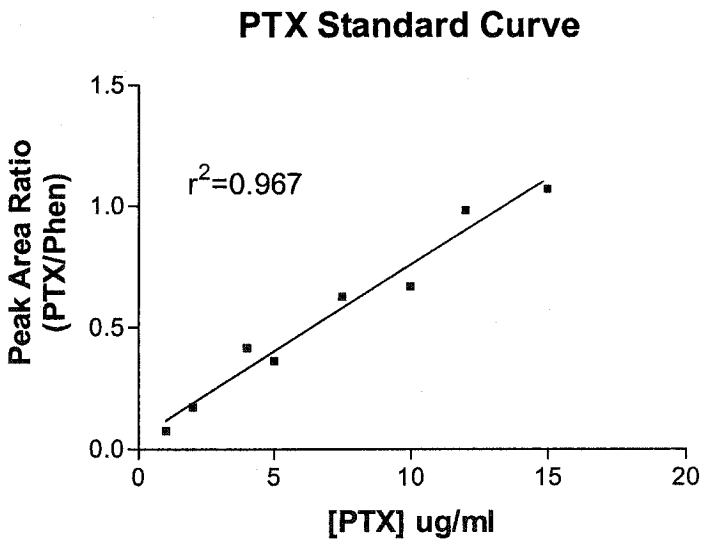

Figure 3-8. Representative standard curves of M-1 and PTX used for HPLC analysis. Known drug concentration (1-15 μg/ml) on the x-axis was plotted against Peak Area Ratio (Drug/Phenacetin) on the y-axis. Peak Area Ratios were calculated from HPLC peak area printout values. Unknown drug levels in mouse serum were determined by calculating the peak area ratio of drug/phenacetin for each sample and substituting this value into the equation of the line derived from each standard curve ($y = mx + b$).

3.3.2.2 Kinetics of M-1 and PTX

Male CD1 mice were injected with M-1 or PTX (100 mg/kg i.p.) and blood was collected at various timepoints (5, 10, 15, 25, 45, 60, 120 minutes) as described in section 2.8.2. Serum was collected by centrifugation and analyzed by HPLC as described in section 2.10. Serum drug values were calculated using the equation of the line from M-1 and PTX standard curves (Fig 3-8). Kinetics of M-1 and PTX *in vivo* are shown in Figure 3-9. HPLC analysis of serum drug levels following M-1 (dashed lines) and PTX (solid lines) injection indicated that both drugs were present in serum following injection of either drug alone. This was expected since the conversion between PTX and M-1 is a reversible reaction that takes place in the blood. M-1 had reached a peak by 10 minutes post-injection while PTX peaked at 15 minutes. The rate of elimination for M-1 (following M-1 injection) and PTX (following PTX injection) was 0.75 μg/ml/min between the 20 and 40 minute timepoints. Serum half-lives of PTX and M-1 were 15 and 20 minutes, respectively.

Levels of PTX and M-1 in serum following M-1 injection reached near equilibrium by 25 minutes, whereas only a small amount of PTX was converted to M-1 following PTX injection (Fig 3-9). This resulted in higher total drug levels (M-1 + PTX) following M-1 injection (Fig 3-10). Since both drugs are active *in vivo*, the combination of PTX and the metabolite in the body will determine the overall biological effects of the drug. While no drugs were detected in serum 120-minutes after PTX injection, detectable amounts of both M-1 and PTX remained following injection of the metabolite.

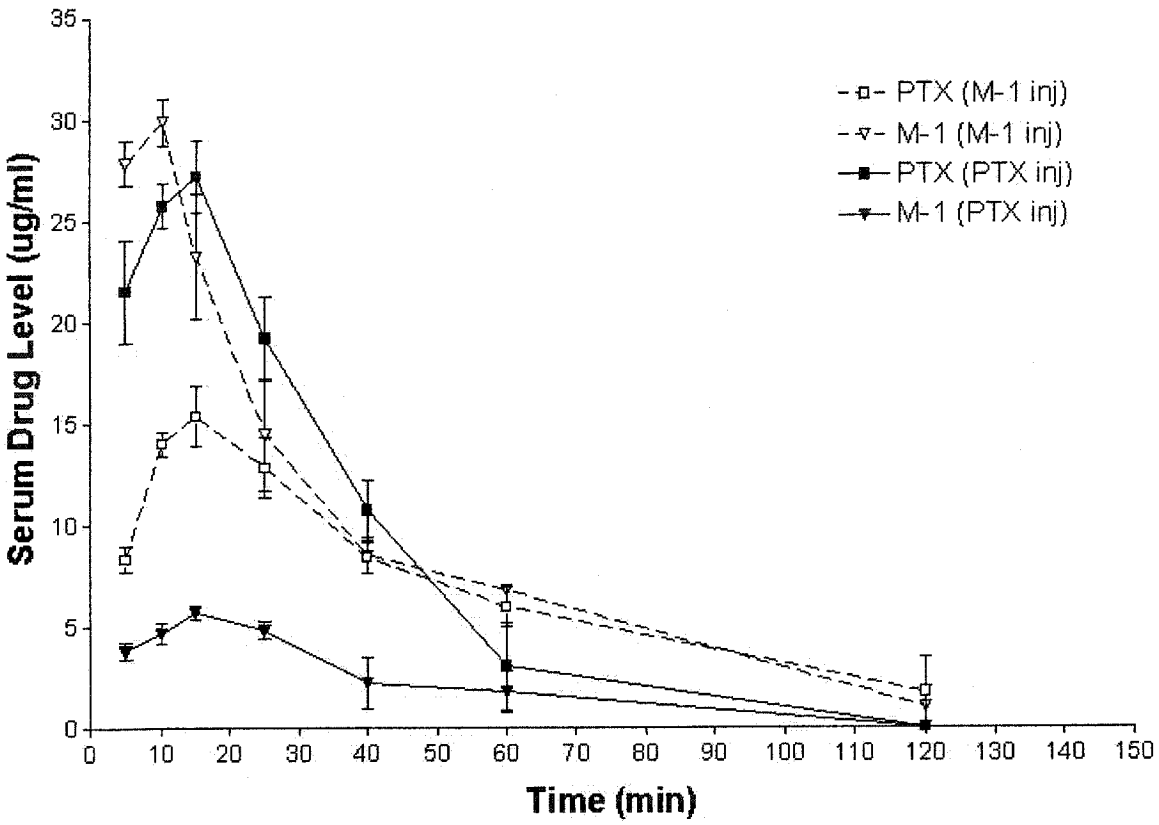

Figure 3-9. Kinetics of M-1 and PTX *in vivo*. Animals were injected with M-1 (dashed lines) or PTX (solid lines) (100 mg/kg i.p.) and serum samples were analyzed by HPLC at 5, 10, 15, 25, 40, 60, and 120 min. Interconversion of PTX and M-1 occurs *in vivo* thus both drugs are detected by HPLC analysis following injection of either drug alone. Rate of elimination between the 20- and 40-minute timepoints was approximately 0.75 μg/ml/min for both PTX and M-1. Each point is mean drug concentration (μg/ml) ± SEM for 4 separate animals.

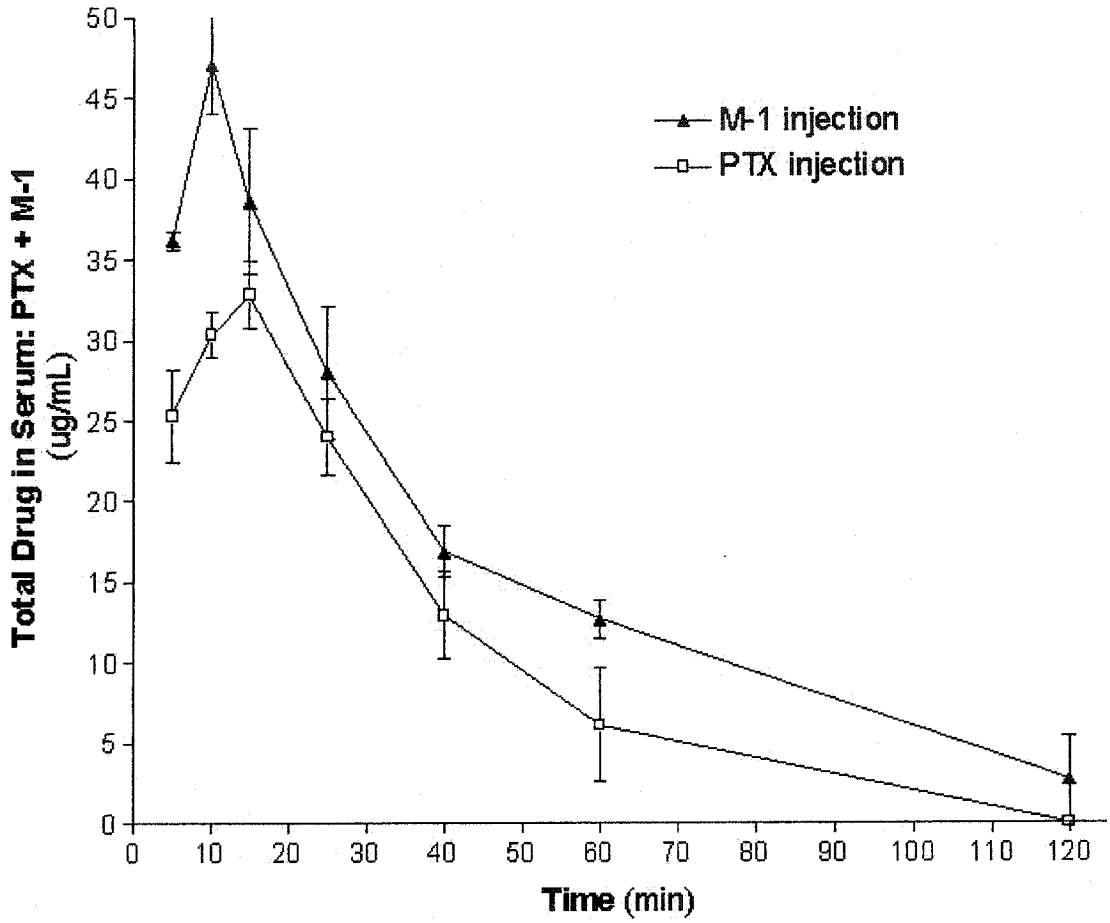

Figure 3-10. Kinetics of M-1 and PTX *in vivo* graphed as total drug (PTX + M-1) in serum. Combined levels of PTX and M-1 give an estimate of relative bioactivity *in vivo*. Each point is mean drug concentration (μg/ml) ± SEM for 4 separate animals.

3.4 INTERACTION OF M-1 AND PTX WITH CIPROFLOXACIN

3.4.1 Interaction of M-1 and PTX with Cipro in Mice

Combination therapy with PTX and the antibiotic ciprofloxacin increased serum levels of PTX and its primary metabolite in humans thereby enhancing the efficacy of PTX therapy (Thomson et al., 1994). A direct interaction between ciprofloxacin and M-1 has never been examined. In order to investigate the possibility of an interaction between ciprofloxacin and M-1 *in vivo*, mice were pre-treated with ciprofloxacin or saline for 9 days before receiving an injection of M-1 or PTX (100 mg/kg i.p.). Blood was collected 30 minutes post-injection and serum was analyzed by HPLC. This timepoint was chosen based on the kinetics experiment described above (Fig 3-9).

HPLC chromatographs showed that ciprofloxacin pre-treatment increased serum drug levels following injection of either PTX or M-1 (Fig 3-11). The increase was most dramatic in the group receiving M-1 injections, where serum M-1 levels were increased 3-fold ($p<0.05$; Fig 3-12) compared to serum M-1 levels in mice not pretreated with ciprofloxacin. A statistically significant 2-fold increase in serum drug levels was achieved in all other groups ($p<0.05$). Since the therapeutic effects of PTX or M-1 depend on the total amount of both active compounds in the body, results were graphed as total drug (PTX + M-1) in the serum at 30 minutes post-injection (Fig 3-13). Total drug levels following M-1 injection alone were significantly higher than following PTX injection alone (23.6 ± 1.7 vs. 15 ± 1.0 μg/mL; $p<0.05$). Ciprofloxacin pre-treatment significantly elevated total drug levels following PTX or M-1 injection ($p<0.05$). The

combination of ciprofloxacin and M-1 produced the highest total drug levels (57 ± 3.3 μg/mL), with a significant increase over PTX with ciprofloxacin pre-treatment (28 ± 4.6 μg/mL; $p<0.05$).

3.4.2 Preliminary Assessment of a Cipro/PTX Interaction in Rats

An interaction between ciprofloxacin and PTX in rats has not previously been examined. Since PTX was administered to rats by injection (32 mg/kg i.p.) and enema (64 mg/kg i.c.) in the TNBS experiments (section 2.11.14), we examined serum PTX levels achieved following both routes of administration with and without Cipro pre-treatment (25 mg/kg i.p.) for 9 days. Figure 3-14 shows that PTX levels in serum were not changed with ciprofloxacin pre-treatment when PTX was given by injection (32 mg/kg i.p.) or enema (64 mg/kg i.c.). PTX levels in serum 20 minutes following PTX injection (32 mg/kg i.p.) were approximately 15 μg/ml. Serum levels at 20-minutes post-enema (64 mg/kg i.c.) were approximately 23 μg/ml.

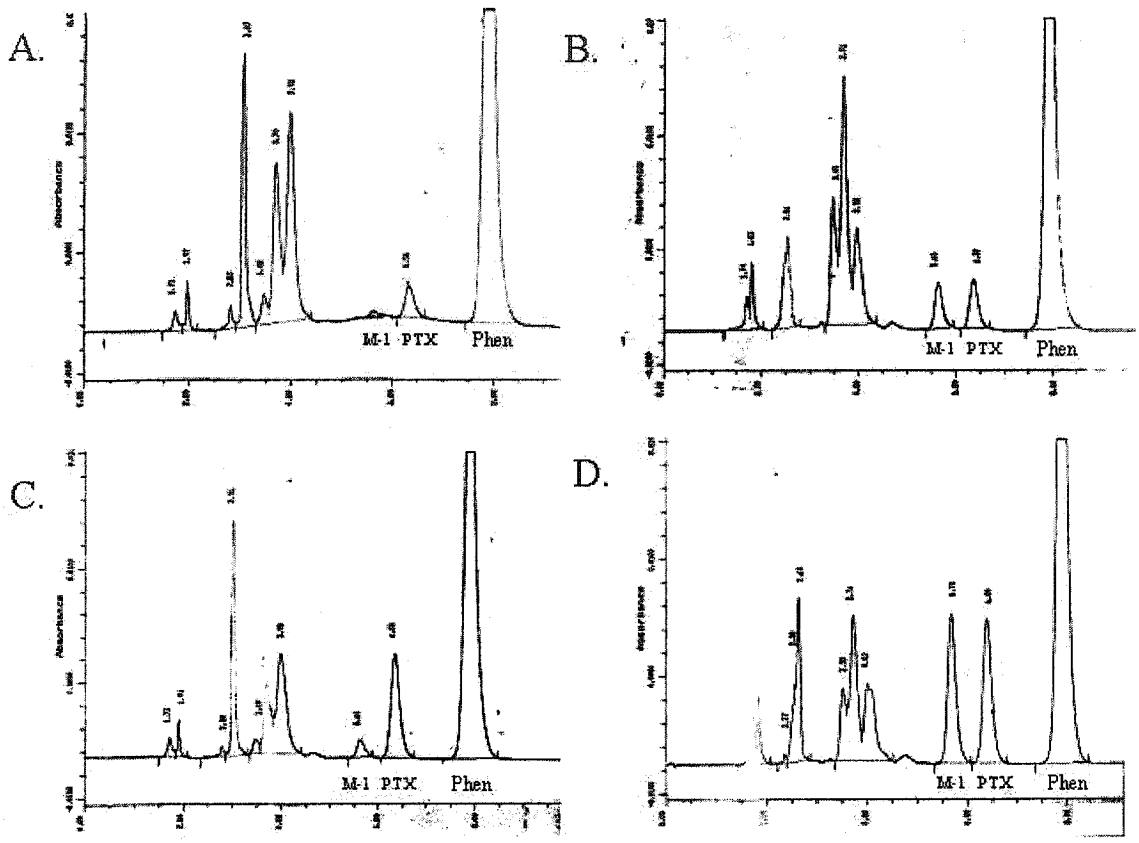

Figure 3-11. Representative HPLC chromatographs demonstrating the effect of ciprofloxacin pre-treatment on serum levels of PTX and M-1. This figure shows the visual difference in HPLC peak area for each drug between treatment groups. Animals were treated with ciprofloxacin (25 mg/kg) or saline for 9 days before receiving an injection of PTX or M-1 (100 mg/kg i.p.). Serum samples were collected 30 minutes after PTX or M-1 injection. **A.** PTX injection (saline pre-treatment). **B.** M-1 injection (saline pre-treatment). **C.** PTX injection (ciprofloxacin pre-treatment). **D.** M-1 injection (ciprofloxacin pre-treatment). Phenacetin (30 μg/mL) was used as the internal standard for all samples so that serum drug levels could be calculated from a standard curve.

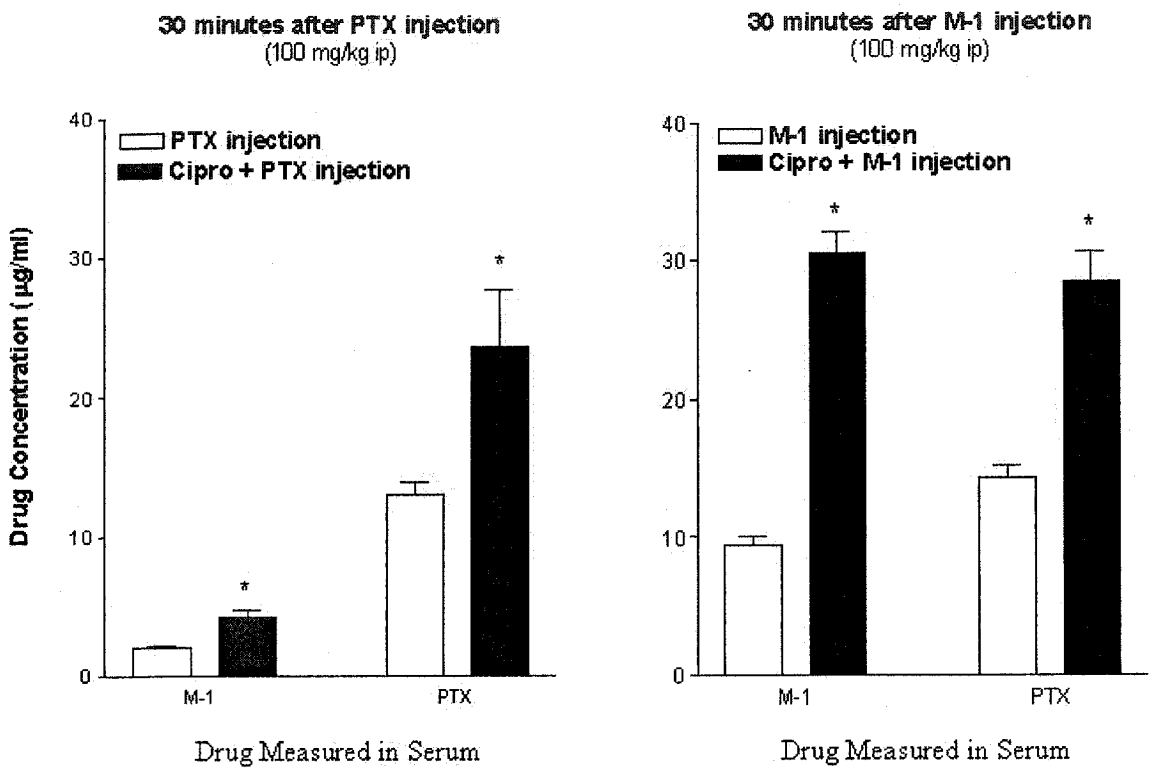

Figure 3-12. Effect of ciprofloxacin pre-treatment on serum levels of PTX and M-1 30-minutes after injection of either drug. Animals were treated with ciprofloxacin (25 mg/kg) or saline for 9 days before receiving an injection of M-1 or PTX (100 mg/kg i.p.). Interconversion of PTX and M-1 takes place *in vivo* thus both compounds are detected in serum after injection of either drug alone. Each bar represents mean drug concentration (µg/ml) ± SEM for 5 animals. Figure is representative of two separate experiments yielding similar results.
* = significant difference from same group without ciprofloxacin pre-treatment; $p<0.05$

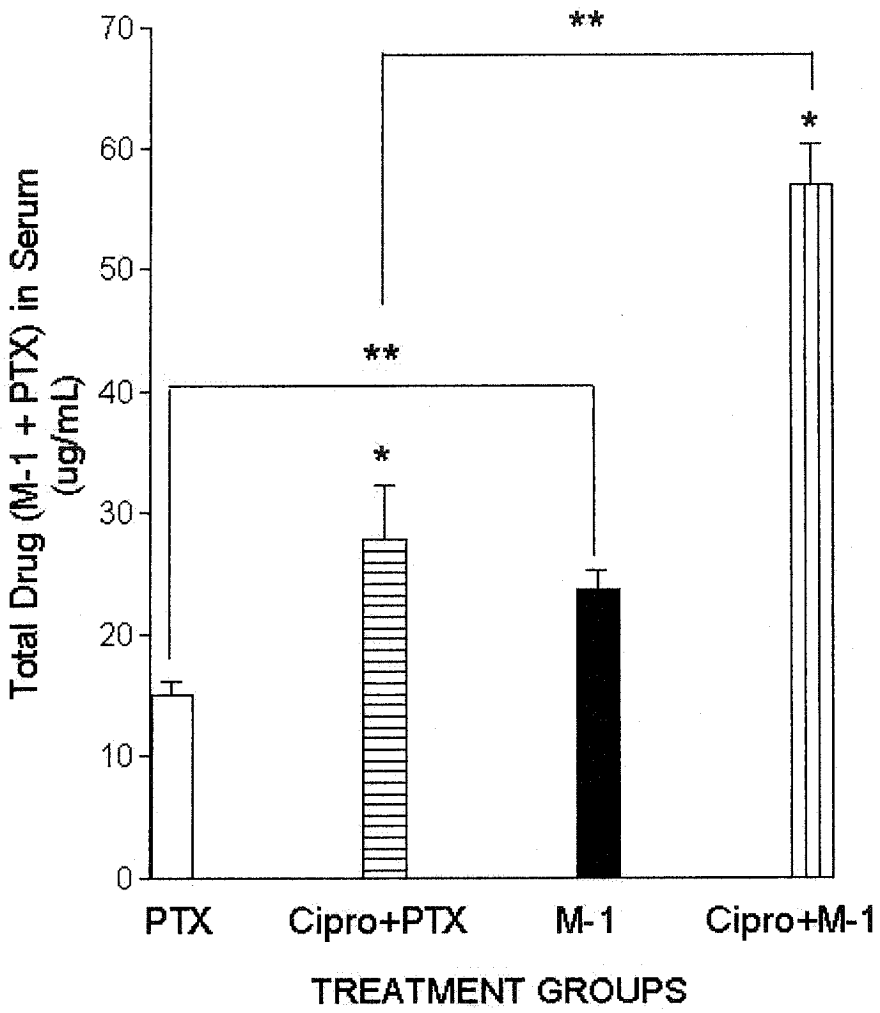

Figure 3-13. Effect of ciprofloxacin pre-treatment on total drug (PTX + M-1) levels in serum 30 minutes after M-1 or PTX injection. Mice were treated with ciprofloxacin (25 mg/kg) of saline for 9 days before receiving an injection of PTX or M-1 (100 mg/kg i.p.). Results are expressed as mean drug concentration (μg/mL) ± SEM for 5 animals. Figure is representative of two separate experiments yielding similar results.
* = significant difference from same group without ciprofloxacin pre-treatment; $p<0.05$
** = significant difference between groups indicated; $p<0.05$

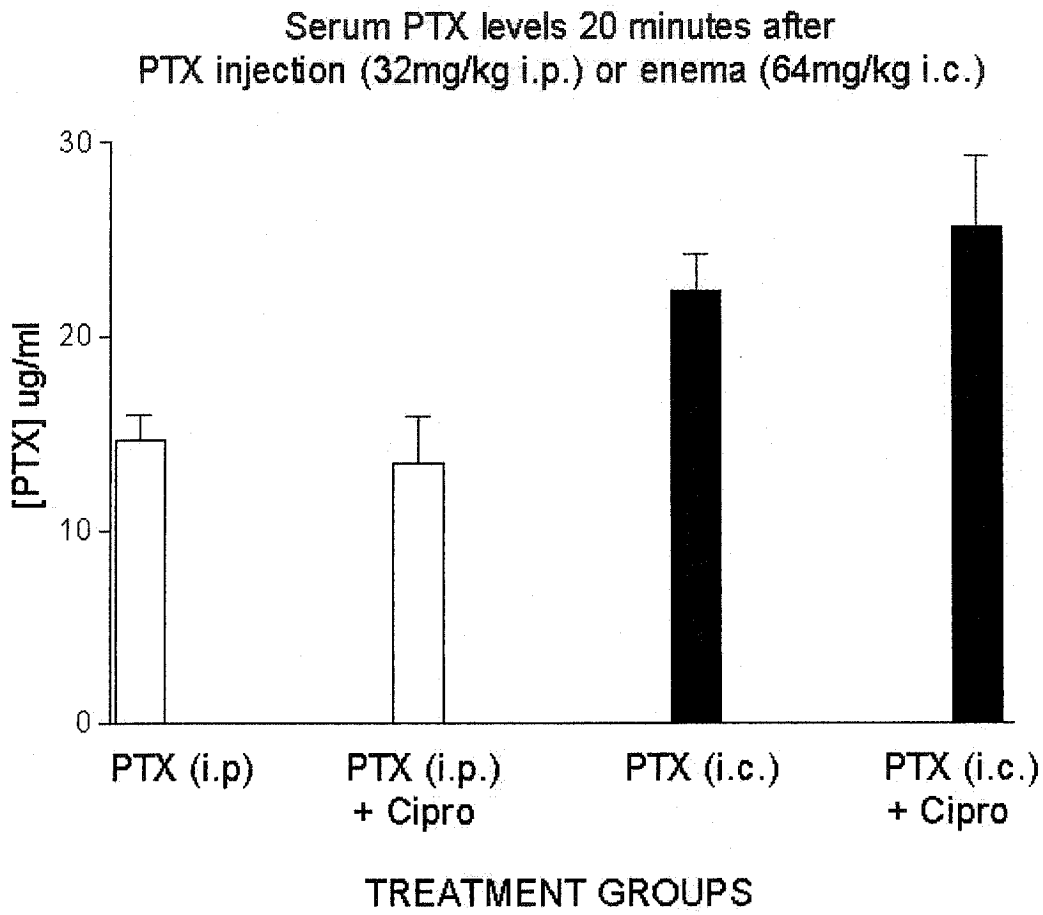

Figure 3-14. Effect of ciprofloxacin pre-treatment on rat serum PTX levels 20 minutes after PTX injection (32 mg/kg i.p.) or enema (64 mg/kg i.c.). Animals were pre-treated with ciprofloxacin (25 mg/kg i.p.) or saline for 9 days before receiving a single PTX injection or enema.

3.5 EFFECTS OF M-1 AND PTX IN TNBS-INDUCED COLITIS

3.5.1 Dose-Response Experiment with TNBS

An initial dose-response experiment was performed in female Sprague-Dawley rats (125-150 g) in order to determine a dose that would produce sufficient reproducible colitis. Previous studies report doses in the range of 15-30 mg/rat using various TNBS preparations and rat strains. We initially tested TNBS at 30 mg/rat (n=3), the most common dose reported in the literature. It was determined that this dose was too high and all animals were sacrificed 5 days after the procedure due to abdominal swelling, lack of fecal output, and emerging evidence of pain behavior. The TNBS used was a powder formulation. We next tested lower doses of TNBS at 15, 17.5, 20, and 25 mg/rat using a 1 M stock solution purchased from Sigma. A dose of 15 mg/rat was chosen as the dose to use in further colitis experiments. Animals receiving 15 mg of TNBS showed reproducible colitis with an average damage score of 6.34. This level of damage was considered sufficient but not excessive. All doses above 15 mg/rat resulted in excessive colon damage and many animals were sacrificed early for ethical reasons. Table 3-1 outlines the results from the TNBS dose-response experiment. In order to further standardize the TNBS dose given to each rat, 90 mg/kg (~12.5-15 mg/rat) was chosen and was administered as described in section 2.11.3. Figure 3-15 shows a cross-section of normal rat colon section (8 μM) that has been stained with hematoxylin and eosin (H&E) in order to visualize normal intestinal tissue architecture. Figure 3-16 compares cross-sections of colon from (A) a saline-treated rat and (B) a rat treated with 90 mg/kg TNBS.

Table 3-1. TNBS DOSE-RESPONSE EXPERIMENT RESULTS

TNBS Dose (mg/rat)	n	Damage Score (Avg)	Colon Weight (g/6cm)	Early Sacrifice (n)
0	4	1	0.6	0/4
15	4	6.34	1.16	0/4
17.5	1	9	1.92	0/1
20	4	9	2.47	2/4
25	4	11.4	*	4/4

* colons not weighed

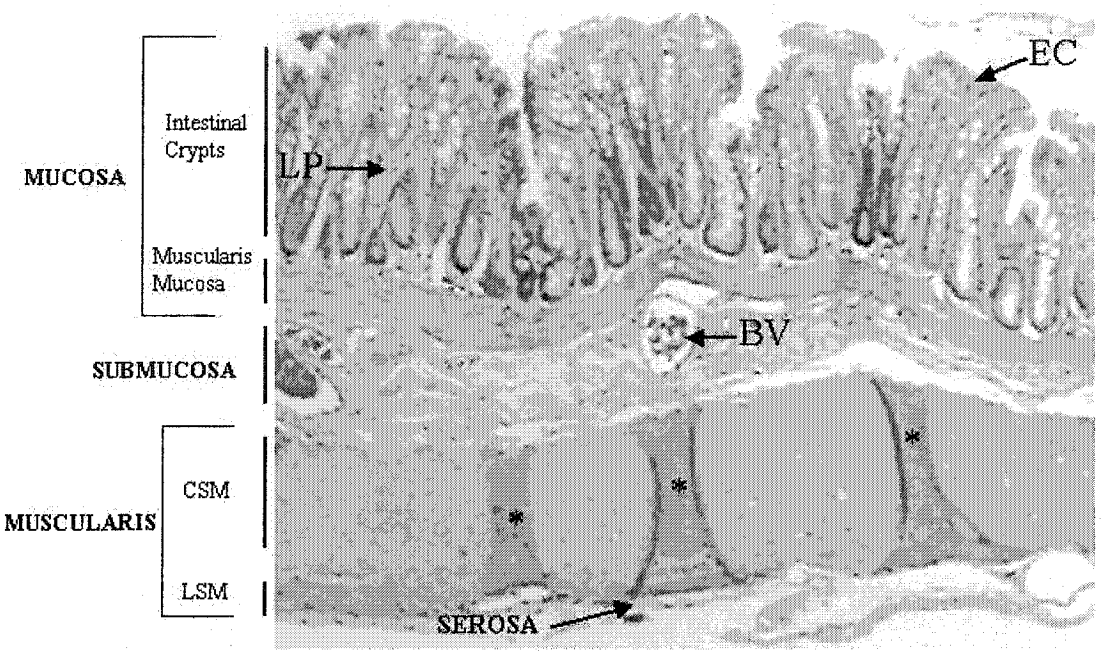

Figure 3-15. Cross-section of a normal rat colon illustrating colon tissue architecture. The four major layers starting at the lumen of the colon are the mucosa (consisting of the intestinal crypts and a two thin bands of circular and longitudinal smooth muscle), the submucosa (containing ECM, BVs, nerves and lymphatic vessels), the muscularis (thick bands of smooth muscle important for contraction), and the serosa (a thin but tough connective tissue layer that supports the intestine). LP=lamina Propria, EC=epithelial cells, BV=blood vessel, CSM=circular smooth muscle, LSM=longitudinal smooth muscle, *=folds in tissue that occurred during mounting (original magnification 100X)

A)

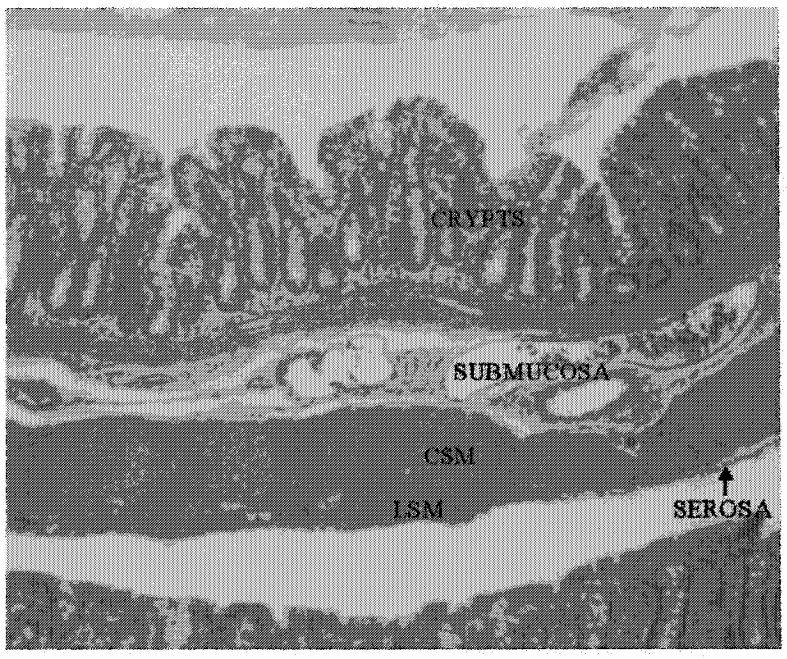

B)

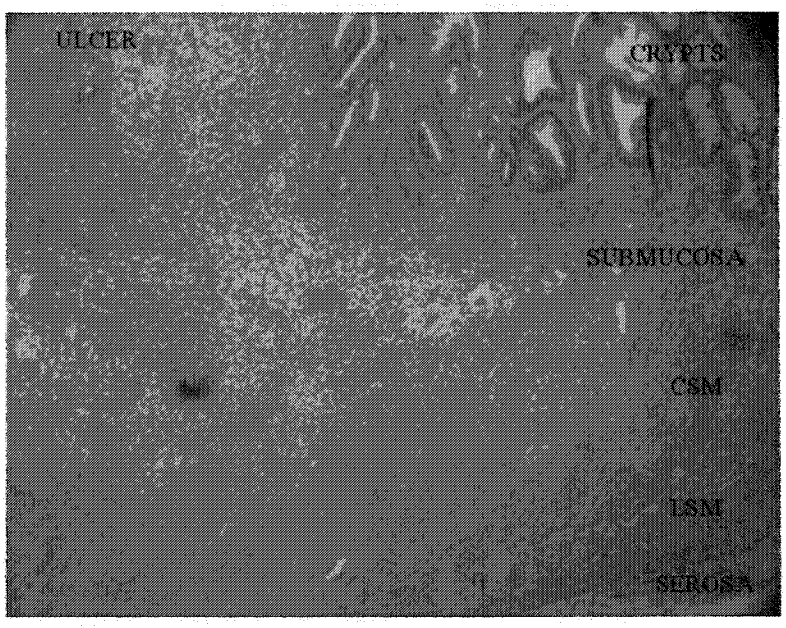

Figure 3-16. Colon sections from (A) saline and (B) TNBS-treated rats (90 mg/kg). Colons were rolled longitudinally, fixed in formalin, and embedded in paraffin before being mounted onto slides (8 μm sections). Sections were stained with hematoxylin and eosin to show tissue morphology. Note the increase in overall thickness of the TNBS-treated colon as well as the dense cellular infiltrate (purple nuclei). There is loss of normal crypt architecture adjacent to sites of ulceration and total crypt loss in the ulcer. CSM=circular smooth muscle, LSM=longitudinal smooth muscle (original mag. 100X)

3.5.2 TNBS-induced Colitis Experiments: Series I

In the first series of experiments, animals received intraperitoneal injections of PTX or M-1 (32 mg/kg) twice daily from days 3-14 of the experiment. The hypothesis was that both PTX and M-1 would attenuate TNBS-induced colitis. Animals were sacrificed on Day 14 and tissue was prepared as described in section 2.11.4.

3.5.2.1 Effect of M-1 and PTX on Colon Weight in TNBS-induced Colitis

Colons were dissected from the peritoneum, were opened longitudinally, cleaned and trimmed to a point 6 cm proximal from the anus. These 6 cm colon segments were weighed. Measuring the weight of the colon tissue (wet weight) gives an estimation of the overall extent of colon damage, since inflammation (due to increased cellular infiltrate) edema (due to inflammation), and fibrosis, increase the weight of the tissue. TNBS-treatment (90 mg/kg) resulted in a significant increase in overall weight of the 6 cm colon segment proximal to the anus that was still evident at day 14 ($0.6 \pm .02$ vs. 1.26 ± 0.1 g; $p<0.05$). Treatment with PTX or M-1 (32 mg/kg i.p. bid) did not affect this TNBS-induced increase in colon weight (Fig 3-17).

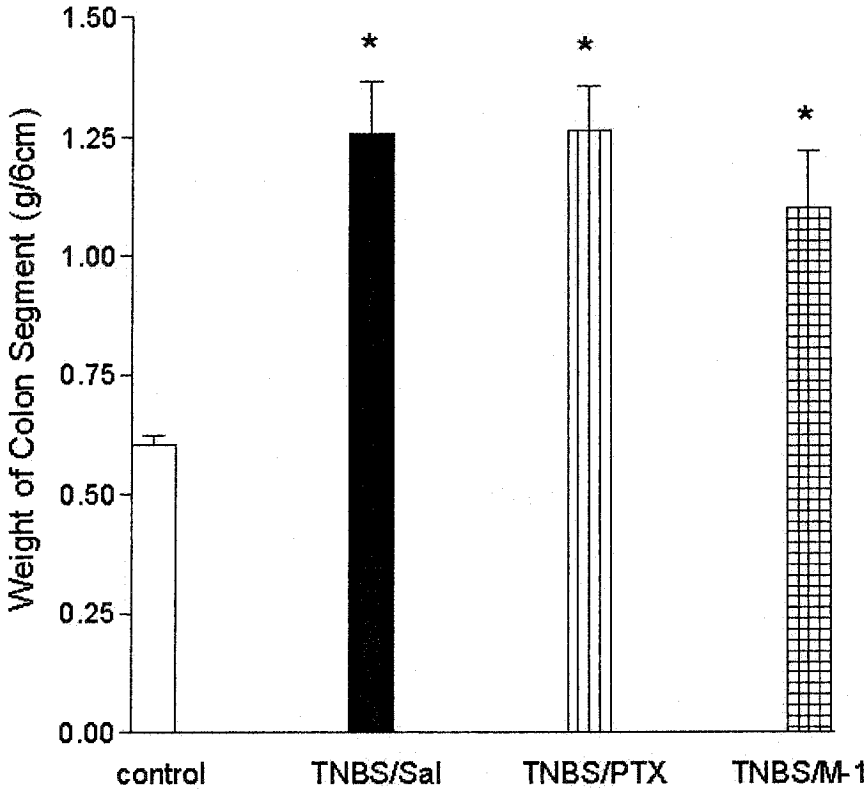

Figure 3-17. Effect of M-1 and PTX on Colon Weight in TNBS-induced Colitis (Series I). Colon wet weight gives a crude estimation of overall colon damage since inflammation, edema, and fibrosis increase colon weight. Rats were treated with M-1 or PTX (32 mg/kg i.p. bid) from days 3-14. Results are mean colon segment weight (g/6 cm) ± SEM (n=10) and are pooled data from two separate experiments with similar results.
* = significant difference from control (saline-treated rats); $p<0.05$

3.5.2.2 *Effect of M-1 and PTX on Colon Damage in TNBS-induced Colitis*

Treatment with TNBS resulted in colitis with an average colon damage score of 6.6 ± 0.5 compared to 1 ± 0.0 in the control group ($p<0.05$). A score of 6 generally represents a colon with a fairly large (>1 cm) area of ulceration. A score of 1 represents a completely normal colon. Treatment with PTX did not improve TNBS-induced colon damage (6.7 ± 0.9). Treatment with M-1 showed a trend toward improvement of colon damage (4.7 ± 0.96; $p=0.07$) but this did not reach statistical significance. Variability within the groups likely prevented achievement of statistical significance indicating that the effects of this drug dose were not consistent enough to show overall significant benefit (Fig 3-18a).

3.5.2.3 Effect of M-1 and PTX on MPO Activity in TNBS-induced Colitis

MPO is an enzyme found predominantly in neutrophils and MPO activity provides an estimation of tissue inflammation. TNBS-treatment resulted in a significant increase in tissue MPO activity compared to controls (9.6 ± 2 vs. 0.5 ± 0.08 units/mg tissue; $p<001$). Treatment with PTX did not significantly reduce TNBS-induced MPO activity in colon tissue (7.04 ± 1.3 units/mg tissue). Treatment with M-1 showed a trend toward reduction of MPO activity (4.9 ± 1.4 units/mg tissue; $p=0.053$) but did not achieve statistical significance. Variability in MPO between colon samples can be quite high (SEM>10 %) so the drug effects need to be very consistent in order to achieve statistical significance (Fig 3-18b).

A)

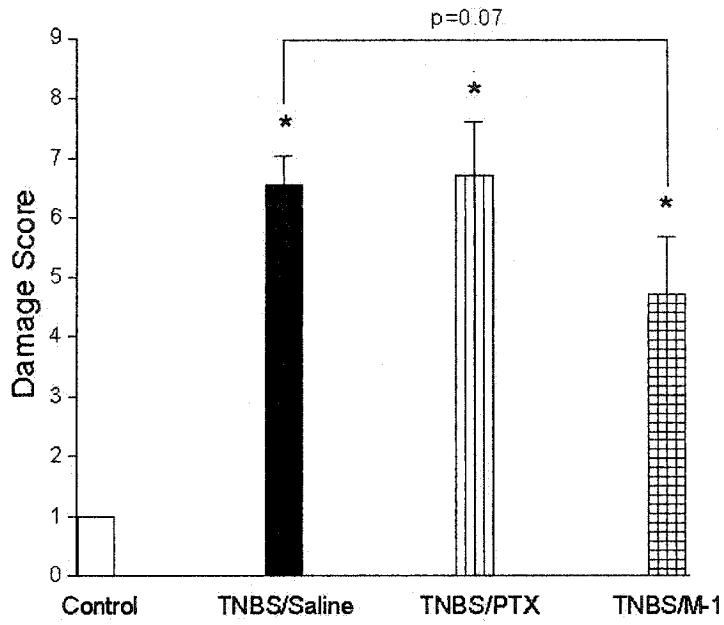

B)

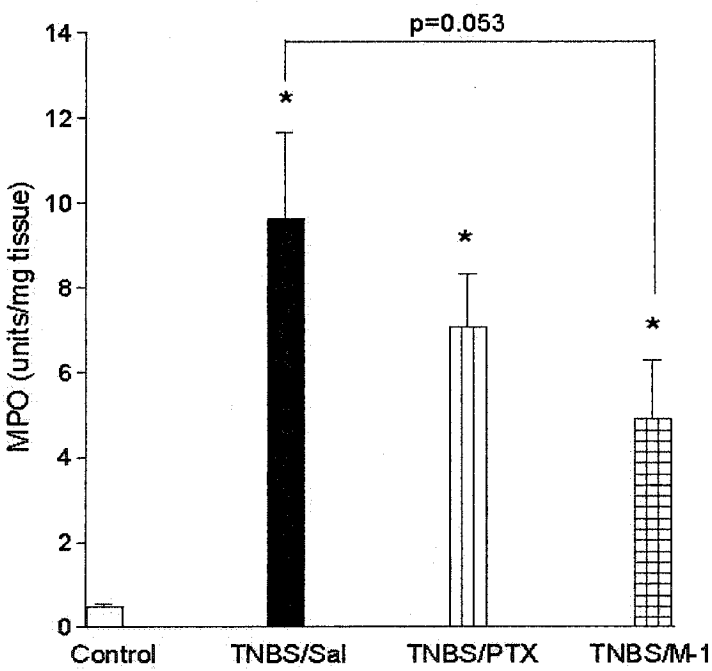

Figure 3-18. Effect of M-1 and PTX on Colon Damage and MPO activity in TNBS-induced Colitis (Series I). Rats were treated with M-1 or PTX (32 mg/kg i.p. bid) from days 3-14. Results are mean ± SEM (n=10) and are pooled data from two separate experiments with similar results.
* = significant difference from controls (saline-treated rats); $p<0.05$

3.5.3 TNBS-Induced Colitis Experiments: Series II

Based on the results from the first series of TNBS experiments (section 3.5.2), it was hypothesized that if the treatment dose of PTX and M-1 was increased, attenuation of TNBS-induced colitis would be achieved. When the dose was doubled to 64 mg/kg (i.p.), mild side effects were observed for approximately 15 minutes after injection of PTX or M-1 (dizziness, excessive licking movements). Rather than increasing the number of injections given per day, it was decided to change the route of administration and deliver the drug directly to the site of damage (the colon). Thus in the second series of experiments, rats received PTX or M-1 (64 mg/kg bid) intracolonically from days 3-14 after TNBS-administration. No side effects were observed. Additional control groups were added in this series to examine the effects of PTX and the novel M-1 on colon tissue in saline-treated rats not exposed to TNBS. Experiments are described in detail in section 2.11.4.

3.5.3.1 Effect of PTX and M-1 on Colon Weight in TNBS-induced Colitis

Measuring colon wet weight gives a crude indication of parameters such as inflammation, edema, and fibrosis occurring in the tissue. Induction of colitis with TNBS caused a significant increase in colon wet weight compared to saline treated controls (1.40 ± 0.2 vs. 0.54 ± 0.02 g/6cm; $p<0.001$) (Fig 3-19). In the TNBS-induced colitis group, treatment with M-1 for 11 days significantly reduced colon segment weight compared to TNBS-treated animals (0.86 ± 0.06 vs. 1.40 ± 0.2 g/6cm; $p<0.001$), while

PTX treatment did not reach statistical significance (1.17 ± 0.1 vs. 1.40 ± 0.2 g/6cm; p=0.074). There was no difference between drug-treated controls and saline-treated controls indicating that PTX and M-1 had no effect on baseline colon segment weight.

3.5.3.2 Effect of PTX and M-1 on Colon Damage in TNBS-induced Colitis

Morphology Damage score (D.S.) was calculated using a well-established scoring system described in section 2.11.5. Treatment with TNBS caused significant colitis with an average damage score of 6.9 ± 0.8 compared to control animals not exposed to TNBS (1 ± 0; $p<0.001$) (Fig 3-20). Intracolonic treatment with PTX or M-1 (64 mg/kg bid) from days 3-14 significantly attenuated the damage induced by TNBS (4.6 ± 0.9 and 4.2 ± 0.6 respectively, vs. 6.9 ± 0.8; $p<0.01$). A damage score of 4 generally corresponds to a small area of ulceration and/or inflammation (<1 cm) without adhesions or episodes of diarrhea. Colons from PTX- and M-1-treated animals not exposed to TNBS were normal in appearance (D.S. = 1). One exception was an M-1 treated animal who received a score of 2 for a small site of hyperemia (redness), possibly a result of the previous enema procedure.

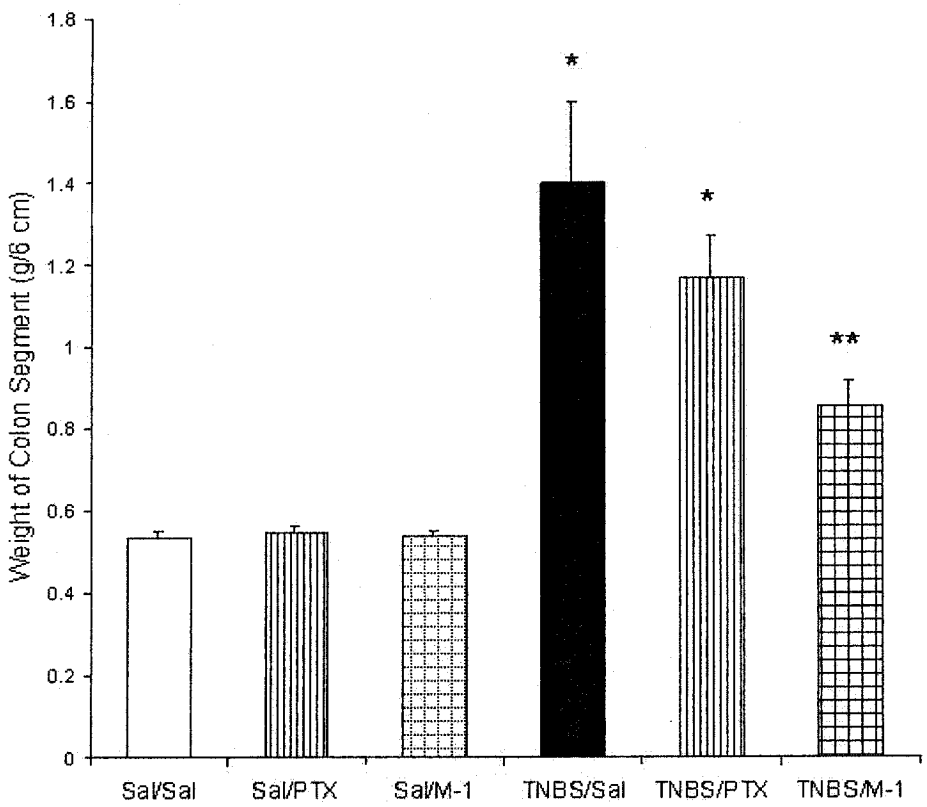

Figure 3-19. Effect of M-1 and PTX on Colon Weight in TNBS-induced Colitis (Series II). Colon wet weight gives a crude estimation of overall colon damage since inflammation, edema, and fibrosis increase colon weight. Rats were treated with M-1 or PTX (64 mg/kg i.c. bid) from days 3-14 following exposure to TNBS (90 mg/kg) or saline. Results are mean colon weight (g/6 cm) ± SEM (n=8) and are pooled data from two separate experiments with similar results.
* = significant difference from control (saline-treated rats); $p<0.05$
** = significant difference from TNBS/Sal; $p<0.05$

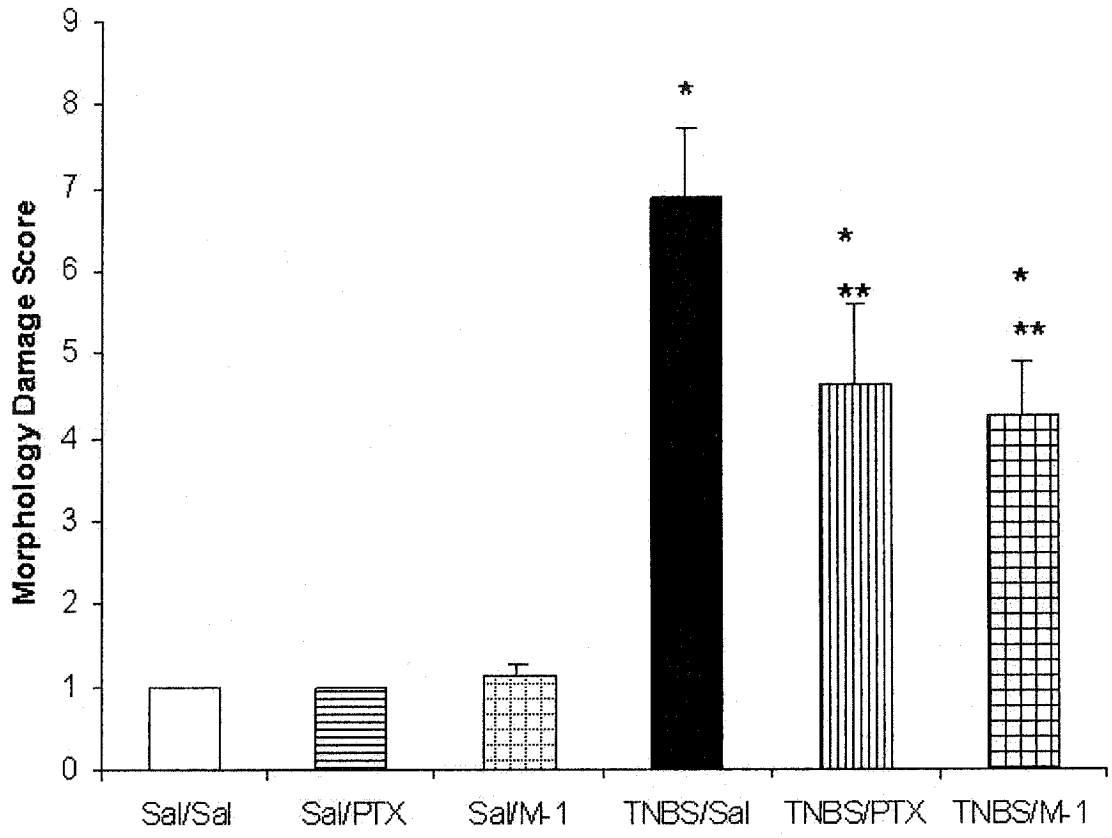

Figure 3-20. Effect of M-1 and PTX on Colon Damage in TNBS-induced Colitis (Series II). Colon Damage was measured using a well-established scoring system described in section 2.11.5. Rats were treated with M-1 or PTX (64 mg/kg i.c. bid) from days 3-14. Results are mean damage score ± SEM (n=8) and are pooled data from two separate experiments with similar results.
* = significant difference from controls (saline-treated rats); $p<0.05$
** = significant difference from TNBS/Sal; $p<0.05$

3.5.3.3 Effect of PTX and M-1 on MPO Activity in TNBS-Induced Colitis

MPO is an enzyme stored in the primary granules of neutrophils that is released upon degranulation and causes tissue destruction. Measuring MPO activity in colon homogenates gives an estimation of neutrophil infiltration and thus inflammation in the tissue. MPO activity is reported in units per mg of tissue, where 1 unit of MPO activity is the activity to convert 1 micromole of H_2O_2 , which corresponds to a change in absorbance of $1.13x10^{-2}$. MPO activity in colon tissue from control animals not exposed to TNBS was very low (0.36 ± 0.1 units/mg tissue). Treatment of control animals with PTX or M-1 had no effect on basal MPO activity (Fig 3-21). Colitis induced by TNBS (90 mg/kg) resulted in significantly elevated tissue MPO levels at day 14 compared to controls (10.1 ± 3 vs. 0.36 ± 0.1 units/mg tissue; $p<0.001$). Intracolonic treatment with PTX or M-1 (64 mg/kg bid) from days 3-14 significantly attenuated the TNBS-induced increase in tissue MPO activity (5.4 ± 2 and 3.7 ± 1 units/mg tissue respectively, vs. 10.1 ± 3 units/mg tissue; $p<0.05$). Tissue for analysis of MPO activity was taken from sites of colon damage. MPO activity in non-involved sections of colon from TNBS-treated rats was similar to controls (data not shown). The change in MPO activity over time in this model corresponded with inflammatory infiltrate in the tissue visualized in H&E-stained colon sections (Fig 3-22). An assessment of MPO activity in colon tissue at 12 and 24 hours post-TNBS (Fig 3-23) revealed an early peak in MPO activity that subsided by 24-hours and was followed by a second peak at 7 days when combined with the data from Fig 3-23. Inflammatory infiltrate in the tissue was not assessed by H&E at these timepoints.

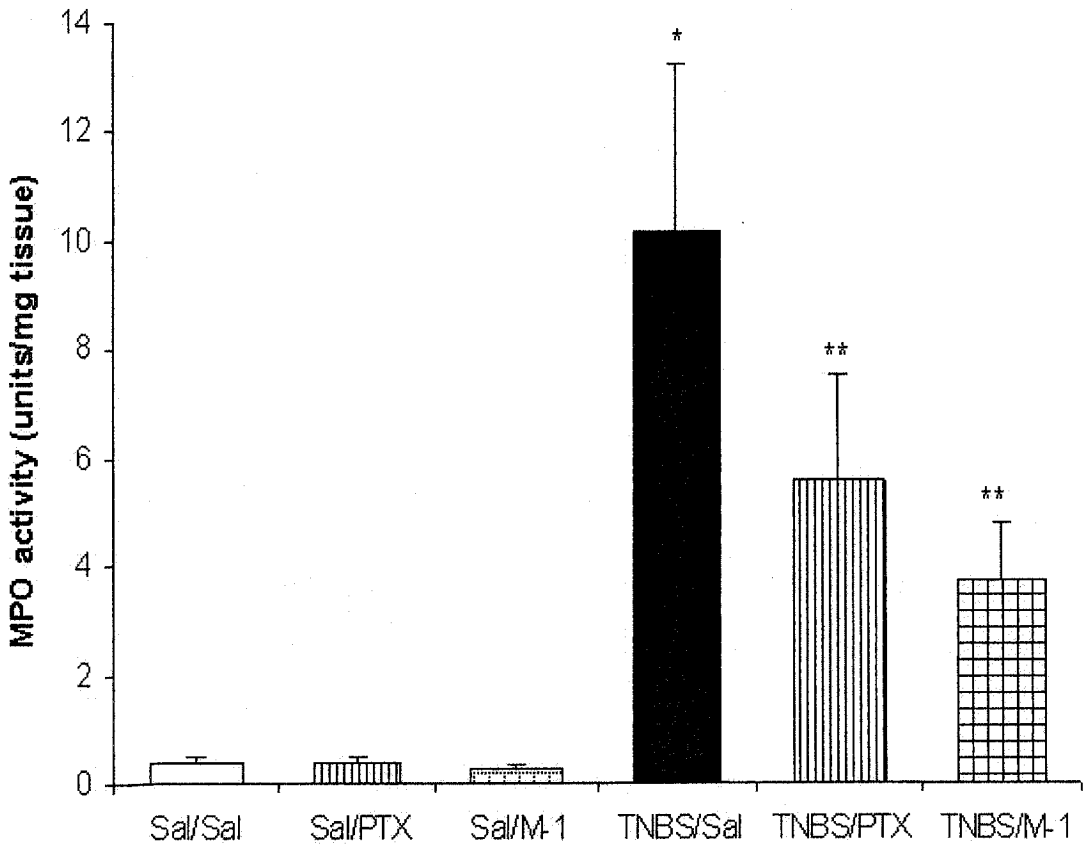

Figure 3-21. Effect of M-1 and PTX on MPO Activity in TNBS-induced Colitis (Series II). MPO is an enzyme synthesized predominantly by neutrophils and MPO activity gives an estimation of inflammation in the colon tissue. Rats were treated with M-1 or PTX (64 mg/kg i.c. bid) from days 3-14. Results are mean MPO activity (units/mg tissue) ± SEM (n=8) and are pooled results from two separate experiments with similar results.

* = significant difference from controls (saline-treated rats); $p<0.05$

** = significant difference from TNBS/Sal; $p<0.05$

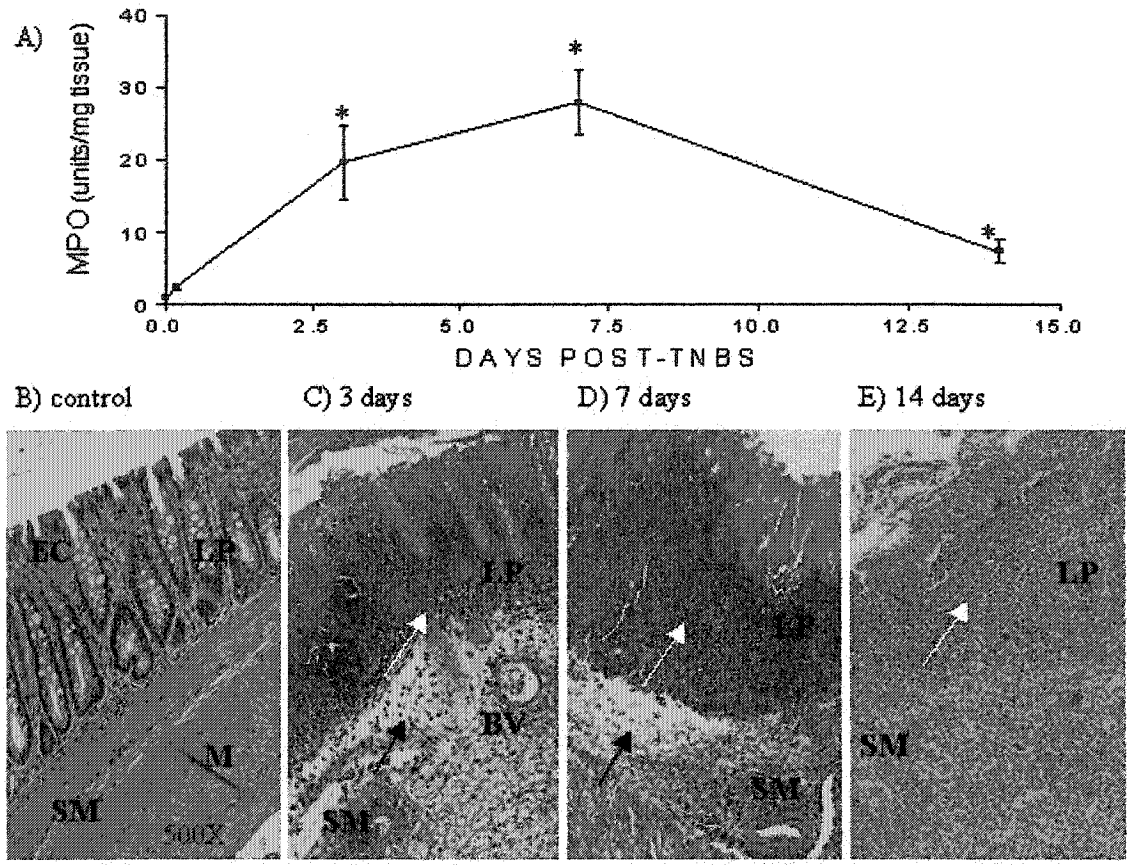

Figure 3-22. Changes in MPO activity and inflammatory infiltrate over time in TNBS-induced colitis. **A.** MPO activity in rat colon tissue was significantly elevated by 3 days post-TNBS and was further increased at day 7 ($p<0.001$). MPO levels decreased by more than 50 % by day 14 but still remained significantly elevated compared to controls ($p<0.001$). These changes in MPO activity correspond with inflammatory infiltrate seen in H&E-stained colon sections (B-E). **B.** Section of colon from a control animal. Note the intact epithelial cell layer (EC), normal crypt formation and basal level of inflammatory cells in the lamina propria (LP) seen as dark purple nuclei. The submucosal layer (SM) is seen as a narrow band between the mucosa and the muscularis (M). **C.** At day 3 post-TNBS, edema was present in the thickened submucosa (black arrows) due to leaky blood vessels (BV). The infiltration of inflammatory cells into the LP (white arrows) corresponded with the significant increase in MPO activity. **D.** At day 7 post-TNBS, there was still evidence of edema in the SM, and the inflammatory infiltrate extending into the LP was thick and dense corresponding with high MPO activity. Note abnormal appearance of the epithelial layer and crypt architecture. **E.** By day 14 post-TNBS, the epithelial layer and crypts were completely destroyed at sites of ulceration and a heavy inflammatory infiltrate was present with increased cellularity in all layers of the intestine. This cellular infiltrate was less dense than at days 3 and 7 and this was reflected in MPO activity.

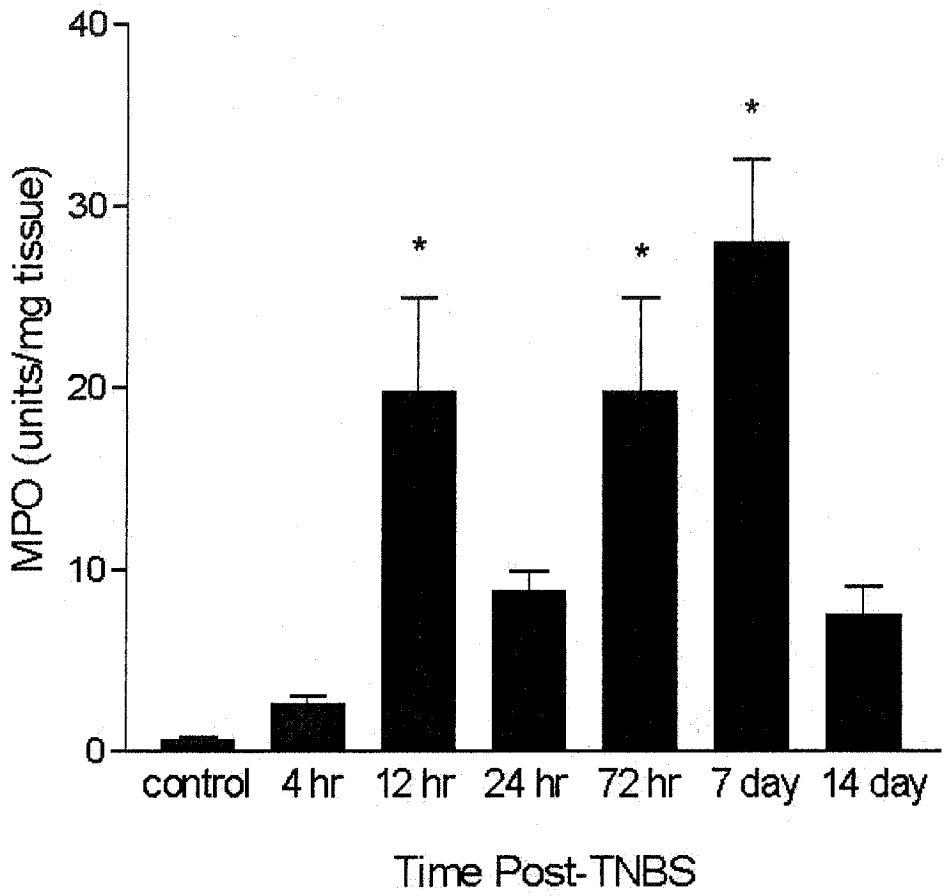

Figure 3-23. Biphasic elevation in MPO activity over time in TNBS-induced colitis. Rats were treated with TNBS (90 mg/kg) and were sacrificed after 12 and 24 hours (n = 3/group). This MPO data was combined with data from Fig 3-23. A biphasic elevation in MPO activity was revealed with an initial peak at 12 hours and a later peak at 7 days post-TNBS.
* = significant difference from control ($p<0.05$)

3.5.4 TNBS-Induced Colitis Experiments: Series III

In the final series of TNBS-experiments, PTX and M-1 (or saline) treatments were initiated 1-hr post-TNBS administration based on the hypothesis that earlier initiation of drug treatment would further enhance the therapeutic effects of M-1 and PTX compared to series II experiments where treatment was initiated 72 hrs post-TNBS.

3.5.4.1 Colon Weight in TNBS-induced Colitis (Series III)

The effect of TNBS on colon segment weight was not significantly different from controls at day 14 when saline treatment was initiated 1 hr post-TNBS (0.9 ± 0.09 vs. 0.06 ± 0.03). There was no significant difference in colon weight between any of the groups in this experiment (Fig 3-24A). Initiating saline treatment 1 hr post-TNBS attenuated the effect of TNBS on colon weight at 7 and 14 days post-TNBS (Fig 3-24B) compared to initiating saline treatment 72 hrs post-TNBS as in Series I and II.

3.5.4.2 Damage Score in TNBS-induced Colitis (Series III)

The effect of TNBS on colon damage was not significantly different from controls at day 14 when saline treatment was initiated 1 hr post-TNBS (3.6 ± 1.3 vs. 1 ± 0.0). There was no significant difference in colon damage between any of the groups in this experiment (Fig 3-25A). Initiating saline treatment 1 hr post-TNBS dampened the effect of TNBS on colon damage at 3, 7, and 14 days post-TNBS (Fig 3-25B).

A)

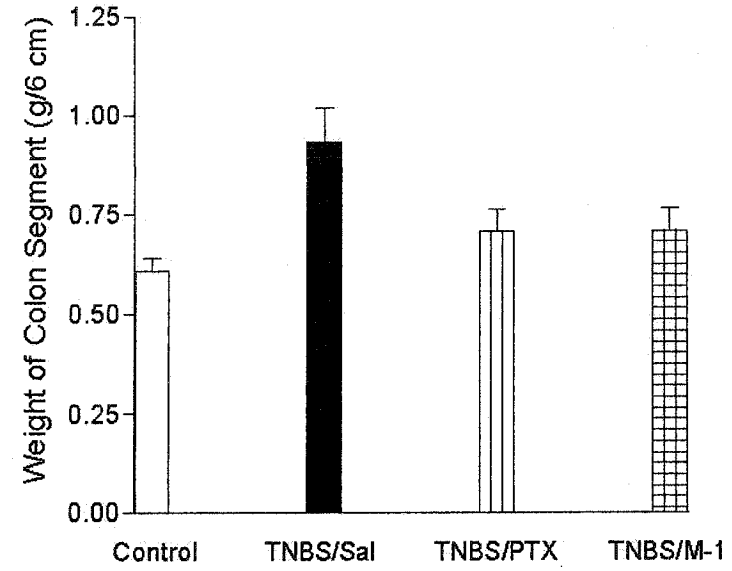

B)

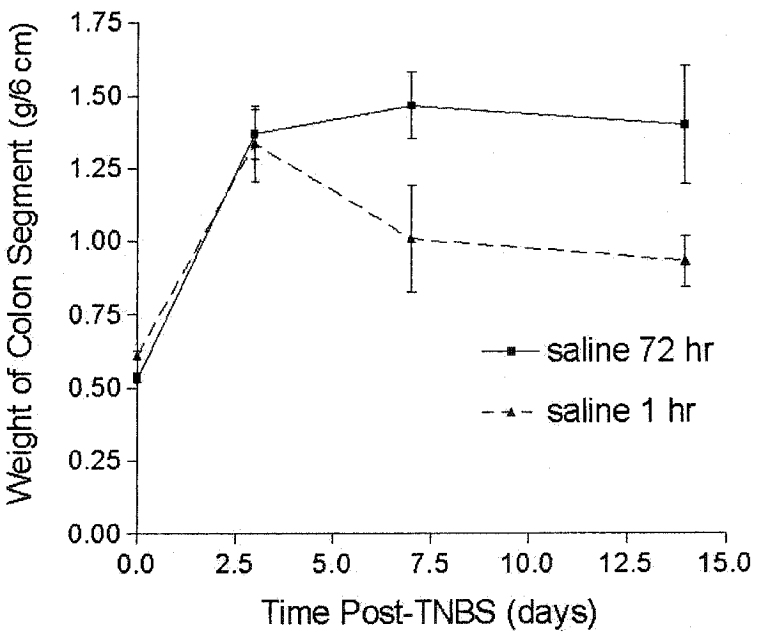

Figure 3-24. Colon Weight in TNBS-induced Colitis (Series III). **A.** Effect of M-1 and PTX treatment (64 mg/kg i.c. bid) on colon segment weight when treatment was initiated 1 hr-post TNBS (90 mg/kg). Saline treatment was initiated 1 hr post-TNBS in the experimental colitis group (TNBS/Sal) as a control. No significant differences were seen between groups. **B.** Washout effect caused by initiating saline treatment (i.c.) 1 hr post-TNBS administration. The effect of TNBS on colon segment weight was diminished when saline treatment was initiated 1hr post-TNBS (saline 1 hr) compared to 72 hrs post-TNBS as in series I and II (saline 72 hr). (n=5)

A)

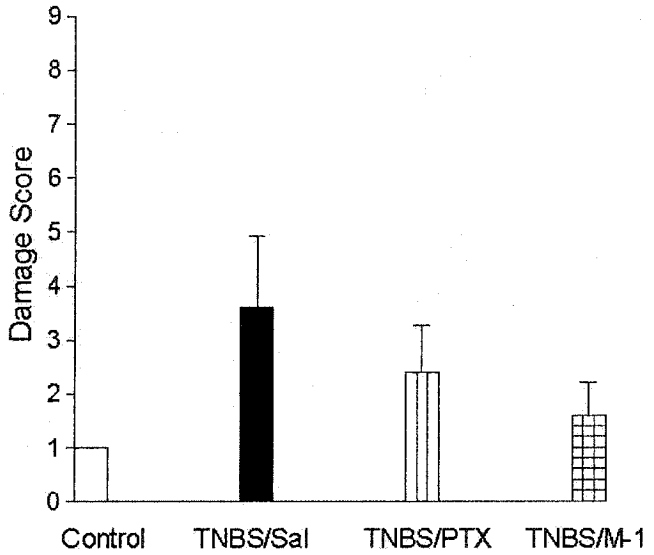

B)

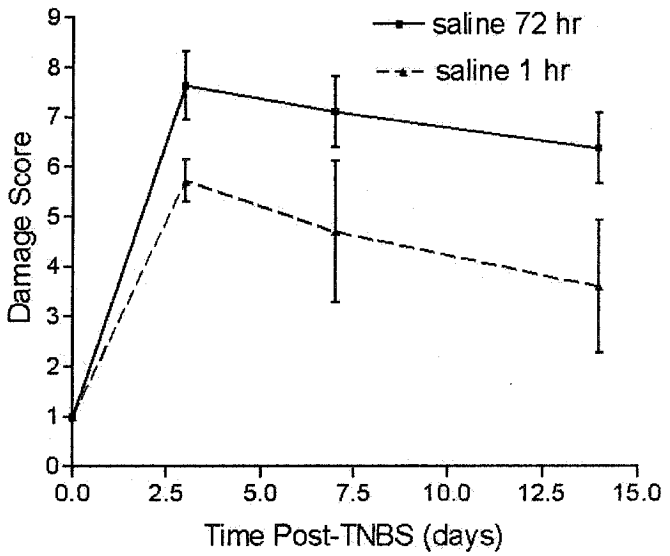

Figure 3-25. Damage Score in TNBS-induced Colitis (Series III). **A.** Effect of M-1 and PTX treatment (64 mg/kg i.c. bid) on colon damage when treatment was initiated 1 hr-post TNBS (90 mg/kg). Saline treatment was initiated 1 hr post-TNBS in the experimental colitis group (TNBS/Sal) as a control. No significant differences were seen between groups. **B.** Washout effect caused by initiating saline treatment (i.c.) 1 hr post-TNBS administration. The effect of TNBS on colon damage was diminished when saline treatment was initiated 1 hr post-TNBS (saline 1 hr) compared to 72 hrs post-TNBS as in series I and II (saline 72 hr). (n=5)

3.5.4.3 *MPO Activity in TNBS-induced Colitis (Series III)*

The effect of TNBS on MPO activity was not significantly different from controls at day 14 when saline treatment was initiated 1hr post-TNBS (2.9 ± 0.6 vs. 1.1 ± 0.9). There was no significant difference in MPO activity between any of the groups in this experiment (Fig 3-26A). Initiating saline treatment 1 hr post-TNBS significantly dampened the effect of TNBS on MPO activity at 3, 7, and 14 days compared to initiating saline treatment 72 hrs post-TNBS ($p<0.05$; Fig 3-26B).

A)

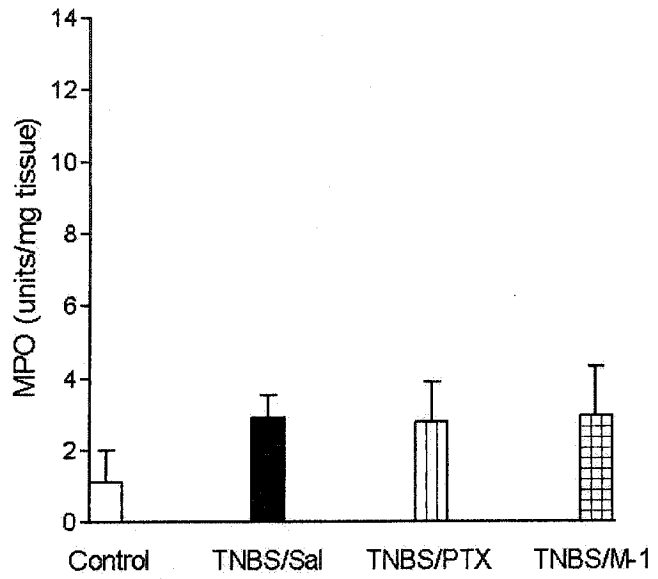

B)

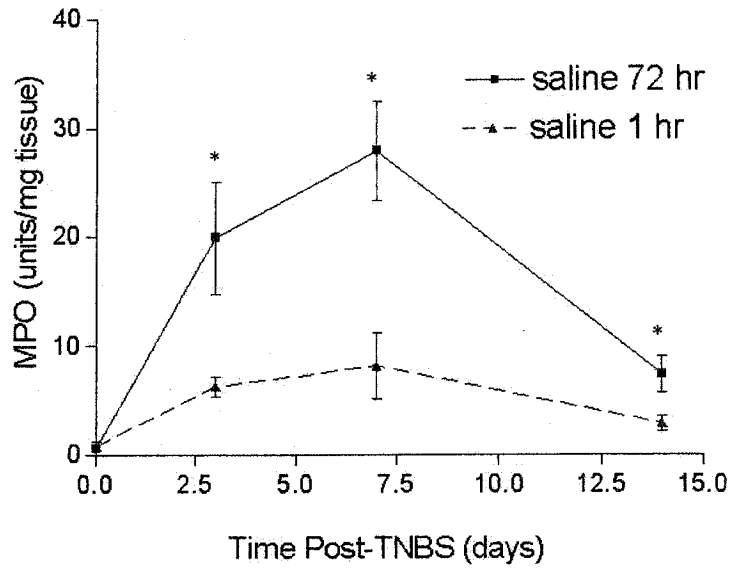

Figure 3-26. MPO Activity in TNBS-induced Colitis (Series III). **A.** Effect of M-1 and PTX treatment (64 mg/kg i.c. bid) on MPO activity when treatment was initiated 1 hr-post TNBS (90 mg/kg). Saline treatment was initiated 1 hr post-TNBS in the experimental colitis group (TNBS/Sal) as a control. No significant differences were seen between groups. **B.** Washout effect caused by initiating saline treatment (i.c.) 1 hr post-TNBS administration. The effect of TNBS on MPO activity was significantly diminished when saline treatment was initiated 1 hr post-TNBS (saline 1 hr) compared to 72 hrs post-TNBS as in series I and II (saline 72 hr). (n=5)
* = significant difference from same timepoint with washout effect ($p<0.05$, t-test).

3.6 EFFECT OF M-1 AND PTX ON FIBROSIS IN TNBS-INDUCED COLITIS

In order to determine if M-1 and PTX exert effects on intestinal fibrosis in TNBS-induced colitis, we examined maximum colon thickness (lumen to serosa) from H&E-stained colon sections (see Fig 3-16) and modified the well-established Sirius Red/Fast Green method of tissue collagen quantitation (section 2.13.1) for use in an inflammatory disease model. We also examined collagen type III by immunohistochemistry of PFA-fixed paraffin-embedded colon sections and collagen type I in colon tissue by Western immunoblotting to determine if these collagens were increased in TNBS-colitis. All tissues examined were from Series II TNBS-experiments.

3.6.1 Effect of PTX and M-1 on Colon Thickness in TNBS-induced Colitis

Colon thickness increases with fibrosis and muscularis overgrowth (along with edema and inflammation) in colon tissue. This is similar to the bowel wall thickening seen in CD. Colon thickness (lumen to serosa) was measured at its maximum point using a light microscope (magnification 25X) with a scale embedded in the eyepiece. The scale units were converted to millimeters (mm) using a standard transparent ruler. Data are expressed as mean maximum colon thickness (mm) ± SEM (Fig 3-27). TNBS induced a significant increase in maximum colon thickness compared to controls at day 14 (2.1 ± 0.2 vs. 0.7 ± 0.05 mm; $p<0.05$). While PTX treatment failed to produce a significant effect, M-1 treatment significantly reduced maximum colon thickness in TNBS-treated rats (1.4 ± 0.1 vs. 2.1 ± 0.2 mm; $p<0.05$).

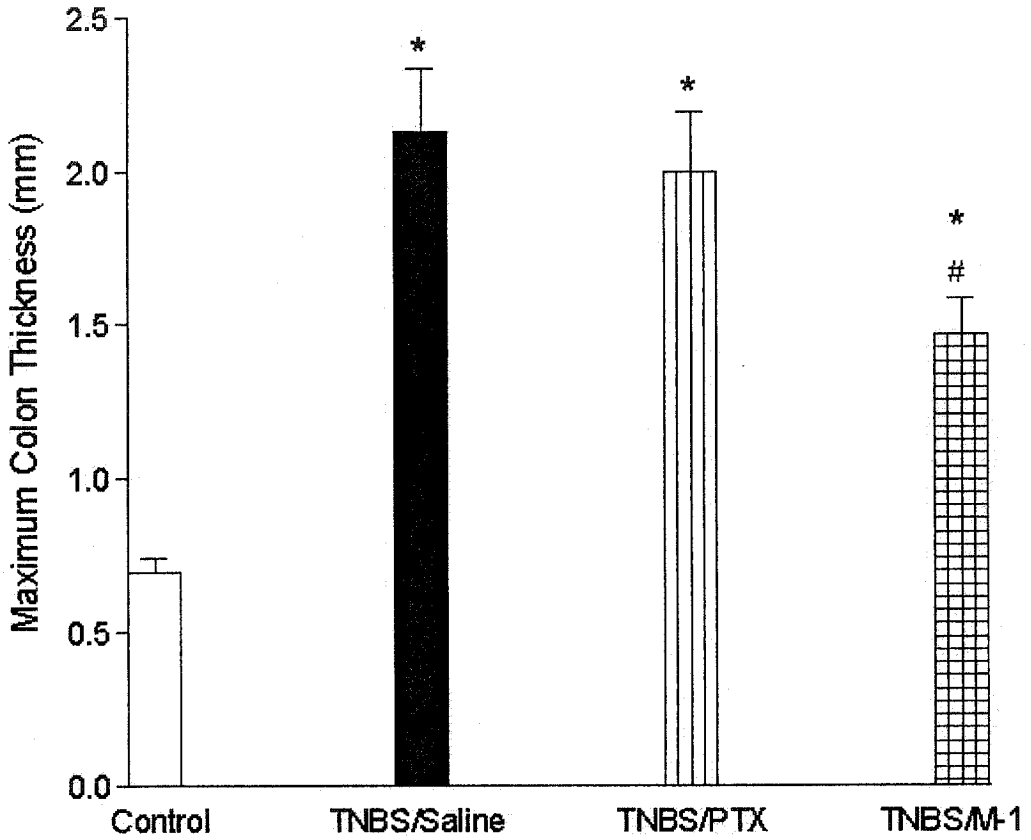

Figure 3-27. Effect of M-1 and PTX on Colon Thickness in TNBS-induced colitis. Maximum bowel thickening was measured as a crude estimate of fibrosis and damage in the tissue. Measurements were taken from slides of H&E-stained colon sections using a light microscope equipped with a scale in the eyepiece (mag 25X). Data are expressed as mean maximum colon thickness (mm) ± SEM and are pooled data from two separate experiments with similar results (n=8).
* = significant difference from controls ($p<0.05$)
# = significant difference from TNBS/Saline ($p<0.05$)

3.6.2 Collagen Quantitation in Colon Tissue by Sirius Red/Fast Green Method

A preliminary assessment of peak absorbance values for Sirius Red and Fast Green was performed (Fig 3-28). A mixture of 1 % Fast Green/ 0.04 % Sirius Red in saturated picric acid was read over a wide range of wavelengths (nm) to determine peak absorbance values for each dye. Peak absorbance for Sirius Red was 535 nm and for Fast Green was 604 nm (Fig 3-28). These were the wavelengths used in the SR/FG (staining and elution) method described in detail in section 2.13.1.

3.6.3 Modification of the SR/FG Method to Measure Collagen in Inflamed Tissue

The well-established method for tissue collagen quantitation, originally described by Lopez-de Leon and Rojkind (1985), was modified for use in an inflammatory disease model. In an inflammatory environment, the protein content of the tissue is increased due to factors such as invading inflammatory cells and hyperproliferation of resident cells, and this must be accounted for when assessing tissue collagen levels. When expressed on a μg collagen/mg protein basis, the collagen "ratio" was not different between saline- and TNBS-treated rats (Fig 3-29). However, it was obvious from the SR/FG-stained colon sections that collagen levels were increased in TNBS-treated colon tissue especially at sites of damage (Fig 3-30). It was apparent that cellular density was increased in colitic tissue as well. Thus, as collagen protein was increasing in the tissue, so was overall protein, resulting in minor changes in the ratio of collagen to total protein. This ratio was therefore corrected for colon weight and protein concentration of the tissue.

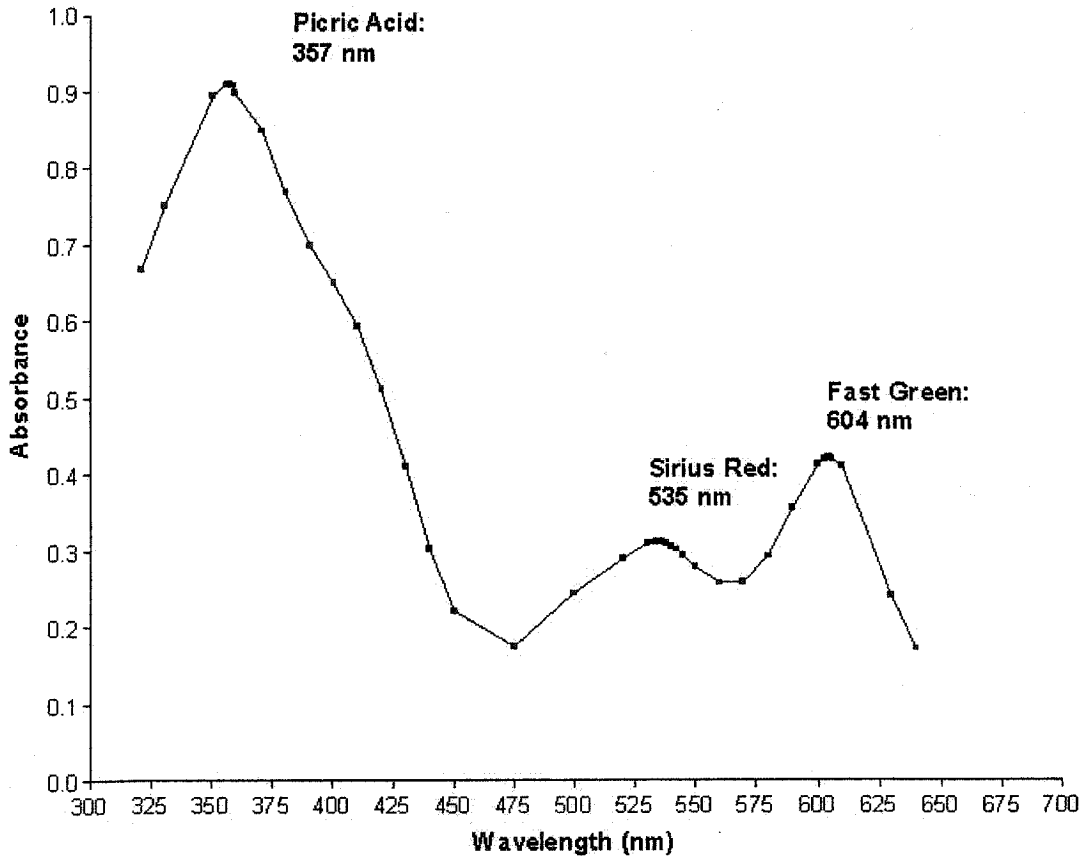

Figure 3-28. Peak absorbance values for Sirius Red and Fast Green using the Milton Roy Spectronic 1001 Plus spectrophotometer. A mixture of 0.1 % Fast green/0.04 % Sirius red in saturated picric acid was read at a wide range of wavelengths (nm) to determine the maximum absorbance values for Sirius Red and Fast Green. These were the values used in the SR/FG collagen quantitation method described in section 2.13.1.

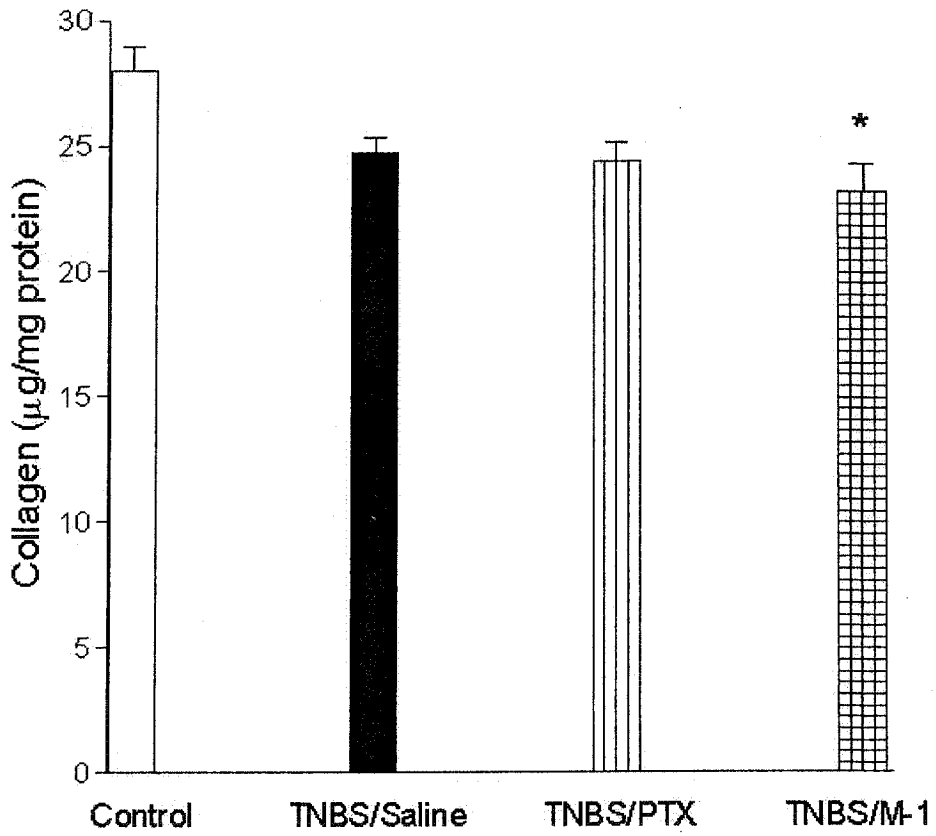

Figure 3-29. Collagen in colon tissue sections using the SR/FG method. Collagen in PFA-fixed paraffin-embedded colon sections (8 µm) was determined using the SR/FG method of staining and elution. Results are expressed as mean collagen (µg/mg protein) ± SEM (n=8).
* = significant difference from controls ($p<0.05$)

A)

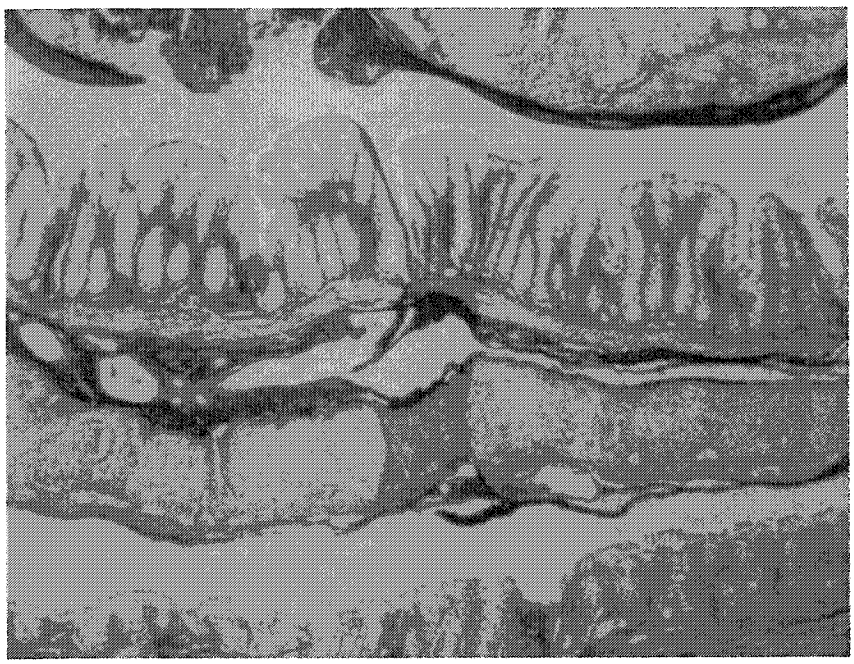

B)

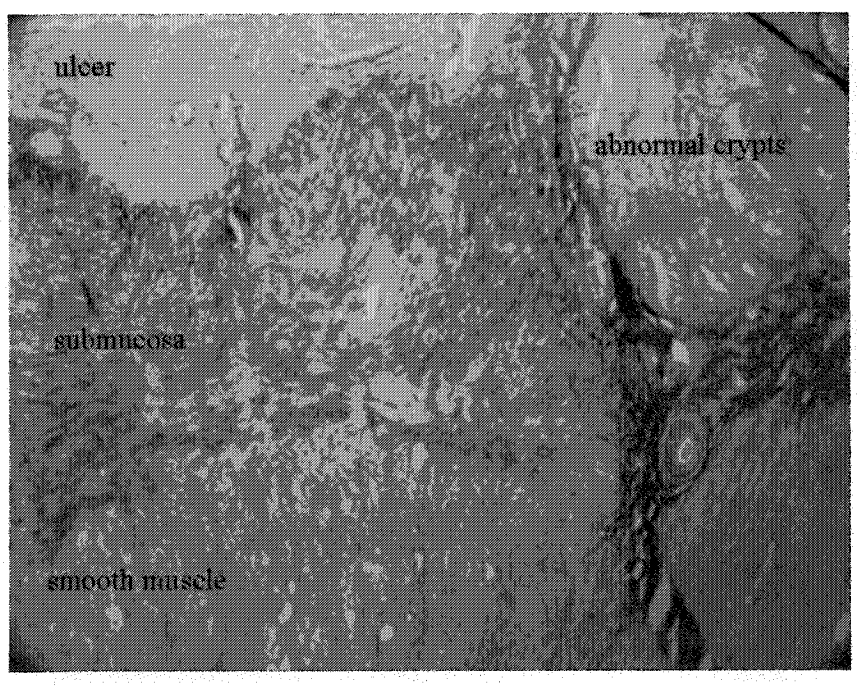

Figure 3-30. Sirius Red/Fast Green-stained colon sections from (A) a control rat and (B) a TNBS-treated rat (90 mg/kg). Sirius Red stains collagen in the presence of picric acid while Fast Green stains protein in general (original magnification 100X).

3.6.4 Effect of M-1 and PTX on Colonic Collagen Levels in TNBS-induced Colitis Corrected for Colon Weight

Collagen levels increased along with overall protein within the inflamed colon tissue, resulting in a minimal change in the "ratio" of collagen to total protein in each 8 μM colon section as assessed by the SR/FG method. In models of fibrosis where this method is traditionally used, there is a predominant increase in ECM protein without a major increase in overall protein content of the tissue. Since each colon section used in the SR/FG experiment was the same length (6 cm) and thickness (8 μm), the collagen ratio was multiplied by the weight of the colon tissue to obtain a more accurate estimate of the relative difference in tissue collagen levels between groups (Fig 3-31). The value obtained from this calculation (mg collagen/g protein x g colon weight) is referred to as modified collagen level corrected for colon weight. TNBS-treatment resulted in a significant increase in colonic collagen level compared to controls (35 ± 5 vs. 15 ± 0.6; $p<0.05$). While PTX did not have a significant effect on collagen, M-1 treatment significantly reduced colonic collagen level compared to TNBS-treated rats (19 ± 1.7 vs. 35 ± 5; $p<0.05$).

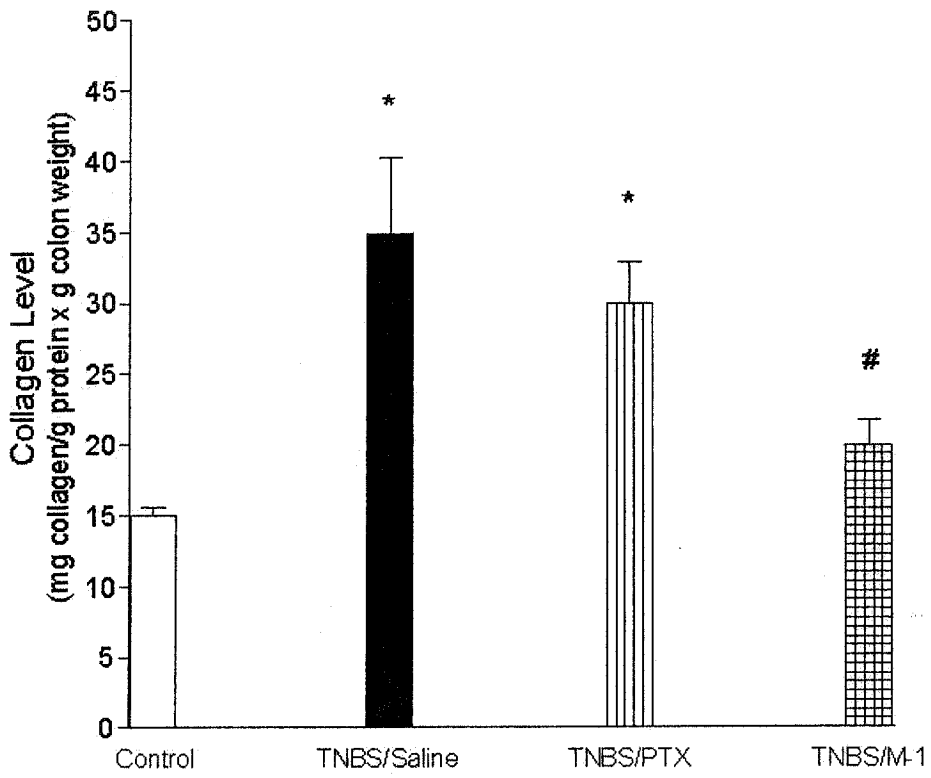

Figure 3-31. Effect of M-1 and PTX on Colonic Collagen Level in TNBS-induced colitis. The value obtained from the SR/FG method of collagen quantitation (mg collagen/g protein) was multiplied by the weight of the colon segment (6 cm) to obtain a modified collagen score corrected for colon weight. Results are mean collagen content (mg collagen/g protein x g colon) ± SEM (n=8) and are pooled results from two separate experiments with similar findings.
* = significant difference from controls ($p<0.05$)
# = significant difference from TNBS/Saline ($p<0.05$)

3.6.5 Correlation Between Collagen Level and Damage Score

In order to further validate our modification of the SR/FG calculation of collagen content, by accounting for the increased colon protein in TNBS-induced colitis due to inflammation, a correlation was performed between the Collagen Level corrected for colon weight (mg collagen/g protein x g colon) and Damage Score. In a model of inflammation-induced colitis, these two variables are expected to show a positive correlation. Figure 3-32 illustrates the significant positive correlation between Collagen Content and Damage Score with a correlation coefficient of 0.872 ($p<0.001$).

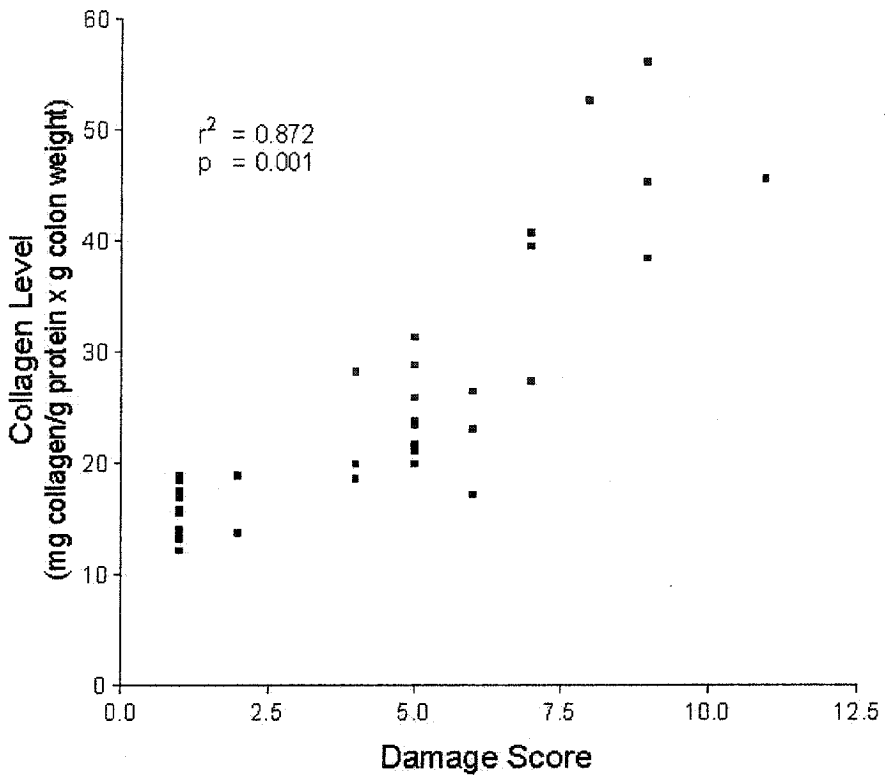

Figure 3-32. Correlation between Damage Score and the modified Collagen Level corrected for colon segment weight (μg collagen/g protein x g colon weight).

3.6.6 Estimation of Colonic Collagen Content (mg collagen / colon segment)

To estimate the true collagen content in rat colon tissue, protein values from a standard protein determination (PD) assay on colon tissue were factored into the equation using frozen colon tissue from TNBS-experiments (Series II). Addition of this value into the equation accounted for the increase in protein concentration in TNBS-treated colon tissue as well as the increase in total protein per 6 cm colon segment (colon weight). The total equation used was: μg collagen/mg protein (SR/FG) x mg protein/g tissue (PD) x g tissue/6 cm colon segment (colon weight). The resulting value for collagen was μg collagen/6 cm colon segment, which was converted to mg collagen/6 cm colon segment (Fig 3-33).

TNBS-treatment significantly increased the amount of collagen in the distal 6 cm of the colon compared to controls (4.1 ± 0.5 vs. 1.5 ± 0.1 mg/6 cm colon segment; $p<0.05$). While treatment with PTX showed a non-significant trend toward inhibition of TNBS-induced collagen accumulation in colon tissue (3.5 ± 0.6 mg/6 cm colon segment), M-1 treatment resulted in significant inhibition compared to TNBS-treated rats (2.2 ± 0.3 vs. 4.1 ± 0.5 mg/6 cm colon segment; $p<0.05$).

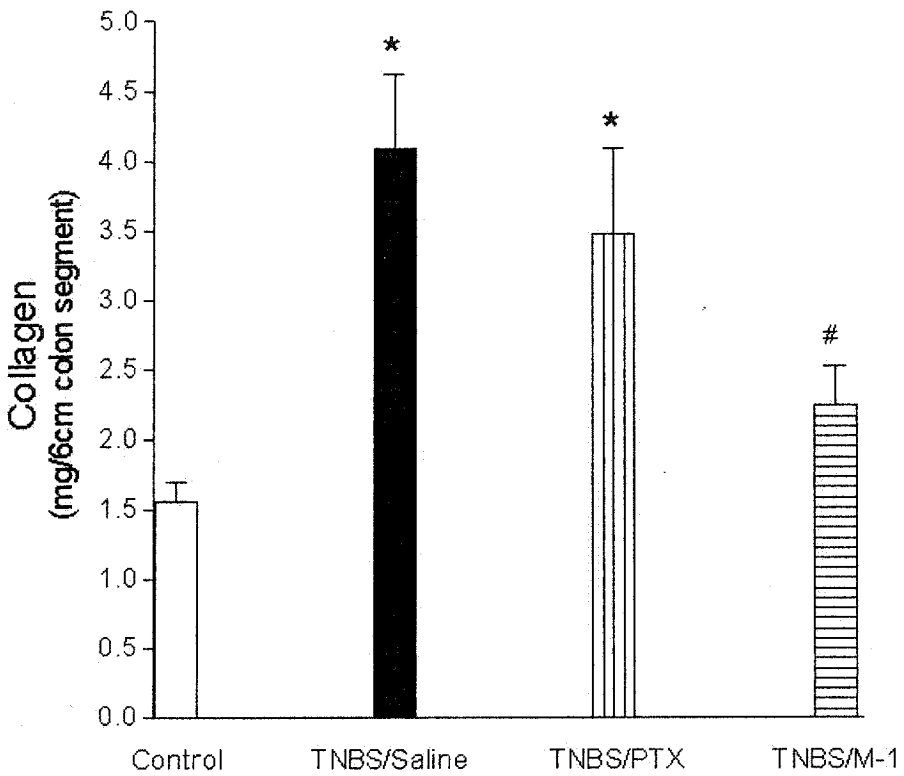

Figure 3-33. Collagen Content expressed as mg collagen per 6 cm colon segment. Collagen was calculated using the following equation: μg collagen/mg protein (SR/FG) x mg protein/g tissue (protein determination) x g tissue/6 cm colon segment (colon weight). Results (μg collagen/6 cm colon segment) were divided by 1000 and are expressed as mean collagen (mg/6 cm colon segment) ± SEM.
N = 8 (control), 5 (TNBS/Saline), 6 (TNBS/PTX), 5 (TNBS/M-1)
* = significant difference from control; $p<0.05$
# = significant difference from TNBS/Saline; $p<0.05$

3.6.7 Immunohistochemical Staining of Collagen Type III in Frozen Colon Tissue

Immunohistochemical staining of collagen type III was performed on frozen colon tissue from saline-treated and TNBS-treated rats in order to determine if this particular collagen is increased in TNBS-induced colitis (see 2.13.2 for details). Collagen type III was visualized with an aminoethylcarbazole reaction (red) and tissue was counterstained with hematoxylin, which stains nuclei (blue). Figure 3-34 illustrates the visible increase in collagen III in the thickened submucosa and smooth muscle layers of colon tissue from TNBS-treated rats (magnification 100X). Figure 3-35 shows a section of smooth muscle from each colon at a higher magnification (800X).

3.6.8 Western Analysis of Collagen Type I in Colon Lysates

Select colon lysates were analyzed by western immunoblotting for collagen type I protein (Fig 3-36). A strong double band was detected at 50 kDa that disappeared when the primary antibody was pre-adsorbed with a blocking peptide (not shown). Three samples from each drug-treated group (lanes 7-9, 12-14) were chosen based on low damage scores (DS 2-4). These animals were considered good "responders" to the drug treatments. Lanes 10 and 11 show one sample from each treatment group with a moderate level of damage (DS 5 and 6). Densitometric analysis of western results revealed a significant increase in collagen type I protein in TNBS-treated colon tissue ($p<0.001$). Collagen type I levels in selected drug-treated tissue samples was significantly reduced compared to TNBS-treated tissue ($p<0.01$).

A)

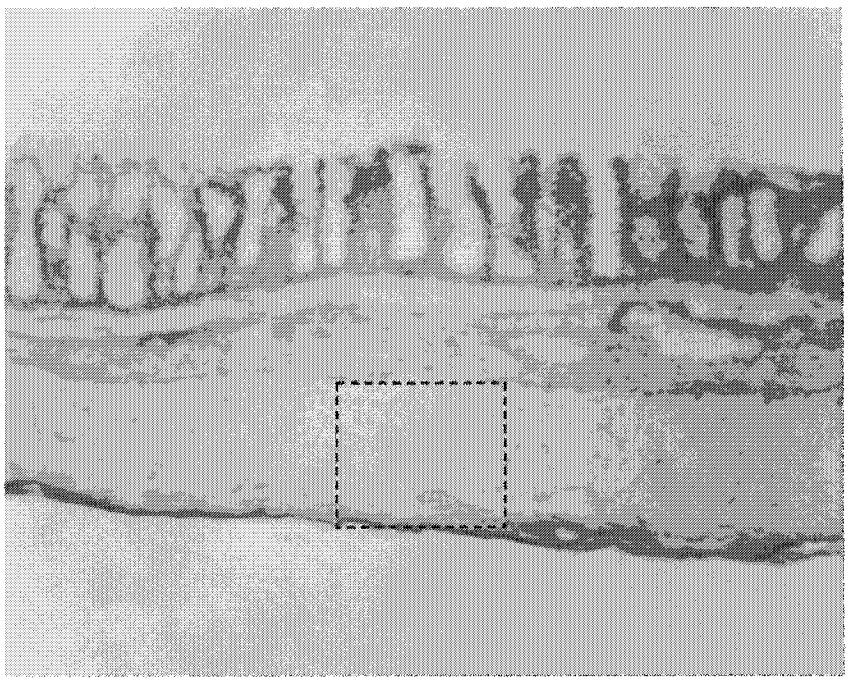

B)

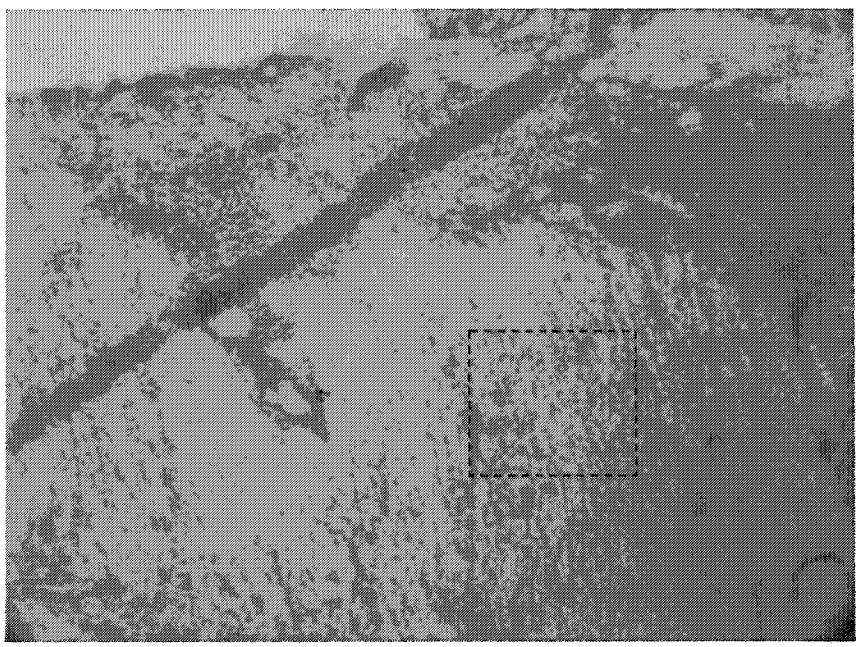

Figure 3-34. Immunohistochemical staining of collagen type III in colon tissue from (A) a saline-treated rat and (B) a TNBS-treated rat (90 mg/kg). Collagen was visualized with aminoethylcarbazole (red) and tissue was counterstained with hematoxylin to visualize nuclei (blue). Magnification 100X. Dashed boxes represent the approximate area of smooth muscle that is enlarged (800X) in Fig 3-35.

A)

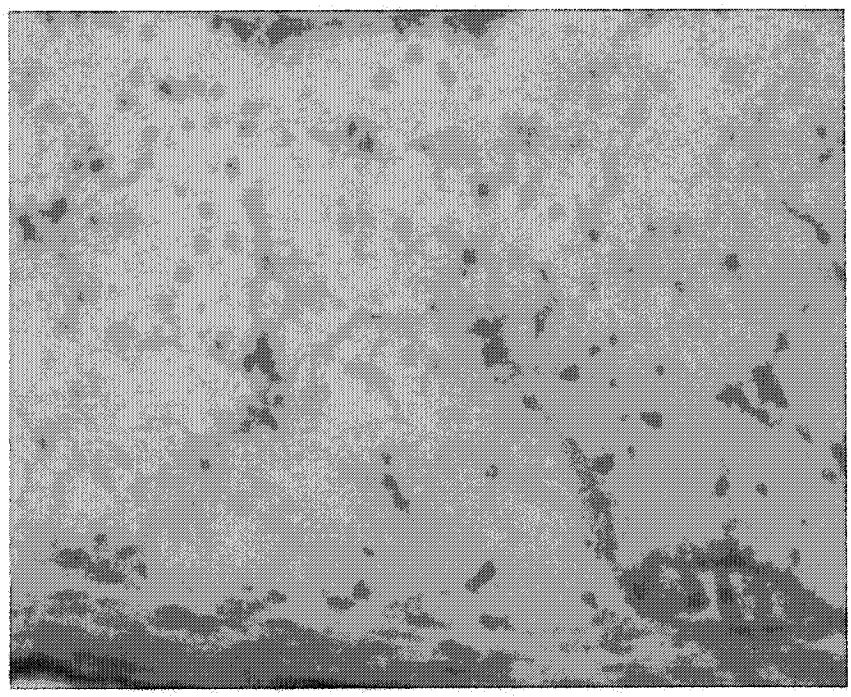

B)

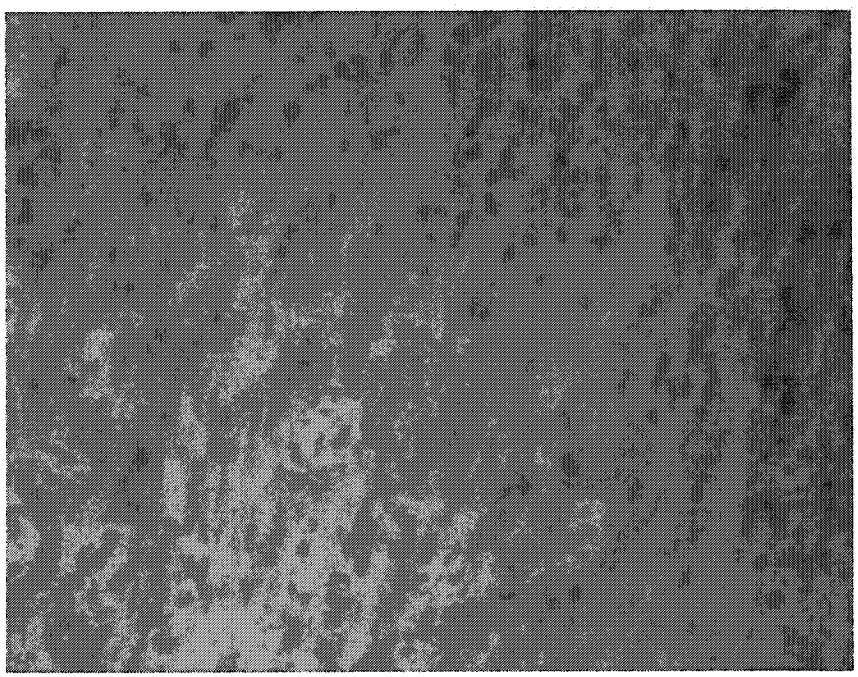

Figure 3-35. Immunohistochemical staining of collagen type III in colon smooth muscle (muscularis) from (A) a saline-treated rat and (B) a TNBS-treated rat. There is increased deposition of collagen in the smooth muscle as well as increased cell density (blue nuclei visible). Collagen accumulation can lead to loss of function of intestinal tissue. Collagen was visualized with aminoethylcarbazole (red) and tissue was counterstained with hematoxylin to visualize nuclei (blue). Magnification 800X.

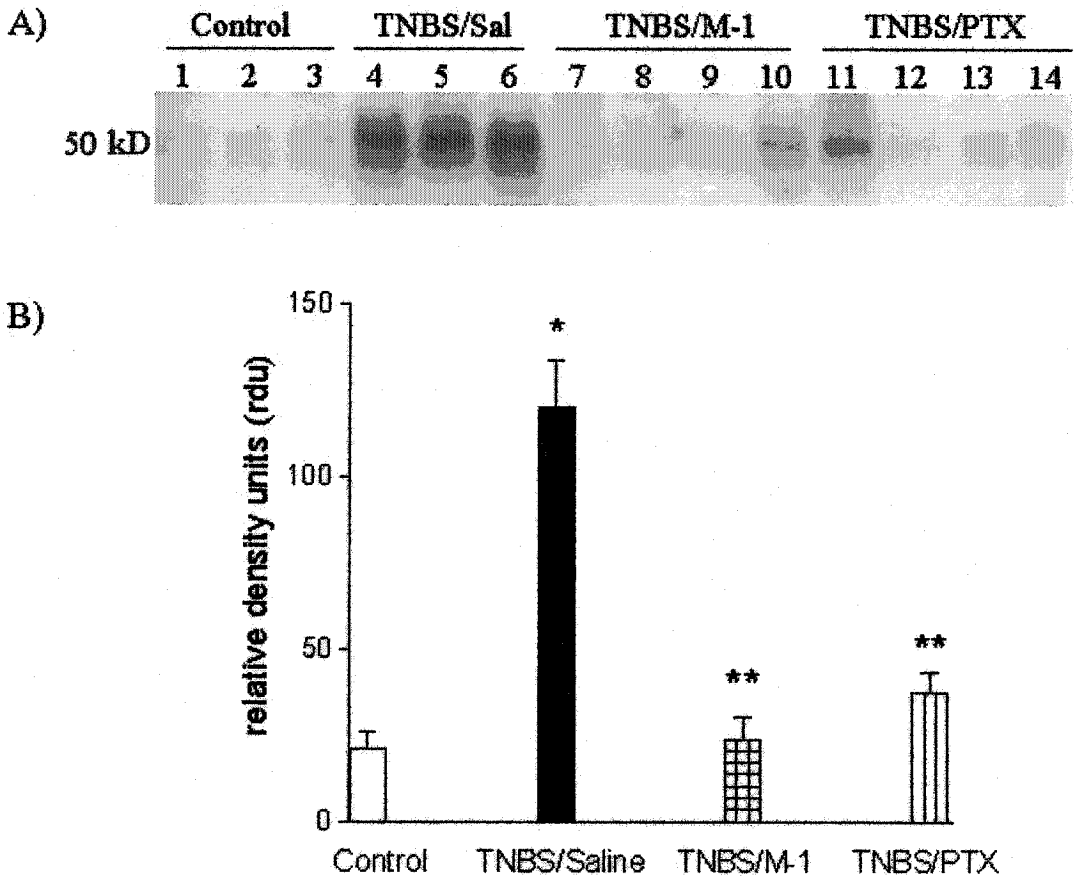

Figure 3-36. Collagen Type I in select colon samples from TNBS experiments (Series II). Collagen type I was assessed (A) by Western blot and (B) densitometric analysis is shown below. A double band was visualized at approximately 50 kDa that disappeared when the primary antibody was pre-absorbed with a blocking peptide. Lanes 1-3 are saline controls, lanes 4-6 are saline-treated colitic animals, lanes 7-9 are good responders in the M-1 colitic group, lanes 12-14 are good responders in the PTX colitic group, and lanes 10 and 11 are drug-treated animals with moderate colon damage remaining.
* = significant difference from controls ($p<0.05$)
** = significant difference from TNBS/Saline ($p<0.05$)

3.7 ASSESSMENT OF INTERLEUKIN-18 IN TNBS-INDUCED COLITIS

It was hypothesized that IL-18 would be elevated in the rat model of TNBS-induced colitis. Colon tissue and serum from TNBS-treated rats were analyzed by ELISA. Protein determination was performed on colon tissue and IL-18 results are expressed as mean IL-18 (pg)/mg protein ± SEM.

3.7.1 IL-18 in Rat Colon Tissue

IL-18 levels in normal rat colon were approximately 50 pg/mg protein. There was a significant decrease in IL-18 by 12-hours post-TNBS (9 ± 2.6 vs. 48 ± 3.9 pg/mg protein; $p<0.05$). A gradual increase in IL-18 occurred between 12-hours and 3-days where there was a significant increase in IL-18 over controls (105 ± 15 vs. 48 ± 3.9 pg/mg protein; $p<0.05$). Colon IL-18 levels gradually returned to control levels by day 14 (Fig 3-37).

3.7.2. IL-18 in Rat Serum

IL-18 could not be detected in rat serum using the Rat IL-18 ELISA kit purchased from Biosource. IL-18 levels in untreated Sprague-Dawley rat serum are reported to be approximately 50 pg/mL and the kit is reported to detect IL-18 levels in the range of 4 – 1000 pg/mL (Biosource ELISA Manual). There was likely a problem with the sensitivity of the kit.

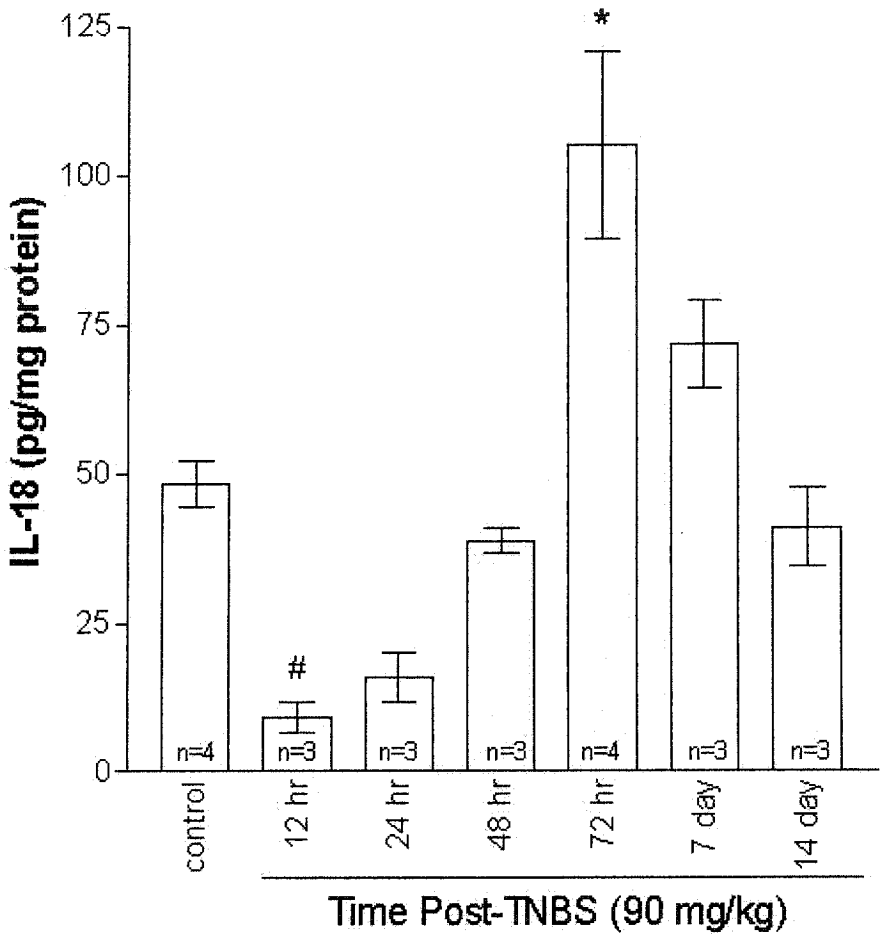

Figure 3-37. Colonic IL-18 levels in TNBS-induced colitis. Rats treated with TNBS (90 mg/kg) were sacrificed at various timepoints and IL-18 in colon tissue was analyzed by ELISA. Control animals received saline. Results are expressed as mean IL-18 (pg/mg protein) ± SEM.
* = significant increase compared to controls ($p<0.05$)
# = significant decrease compared to controls ($p<0.05$)

3.8 MOLECULAR EVENTS IN TNBS-INDUCED COLITIS

Several type I inflammatory cytokines elevated in CD exert their effects via activation of the transcription factor nuclear factor-kappa B (NF-κB), including IL-18. It was hypothesized that NF-κB p65 would be elevated in TNBS-colitis. The role of mitogen-activated protein kinases (MAPKs) in IBD are currently being investigated but this is a very recent field. In order to determine the relative importance of these signaling proteins in TNBS-induced colitis in the rat, Western immunoblotting of rat colon tissue was performed. Proteins assessed were NF-κB, JNK1, p-JNK, p38 MAPK, and p-p38 MAPK. Phospho-ATF-2, activated by both JNK and p38 MAPK, was also assessed.

3.8.1 Changes in Colonic NF-κB Levels in TNBS-Induced Colitis

NF-κB p65 was significantly elevated in TNBS-treated colon tissues at 4 hrs and 3 days post-TNBS ($p<0.05$) and gradually returned to baseline by 14 days (Fig 3-38).

3.8.2 Changes in colonic MAPK levels in TNBS-induced colitis

JNK1 and p-JNK levels were elevated at 4 hrs post-TNBS. The MAPK p38 was transiently decreased at 4 hrs post-TNBS and at day 14 as well (Fig 3-39). Phospho-p38 levels followed the same pattern as p38 levels but were much lower. Phospho-ATF-2 was decreased at 4 hrs post-TNBS and gradually increased over time.

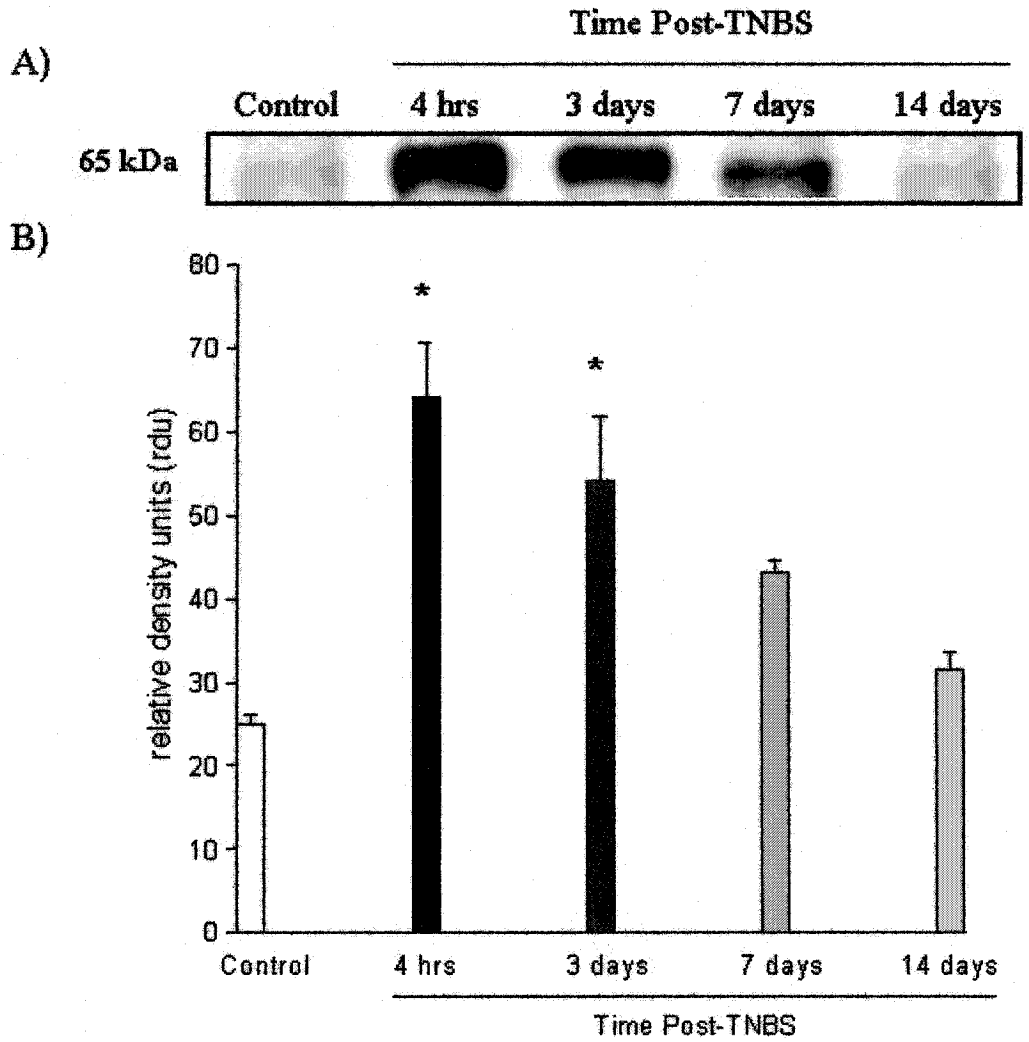

Figure 3-38. Colonic NF-κB levels in TNBS-induced colitis. **A.** Western immunoblotting of NF-κB p65 (65 kD) in colon lysates at various timepoints following TNBS administration showed that NF-κB levels were increased by 4 hrs post-TNBS and gradually decreased over time. **B.** Densitometry showed that NF-κB levels were significantly elevated at 4 hrs and 3 days post-TNBS compared to controls ($p<0.05$; $n=3$). The antibody detected total NF-κB p65 protein in rat colon lysates.

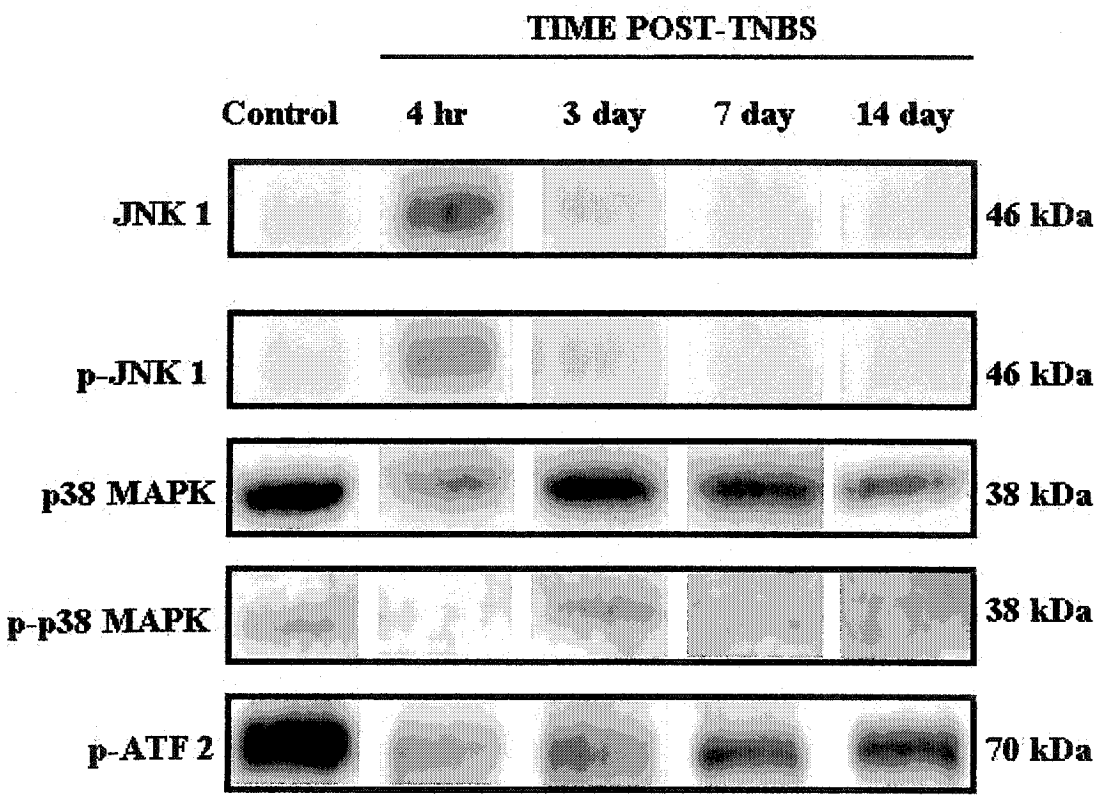

Figure 3-39. Colonic levels of MAPK in TNBS-induced colitis. In order to identify novel signaling molecules involved in TNBS-induced colitis, colonic levels of JNK 1, p-JNK 1, p38 MAPK, p-p38 MAPK, and p-ATF-2 (downstream target of both JNK and p38 pathways) levels were assessed by Western immunoblotting across a range of timepoints from 4 hours to 14 days post-TNBS. The role of MAPKs in human IBD is a very recent field of investigation. Representative bands are shown in figure (n=3). Loading was verified by amido black-staining of immunoblot membranes.

3.8.3 Changes in Colonic TGF-β and PDGF-B Levels in TNBS-induced Colitis

It was hypothesized that PDGF-B may be involved in fibrosis associated with TNBS-induced colitis. Two profibrogenic cytokines PDGF-B and TGF-β1 were assessed in colon tissues by Western immunoblotting. TGF-β1 (25 kDa) was decreased at 4 hrs post-TNBS and returned to control levels at later timepoints (Fig 3-40). PDGF-B was undetectable in control tissues and in early colitis. PDGF-B, detected as PDGF-BB (25 kDa) and PDGF-AB (27 kDa) dimers, was detectable from days 3 to 14 post-TNBS.

3.9 EFFECT OF M-1 AND PTX ON NF-κB ACTIVITY IN VITRO

3.9.1 Effect of TNF-α, IL-1β and IL-18 on NF-κB Nuclear Translocation in IECs

IEC cells exhibited varied intensity of basal NF-κB staining from experiment to experiment. Control cells under basal stimulation (DMEM + 1 % FBS) consistently stained positive for NF-κB p65 in both the nucleus and the cytoplasm (Fig 3-41). Both TNF-α (50 mg/ml) and IL-1β (50 mg/ml) stimulated nuclear translocation of NF-κB p65 with intense nuclear staining and weak cytoplasmic staining. IL-18 did not stimulate nuclear translocation of NF-κB p65 as assessed by immunocytochemistry (ICC).

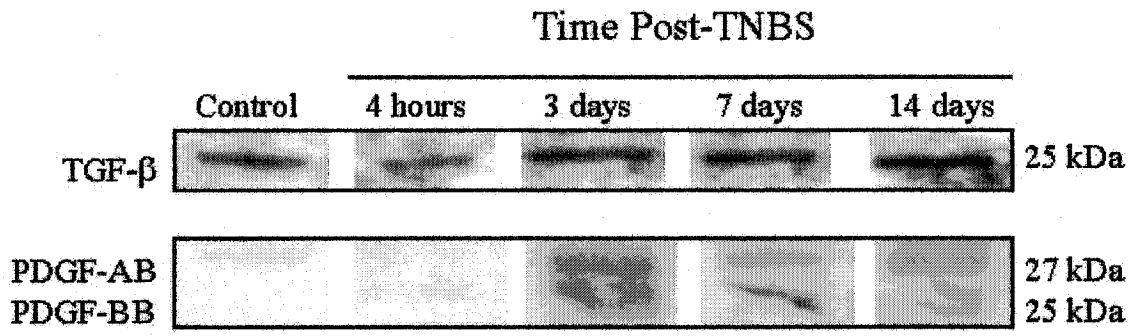

Figure 3-40. Colonic TGF-β and PDGF-B levels in TNBS-induced colitis. Cytokines were detected as dimers by Western analysis. Both PDGF-AB (27 kDa) and PDGF-BB (25 kDa) were detected from 3 days – 14 days. TGF-β (25 kDa) was detectable at all timepoints with a transient depression at 4 hrs post-TNBS.

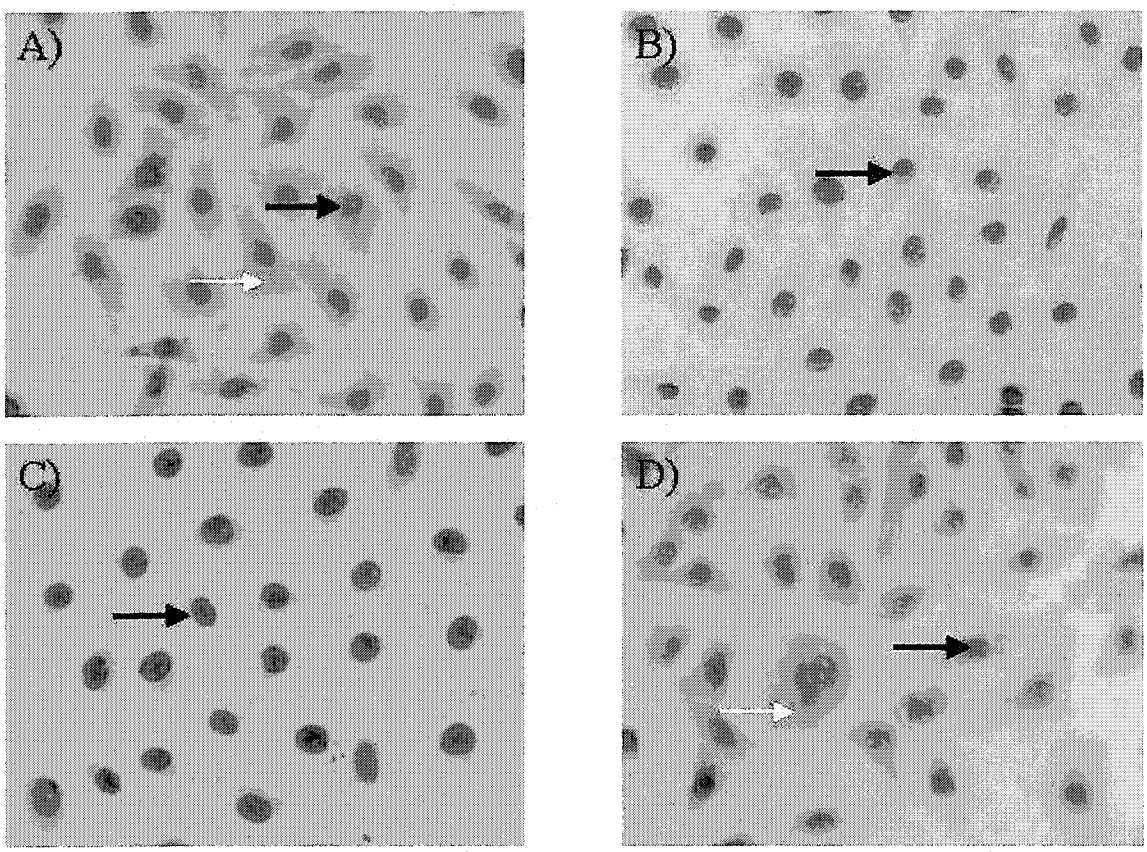

Figure 3-41. Effect of TNF-α, IL-1β and IL-18 on nuclear translocation of NF-κB in intestinal epithelial cells. **A.** Control cells under basal stimulation (DMEM + 1%FBS) consistently show both cytoplasmic (white arrow) and nuclear (black arrow) staining for NF-κB p65. **B.** TNF-α (50 ng/ml). **C.** IL-1β (50 ng/ml). **D.** IL-18 (50 ng/ml). Both TNF-α and IL-β stimulated nuclear translocation of NF-κB p65. Cells were fixed 1 hour after stimulation with cytokines.

3.9.2 Effect of IL-18 on NF-κB Activation in IEC-6 Cells by Western Immunoblotting

Results from ICC experiments suggested that IL-18 did not activate NF-κB in cultures IEC-6 cells (Fig 3-41). NF-κB was therefore assessed in nuclear fractions from IEC-6 cells treated with IL-18 (50 ng/ml or 100 ng/ml) for 1 or 2 hours to determine if IL-18 stimulates activation of NF-κB in these cells (Fig 3-42). There was no difference between controls and IL-18-treated groups. IL-18 did not activate NF-κB in IEC-6 cells under the culture conditions tested, consistent with the ICC results.

3.9.3 Effect of M-1 and PTX on Cytokine-Stimulated Activation of NF-κB *in vitro*

TNF-α (50 ng/ml) and IL-1β (50 ng/ml) treatment for 1 hour resulted in clusters of IEC-6 cells with dense nuclear staining indicating nuclear translocation of NF-κB p65. Both PTX and M-1 treatment (1 mg/ml) blocked cytokine-stimulated nuclear translocation of NF-κB p65 (Fig 3-43). There was no difference between drug-treated wells and control wells (not shown). Wells not exposed to primary antibody showed no staining. Drugs were added 10 minutes before cytokines. Cells were fixed 1 hour after addition of cytokines.

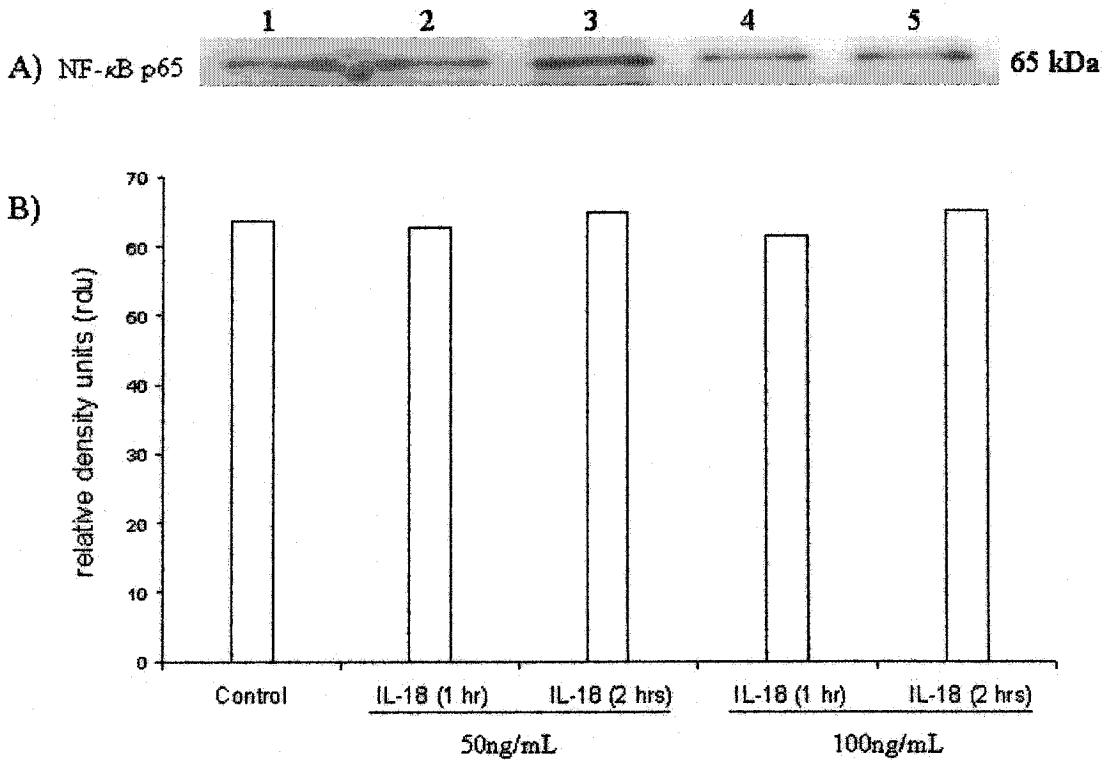

Figure 3-42. Effect of IL-18 on NF-κB activation in IEC-6 cells by Western analysis. Epithelial cells were treated with recombinant rat IL-18 (50 or 100 ng/mL) for 1 or 2 hrs. Nuclear proteins were extracted. **A.** Western immunoblotting of nuclear lysates using a NF-κB p65 polyclonal antibody. **B.** Densitometric analysis of NF-κB p65 levels in nuclear lysates from IECs treated with rrIL-18. Blots were stained with amido black to ensure equal loading of nuclear protein (20 μg/lane).

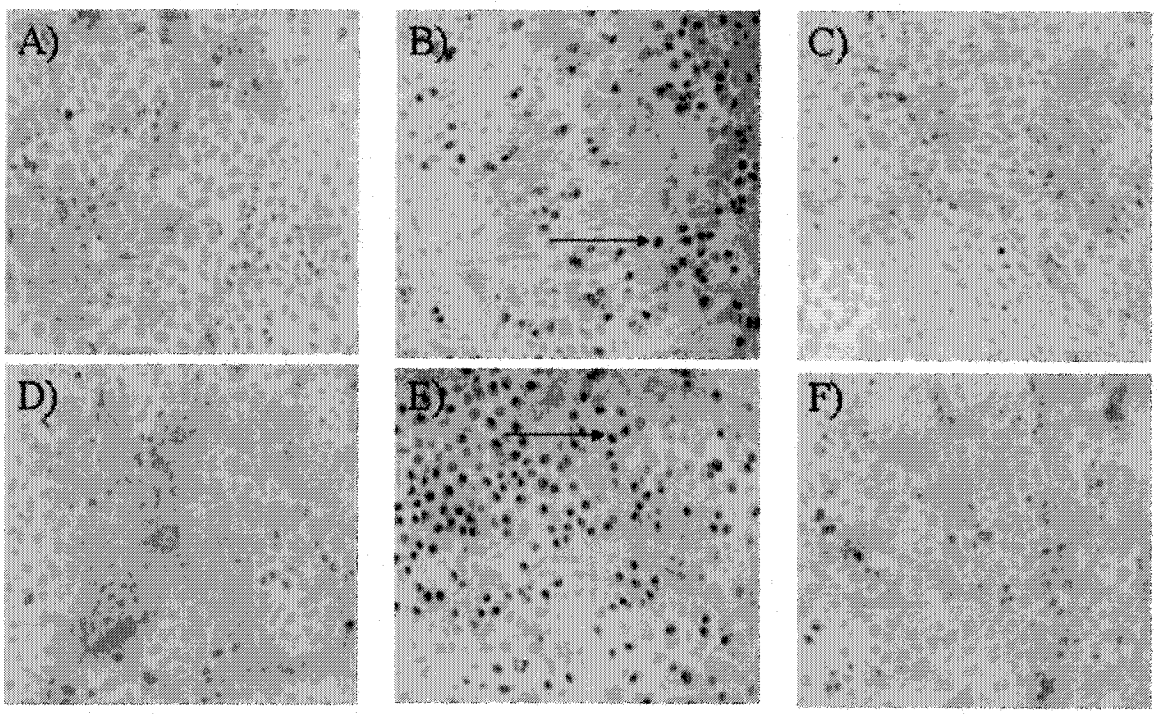

Figure 3-43. Effect of M-1 and PTX on cytokine-induced NF-κB p65 activation *in vitro*. Rat intestinal epithelial cells (IECs) were stimulated with TNF-α (50 ng/ml) or IL-1β (50 ng/ml) for 1 hr in the presence and absence of M-1 or PTX (1 mg/ml). Immunocytochemistry was performed to visualize nuclear translocation of NF-κB p65. This antibody was not specific for phosphorylated NF-κB p65 so staining was visible in the cytoplasm as well as nucleus. In activated cells, concentrated staining was seen in the nucleus (black arrows). **A**. TNF-α in the presence of M-1. **B**. TNF-α alone. **C**. TNF-α in the presence of PTX. **D**. IL-1β in the presence of M-1. **E**. IL-1β alone. **F**. IL-1β in the presence of PTX. Drugs were added 10 minutes prior to cytokines. Each treatment was performed in duplicate. There was no difference between control and drug-treated wells (control not shown).

Chapter 4

DISCUSSION

This thesis was an examination of the anti-fibrogenic and anti-inflammatory effects of a novel metabolite of pentoxifylline (M-1) in comparison with the parent compound (PTX). The results of these investigations indicate that M-1 (1-(R/S-5-hydroxyhexyl)-3,7-dimethylxanthine) is an effective anti-fibrotic agent, *in vitro* and *in vivo*, that may be useful in the treatment of both inflammation and fibrosis associated with human Crohn's disease (CD). This would be a major advance in the field of gastroenterology since there is currently no treatment aimed at preventing or reversing fibrosis in CD, a complication that leads to surgical intervention in the majority of patients. We have examined cytokines and signaling molecules in TNBS-induced colitis, an experimental model of CD, which may identify novel therapeutic targets. Biological effects of M-1 may be enhanced *in vivo* by taking advantage of a pharmacologic drug interaction with the antibiotic ciprofloxacin that produces significantly elevated serum levels of active drug. Our findings and their significance will be discussed in detail below.

We have developed a simple, reproducible, and inexpensive method to synthesize racemic M-1 from PTX using a non-selective chemical reduction reaction with an average percent yield greater than 80 % (see methods section 2.6.1). This method was a simple modification of a previous method developed in our lab that produced a yield of less than 50 %, meaning that the weight of recovered product was less than 50% weight of the starting compound, PTX. This previous method will be referred to as the original method of M-1 synthesis. Two additional extractions from dichloromethane were performed in the modified method in order to recover more of the metabolite from the

aqueous phase. The product was identified as M-1 by ^{1}H-NMR spectroscopy (Fig 3-1), and HPLC analysis of M-1 standards confirmed that no contaminating PTX was present in the compound (Fig 3-8). The ratio of M-1R and M-1S in the recovered product could have been verified by chiral HPLC but this technology was unavailable to us. Since the synthesis method employed was a non-selective chemical reduction reaction, as opposed to an enzymatic or enantioselective reaction, it can be assumed that the product is a racemic mixture (1:1) of M-1 enantiomers (Ege, 1994).

PDGF is a pro-fibrogenic growth factor implicated in the pathogenesis of many fibrotic diseases, including liver fibrosis (Peterson and Williams, 1987; Peterson and Isbrucker, 1990; Isbrucker and Peterson, 1992; Peterson, 1993; Gressner, 1992), scleroderma (Raoul *et al.*, 2004), collagenous colitis (Peterson and Huet, 1996), atherosclerosis (Ostman and Heldin, 2001), and lung and kidney fibrosis (Heldin and Westermark, 1999). It is likely involved in the development of intestinal fibrosis associated with Crohn's disease (Assche, 2001; Lawrance *et al.*, 2001; Kumagai *et al.*, 2000; Beck and Podolsky, 1999). Excess proliferation and collagen synthesis by fibroblasts and fibroblast-like cells are hallmarks of fibrosis in any organ system. We have shown that PDGF is a potent mitogen for non-confluent fibroblasts, yet stimulates collagen synthesis in confluent fibroblast monolayers (Isbrucker and Peterson, 1998). Another group reported that low-dose PDGF (1 ng/ml) stimulated collagen synthesis by wound fibroblasts, while a higher concentration (30 ng/ml) stimulated fibroproliferation (Lepisto *et al.*, 1995). These results suggest that proliferation and collagen synthesis by fibroblasts are two independent processes, both regulated by PDGF. Examining drug

effects on PDGF-stimulated events *in vitro* therefore provides rationale to examine their effects *in vivo* in animal models of fibrosis.

Our initial characterization of M-1 *in vitro* demonstrated that the racemic metabolite inhibited PDGF-stimulated human skin fibroblast proliferation (Fig 3-3) and collagen synthesis (Fig 3-6) in a dose-dependent manner. When compared to the inhibitory effects of PTX, M-1 inhibited PDGF-driven fibroproliferation and collagen synthesis with a 50 %-inhibition concentration (IC_{50}) that was approximately 33 % lower for M-1 than for PTX. There was a statistically significant difference in the inhibitory effects of M-1 and PTX at 240 μM ($p<0.05$), indicating that M-1 is pharmacologically more potent than PTX at this dose. This finding is consistent with a previous study from our lab investigating the effects of an experimental M-1 preparation, supplied by Hoescht, on PDGF-driven collagen synthesis by cultured porcine myofibroblasts (Isbrucker and Peterson, 1994; Isbrucker and Peterson, 1998). This previous study reported that M-1 was more potent than PTX with a similar level of inhibition observed. M-1 (240 μM) inhibited PDGF-stimulated collagen synthesis by close to 100 %, while the same dose of PTX inhibited collagen synthesis by only 60 % compared to controls not exposed to PDGF, consistent with the findings presented in this thesis. These results suggest that M-1 previously synthesized by Hoescht had the same pharmacological properties as our racemic M-1.

A previous study investigating the effects of racemic M-1, synthesized by the original chemical method developed by our group, reported that M-1 was equally as

effective as PTX at inhibiting PDGF-stimulated proliferation of cultured dermal fibroblasts (Peterson, 1996). The increased potency of M-1 in the present experiments likely reflects a difference in the fibroblasts themselves, since a proliferation assay comparing inhibition of PDGF-driven fibroproliferation by M-1 (synthesized by the original and modified methods), confirmed equivalent potency *in vitro*. All M-1 preparations exhibited the same biological activity with higher potency than PTX at 240 μM (Fig 3-4). These cultured fibroblasts have undergone several passages since the previous study in 1996 (Peterson, 1996) and it is possible that expression of molecular targets for M-1 (or PTX) may have changed over time resulting in an altered response to one, or both, of the drugs. Different culture or experimental conditions could also be a factor. Since excessive proliferation and collagen synthesis by fibroblasts are hallmark events in fibrosis, the *in vitro* results presented in this thesis suggest that M-1 could be a useful anti-fibrotic agent.

The molecular targets of M-1 in the inhibition of PDGF-driven fibroproliferation and collagen synthesis remain to be determined but molecular mechanisms have now been described for PTX. Understanding the mechanisms of PTX effects will provide a foundation from which to explore the molecular effects of M-1 in future studies. AP-1 (activator protein-1) describes a family of transcription factors that consists of proteins such as c-Jun, c-Fos, and ATF-2 (activating transcription factor-2), that modulate target gene expression as homodimers and heterodimers (Ghosh, 2002). AP-1 regulates cell proliferation and survival in response to many stimuli (Shaulian and Karin, 2002). Recently, our group has shown that PTX interrupts PDGF-driven fibroproliferation by

inhibiting PDGF-induced expression of *c-jun*, but not *c-fos*, and PTX inhibited phosphorylation of endogenous c-Jun protein at serine residue 73 (Peterson *et al.*, 2002). Antisense to *c-jun* also inhibited PDGF-induced fibroproliferation in this study. Inhibitory effects on c-Jun phosphorylation lead to decreased c-Jun-containing AP-1 dimers thereby modulating expression of AP-1-regulated target genes. This is a novel mechanism of action for PTX, which is generally described as a PDE inhibitor. Our lab had previously shown that PTX inhibition of PDGF-driven fibroproliferation was independent of effects on cAMP (Peterson *et al.*, 1998), adenosine receptors (Peterson et al., 1996) or PDGF receptors (Slyz and Peterson, 1994). PTX has been reported to mediate PDGF-driven proliferation of vascular smooth muscle (VSMC) cells via a cAMP/PKA-dependent pathway (Chen *et al.*, 1999), and to inhibit PDGF-induced fibroproliferation of myofibroblasts via inhibition of extracellular signal-regulated kinase (ERK) and *c-fos* (Pinzani *et al.*, 1996), indicating possible cell- and tissue-specific differences in signaling mechanisms of fibroproliferation and thus PTX action.

Mechanisms of inhibition of fibroblast collagen synthesis by PTX are beginning to be elucidated. PTX decreased α1(I) and α1(III) collagen mRNA levels in a swine model of hepatic fibrosis (Isbrucker and Peterson, 1994). PTX was recently reported to down-regulate basal and TGF-β-induced collagen α1(I) and α1(III) mRNA levels in VSMC via a cAMP/PKA-dependent mechanism suggesting that PDE is an important target in these cells (Chen *et al.*, 1999). PTX has also been reported to suppress TGF-β-induced α1(I), α2(I), and α1(III) procollagen mRNA transcription in dermal fibroblasts via down-regulation of the transcription factor, nuclear factor-1 (NF-1) (Duncan *et al.*,

1995), which is known to mediate TGF-β-induced procollagen gene expression (Ghosh, 2002). In addition to inhibitory effects on procollagen gene expression, PTX also increases collagenase activity in certain fibroblast cultures (Berman *et al.*, 1989), highlighting another anti-fibrogenic role for PTX.

The role of *c-jun* in the ability of PTX to inhibit PDGF-stimulated collagen synthesis remains to be determined. Occupancy of AP-1 sites in type I procollagen genes (*COLIAI, COL1A2*) has been reported to suppress procollagen gene transcription in mesangial cells (Silbiber *et al.*, 1999; Ghosh, 2002). However, AP-1-binding induces *COL1A1* expression in rat fibroblasts (Slack *et al.*, 1995) indicating cell-type specific differences in procollagen gene regulation. Studies have shown that AP-1 stimulation is important for basal procollagen gene expression in dermal fibroblasts (Gao *et al.*, 2004), and also induces activation of hepatic myofibroblasts and collagen synthesis by these cells (Armendariz-Borunda *et al.*, 1994). A very recent study showed that SP600125, a JNK (c-Jun N-terminal kinase) inhibitor, blocked PDGF-induced proliferation and collagen synthesis in pancreatic myofibroblasts by inhibiting AP-1 activation (Masamune *et al.*, 2004). Thus, inhibition of c-Jun by PTX likely accounts, at least in part, for its inhibitory effects on cytokine-induced, as well as basal collagen synthesis in fibroblasts and myofibroblasts.

We have demonstrated that racemic M-1 inhibits the fibrogenic effects of PDGF on fibroblasts *in vitro* but its effects *in vivo* were previously unexplored. Injection of M-1 (32 and 100 mg/kg i.p.) into C57BL/6 mice revealed no signs of toxicity. Signs of

toxicity include dizziness (rotating head movements), lethargy, and hypersalivation (excessive licking movements). HPLC analysis of serum collected 20 minutes after M-1 injection showed that both M-1 and PTX were present. A kinetics experiment was performed in CD1 mice to compare the absorption, elimination, and metabolism of M-1 and PTX *in vivo* (see methods 2.8.2). M-1 and PTX (100 mg/kg) were administered by intraperitoneal route and serum was collected at various timepoints for HPLC analysis. No signs of toxicity were observed in CD1 mice with this dose of drug.

Examination of M-1 kinetics compared to PTX revealed that both drugs reached peak serum levels 10-15 minutes after i.p. injection with similar α-elimination rates of 0.75 μg/ml/min. The serum half-lives of M-1 and PTX were 15 and 20 minutes, respectively. Differences in the metabolic profiles of the two compounds were observed by analyzing the conversion of M-1 to PTX *in vivo* and vice versa (Fig 3-19). Following injection of PTX, very little M-1 was detected in the serum. Following M-1 injection, the levels of M-1 and PTX in serum reached equilibrium by 40 minutes, indicating that PTX is a major metabolite formed from racemic M-1 *in vivo*. A recent study demonstrated that reversible interconversion of PTX and M-1 takes place rapidly in human erythrocytes (CYP450-independent mechanism) with the conversion of M-1 → PTX being favored 4-fold over PTX → M-1, consistent with our findings in mice (Nicklasson *et al.*, 2002). The rate of conversion of M-1S to PTX was 4-fold higher than conversion of M-1R in this study, and the authors indicate that liver enzymes likely participate in conversion of M-1R to PTX *in vivo*. In support of this, conversion of M-1R back to PTX has been reported in human liver microsomes and is thought to occur partially via CYP1A2 and

also via an unidentified CYP450-independent mechanism, which could include cytosolic oxidases (Lillibridge *et al.*, 1996; Lee *et al.*, 1997).

Since both PTX and racemic M-1 are active *in vivo*, the higher total drug levels (M-1 + PTX) achieved in serum following M-1 injection would likely result in enhanced therapeutic effectiveness of this compound (Figs 3-10 and 3-13). The total drug levels achieved in mouse serum following M-1 and PTX injection were 171 μM and 125 μM, respectively, near the concentration at which significant anti-fibrogenic effects were seen *in vitro* (240 μM). Given that M-1 had more potent anti-fibrogenic effects than PTX *in vitro*, the higher levels of M-1 achieved by injecting the metabolite directly, could result in enhanced anti-fibrogenic effects *in vivo*. The anti-fibrogenic effects of PTX and M-1 were examined in the TNBS-model of colitis and will be discussed shortly.

An *in vivo* drug interaction between the quinolone antibiotic ciprofloxacin and PTX has been demonstrated in humans that resulted in elevated plasma levels of PTX and M-1 with enhanced therapeutic benefit of PTX administration (Thompson *et al.*, 1994). Our group has reproduced this interaction in mice and demonstrated that pre-treatment of CD1 mice with ciprofloxacin (25 mg/kg) for 9 days resulted in a 2-fold increase in serum concentrations of PTX and M-1 compared to controls (Wornell and Peterson, 1997; Peterson *et al.*, 2004). Increased serum drug levels were predominantly due to inhibition of CYP1A2 catalytic activity but were not due to decreased protein levels of the enzyme as assessed by Western immunoblotting (Peterson *et al.*, 2004). This is consistent with the role of ciprofloxacin as a competitive inhibitor of the CYP1A2 enzyme (Fuhr *et al.*,

1992; Herrlin *et al.*, 2000). Increased serum drug levels in mice would likely increase the *in vivo* therapeutic benefit of PTX, as was reported in humans (Thompson *et al.*, 1994), and this should be further examined in murine models of disease.

A goal of this thesis work was to determine if a similar interaction exists between ciprofloxacin (Cipro) and M-1 since this had never been investigated. As expected, a 2-fold increase in serum drug levels was seen 30-minutes after PTX injection (100 mg/kg i.p.) in the Cipro-pre-treated group, consistent with our previously published results (Peterson *et al.*, 2004). In the Cipro/M-1 group, there was a significant 2-fold increase in PTX serum levels and a 3-fold increase in serum M-1 levels seen at 30 minutes post-injection (Fig 3-12). In combination with higher total drug levels (PTX + M-1) achieved in serum following M-1 injection compared to PTX, this interaction resulted in significantly elevated total serum drug levels in the Cipro/M-1 group (240 μM) compared to all other groups (Fig 3-13). The drug level achieved (240 μM) is a concentration we routinely use *in vitro*. The 3-fold increase in M-1 levels in the Cipro/M-1 group suggested that an additional pathway of M-1 metabolism was blocked since a 2-fold increase was seen in all other groups (see Fig 4-1 for metabolic pathways of PTX and M-1).

CYP1A2 is important for the N-demethylation of PTX and M-1 to M-6 and M-7, respectively (Peterson *et al.*, 2004). Also, CYP1A2 plays a partial role in the conversion of M-1R back to PTX (Lee *et al.*, 1997). Interestingly, CYP3A4 has recently been described as the major enzyme responsible for the conversion of M-1R to M-3b (*trans*-

4,5-diol of M-1) which is a metabolite of M-1R formed *in vivo* (Shin *et al.*, 1998). Ciprofloxacin is known to be a potent competitive inhibitor of CYP3A4 (McLellan *et al.*, 1996). This likely explains the dramatic elevation in M-1 levels seen with the Cipro/M-1 combination since pathways to three of its metabolites (M-6, M-3b and PTX) are inhibited by ciprofloxacin. Inhibition of CYP1A2 and CYP3A4 by ciprofloxacin is competitive in nature and therefore pretreatment with ciprofloxacin is likely not necessary to achieve increased serum levels of PTX and M-1.

The combination of M-1 and ciprofloxacin should be examined in animal models of disease. Since ciprofloxacin is commonly prescribed to human CD patients to prevent or treat bacterial overgrowth (Sartor, 2004; Castiglione *et al.*, 2003), the combination of ciprofloxacin with M-1 in these patients could be particularly advantageous. The therapeutic effects of this drug combination should first be examined in a murine model of CD (e.g. TNBS-induced colitis). Ciprofloxacin itself has been shown to attenuate colitis in the IL-10 knockout (IL-10-/-) mouse model, a disease model where colitis is triggered by exposure to bacteria (Madsen *et al.*, 2000). Ciprofloxacin has also shown acute improvements in DSS-induced murine colitis although it failed to protect in chronic colitis (Hans *et al.*, 2000). Therefore, a "ciprofloxacin only" control group would be important if this drug interaction is examined in murine colitis to separate out the effects of ciprofloxacin alone on colitis. It should be mentioned that mild transient toxicity was observed in our Cipro/M-1 group (lethargy for 10-15 minutes) due to the high serum drug levels achieved, therefore dosing should be further examined. Signs of toxicity were not observed in any other treatment group.

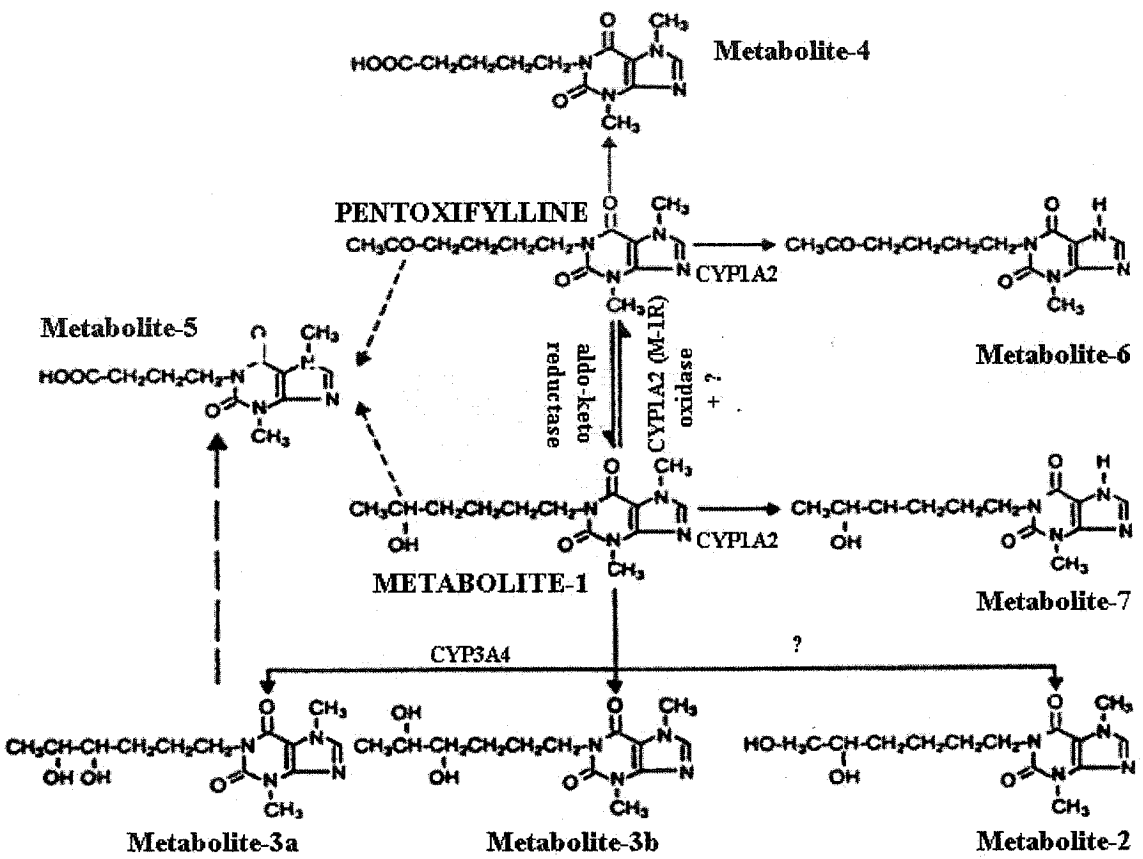

Figure 4-1. Metabolic pathways of PTX and M-1 (adapted from Ward and Clissold, 1987). M-5 and M-1 are the major metabolites of PTX. M-5 is the major product detected in urine. PTX, M-7, and M-3b are the major metabolites of M-1. M-1 and PTX are not detected in urine indicating complete metabolism of these compounds *in vivo*.

TNBS-induced fibrosis has been studied in animal models of pulmonary interstitial fibrosis (Kimura *et al.*, 1992; Zhang-Hoover *et al.*, 2000), pancreatic fibrosis (Puig-Divi *et al.*, 1996; Haber *et al.*, 1995), and chronic cholangitis (Mourelle *et al.*, 1995) but few studies have examined intestinal fibrosis in TNBS-induced colitis, a model of human CD. Intestinal fibrosis in a rat model of TNBS-induced colitis was previously reported by our group (Peterson and Davey, 1997). Fibrosis in human CD proceeds despite the use of anti-inflammatory and immunosuppressant agents, culminating in surgical bowel resection in more than 50 % of the CD population (Schuppan *et al.*, 2000). There are currently no medicinal treatments aimed at preventing or reversing fibrosis in CD (van Assche *et al.*, 2004). A major goal of this thesis project was to examine the effects of M-1 *in vivo*, in comparison with the parent compound PTX, on inflammation and intestinal fibrosis in a rat model of TNBS-induced colitis.

We chose rats for the present investigations since this model had previously been used in our lab (Peterson and Davey, 1997; Peterson *et al.*, 2000) and since mice are particularly resistant to the development of intestinal fibrosis (Lawrance *et al.*, 2003). Since many species differences exist with regard to drug metabolism (McLellan *et al.*, 1996) and drug interactions (Chen *et al.*, 2004), it could not be assumed that the ciprofloxacin interaction would occur in rats even though it has now been demonstrated in humans and mice. A preliminary examination of PTX and ciprofloxacin in rats showed no difference in serum PTX levels with ciprofloxacin pre-treatment (Fig 3-14), thus we did not explore this interaction further in the rat model of CD.

TNBS (90 mg/kg; 12.5-15 mg/rat) was chosen for our investigations based on the results of a preliminary dose-response experiment (Table 3-1). This dose was consistent with other studies using young adult rats (Torres *et al.*, 1999; Miampamba *et al.*, 1998; Tatsumi *et al.*, 1996). The most common TNBS doses reported in the literature are 25-30 mg/rat (Morris *et al.*, 1989; Jacobson *et al.*, 1997; Messaoudi *et al.*, 1999; Moreels *et al.*, 2001; Togawa *et al.*, 2002); however, on further investigation these rats were generally twice as heavy as our rats (>300 g) and doses worked out to be in the range 80-100 mg/kg. Thus 90 mg/kg TNBS was a standard dose based on weight for the rat. This dose caused reproducible colon damage (average damage score: 6.7) and inflammation (average MPO activity: 10 units/mg tissue) and provided a good reference from which to compare the effects of PTX and M-1 *in vivo*.

The damage score achieved in the present studies was higher than the average damage scores achieved previously in our lab using the TNBS model (average damage score 4.5-5.0) (Peterson and Davey, 1997; Peterson *et al.*, 2000). The scale used to calculate damage score in one study (Peterson and Davey, 1997) was an older version (Wallace *et al.*, 1989) of the scale used in the present investigation (Wallace *et al.*, 1992) that did not take into account the presence of adhesions (add 1-2 points) or diarrhea (add 1 point). The previous study examined a different timepoint as well (5 days post-TNBS). Another previous study using the same scoring system and timepoint reported and average damage score of 5.0 but these rats were larger than our rats (Peterson *et al.*, 2000). Thus, there is some variability in the literature regarding damage score that is likely due to differences in TNBS dose, rat weight and strain, and the exact method used

to measure colon damage. Nonetheless, the damage achieved in the present investigations was consistent from experiment to experiment when the same parameters were used (Series I: 6.6 ± 0.5; series II: 6.9 ± 0.8).

In series I (drug dose 32 mg/kg i.p. bid) and series II (drug dose 64 mg/kg i.c. bid) experiments, colitis was induced with TNBS (90 mg/kg) at the onset of the experiment and drug treatments were not initiated for 72 hours to ensure development of a strong response to the hapten. Evaluation of H&E-stained colon sections revealed that intestinal crypt distortion, edema, and inflammatory infiltrate, hallmarks of active CD (Cotran *et al.*, 1999), were evident by 72 hrs post-TNBS (Fig 2-23). Visible changes in the amount of inflammatory infiltrate in colon tissue over time in response to TNBS corresponded with values obtained for colonic MPO activity, with the highest elevation seen at 7 days post-TNBS (Fig 3-23). Ulceration featuring total loss of intestinal crypt architecture was evident at day 14. Colon thickness, and cellularity through all layers of the colon, were also visibly increased at this timepoint. Although specific cell-types were not identified in these studies, increased cellularity in human IBD is due to invading inflammatory cells as well as hyperproliferation of resident cells, including smooth muscle cells and fibroblasts involved in fibrosis (Pucilowska *et al.*, 2000; Lawrance *et al.*, 2001).

MPO activity remained significantly elevated at day 14 indicating that neutrophils are a significant component of the inflammatory infiltrate present at this timepoint (Fig 3-18b and 3-22). Examination of MPO activity in rat colon tissue at 12 hours and 24 hours post-TNBS, indicated that there was a biphasic elevation in MPO activity with an early

elevation at 12 hours that declines by 24 hours, and a second elevation through the later stages of TNBS-induced colitis (Fig 3-23). Data gathered from these samples was combined with the data in Fig 3-22. A biphasic neutrophil (NT) response is plausible (Dalmarco *et al.*, 2002; Kalff *et al.*, 1999; Rao *et al.*, 1994; Cooray, 1996; Yamada *et al.*, 1993; Fainsilber *et al.*, 1988), where NTs may participate in an initial innate immune response triggered by ethanol, increased mucosal permeability, or bacterial components, followed by a second wave of NTs as the T cell-driven chronic immune response develops. Few studies have examined changes in inflammatory infiltrate over time in TNBS-induced colitis, especially at the 12-hour timepoint, and this should be addressed in a separate study.

In the first series of TNBS experiments, PTX and M-1 (32 mg/kg bid) were administered by intraperitoneal injection (i.p.) from days 3-14 after colitis induction (n=10 per group). The results indicated that this dosing schedule did not have significant therapeutic effects on damage or inflammation in this model, although a trend toward improvement was seen in the M-1-treated colitic rats compared to saline-treated colitic rats where M-1 treatment reduced Damage Score (38 % decrease; p=0.07) and MPO activity (56% decrease; p=0.053) to near significant levels (Fig 3-18). With an increased number of animals (ex. 15-20/group) these effects likely would have reached statistical significance. We decided to double the dose of PTX and M-1 (64 mg/kg i.p.) in series II experiments with the aim of improving their effects in TNBS-induced colitis but mild signs of toxicity (e.g. hypersalivation) were observed after injection. Similar side effects were reported at this dose by a previous student from our lab. PTX has been administered

(i.p.) in rats at much higher doses, up to 300 mg/kg, and a dose of 70 mg/kg (i.p.) in rats is considered comparable to doses administered to humans with circulatory disorders (Abdel-Salam *et al.*, 2003). Nonetheless, we decided to administer the drug directly to the site of action (64 mg/kg intracolonically) and no signs of toxicity were observed. Intracolonic PTX at 100 mg/kg had previously been administered without side effects (Peterson and Davey, 1997). The lack of side effects with i.c. administration is likely due to slower absorption by the intracolonic route compared to i.p. injection.

Series III experiments revealed that the effects of TNBS were attenuated when intracolonic treatments, including saline, were initiated 1 hour after TNBS, suggesting a "wash-out" effect (Figs 3-24 – 3-26). It was therefore important to initiate intracolonic treatments after establishment of colitis in the TNBS model. In series II experiments, intracolonic treatment with PTX or M-1 (64 mg/kg bid) from days 3-14 significantly attenuated colon damage and inflammation associated with TNBS-colitis (Fig 3-20 and 3-21). These results are consistent with previous studies examining the effects of PTX in experimental colitis (Peterson and Davy, 1997; Murthy *et al.*, 1999), as well as a study investigating a novel M-1R compound, lisofylline, in TNBS-induced colitis (Sturm *et al.*, 2002). There were no significant differences between the effects of PTX and M-1 on colon damage or MPO activity, indicating that these drugs have similar anti-inflammatory effects in TNBS-induced colitis even though their mechanisms of action may be different (Bursten *et al.*, 1994; Coon *et al.*, 1999; Jimenez *et al.*, 2001; Sturm *et al.*, 2002). M-1S is believed to have pharmacological properties similar to PTX but few studies have examined this (Aviado and Dettlebach, 1984; Tranquille *et al.*, 1991;

Sullivan *et al.*, 1988; Bright *et al.*, 1998). Studies have instead focused on the properties of lisofylline, an experimental M-1R compound, and have found it to be a potent anti-inflammatory agent with biological properties distinct from PTX (Rice *et al.*, 1994; Bursten *et al.*, 1994; Bright *et al.*, 1998; Coon *et al.*, 1999).

Many anti-inflammatory effects of M-1R are attributed to its potent suppression (800 times more potent than PTX) of phosphatidic acid (PA) generation (Rice *et al.*, 1994; Bursten *et al.*, 1994; Sturm and Dignass, 2002) and TNF-α synthesis (Hasegawa *et al*, 1997; Fiorucci *et al.*, 1998). Anti-inflammatory effects of PTX are often attributed to inhibition of NF-κB activation (Jimenez *et al.*, 2001; Chen *et al.*, 2003; Biswaz *et al.*, 1994) and elevation of cAMP due to inhibition of PDE (Streiter *et al.*, 1988; Bruynzeel *et al.*, 1997). The anti-inflammatory effects of lisofylline are presumed to be independent of PDE inhibition (Wattanasirichaigoon *et al.*, 2000) and lisofylline has been reported not to block NF-κB activation in response to TNF-α (Bursten *et al.*, 1994) or hyperoxia-induced lung injury (George *et al.*, 2002). Moreover, lisofylline is reported to block activation of cAMP response element binding protein (CREB) (George *et al.*, 2002; Bolick *et al.* 2003), a protein that is activated in response to PTX (Jimenez *et al.*, 2001; Lee *et al.*, 1997; Staak *et al.*, 1997). The racemic nature of the M-1 used in our studies means that the combined mechanisms of M-1R and M-1S will be exhibited *in vivo* and will likely encompass mechanisms both similar and distinct from PTX.

In contrast to the similar anti-inflammatory effects of PTX and M-1 in TNBS-induced colitis, only M-1 inhibited the TNBS-induced increase in total intestinal collagen

levels, suggesting that M-1 has superior anti-fibrotic activity *in vivo* compared to PTX. M-1 significantly attenuated TNBS-induced increases in colon weight (Fig 3-19) and colon thickness (Fig 3-27). Colon weight and thickness provide a crude estimate of the overall levels of edema, inflammation, and fibrosis in the tissue. Analysis of H&E-stained colon sections at day 14 post-TNBS (Figs 3-16 and 3-22) revealed that edema in the tissue had subsided by this timepoint compared to earlier timepoints (Fig 3-22). There was no visual difference in inflammatory infiltrate between H&E-stained colons from PTX and M-1-treated rats, which was supported by the similar effects of PTX and M-1 on MPO activity (Fig 3-21). The different effects of M-1 and PTX on colon weight and thickness could therefore be attributed, at least in part, to fibrosis in the tissue. We examined collagen deposition in colon tissue by a Sirius Red/Fast Green-staining method, immunohistochemistry, and Western analysis. The results are discussed below.

This is one of the few studies to examine the effects of pharmacologic agents on inflammation-induced fibrosis in an animal model of colitis. Total collagen deposition in the colon was measured using the Sirius Red/Fast Green (SR/FG) method of tissue collagen quantitation originally described by Lopez de Leon and Rojkind (1985) and previously established in the TNBS model (Peterson and Davey, 1997). Sirius Red stains fibrillar collagen in the presence of picric acid. Analysis of collagen (μg) as a ratio of total protein (mg) using the SR/FG method showed no difference between control and TNBS-treated tissues indicating that the "ratio" itself was not changed (Fig 3-29). Treatment with M-1 resulted in a small but significant decrease in the ratio of collagen to total protein, suggesting that as overall protein in the colon was increasing, collagen

accumulation was being inhibited. Results from IHC and western analysis clearly demonstrated that collagen type III (Fig 3-35) and collagen type I (Fig 3-36) were elevated in TNBS-induced colitis. Elevated levels of collagens type III and type I are characteristic of disease-related fibrosis, including intestinal fibrosis seen in human Crohn's disease (Geboes *et al.*, 2000; Gonzalez *et al.*, 2004; Kershenobich-Stalnikowitz and Weissbrod, 2003).

Visual inspection of SR/FG-stained colon sections also demonstrated that total collagen in TNBS-treated tissue was clearly increased compared to controls (Fig 3-30). H&E-stained tissues demonstrated that overall cellularity was higher in tissue from colitic rats (Fig 3-16). In order to account for the overall increase in protein/cellularity in TNBS-exposed tissue, the collagen ratio (μg collagen/mg protein) was corrected for the total weight of each 6cm colon segment. This modified collagen score revealed that collagen was significantly increased in the TNBS group compared to controls (Fig 3-31), which supported the results from visual analysis of SR/FG-stained tissue, as well as IHC and Western analysis of collagen types III and I, respectively. Unfortunately, an anti-rat collagen type I antibody for use in IHC was not commercially available, nor could we consistently detect collagen type III by Western analysis using an anti-rat collagen type III antibody we had purchased from Sigma. The modified collagen score showed a significant positive correlation with damage score (Fig 3-32), which would be expected in a model of inflammation-induced fibrosis. When this modified collagen score was further corrected for the increased protein concentration in TNBS-exposed tissue due to inflammatory infiltrate and excessive proliferation of resident mesenchymal cells, an

estimate of the absolute collagen content of colon tissue (mg collagen/6 cm colon segment) was obtained and demonstrated that colonic collagen was significantly increased in TNBS-colitis (Fig 3-33).

Other investigators have assessed SR-stained collagen by qualitative visual histochemical analysis (Last *et al.*, 2004) often accompanied by development of a semi-quantitative scoring system (Du *et al.*, 2001), automated digital image analysis (Ejeil *et al.*, 2003), computerized histomorphometry (Murphy and Nicholson, 2003), and Sirius Red-polarizing microscopy-morphometry, which can distinguish between certain types of collagen by their unique fibril properties (Che and Huang, 1999). These methods produce a ratio of SR-stained area to the total area of the tissue section, similar to the elution method of Lopez de Leon and Rojkind (1985). The original SR/FG method was found to correlate with morphometry results (Gascon-Barre *et al.*, 1989). The method described in this study provides a simple method of quantitating tissue collagen by extending the calculations from the original SR/FG method to account for changes in tissue composition that may occur in inflamed tissues. This modification seems intuitive but has not been described in the literature. Accounting for changes in protein concentration and tissue weight using the SR/FG method will likely be useful to other investigators attempting to quantitate collagen in inflamed tissue.

In support of our modification to the calculation of collagen content from SR/FG-stained tissues, Sanai and colleagues (1999) recently reported substantial increases in collagens type I and III visualized by IHC in allergic nasal membranes compared to

controls, with significant thickening of the collagen-containing basement membrane region, but could show no difference in total collagen levels using the SR/FG method. This being a model of inflammation-induced fibrosis, it is quite possible that increases in inflammatory infiltrate and other proteins in the nasal membranes paralleled the increase in collagen, resulting in no change in the "ratio" of collagen to total protein. Using the original SR/FG calculations (Lopez de Leon and Rojkind, 1985), a change in collagen level will only be detected if it is greater in magnitude than the change in total tissue protein.

In our study, colitic rats had significantly increased intestinal collagen levels compared to non-colitic controls, indicative of TNBS-induced intestinal fibrosis (Figs 3-31 and 3-33). Only treatment with M-1 significantly reduced total collagen deposition and thus intestinal fibrosis in this model. This is likely a combination of the more potent anti-fibrogenic effects of M-1, as seen in our *in vitro* studies (Figs 3-3 and 3-6), and the higher total drug levels achieved *in vivo* following direct administration of the metabolite compared to PTX (Fig 3-14). The lack of effect of PTX on total collagen is in agreement with previous results from our lab where acute PTX treatment failed to reduce collagen levels in TNBS-induced colitis using the original SR/FG method (Peterson and Davey, 1997). PTX may have selective inhibitory effects on collagen type I in TNBS-colitis as indicated by Western analysis of colon tissue from select animals who showed a good response to PTX (e.g. low damage score) (Fig 3-36). This will be further assessed by our group. It should be noted that PTX has attenuated fibrosis in other disease models including glomerulonephritis (Lin *et al.*, 2002), Peyronie's disease (Valente *et al.*, 2003),

and hepatic fibrosis (Peterson, 1993), and it is possible that a higher dose or longer treatment period could have improved the effect of PTX on TNBS-induced fibrosis. PTX has also reversed intestinal collagen deposition in human collagenous colitis patients, resulting in clinical remission in several patients (Peterson and Tanton, 1996). Thus the anti-fibrotic effects of PTX *in vivo* are worthy of further investigation, especially since PTX is a well-known and affordable drug that is already routinely prescribed to humans. Nonetheless, at the dose tested, only M-1 exhibited significant effects on TNBS-induced total colonic collagen deposition and this compound should be assessed in other animal models of fibrosis.

In an attempt to identify cytokines involved in the fibrosis associated with TNBS-induced colitis, we examined the levels of two pro-fibrogenic cytokines, PDGF-B and TGF-β1, in colon tissues by Western analysis. Preliminary results revealed that there was a decrease in TGF-β1 4 hours after TNBS administration that returned to baseline by day 3 (Fig 3-41), indicating that TGF-β1 is likely not involved in TNBS-induced fibrosis. The depression in TGF-β1 levels at 4-hours post-TNBS could result in loss of immunoregulatory effects of TGF-β at this timepoint. Although some studies report increased expression of TGF-β in areas of active CD lesions (Xian *et al.*, 1999), TGF-β signaling is generally inhibited in IBD resulting in loss of the "anti-inflammatory" effects of TGF-β (Fiocci *et al.*, 2001; Monteleone *et al.*, 2001). In fact, murine TNBS-colitis was attenuated by intranasal administration of a plasmid expressing TGF-β under the control of a constitutive promoter (Kitani *et al.*, 2000). The fibrogenic consequences of TGF-β therapy in IBD are unexplored. Activators of NF-κB (e.g. TNF-α, IL-18, and IL-1β) are

elevated in human CD and induce the production of Smad 7, an endogenous inhibitor of TGF-β signaling (Bitzer *et al.*, 2000). IFN-γ, the hallmark T_H1 cytokine, also suppresses TGF-β signaling (Ulloa *et al.*, 1999). It is generally accepted that in the face of a strong T_H1 response, as seen in human CD and in TNBS-colitis, it would be difficult for TGF-β to exert its anti-inflammatory (or pro-fibrogenic) effects.

In contrast to TGF-β, PDGF-B was barely detectable in control tissues but was elevated in colitic tissue from days 3-14 post-TNBS. This suggests that PDGF may play an active role in fibrogenesis in TNBS-colitis by stimulating proliferation and collagen synthesis by fibroblasts, myofibroblasts, and smooth muscle cells. Evidence has suggested that PDGF and its receptors are increased in CD lesions (Kumagi *et al.*, 2001) and that CD fibroblasts are hypersensitive to the effects of PDGF *in vitro* (Lawrance *et al.*, 2001). A study by Peterson and Tanton (1996) suggested that PDGF (and not TGF-β, TNF-α or TNF-β) is involved in fibrosis associated with human collagenous colitis. The results from our investigation are preliminary and need to be repeated.

Assessment of the pro-inflammatory cytokine IL-18 by ELISA in TNBS-induced colitis revealed that colonic IL-18 levels were significantly increased 3-days after colitis induction, following a sharp depression that was seen by 4 hours (Fig 3-37). The 2-fold increase in colonic IL-18 in our study is consistent with the increase in IL-18 recently reported in the murine model of DSS-induced colitis (Loher et al., 2004). Since IL-18 is constitutively produced by intestinal epithelial cells (IEC) in the healthy colon (Takeguchi *et al.*, 1997), the initial depression in IL-18 could be a result of physical

damage to the epithelium caused by administration of TNBS and ethanol. The release of IL-18 from TNBS-exposed epithelial cells could play an important role in initiating an immune response to TNBS (Kanai *et al.*, 2001; Kashiwaruma *et al.*, 2002; Komai-Koma *et al.*, 2003; Sugawara *et al.*, 2001; Gracie *et al.*, 2003). Niak and colleagues (1999) reported that keratinocytes (dermal epithelial cells) secrete biologically active IL-18 when exposed to dinitrochlorobenzene (DNCB), a contact sensitizer with similar properties to TNBS. The peak seen at day 3 would likely constitute IL-18 produced by recovering epithelial cells as well as IL-18 produced by monocytes, macrophages, and NK cells that have migrated into the inflamed tissue (Gracie *et al.*, 2003). IL-18 levels returned to normal by day 7 consistent with a role for IL-18 in the developing immune response in TNBS-induced colitis, including effects on T cell recruitment and activation (Kanai *et al.*, 2001; Komai-Koma *et al.*, 2003). That the peak elevation in IL-18 at day 3 preceded the peak in MPO activity seen at day 7 in our studies coincides with the recently reported role of IL-18 in neutrophil recruitment (Netea *et al.*, 2000; Cannetti *et al.*, 2003) and activation (Whyman *et al.*, 2002; Leung *et al.*, 2001). The initial release of IL-18 from the intestinal epithelium following TNBS administration may have played a role in the early peak in MPO activity observed at 12-hours post-TNBS (Fig 3-33). IL-18-mediated neutrophil recruitment is reported to occur indirectly via the induction of TNF-α and LTB_4, a potent NT chemoattractant (Cannetti *et al.*, 2003). Activated neutrophils, in turn, play a role in the processing of pro-IL-18 to its mature form (Sugawara *et al.*, 2001).

Since the ELISA kit likely detected both pro-IL-18 and mature IL-18, it cannot be assumed that the IL-18 detected was biologically active *in vivo*. The primary source of IL-18 in control tissue was likely the IECs, which secrete only pro-IL-18 under normal circumstances (Takeuchi *et al.*, 1997). In colitic tissue, the visual abundance of inflammatory cells in tissue sections, along with sustained damage to the epithelium, indicate that inflammatory cells are likely the major source of IL-18 at day 3. Activated immune cells process and secrete IL-18 in its biologically active form (Gracie *et al.*, 2003). Circulating monocytes secrete pro-IL-18, as do keratinocytes and IECs, which may then be processed by enzymes released in the inflamed tissue (Sugawara *et al.*, 2001). Thus, much of the IL-18 detected in colitic tissue at day 3 was likely mature IL-18. In human CD, elevated levels of bioactive IL-18 have been detected in biopsy samples from active lesions (Pizarro *et al.*, 1999).

Visual inspection of H&E-stained colon sections revealed that the inflammatory infiltrate in the lamina propria was most dense 7 days after colitis induction, yet IL-18 levels were decreasing at this time. This indicates that the cytokine profile may change in the later phase of TNBS-induced colitis. There is evidence to support a shift in cytokine and chemokine expression in early versus late experimental colitis (Spencer *et al.*, 2002; Ajuebor *et al.*, 2001). The dramatic elevation in MPO at 7 days post-TNBS may also indicate that neutrophils comprise a larger percentage of the inflammatory infiltrate at this timepoint compared to macrophages and NK cells, contributing to the decreasing IL-18 levels. IL-18 could not be detected in rat serum and this was a defect of the IL-18 kit used (Biosource International), a defect that was encountered by another group using the

same kit (personal communication). Unfortunately, this is the only rat IL-18 ELISA kit available commercially. The lack of detection likely reflects diminished sensitivity of the kit. Serum IL-18 levels may be a useful clinical marker of human CD versus UC (Furuya *et al.*, 2002). Recently, our group has reported increased serum levels of IL-18 in collagenous colitis patients compared to controls with irritable bowel syndrome (Peterson *et al.*, 2003). IL-18 levels correlated with pro-collagen III N-terminal peptide (PIIINP) in this study, a serological marker of active fibrosis. It would have been interesting to determine if serum IL-18 levels were elevated in TNBS-induced colitis since this has not been investigated. Since IL-18 levels were already at their peak when drug treatment was initiated, it is unlikely that therapeutic effects of M-1 or PTX were due to inhibition of IL-18 levels. However, since IL-18 and other cytokines implicated in CD (e.g. TNF-α and IL-1β) exert many effects via activation of the transcription factor NF-κB, the levels of this transcription factor were examined in TNBS-induced colitis.

Assessment of NF-κB by Western analysis followed by densitometry in TNBS-colitis revealed that NF-κB p65 protein levels were significantly increased in colon lysates by 4 hours post-TNBS and gradually returned to baseline by day 14 (Fig 3-38). The sustained increase in NF-κB was not surprising in light of the mounting evidence that NF-κB plays an important role in the inflammatory events associated with experimental colitis as well as human CD. Neurath and colleagues (1996) demonstrated the important role of NF-κB in murine TNBS-colitis when they showed that administration of antisense phosphorothioate oligonucleotides to the p65 subunit of NF-κB abrogated established colitis. This study supports our finding of sustained NF-κB

elevation in the TNBS model. If NF-κB was increased only transiently in early colitis development, antisense therapy would not have reversed established colitis. If NF-κB remained elevated after colitis was established and played a role in active colitis, then neutralization of NF-κB in established colitis would have therapeutic effects. Antisense to NF-κB p65 was recently reported to attenuate fibrosis in a newly developed murine model of inflammation-induced intestinal fibrosis (Lawrance *et al.*, 2003), likely by the indirect effect of reducing inflammation rather than a direct effect on fibrosis (MacDonald, 2003). Rogler and colleagues (1998) reported that in addition to macrophages and other immune cells, intestinal epithelial cells are a major site of increased NF-κB activation in inflamed CD mucosa. They used an antibody that specifically recognized activated NF-κB p65 by binding to a site generally blocked by the inhibitor of κB (IκB) protein. Unfortunately, a phospho-specific NF-κB p65 antibody targeted against rat protein was not commercially available during our studies.

The pro-inflammatory cytokines IL-18, IL-1β and TNF-α are important mediators of inflammation in IBD and all three are known to signal through the activation of NF-κB (Stevens *et al.*, 1996; Gracie *et al.*, 2003). Both IL-1β and TNF-α have been shown to activate NF-κB in IEC-6 cells, a normal rat intestinal epithelial cell line (Hellerbrand *et al.*, 1996). This study showed that intercellular adhesion molecule-1 (ICAM-1) expression on IEC-6 cells was increased in response to TNF-α and IL-1β by an NF-κB-dependent mechanism. ICAM-1 expression, and secretion of soluble ICAM-1, are elevated in IBD (Dippold *et al.*, 1993) and epithelial cells may therefore play a role in the development of inflammation in IBD by recruiting inflammatory cells such as neutrophils

into the area. In order to determine if racemic M-1 affects NF-κB activation, we compared the effects of PTX and M-1 on cytokine-stimulated NF-κB p65 nuclear translocation in IEC-6 cells by immunocytochemistry (ICC). IL-18 did not activate NF-κB in IECs, as assessed by ICC (Fig 3-41) or Western analysis of nuclear protein (Fig 3-42), likely indicating that under normal culture conditions these cells do not express enough of the functional IL-18R complex to observe activation of NF-κB within the cell. IL-18R expression by IECs has not been examined. Functional IL-18R was shown to be increased on macrophages, vascular endothelial cells and vascular smooth muscle cells in atherosclerotic lesions compared to cells from control tissue. IL-18Rs were up-regulated on these cell-types *in vitro* by exposure to TNF-α and IL-1β, cytokines implicated in atherosclerosis (Gerdes *et al.*, 2002). It is possible that low-level receptor expression on IECs is up-regulated by inflammatory mediators in human CD but this remains to be determined. In fact, in an initial ICC experiment during this study, NF-κB was activated in IECs in response to IL-18 but this could not be repeated despite many attempts. It may have been that some unidentified stimulus in the culture environment (e.g. hypoxia, bacterial contamination, increased insulin in the media) could have activated the cells and caused up-regulation of IL-18R. It could also be that the cells were at a very low passage number, directly from ATCC, and may have expressed higher levels of IL-18R in early passages. Whatever the reason, both PTX and M-1 blocked NF-κB activation at all timepoints tested following IL-18 administration in this particular experiment.

Anti-inflammatory effects of PTX, including inhibition of inflammatory cytokine release (e.g. TNF-α, IL-1β, and IL-18) and cytokine signaling, are often attributed to

inhibition of NF-κB activation (Jimenez *et al.*, 2001; Chen *et al.*, 2003). It was therefore not surprising that PTX blocked nuclear translocation of NF-κB in response to IL-1β and TNF-α in IECs at all timepoints assessed (Fig 3-42). The finding that racemic M-1 blocked NF-κB activation *in vitro* was not predicted, since M-1R (lisofylline) was reported not to block TNF-α-induced activation of NF-κB in cultured macrophages (Bursten *et al.*, 1994). This discrepancy may indicate that the S-isoform of M-1 is capable of inhibiting NF-κB activity, similar to PTX. The dose of M-1 used in our study (~3 mM) was higher than the dose of lisofylline (100 μM) used by Bursten and colleagues (1994). Inhibition of NF-κB by M-1 in our study could therefore represent a dose-dependent, enantiomer specific, or cell-type specific effect. Our group is currently examining the effects of drug-dose and cell-type on inhibition of NF-κB activation by M-1 *in vitro*. Nonetheless, the results presented here suggest that inhibition of NF-κB activation by PTX, and likely by racemic M-1, is an important mechanism by which these drugs exert their anti-inflammatory effects. Since important pro-inflammatory cytokines in colitis activate transcriptional responses via NF-κB activation, inhibition of NF-κB by PTX and M-1 would contribute to the anti-inflammatory effects observed in the TNBS model, especially since NF-κB was the most dramatically elevated signaling molecule assessed (Fig 3-40).

Two MAPKs, JNK/SAPK and p38 MAPK, were also assessed in colon tissue from TNBS-treated rats (see Fig 4-2 for traditional MAPK signaling cascades). JNK-1 and p-JNK were increased 4 hours after colitis induction but returned to normal levels at all later timepoints assessed (Fig 3-41). JNK is an upstream kinase for c-Jun

phosphorylation and therefore regulates formation of AP-1 transcription factors. We have recently shown that PTX is capable of inhibiting c-Jun phosphorylation in human fibroblasts contributing to the anti-proliferative effects of PTX (Peterson *et al.*, 2002). It has been demonstrated that JNK activation is important for T cell proliferation (Dong *et al.*, 1998) and is an important mediator of T_H1 cell differentiation (Dong *et al.*, 2000; Yang *et al.*, 1998). It is unclear at what timepoint JNK activation returns to baseline in the TNBS-model (sometime between 4 and 72 hrs). It is tempting to speculate that inhibition of this transient increase in JNK activation (using a specific JNK inhibitor for instance) in TNBS-colitis could hinder the development of colitis by targeting T_H1 development and subsequent cytokine synthesis. JNK is a positive regulator of TNF-α translation and thus the increase in JNK activity in early TNBS-colitis may drive inflammatory cytokine production (Swantek *et al.*, 1997).

JNK inhibition in experimental colitis has not yet been examined but inhibition of the JNK cascade for therapeutic purposes has become a hot topic of investigation (review Bogoyevitch *et al.*, 2004). Studies have shown that JNK inhibition attenuates joint destruction in experimental arthritis (Han *et al.*, 2001) and prevents connective tissue growth factor (CTGF) induction by TGF-β in human lung fibroblasts thereby preventing collagen synthesis (Utsugi *et al.*, 2003), implicating JNK as a possible mediator of tissue remodeling and fibrosis. The transient nature of JNK elevation in TNBS-colitis may be a result of negative regulation of JNK by NF-κB in this model. Inhibition of JNK by NF-κB is now well-documented in the literature (Varfolomeev and Ashkenazi, 2004; Deng *et*

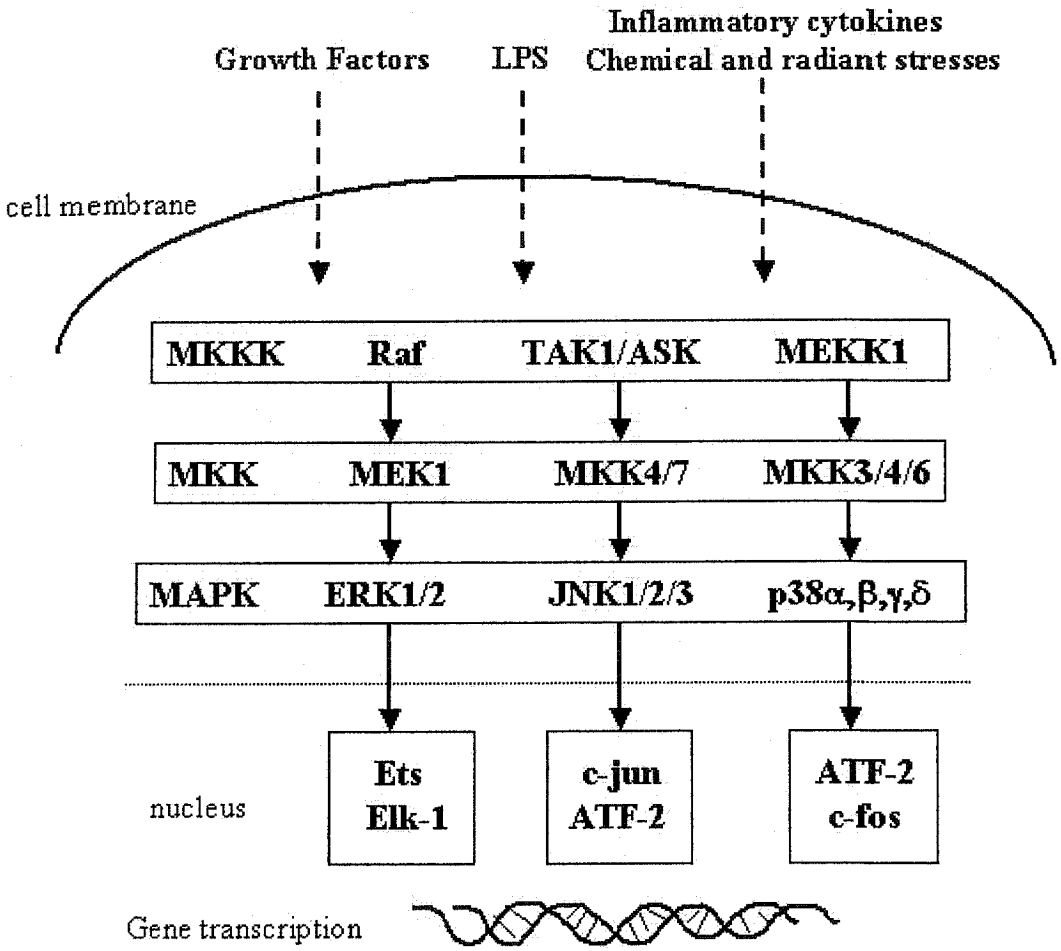

Figure 4-2. Classical MAPK signaling cascades.

al., 2003; Tang *et al.*, 2002; Tang *et al.*, 2001). Sustained activation of NF-κB inhibits cytokine-induced JNK activation (Zhang and Chen, 2004).

The p38 MAPK was not increased in TNBS-colitis. In fact, there was a transient depression in p38 protein levels at 4 hrs post-TNBS accompanied by a depression in p-p38 (Fig 3-41). This was surprising since the role of p38 MAPK in mediating inflammatory responses in various human disorders is receiving attention in the literature (Lowenberg *et al.*, 2004; Lee *et al.*, 2000; Salituro *et al.*, 1999). The p38 MAPK is the most widely studied MAPK and it is well known to participate in intracellular signaling cascades resulting in inflammation (Lee *et al.*, 1999; Van den Blink *et al.*, 2002). Activation of p38 MAPK was required for development of a dermal contact hypersensitivity response to 2,4-dinitro-1-fluorobenzene (DNFB), a hapten compound related to TNBS (Takanami-Ohnishi *et al.*, 2002), thus we expected that p-p38 would be increased in TNBS-colitis.

The role of p38 MAPK in human IBD is somewhat controversial. A recent investigation of MAPKs in human IBD revealed that levels of p-p38, p-JNK1/2 and p-ERK1/2 were all significantly increased in colonic mucosa from CD patients compared to controls (Waetzig *et al.*, 2002). Protein levels of p38 and JNK were slightly increased in CD in this study whereas ERK protein levels were decreased. Another study reported that both p38 and JNK activity were increased in human CD (Hommes *et al.*, 2002). Treatment with a dual p38/JNK inhibitor, CNI-1493, in this study strongly reduced

clinical disease activity in human CD patients. Only inhibition of JNK-phosphorylation was detected *in vivo* and thus the beneficial effects of CNI-1493 treatment were attributed to JNK inhibition only. Thus a clear role for p38 in CD still has not been determined. A clinical trial using a selective p38 inhibitor is currently underway (Waetzig and Schreiber, 2003).

Our finding of reduced p38 activity in TNBS-colitis may represent a limitation of using an animal model to mimic human disease. Interestingly, a recent study of murine TNBS-colitis reported a dichotomal role of inhibiting p38 MAPK with a selective inhibitor, SB203580 (Ten Hove *et al.*, 2002). This group saw a transient increase in p38 activity in mice following TNBS administration, which may reflect a species difference in the response to TNBS. Treatment with the p38 inhibitor resulted in increased weight loss, increased colon weight, and increased TNF-α production in colitic mice compared to untreated colitic mice, while decreased lymphocyte numbers, and decreased IFN-γ and IL-12 production were observed. The authors speculate that inhibition of p38 may abrogate p-38 MAPK-mediated protective functions of immune cells while exacerbating the production of TNF-α, a pivotal cytokine in IBD. Our results suggest that inhibition of p38 MAPK in TNBS-induced rat colitis may not have any beneficial effect.

ATF-2 is a transcription factor that is phosphorylated through both JNK and p38 pathways (Reimold *et al.*, 2001). Our finding of decreased p-ATF-2 levels in TNBS-colitis is interesting in light of a recent study that reported that CD patients who respond to Infliximab (anti-TNF-α) therapy show increased p-ATF-2 following treatment,

whereas non-responders have low p-ATF-2 levels in colonic biopsies (Waetzig *et al.*, 2003). All CD patients in this study showed a transient increase in p-p38 after Infliximab treatment but only the responders exhibited increased p-ATF-2, a downstream target of p38. A recent study using ATF-2-deficient mice concluded that ATF-2 is essential for maximal immediate induction of adhesion molecules and cytokine genes in response to LPS, T cell activation, and viral infection, but may actually protect against overactive immune responses (Reimold *et al.*, 2001). The role of this transcription factor in IBD should be further explored.

Chapter 5

SUMMARY, SIGNIFICANCE AND FUTURE STUDIES

This thesis examined the *in vitro* and *in vivo* effects of a racemic M-1 (1-(R/S-5-hydroxyhexyl)-3,7-dimethylxanthine), a major metabolite of PTX. We have developed a simple, reproducible and inexpensive method to produce the metabolite with an excellent recovery rate of greater than 80 % of starting compound with equivalent biological activity from batch to batch. This work demonstrated that racemic M-1 is more potent than PTX *in vitro* at inhibiting PDGF-stimulated proliferation and collagen synthesis of cultured fibroblasts. Fibroproliferation and collagen synthesis are the hallmark events of fibrosis and these findings suggest that M-1 may be a useful anti-fibrogenic compound *in vivo*. We are currently examining the effects of M-1 in models of fibrotic diseases such as liver fibrosis and scleroderma.

Our investigation of the anti-inflammatory and anti-fibrogenic effects of M-1 in a rat model of human CD revealed that while PTX and M-1 share similar anti-inflammatory effectiveness in the model, with significant reduction of ulceration and inflammation, only M-1 protected rats from inflammation-induced intestinal fibrosis. This is a very important finding since there is currently no treatment aimed at preventing or reversing fibrosis in CD. Fibrosis in CD is a major cause of morbidity that leads to surgical intervention in over 50 % of patients. This is an enormous burden to health care since CD is highly prevalent in North America. Development of an inexpensive treatment that could target both inflammation and fibrosis in CD would be a major advance in the field of gastroenterology. Since intracolonic therapy is not the most desirable dosage form, an oral formulation of M-1 that is activated in the colon (similar to a currently available 5-ASA derivative for CD) could be quite effective. M-1 would likely be beneficial in other forms of IBD including collagenous colitis and ulcerative colitis.

Toxicity and dosing of racemic M-1 must be examined in humans before this can be explored.

Characterization of fibrosis in TNBS-induced colitis revealed dramatic elevations in type I and type III collagen, consistent with the human disease. This suggests that the TNBS model, using our particular parameters, is useful for the study of inflammation-induced fibrosis and could aid investigators in identifying other therapeutic strategies to treat intestinal fibrosis in IBD. We have also modified a well-established method for measuring tissue collagen (Lopez de Leon and Rojkind, 1985) to account for changes in tissue architecture that often accompany inflammation. This modification allows the investigator to measure the absolute amount of collagen in a given tissue by working backward through a series of factors including tissue weight and tissue protein concentration. This could help other investigators who have encountered frustrations in trying to measure collagen in inflamed tissues. PDGF was implicated as a possible mediator of fibrosis in TNBS-induced colitis and ongoing studies in our lab are investigating the role of PDGF in human IBD. Since we have shown that PTX and M-1 target PDGF-mediated fibrogenic events *in vitro*, and that M-1 is more potent than PTX in this respect, this could explain the enhanced anti-fibrotic effects of M-1 seen in this model. The role of PTX in the inhibition of collagen type I in TNBS-colitis needs to be further examined.

Characterization of molecular events associated with TNBS-induced colitis revealed a sustained increase in colonic NF-κB p65 levels, confirming that this transcription factor is an important therapeutic target in this model. Our *in vitro* studies indicated that both PTX and M-1 were able to block NF-κB activation in IECs and thus

NF-κB is likely an important molecular target of these drugs in TNBS-induced colitis. Studies are underway in our lab to further examine the effects of M-1 on NF-κB *in vitro* and future studies should examine this effect *in vivo*. A transient increase in p-JNK was also observed that could be targeted in future studies using a specific JNK inhibitor. The MAPK p38 did not appear to play a significant role in TNBS-induced colitis since it was transiently decreased in the model. The relevance of this finding to human CD is currently unclear since the role of MAPKs in IBD is a very recent field of investigation. A sustained decrease in p-ATF-2, a downstream target of p38 MAPK, could indicate that diminished signaling via this pathway contributes to the development of colitis. Recent data from a study of human CD suggests that this could be a possibility since CD patients who respond to the therapeutic agent Infliximab show enhanced phosphorylation of ATF-2 (Waetzig *et al.*, 2003). The role of MAPKs in human IBD is a field that is currently under heavy investigation. In the meantime, investigators should continue to explore the role of MAPKs in various experimental models of colitis.

Investigation into the kinetics of M-1 compared to PTX revealed that higher levels of active drug (PTX + M-1) were achieved following direct administration of the metabolite. This could also explain the enhanced effects of M-1 in TNBS-induced colitis. M-5 is also an active metabolite of PTX and should be assessed in future HPLC analyses in order to completely determine the levels of active drug achieved following PTX or M-1 administration. We did not have a pure sample of M-5 thus we could not identify this peak by HPLC. An interaction with the antibiotic ciprofloxacin in mice demonstrated that dramatically elevated levels of M-1 were achieved *in vivo* following M-1 administration, likely due to inhibition of multiple pathways of M-1 metabolism by

ciprofloxacin. The interaction between M-1 and ciprofloxacin is a novel finding. Since ciprofloxacin is commonly prescribed to CD patients, the combination of this antibiotic with M-1 could be particularly advantageous in the treatment of human CD and perhaps other forms of IBD as well. This interaction should first be examined in a murine model of CD, such as TNBS-induced colitis.

This was the first study to examine the combined effects of M-1R and M-1S (racemic M-1) *in vivo* and our results suggest that M-1 has potential as a therapeutic anti-inflammatory and anti-fibrogenic agent. Previous studies have examined the anti-inflammatory properties of lisofylline, an experimental M-1R compound. Synthesis of an enantiomerically pure compound is extremely expensive and should only be undertaken after careful consideration of production and development costs versus the actual therapeutic advantages of enantiospecificity, usually in terms of reducing toxicity (Pifferi and Perucca, 1995). No studies report toxic effects of M-1S or other PTX metabolites and therefore commercial development of a pure M-1R compound may not be warranted. Racemic M-1 would be a much cheaper alternative to lisofylline and would harness effects of both M-1R and the novel M-1S enantiomer whose molecular effects remain to be elucidated.

REFERENCES

Abbas A, Murphy KM, Sher A. Functional diversity of helper T lymphocytes. Nature 1996; 383: 787-793

Abdel-Salam OME, Baiuomy AR, El-Shenaway SM, Armid MS. The anti-inflammatory effects of the phosphodiesterase inhibitor pentoxifylline in the rat. Pharmacol Res 2003; 47: 331-340.

Adams CL, Kobets N, Meiklejohn GR, Millington OR, Morton AM, Rush CM, Smith KM, Garside P. Tracking lymphocytes in vivo. Arch Immunol Ther Exp (Warsz) 2004; 52(3): 173-187.

Ajuebor MN, Hogaboam CM, Kunkel SL, Proudfoot AE, Wallace JL. The chemokine RANTES is a crucial mediator of the progression from acute to chronic colitis in the rat. J Immunol 2001; 166: 552-558.

Akobeng AK, Zachos M. Tumor necrosis factor-alpha antibody for induction of remission in Crohn's disease. Cochrane Database Syst Rev 2004; (1): CD003547.

Anderson KN (ed). Mosby's medical, nursing, and allied health dictionary 5th edition. Mosby; USA: 1998.

Andrews NC, Faller DV. A rapid micropreparation technique for extraction of DNA-binding proteins from limiting numbers of mammalian cells. Nucl Acids Res 1991; 19(9): 2499.

Andus T, Targan SR, Deem R, Toyoda H. Measurement of tumor necrosis factor alpha mRNA in small numbers of cells by quantitative polymerase chain reaction. Reg Immunol 1993; 5(1): 11-17.

Armendariz-Borunda J, Sinkevich CP, Roy N, Raghow R, Kang AH, Seyer JM. Activation of Ito cells involves regulation of AP-1 binding proteins and induction of type I collagen gene expression. Biochem J 1994; 15: 817-824.

Assche VG. Can we influence fibrosis in Crohn's disease? Acta Gastroenterol Belg 2001; 64(2): 193-196.

Atamas SP. Complex cytokine regulation of tissue fibrosis. Life Sciences 2002; 72: 631-643.

Aviado D, Dettelbach H. Pharmacology of PTX: a hemorrheologic agent for the treatment of intermittent claudication. Angiology 1984; 35: 407-417.

Azam T, Novick D, Bufler P, Yoon D-Y, Rubinstein M, Dinarello CA, Kim SH. Identification of a critical Ig-like domain in IL-18 receptor A and characterization

of a functional IL-18 receptor complex. J Immunol 2003; 171: 6574-6580.

Barnes PJ, Karin M. Nuclear factor-kappaB: a pivotal transcription factor in chronic inflammatory diseases. N Eng J Med 1997; 336: 1066-1071.

Bateman JF, Lamande SR, Ramshaw JAM. Collagen superfamily. In Comper WD (ed). Extracellular Matrix Volume 2: Molecular components and interactions. Amsterdam, The Netherlands; Harwood Academic Publishers, 1996: 22-67.

Beck PL, Podolsky DK. Growth factors in inflammatory bowel disease. Inflamm Bowel Dis 1999; 5(1): 44-60.

Beelan DW, Sayer HG, Franke M, Scheulen ME, Quabeck K, Mohnke M, Oidtmann M, Schaefer UW. Constant intravenous pentoxifylline infusions in allogenic marrow transplant recipients: results of a dose escalation study. Bone Marrow Transpl 1993; 12: 363-370.

Beermann B, Ings R, Mansby J, Chamberlain J, MacDonald A. Kinetics of intravenous and oral pentoxifylline in healthy subjects. Clin Pharmacol Ther 1985; 37: 25-28.

Benbernou N, Esnaukt S, Potron G, Guenounou M. Regulatory effects of pentoxifylline on T-helper cell-derived cytokine production in human blood cells. J Cardiovasc Pharmacol 1995; 25(Suppl 2): S75-S79.

Berman B, Duncan MR. Pentoxifylline inhibits the proliferation of human fibroblasts derived from keloid, scleroderma, and morphea skin and their production of collagen, glycosaminoglycan, and fibronectin. Br J Dermatol 1990; 123: 339-346.

Berrin MC, McKay DM, Perdue MH. Immune-epithelial interactions in host defense. Am J Trop Med Hyg 1999; 60(4 Suppl): 16-25.

Bianco JA, Appelbaum FR, Nemunaitis J, Almgren J, Andrews F, Kettner P, Shields A, Singer JW. Phase I-II trial of pentoxifylline for the prevention of transplant-related toxicities following bone marrow transplantation. Blood 1991; 78(5): 1205-1211.

Bienvenu J, Doche C, Gutowski MC, Lenoble M, Lepape A, Perdrix JP. Production of proinflammatory cytokine and cytokines involved in the TH1/TH2 balance is modulated by pentoxifylline. J Cardiovasc Pharmacol 1995; 25(Suppl 2): S80-S84.

Bilsborough J, Viney JL. Getting to the guts of immune regulation. Immunology 2002; 106: 139-143.

Biswas DK, Ahleers CM, Dezube BJ, Pardee AB. Pentoxifylline and other protein kinase C inhibitors down-regulate HIV-LTR NF-kappaB induced gene expression. Mol Med 1994; 1(1): 31-43.

Bitzer M. A mechanism of suppression of TGF-β/Smad signaling by NF-κB/RelA. Genes Dev 2000; 14: 187-197.

Blanchard MG, Peterson TC. Increased level of antifibrotic drugs due to selective inhibition of CYP1A2. Hepatology 1999; 30: 558A.

Bluestone JA, Abbas AK. Natural versus adaptive regulatory T cells. Nat Rev Immunol 2003; 3(3): 253-257.

Bogoyevitch MA, Boehm I, Oakley A, Ketterman AJ, Barr RK. Targeting the JNK MAPK cascade for inhibition: basic science and therapeutic potential. Biochem Biophys Acta 2004; 1697: 89-101

Bohr J; Olesen M; Tysk C and Jarnerot G. Collagenous colitis and lymphocytic colitis: a clinical and histopathological review. Canadian Journal of Gastroenterology 2000; 14(11): 943-947.

Bolick DT, Hatley ME, Srinivasan S, Hedrick CC, Nadler JL. Lisofylline, a novel anti-inflammatory compound, protects mesangial cells from hyperglycemia- and angiotensin II-mediated extracellular matrix deposition. Endocrinology 2003; 144(12): 5227-5231.

Born TL, Thomassen E, Bird TA, Sims JE. Cloning of a novel receptor subunit, AcPL, required for interleukin-18 signaling. J Biol Chem 1998; 273: 29445-29450.

Boughton-Smith NK, Wallace JL, Whittle BJ. Relationship between arachidonic acid metabolism, myeloperoxidase activity, and leukocyte infiltration in a rat model of inflammatory bowel disease. Agents Actions 1988; 25(1-2): 115-123.

Bouma G, Kaushiva A, Strober W. Experimental murine colitis is regulated by two genetic loci, including one on chromosome 11 that regulates IL-12 responses. Gastroenterology 2002; 123(2): 554-565.

Bradley PP, Priebat DA, Christensen RD, Rothstein G. Measurement of cutaneous inflammation: estimation of neutrophil content with an enzyme marker. J Invest Dermatol 1982; 78(3): 206-209.

Bright JJ, Du C, Coon M, Sriram S, Klaus SJ. Prevention of experimental allergic encephalomyelitis via inhibition of IL-12 signaling and IL-12-mediated Th1 differentiation: An effect of the novel anti-inflammatory drug lisofylline. J Immunol 1998; 161: 7015-7022.

Bruynzeel I, van der Raaij LM, Willemze R, Stoof TJ. Pentoxifylline inhibits human T-cell adhesion to dermal endothelial cells. Arch Dermatol Res 1997; 289(4): 189-193.

Bursten S, Weeks R, West J, Le T, Wilson T, Porubek D, Bianco JA, Singer JW, Rice GC. Potential role for phosphatidic acid in mediating the inflammatory responses to TNF-α and IL-1β. Circ Shock 1994; 44: 14-29.

Burgeson RE, Nimni ME. Collagen types: molecular structure and tissue distribution. Clin Orthop 1992; 282: 250-272.

Camoglio L, Juffermans NP, Peppelenbosch M, te Velde AA, ten Kate FJ, van Deventer SJH, Kopf M. Contrasting roles of IL-12p40 and IL-12p35 in the development of hapten-induced colitis. Eur J Immunol 2002; 32: 261-269.

Cannetti CA, Leung BP, Culshaw S, McInnes IB, Cunha FQ, Liew FY. IL-18 enhances collagen-induced arthritis by recruiting neutrophils via TNF-α and leukotriene B_4. J Immunol 2003; 171: 1009-1015.

Casini-Raggi V, Kam L, Chong YJT, Fiocci C, Pizarro TT, Cominelli F. Mucosal imbalance of IL-1 and Il-1 receptor antagonist in inflammatory bowel disease: a novel mechanism of chronic intestinal inflammation. J Immunol 1995; 154: 2434-2440.

Castiglione F, Rispo A, Di Gorolamo E, Cozzolino A, Manguso F, Gassia R, Mazzacca G. Antibiotic treatment of small bowel bacterial overgrowth in patients with Crohn's disease. Aliment Pharmacol Ther 2003; 18(11-12): 1107-1112.

Che D and Huang X. Chronic obstructive pulmonary disease and pulmonary structural remodeling. Zhonghua Jie He He Hu Xi Za Zhi 1999; 22(8): 472-474.

Chen Q, Tan E, Strauss J, Zhang Z, Fenyk-Melody J, Booth-Genthe C, Rushmore T, Stearns R, Evans D, Baillie T, Tang W. Effect of quinidine on the 10-hydroxylation of R-warfarin: species differences and clearance projection. J Pharmacol Exp Ther 2004; [e-pub ahead of print]

Chen Y-M, Wu KD, Tsai TJ, Hseih BS. Pentoxifylline inhibits PDGF-induced proliferation and TGF-β-stimulated collagen synthesis by vascular smooth muscle cells. J Mol Cell Cardiol 1999; 31(4): 773-783.

Chen Y-M, Tu C-J, Hung K-Y, Wu K-D, Tsai T-J, Hsieh B-S. Inhibition by pentoxifylline of TNF-α-stimulated fractalkine production in vascular smooth muscle cells: evidence for mediation by NF-κB down-regulation. Brit J Pharmacol 2003; 138: 950-958.

Ciechanover A. The ubiquitin-proteosome proteolysis pathway. Cell 1994; 79: 13-21.

Closa D, Folch-Puy E. Oxygen free radicals and the systemic inflammatory response. IUBMB Life 2004; 56(4): 185-191.

Coon ME, Diegel M, Leshinsky N, Klaus SJ. Selective pharmacologic inhibition of murine and human IL-12-dependent Th1 differentiation and IL-12 signaling. J Immunol 1999; 163(12): 6567-6574.

Cooray R. Formylmethionyl-leucyl-phenylalanine-induced chemiluminescence responses in bovine polymorphonuclear leukocytes. Comp Immunol Microbiol Infect Dis 1996; 19(1): 1-8.

Cotran RS, Kumar V, Collins T (eds). The Gastrointestinal Tract. In: Robbins Pathologic Basis of Disease (6^{th} ed). WB Saunders Co.; Philadelphia, PA: 1999.

Crouch SPM, Fletcher J. Effect of ingested pentoxifylline on neutrophil superoxide production. Infect Immun 1992; 60(11): 4504-4509.

Culav EM, Clark CH, Merrilees MJ. Connective tissues: matrix composition and its relevance to physical therapy. Phys Ther 1999; 79: 308-319.

Dai S-M, Matsuno H, Nakamura H, Nishioka K, Yudoh K. Interleukin-18 enhances monocyte tumor necrosis factor α and interleukin-1β production induced by direct contact with T lymphocytes. Arthritis Rheum 2004; 50(2): 432-443.

Dalmarco EM, Frode TS, Medeiros YS. Effects of methotrexate upon inflammatory parameters induced by carrageenan in the mouse model of pleurisy. Mediators Inflamm 2002; 11(5): 299-306.

Dasgupta A, Ramasway K, Giraldo J, Taniguchi M, Amenta PS, Das KM. Colon epithelial protein induces oral tolerance in the experimental model of colitis by trinitrobenzenesulfonic acid. J Lab Clin Med 2001; 138: 257-269.

Depoortere I, Thijs T, Van Assche G, Keith JC Jr, Peeters TL. Dose-dependent effects of recombinant human interleukin-11 on contractile properties in rabbit 2,4,6-trinitrobenzene sulfonic acid colitis. J Pharmacol Exp Ther 2000; 294(3): 983-990.

Depoortere I, Van Assche G, Peeters TL. Motilin receptor density in inflamed and non-inflamed tissue in rabbit TNBS-induced colitis. Neurogastroenterol Motil 2001; 13(1): 55-63.

Deng Y, Ren X, Yang L, Lin Y, Wu, X. A JNK-dependent pathway is required for TNF-α-induces apoptosis. Cell 2003; 115: 61-70.

D'Haens G, Swijsen C, Noman M, Lemmens L, Ceuppens J, Agbahiwe H, Geboes K, and Rutgeerts P. Etanercept in the treatment of active refractory Crohn's disease: A single-center pilot trial. Am J Gastroenterol, 2001; 96(9): 2564-2568.

Diegelmann RF, Evans MC. Wound healing: an overview of acute, fibrotic and delayed healing. Front Biosci 2004; 9: 283-289.

Dinarello CA. Interleukin-1, interleukin-1 receptors and interleukin-1 receptor antagonist. Int Rev Immunol 1998; 16: 457-499.

Dionne S, D'Agata ID, Hiscott J et al. Colonic explant production of IL-1 and its receptor antagonist is imbalanced in inflammatory bowel disease. Clin Exp Immunol 1998; 112: 435-442.

Dippold W; Wittig B; Schwaeble W; Mayer W; Mayer zum Buschenfelde KH. Expression of intercellular adhesion molecule 1 (ICAM-1, CD54) in colonic epithelial cell. Gut 1993: 34: 1593-1597

Dohlman JG, Payan DG, Goetzl EJ. Generation of a unique fibroblast-activating factor by human monocytes. Immunology 1984; 52(3): 577-84.

Dong C, Yang DD, Wysk M, Whitmarsh AJ, Davis RJ, Flavell RA. Defective T cell differentiation in the absence of Jnk1. Science 1998; 282: 2092-2095.

Dong C, Yang DD, Tournier C, Whitmarsh AJ, Xu J, Davis RJ, Flavell RA. JNK is required for effector T cell function but not for T cell activation. Nature 2000; 405: 91-94.

Du X, Weng H, Cai W. Histological changes in 20 hepatic fibrosis patients with chronic hepatitis B after recombinant human interferon-gamma treatment. Zhonghua Gan Zang Bing Za Zhi 2001; 9(5): 273-275.

Duncan MR, Hasan A, Berman. Pentoxifylline, Pentifylline, and interferons decrease type I and type III procollagen mRNA levels in dermal fibroblasts: Evidence for mediation by nuclear factor-1 down-regulation. J Invest Dermatol 1995; 104(2): 282-286.

Ege S. Stereochemistry. In: Hamann KP, Williams J, Wise K, Merill L, Roll M (eds). Organic Chemistry: Structure and Reactivity. D.C. Heath and Co.; USA, 1994: pp. 196-240.

Ejeil AL, Gaultier F, Igondjo-Tchen S, Senni K, Pellat B, Godeau G, Gogly B. Are cytokines linked to collagen breakdown during periodontal disease progression? J Periodontol 2003; 74(2): 196-201.

Elliott SN, Wallace JL. Neutrophil-mediated gastrointestinal injury. Can J Gastroenterol 1998; 12(8): 559-568.

Elson CO, Sartor RB, Tennyson GS, Riddell RH. Experimental models of inflammatory bowel disease. Gastroenterology 1995; 109(4): 1344-1367.

Ely H. Pentoxifylline therapy in dermatology: a review of localized hyperviscosity and its effects on the skin. Dermatol Clin 1988: 6:585-608.

Esche C, de Benedetto A, Beck LA. Keratinocytes in atopic dermatitis: inflammatory signals. Curr Allergy Asthma Rep 2004; 4(4): 26-284.

Fainsilber Z, Feinman L, Shaw S, Lieber CS. Biphasic control of polymorphonuclear cell migration by Kupffer cells. Effect of exposure to metabolic products of ethanol. Life Sci 1988; 43(7): 603-608.

Fantuzzi G, Reed DA, Dinarello CA. IL-12-induced IFN-γ is dependent on caspase-1 processing of the IL-18 precursor. J Clin Invest 1999; 104: 761-767.

Farmer RG, Whelan G, Fazio VW. Long-term follow up of patients with Crohn's disease. Relationship between the clinical pattern and prognosis. Gastroenterology 1985; 88: 1818-1825.

Farmer RG, Michener WM. Association of inflammatory bowel disease in families. Front Gastrointest Res 1986; 11: 17-26.

Feagan BG. Maintenance therapy for inflammatory bowel disease. Am J Gastroenterol 2003, 98(12): S6-S17.

Fedorak RN and Thomson ABR. Inflammatory Bowel Disease. In: Thomson ABD and Shaffer EA (eds). First Principles of Gastroenterology: The Basis of Disease and Approach to Management (4th ed). Mississauga: Canadian Association of Gastroenterology/Astra Zeneca, 2000: 326-372.

Fidler JM. Induction of hapten-specific immunological tolerance and immunity in B lymphocytes. VII. Correlation between trinitrobenzene sulfonic acid administration, serum trinitrophenyl content, and level of tolerance. Cell Immunol 1985; 94: 285-291.

Fiersten GS. Etiology and pathogenesis of rheumatoid arthritis. In: Kelly WN (ed). Textbook of Rheumatology 5th Edition. Philadelphia: WB Saunders,1996: pp. 851-897.

Filosso PL, Turello D, Magnoni MS. Chronic inflammation and airway remodeling

in asthma. Importance of an early treatment. Minerva Pediat 2003; 55(4): 323-329.

Finco TS, Baldwin AS. Mechanistic aspects of NF-κB regulation: the emerging role of phosphorylation and proteolysis. Immunity 1995; 3: 263-272.

Fiocci C. Intestinal inflammation: a complex interplay of immune and nonimmune cell interaction. Am J Physiol Gastrointest Liver Physiol 1997; 273(36): G769-G775

Fiocci C. Inflammatory bowel disease: etiology and pathogenesis. Gastroenterology, 1998; 115: 182-205.

Fiocci C. TGF-β/Smad signaling defects in inflammatory bowel disease: mechanisms and possible novel therapies for chronic inflammation. J Clin Invest 2001; 108(4): 523-526.

Fiorucci S, Antonelli E, Migliorati G, Santucci L, Morelli O, Federici B, Morelli A. TNFα processing enzyme inhibitors prevent aspirin-induced TNF-α release and protect against gastric mucosal injury in rats. Aliment Pharmacol Ther 1998; 12: 1139-1153.

Fuhr U, Anders EM, Mahr G, Sorgel F, Staib AH. Inhibitory potency of quinolone antibacterial agents against cytochrome P4501A2 activity in vivo and in vitro. Antimicrob Agents Chemother 1992; 36: 942-948.

Furuya D, Yagihashi A, Komatsu M, Masashi N, Tsuji N, Kobayashi D, Watanabe N. Serum interleukin-18 concentrations in patients with inflammatory bowel disease. J Immunother 2002; 25(Suppl 1): S65-S67.

Gabianni G. The myofibroblasts in wound healing and fibrocontractive disorders. J Pathol 2003; 200: 500-503.

Gascon-Barre M, Huet PM, Belgiorno J, Plourde V, Coulombe PA. Estimation of collagen content of liver specimens. Variation among animals and among hepatic lobes in cirrhotic rats. J Histochem Cytochem 1989; 37(3): 377-381.

Gao C-F, Wang H, Wang A-H, Wan W-D, Wu Y-A, Kong X-T. Transcriptional regulation of human α1(I) procollagen gene in dermal fibroblasts. World J Gastroenterol 2003; 10(10): 1447-1451.

Geboes KP, Cabooter L, Geboes K. Contribution of morphology for the comprehension of mechanisms of fibrosis in inflammatory enterocolitis. Acta Gastroenterol Belg 2000; 63(4): 371-376.

George CLS, Fantuzzi C, Bursten S, Leer L, Abraham E. Effects of lisofylline on hyperoxia-induced lung injury. Lung Cell Mol Physiol 1999; 20: L776-L785.

Gerdes N, Sukhova GK, Libby P, Reynolds RS, Young JL, Schonbeck U. Expression of interleukin (IL)-18 and functional IL-18 receptor on human vascular endothelial cells, smooth muscle cells, and macrophages: implications for atherogenesis. J Exp Med 2002; 195: 245-257.

Ghayur T, Banerjee S, Hugunun M, Butler D, Herzog L, Carter A, Quintal L, Sekut L, Talanian R, Paskind M et al. Caspase-1 processes IFN-gamma-inducing factor and regulates LPS-induced IFN-gamma production. Nature 1997; 386: 619-623.

Ghoreschi K, Rocken M. Immune deviation strategies in the therapy of psoriasis. Curr Drug Targets Inflamm Allergy 2004; 3(2): 193-198.

Ghosh AK. Factors involved in the regulation of type I collagen gene expression: implication in fibrosis. Exp Biol Med 2002; 227(5): 301-314.

Ghosh S, Baltimore D. Activation in vitro of NF-κB by phosphorylation of its inhibitor IκB. Nature 1990; 344: 678-682.

Gillespie MT, Horwood NJ. Interleukin-18: perspectives on the newest interleukin. Cytokine Growth Factor Rev 1998; 9(2): 109-116.

Goldstein ES, Marion JF, Present DH. 6-mercaptopurine is effective in Crohn's disease without concomitant steroids. Inflamm Bowel Dis 2004; 10(2): 79-84.

Gonzalez A, Lopez B, Diez J. Fibrosis in hypertensive heart disease: role of the renin-angiotensin-aldosterone system. Med Clin North Am 2004; 88(1): 83-97.

Gotsman I, Shlomai A, Alper R, Rabbana E, Engelhardt D, Ilan Y. Amelioration of immune-mediated experimental colitis: tolerance induction in the presence of preexisting immunity and surrogate antigen bystander effect. JPET 2001; 926-932.

Gracie JA, Robertson SE, McInnes IB. Interleukin-18. J Leukoc Biol 2003; 73: 213-224.

Green L-F, Chen WC. Shaping the nuclear action of NF-κB. Nat Rev Mol Cell Biol 2004; 5: 392-401.

Green L-F, Chen WC. Regulation of NF-κB action by reversible acetylation. Novartis Found Symp 2004; 259: 208-217; discussion 218-225.

Gressner AM. Hepatic fibrogenesis: the puzzle of interacting cells, fibrogenic cytokines, regulatory loops, and extracellular matrix molecules. Z Gastroenterol 1992; 30(Suppl 1): 5-16.

Grisham MB, Volkmer C, Tso P, Yamada T. Metabolism of trinitrobenzene sulfonic acid by the rat colon produces reactive oxygen species. Gastroenterology 1991; 101(2): 540-547.

Gu Y, Kuida K, Tsutsui H, Ku G, Hsaio K, Fleming MA, Hayashi N, Hagashino K, Okamura H, Nakanishi K et al. Activation of interferon-gamma inducing factor mediated by interleukin-1beta converting enzyme. Science 1998; 275: 206-209.

Haber PS, Keough GW, Apte MV et al. (1999). Activation of pancreatic stellate cells in human and experimental pancreatic fibrosis. Am J Pathol, 155: 1087-1095.

Hamilos DL, Lund VJ. Etiology of chronic rhinosinusitis: the role of fungus. Ann Otol Rhinol Laryngol Suppl 2004; 193: 27-31.

Hanada T, Yoshimura A. Regulation of cytokine signaling and inflammation. Cytokine Growth Factor Rev 2002; 13: 413-421.

Hanauer SB, Feagan BG, Lichtenstein GR, et al. Maintenance infliximab for Crohn's disease: the ACCENT 1 randomized trial. Lancet, 2002; 359: 1541-1549.

Hans W, Scholmerich J, Gross V, Falk W. The role of the resident intestinal flora in acute and chronic dextran sulfate sodium-induced colitis in mice. Eur J Gastroenterol Hepatol 2000; 12(3): 267-273.

Harper PH, Fazio VW, Lavery IC, Jagelman DG, Weakley FL, Farmer RG, Easley KA. The long-term outcome in Crohn's disease. Dis Colon Rectum 1987, 30: 174-179.

Hasegawa N, Oka Y, Nakayama M, Berry GL, Bursten S, Rice J, Raffin TC. The effects of post-treatment with lisofylline, a phosphatidic acid generation inhibitor, on sepsis-induced acute lung injury in pigs. Am J Respir Crit Care Med 1997; 155: 928-936.

Hecht G, Savkovic, SD. Review article: Effector role of epithelia in inflammation – interaction with bacteria. Aliment Pharmacol Ther 1997; 11(Suppl 3): 64-68.

Heldin C-H, Westermark B. Mechanism of action and in vivo role of platelet-derived growth factor. Physiol Rev 1999; 79(4): 1283-1316.

Hellerbrand C; Jobin C; Sartor RB. NF-κB mediates cytokine induced expression of ICAM-1 in IEC-6 cells (abstr). Gastroenterology 1996; 110: A329.

Herrlin K, Segerdahl M, Gustafsson LL, Kalso E. Methadone, ciprofloxacin, and adverse drug reactions. Lancet 2000; 356: 2069-2070.

Hewitson TD, Martic M, Kelynack KJ, Pedagogos E, Becker GJ. Pentoxifylline reduces in vitro renal myofibroblast proliferation and collagen secretion. Am J Nephrol 2000; 20(1): 82-88.

Hodgson PD, Peterson TC. Effect of PTX in a heterologous serum model of fibrosis. Hepatology 1995; 22:4.

Hollander D, Vadheim CM, Brettholz E, Petersen GM, Delahunty T, Rotter JI. Increased intestinal permeability in patients with Crohn's disease and their relatives. A possible etiologic factor. Ann Intern Med 1986; 105(6): 883-885.

Holmes S, Abrahamson JA, Al-Mahdi N, Abdel-Meguid SS, Ho YS. Characterization of the in vitro and in vivo activity of monoclonal antibodies to human IL-18. Hybridoma 2000; 19: 363-367.

Homaidan FR, Zhao L, Palaia T, Donovan V, Burakoff R. Morphological and functional changes in the colonic epithelial cells in a rabbit model of colitis. Inflammation 1999; 23(2): 191-205.

Hommes D, Van den Blink B, Plasse T, Bartelsman J, Xu C, MacPherson B, Tytgat G, Peppelenbosch M, Van Deventer S. Inhibition of stress-activated MAP kinases induces clinical improvement in moderate to severe Crohn's disease. Gastroenterology 2002; 12: 7-14.

Hommes DW, Van Deventer SJ. Endoscopy in inflammatory bowel disease. Gastroenterology 2004; 126(6): 1561-1573.

Hugot JP, Laurent-Puig P, Gower-Rousseau C, Caillat-Zucman S, Beaugerie L, Dupas J-L, Gossun AV, Bonaiti-Pellie C, Cortot A, Thomas G, GETAID. Linkage analysis of chromosome 6 loci, including HLA, in familial aggregations of Crohn's disease. Am J Med Genet 1994; 52: 207-213.

Hugot JP, Laurent-Puig P, Gower-Rousseau C, Olson JM, Lee JC, Beaugerie L, GETAID, Orholm M, Bonaiti-Pellie C, Weissenbach L, Methew CG, Lennard-Jones JE, Cortot A, Colombel J-F, Thomas G. Mapping of a susceptibility locus for Crohn's disease on chromosome 16. Nature 1996: 379: 821-823.

Hurgin V, Novick D, Rubinstein M. The promoter of IL-18 binding protein: activation by IFN-γ-induced complex of IFN regulatory factor 1 and CCAAT/enhancer binding protein β. PNAS 2002; 99(26): 16957-16962.

Hyodo Y, Matsui K, Hayashi N, Tsutsui H, Kashiwamara S, Yamauchi H, Hiroishi K,

Takeda K, Tagawa Y, Iwakura Y et al. IL-18 up-regulates perforin-mediated NK activity without increasing perforin messenger RNA expression by binding to constitutively expressed IL-18 receptor. J Immunol 1999; 162: 1662-1668.

Im SH, Kim SH, Azam T, Venkatesh N, Dinarello CA, Fuchs S, Souroujon MC. Rat interleukin-18 binding protein: cloning, expression, and characterization. J Interferon Cytokine Res 2003; 22(3): 321-328.

Inagaki-Ohara K, Hanada T, Yoshimura A. Negative regulation of cytokine signaling and inflammatory diseases. Curr Opin Pharmacol 2003; 3: 435-442.

Incandela L, De Sanctis MT, Cesarone MR, Belcaro G, Nicolaides AN, Geroulakos G, Ramaswami G. Short-range intermittent claudication and rest pain: microcirculartory effects of pentoxifylline in a randomized controlled trial. Angiology 2002; 53(Suppl 1): S27-S30.

Isaacs KL, Sartor RB, Haskill S. Cytokine messenger RNA profiles in inflammatory bowel disease mucosa detected by polymerase chain reaction amplification. Gastroenterology 1992; 103: 1587-1595.

Isbrucker RA, Peterson TC. Collagens a (I) and a (III) mRNA levels are increased in a porcine model of hepatic fibrosis and reduced by pentoxifylline. Gastroenterol 1994; 106(4): 1086.

Isbrucker RA, Peterson TC. Effect of PDGF, PTX and M-1 on collagen synthesis in porcine hepatic stellate cells. Hepatology 1995; 22:4.

Isbrucker RA, Peterson TC. Platelet-derived growth factor and pentoxifylline modulation of collagen synthesis in myofibroblasts. Toxicol Appl Pharmacol 1998; 149:120-126.

Jacobson K, McHugh K, Collins SM. The mechanism of altered neural function in a rat model of acute colitis. Gastroenterology 1997; 112: 156-162.

Jeziorska M, Haboubi N, Schofield P, Woolley DE. Distribution and activation of eosinophils in inflammatory bowel disease using an improved Immunohistochemical technique. J Pathol 2001; 194(4): 484-492.

Jimenez JL, Punzon C, Nevarro J, Munoz-Fernandez MA, Fresno M. Phosphodiesterase-4 inhibitors prevent cytokine secretion by T lymphocytes by inhibiting nuclear factor kappa-B and nuclear factor of activated T cells activation. J Pharmacol Exp Ther 2001; 299(2): 753-759.

Jobin C and Sartor RB. The IκB/NF-κB system: a key determinant of mucosal inflammation and protection. Am J Physiol Cell Physiol 2000; 278: C451-C462.

Kalff JC, Buchholz BM, Eskandari MK, Hierholzer C, Schraut WH, Simmons RL, Bauer AJ. Biphasic response to gut manipulation and temporal correlation of cellular infiltrates in muscle dysfunction in rat. Surgery 1999; 126(3): 498-509.

Kanai T, Wantanabe M, Okazawa A, Nakamuru K, Okamoto M, Naganuma M, Ishii H, Ikeda M, Kurimoto M, Hibi T. Interleukin 18 is a potent proliferative factor for intestinal mucosal lymphocytes in Crohn's disease. Gastroenterology 2000; 119: 1514-1523.

Kanai T, Wantanabe M, Okazawa A, Sato T, Yamazaki M, Okamoto S, Ishii H, Totsuka T, Tiyama R, Ikeda M, Kurimoto M, Takeda K, Akira S, Hibi T. Macrophage-derived IL-18-mediated intestinal inflammation in the murine model of Crohn's disease. Gastroenterology 2001; 121(4): 875-888.

Kaser A, Novick D, Rubinstein M, Siegmund B, Enrich B, Koch RO, Vogel W, Kim SH, Dinarello CA. Interferon-α induces IL-18 binding protein in chronic hepatitis C patients. Clin Exp Immunol 2002; 129: 332-338.

Kashiwaruma S-I, Ueda H, Okamura H. Roles of interleukin-18 in tissue destrucyion and compensatory reactions. J Immunother 2002; 25(Suppl 1): S4-S11.

Kennedy DW. Pathogenesis of chronic rhinosinusitis. Ann Otol Rhinol Laryngol Suppl 2004; 193: 6-9.

Kershenobich-Stalnikowitz D, Weissbrod AB. Liver fibrosis and inflammation. A review. Ann Hepatol 2003; 2(4): 159-163.

Kielty CM, Hopkinson I, Grant ME. Collagen: the collagen family, structure and organization in the extracellular matrix. In: Royce PM, Steinmann BS (eds). Connective Tissue and its Heritable Disorders: Molecular, Genetic, and Medical Aspects. New York, NY; Wiley-Liss, 1993: 103-147.

Kim KH, Lichtenstein GR. Refractory inflammatory bowel disease. Curr Treat Options Gastroenterol 2004; 7(3): 201-211.

Kim Y-M, Im JY, Han SH, Kang HS, Choi I. IFN-γ up-regulates IL-18 gene expression via IFN consensus sequence-binding protein and activator protein-1 elements in macrophages. J Immunol 2000; 165: 3198-3205.

Kimura R, Hu H, Stein-Steillien J. Delayed-type hypersensitivity responses regulate collagen deposition in the lung. Immunology 1992, 77(4): 550-555.

Kitani A, Fuss IJ, Nakamura K, Schwartz OM, Usui T, Strober W. Treatment of experimental (trinitrobenzenesulphonic acid) colitis by intranasal administration

of transforming growth factor (TGF)-β1 plasmid: TGF-β1-mediated suppression of T helper cell type I response occurs by interleukin (IL)-10 induction and IL-12 receptor β2 chain downregulation. J Exp Med 2000; 192(1): 41-52.

Kohno K, Kataoka T, Ohtsuki Y, Suemoto I, Okamoto M, Usui M, Ikeda M, Kurimoto M. IFN-γ-inducing factor (IGIF) is a co-stimulatory factor on the activation of Th1 but not Th2 cells and exerts its effect independently of IL-12. J Immunol 1997; 158: 1541-1550.

Kojima H, Aizawa Y, Yanai Y, Nagaoka K, Takeuchi M, Ohta T, Ikegami H, Ikeda M, Kurimoto M. An essential role for NF-κB in IL-18-induced IFN-γ expression in KG-1 cells. J Immunol 1999; 162: 5063-5069.

Komai-Koma M, Gracie A, Wei X-Q, Xu D, Thomson N, McInnes IB, Liew FY. Chemoattraction of human T cells by IL-18. J Immunol 2003; 170: 1084-1090.

Krawisz JE, Sharon P, WF. Quantitative assay for acute intestinal inflammation based on myeloperoxidase activity. Gastroenterology 1984; 87: 1344-1350.

Kuby, JA, Goldsby RA, Kindt TJ, Osborne BA. T cell Maturation, Activation, and Differentiation. In: Folchetti N, Tannenbaum J, Hadler GL, O'Lavin D (eds). Kuby Immunology 4th ed. WH Freeman and Co.; New York, USA; 1998: 239-268.

Kuboyama S. Increased circulating IL-1 receptor antagonist in patients with inflammatory bowel disease. Kurume Med J 1998; 45: 33-37.

Kumagai S, Ohtani H, Nagai T, Funa K, Hiwatashi NO, Shimosegawa Nagura H. Platelet-derived growth factor and its receptors are expressed in areas of both active inflammation and active fibrosis in inflammatory bowel disease. Tohoku J Exp Med 2001; 195(1): 21-33.

Kuno K, Matsushima K. The IL-1 receptor signaling pathway. J Leukoc Biol 1994; 56: 542-547.

Last JA, Ward R, Temple L, Pinkerton KE, Kenyon NJ. Olvalbumin-induced airway inflammation and fibrosis in mice also exposed to ultrafine particles. Inhal Toxicol 2004; 16(2): 93-102.

Lawrance IC, Maxwell L, Doe W. Altered response of intestinal mucosal fibroblasts to profibrogenic cytokines in inflammatory bowel disease. Inflammatory Bowel Diseases 2001, 7(3): 226-236.

Lawrance IC, Wu F, Liete AZ, Willis J, West GA, Fiocci C, Chakravarti S. A murine model of chronic inflammation-induced intestinal fibrosis down-refulated by antisense NF-kappaB. Gastroenterology 2003; 125(6): 1250-1261.

Lederer JA, Perez VL, DesRoaches L, Kim SM, Abbas AK, Lichtman AH. Cytokine transcriptional events during helper T cell subset differentiation. J Exp Med 1996; 184(2): 397-406.

Lee JC, Kassis S, Kumar S, Badger A, Adams JL. p38 mitogen-activated protein kinase inhibitors-mechanisms and therapeutic potentials. Pharmacol Ther 1999; 82: 389-397.

Lee JC, Kumar S, Griswold DE, Underwood DC, Votta BJ, Adams JL. Inhibition of p38 MAP kinase as a therapeutic strategy. Immunopharmacology 2000; 47: 185-201.

Lee KS, Cottam HB, Houglum K, Wasson DB, Carson D, Chojikier M. Pentoxifylline blocks hepatic stellate cell activation independently of phosphodiesterase inhibitory activity. Am J Physiol 1997; 273(5 Pt 1): G1094-G1100.

Lee SH, Slattery JT. Cytochrome P450 isozymes involved in lisofylline metabolism to pentoxifylline in human liver mocrosomes. Drug Metab Dispos 1997; 25(12): 1354-1358.

Lefrancois L, Puddington L. Extrathymic intestinal T cell development: Virtual reality? Immunol Today 1995; 16: 16-21.

Lepisto J, Peltonen J, Vaha-Kreula M, Niinikoski J, Laato M. Platelet-derived growth factor isoforms PDGF-AA, -AB and –BB exert specific effects on collagen gene expression and mitotic activity of cultured human wound fibroblasts. Biochem Biophys Res Comm 1995; 209(2): 393-399.

Leung BP, Culshaw S, Gracie JA, Hunter D, Canetti CA, Campbell C, Cunha F, Liew F, McInnes IB. A role for IL-18 in neutrophil activation. J Immunol 2001; 167: 2879-2886.

Leung DY, Boguniewicz M, Howell MD, Nomura I, Hamid QA. New insights into atopic dermatitis. J Clin Invest 2004; 113(5): 651-657.

Li MC, He SH. IL-10 and its related cytokines for treatment of inflammatory bowel disease. World J Gastroenterol 2004; 10(5): 620-625.

Ligumsky M, Simon PL, Karmeli F, Rachmilewitz D. Role of interleukin-1 in inflammatory bowel disease – enhanced production during active disease. Gut 1990; 31: 686-689.

Lillibridge JA, Kalhorn TF, Slattery JT. Metabolism of lysofylline and pentoxifylline in human liver microsomes and cytosol. Drug Metab Dispos 1996; 24(11): 174-179.

Lim W-C, MMBS (S'pore), M.Med (Internal Medicine), MRCP (UK), Hanauer SP. Emerging biologic therapies in inflammatory bowel disease. Rev Gastroenterol Disord 2004; 4(2): 66-85.

Linden DR, Sharkey KA, Mawe GM. Enhanced excitability of myenteric AH neurons in the inflamed guinea-pig distal colon. J Physiol 2003; 547(Pt 2): 589-601.

Linden DR, Sharkey KA, Ho W, Mawe GM. Cyclooxygenase-2 contributes to dysmotility and enhanced excitability of myenteric AH neurons in the inflamed guinea-pig distal colon. J Physiol 2004; 557(Pt 1): 191-205.

Linsenmayer TF. Collagen. In: Hay ED (ed). Cell Biology of Extracellular Matrix. New York, NY: Plenum Press; 1991: 7-44.

Liu ZG, Han J. Cellular responses to tumor necrosis factor alpha. Curr Issues Mol Biol 2001; 3: 79-90.

Liu Z, Geboes K, Colpaert S, D'Haens GR, Rutgeerts P, Ceuppens JL. IL-15 is highly expressed in inflammatory bowel disease and regulates local T-cell dependent cytokine production. J Immunol 2000; 164: 3608-3615.

Lo SK. Capsule endoscopy in the diagnosis and management of inflammatory bowel disease. Gastrointest Endosc Clin N Am 2004; 14(1): 179-193.

Loftberg R, Neurath M, Ost A, Petterson S. Topical NF-κB p65 antisense oligonucleotides in patients with active distal colonic IBD. A randomized controlled pilot trial. Gastroenterology 2002; 122: A60.

Loher F, Bauer C, Landauer N, Schmall K, Seigmund B, Lehr HA, Dauer M, Schoenharting M, Endres S, Eigler A. The interleukin-1β-converting enzyme inhibitor pralnacasan, reduces dextran sulfate sodium-induced murine colitis and T helper 1 T-cell activation. JPET 2004; 308: 583-590.

Lopez de Leon A, Rojkind M. A simple micromethod of for collagen and total protein determination in formalin-fixed paraffin-embedded sections. J Histochem Cytochem 1985; 33: 737-743.

Lowenberg M, Peppelenbosch MP, Hommes DW. Therapeutic modulation of signal transduction pathways. Inflamm Bowel Dis 2004; 10(Suppl 1): S52-S57.

Lynch S, Kelleher D, McManus R et al. RAG1and RAG2 expression in human intestinal epithelium: Evidence of extrathymic T cell differentiation. Eur J Immunol 1995; 25: 1143-1147.

MacDermott RP. Alterations in the mucosal immune system in ulcerative colitis

and Crohn disease. Med Clin North Am 1994; 78(6): 1207-1231.

Madara J. Pathobiology of the intestinal epithelial barrier. J Pathol 1990; 137: 1273-1281.

Madsen KL, Doyle JS, Tavernini MM, Jewell LD, Rennie RP, Fedorak RN. Antibiotic therapy attenuates colitis in interleukin 10 gene deficient mice. Gastroenterol 2000; 118(6): 1094-1105.

Maeda M, Watanabe N, Neda H, Yamauchi N, Okamoto T, Sasaki H, Tsuji Y, Akiyama S, Tsuji N, Niitsu Y. Serum tumor necrosis factor activity in inflammatory bowel disease. Immunopharmacol Immunotoxicol 1992; 14(3): 451-461.

Maerten P, Shen C, Colpaert S, Liu Z, Bullens DAM, Van Assche G, Penninckx F, Geboes K, Vanham G, Rutgeerts P, Ceuppens JL. Involvement of interleukin-18 in Crohn's disease: evidence from in vitro analysis of human gut inflammatory cells and from experimental colitis models. Clin Exp Immunol 2004; 135: 310-317.

Mahida YR, Wu K, Jewell DP. Enhanced production of interleukin-1B by mononuclear cells isolated from mucosa with active ulcerative colits or Crohn's disease. Gut 1989; 30: 835-838.

Mantovani A, Garlanda C. Novel pathways for negative regulation of inflammatory cytokines centered on receptor expression. Dev Biol Stand 1999; 97: 97-104.

Marks SL, Merchant S, Foil C. Pentoxifylline: wonder drug? J Am Anim Hosp Assoc 2001; 37(3): 218-219.

Masamune A, Kikuta K, Suzuki N, Satoh M, Shimosegawa T. A c-jun N-terminal kinase inhibitor SP600125 blocks activation of pancreatic stellate cells. J Pharmacol Exp Ther 2004 [e-pub ahead of print].

Matsui K, Yoshimoto T, Tsutsui H, Hyodo Y, Hayashi N, Hiroishi K, Kawada N, Okamura H, Makanishi K, Higashino K. Propionibacterium acnes treatment diminishes CD4+ NK1.1+ T cells but induces type 1 T cells in the liver by induction of IL-12 and IL-18 production by Kupffer cells. J Immunol 1997; 159: 97-106.

Matsumoto S, Tsuji-Takayama K, Aizawa Y, Koide K, Takeuchi M, Ohta T, Kurimoto M. Interleukin-18 activates NF-κB in murine T Helper Type 1 cells. Biochim Biophys Res Comm 1997; 234: 454-457.

McCormack G, Moriarty D, O'Donoghue DP, McCormick PA, Sheahan K, Baird AW. Tissue cytokine and chemokine expression in inflammatory bowel disease.Inflamm Res 2001; 50(10): 491-495.

McLellan RA, Drobitch RK, Manshouwer M, Renton KW. Fluoroquinolone antibiotics inhibit cytochrome P450-mediated microsomal drug metabolism in rat and human. Drug Metab Dispos 1996; 24(10): 1134-1138.

Mee JB, Alam Y, Groves RW. Human keratinocytes constitutively produce but do not process interleukin-18. Brit J Dermatol 2000; 143: 330-336.

Messaoudi M, Desor D, Grasmuck V, Joyeux M, Langlois A, Roman FJ. Behavioral evaluation of visceral pain in a rat model of colonic inflammation. NeuroReport 1999; 10: 1137-1141.

Miampamba M, Parr EJ, McCafferty D-M, Wallace LJ, Sharkey KA. Effect of intracolonic benzalkonium chloride on trinitrobenzene sulphonic acid-induced colitis in the rat. Aliment Pharmacol Ther 1998; 12: 219-228.

Miller A, Lider O, Roberts AB, Sporn M, Weiner HL. Suppressor T cells generated by oral tolerance to myelin basic protein suppress both in vitro and in vivo immune responses by the release of TGF-β following antigen-specific triggering. Proc Natl Acad Sci USA 1992; 89: 421-425.

Monteleone G, Trapasso F, Parrello T, Biancone L, Stella A, Iuliano R, Luzza F, Fusco A, Pallone F. Bioactive IL-18 expression is up-regulated in Crohn's disease. J Immunol 1999; 163(1): 143-147.

Monteleone G, Kumberova A, Croft NM, McKenzie C, Steer HW, MacDonald TT. Blocking Smad 7 expression restores TGF-β signaling in chronic inflammatory bowel disease. J Clin Invest 2001; 108(4): 601-609.

Monteleone I, Vavassori P, Biancone L, Monteleone G, Pallone F. Immunoregulation in the gut: success and failures in human disease. Gut 2002; 50(Suppl III): iii60-iii64.

Moreels TG, de Man JG, Dick JMC, Nieuwendijk RJ, de Winter BY, Lefebvre RA, Herman AG, Pelckmans PA. Effect of TNBS-induced morphological changes on pharmacological contractility of the rat ileum. Eur J Pharmacol 2001; 423: 211-222.

Morris GP, Beck PL, Herridge MS, Depew WT, Szewezuk MR, Wallace JL. Hapten-induced model of chronic inflammation and ulceration in the rat colon. Gasrtoenterology 1989; 96: 795-803.

Mosman TR, Coffman RL. Th1 and Th2 cells: different patterns of lymphokine secretion lead to different functional properties. Ann Rev Immunol 1989; 7: 145-173.

Muller R, Lehrach F. Haemorheological role of platelet-aggregation and hypercoagulability in microcirculation: theoretical approach with pentoxifylline. Pharmatherapeutica 1980; 2: 372-379.

Muneta Y, Goji N, Mikami O, Shimoji Y, Nakajima Y, Yokomizo Y, Mori Y. Expression of interleukin-18 by porcine airway and intestinal epithelium. J Interferon Cytokine Res 2002; 22(8): 883-889.

Murano M, Maemura K, Hirata I, Toshina K, Nishikawa T, Hamamoto N, Sasaki S, Saitoh O, Katsu K. Therapeutic effect of intracolonically administered nuclear factor kappa B (p65) Antisense ologonucleotide on mouse dextran sulphate sodium (DSS)-induced colitis. Clin Exp Immunol 2000; 120: 51-58.

Murch SH. Local and systemic effects of macrophage cytokines in intestinal inflammation. Nutrition 1998; 14: 780-783.

Murphy GJ, Nicholson ML. Rapamycin has no effect on fibrosis-associated gene expression or extracellular matrix accumulation when administered to animals with established or early allograft vasculopathy. J Thorac Cardiovasc Surg 2003; 126(6): 2058-2064.

Murthy S, Cooper HS, Yoshitake H, Meyer C, Meyer CJ, Murthy NS. Combination therapy of pentoxifylline and TNFalpha monoclonal antibody in dextran sulphate sodium-induced mouse colitis. Aliment Pharmacol Ther 1999, 13(2): 251-260.

Mytar B, Woloszyn M, Ruggerio I, Pryjma J, Zembala M. Monocyte-mediated regulation of the antigen-driven IFN gamma production by T cells. Immunol Invest 1995; 24(6): 897-906.

Naik SM, Cannon G, Burbach GJ, Singh SR, Swerlick RA, Wilcox JN, Ansel JC, Caughman SW. Human keratinocytes constitutively express interleukin-18 and secrete biologically active interleukin-18 after treatment with pro-inflammatory mediators and dinitrochlorobenzene. J Invest Dermatol 1999; 113(5): 766-772.

Naumann M, Scheidereit C. Activation of NF-kappa B in vivo is regulated by multiple phosphorylations. EMBO J 1994; 13(19): 4597-607.

Neish AS. The gut microflora and intestinal epithelial cells: a continuing dialogue. Microbes and Infection 2002; 4: 309-317.

Netea MH, Fantuzzi G, Kullburg BJ, Stuyt RJL, Pulido EJ, McIntyre RC Jr., Joosten LAB, Van der Meer JWM, Dinarello CA. Neutralization of IL-18 reduces neutrophil tissue accumulation and protects mice against lethal *Escherichia coli* and *Salmonella typhimurium* endotoxemia. J Imuunol 2000; 164: 2644-2649.

Neurath MF, Fuss I, Kelsall BL, Stuber E, Strober W. Antibodies to interleukin-12 abrogate established experimental colitis in mice. J Exp Med 1995; 182(5): 1281-1290.

Neurath MF, Fuss I, Kelsall BL, Presky BH, Waegell W, Strober W. Experimental granulomatous colitis in mice is abrogated by induction of TGF-beta-mediated oral tolerance. J Exp Med 1996; 183(6): 2605-2616.

Neurath MF, Petterson S, Meyer zum Buschenfelde KH, Strober W. Local administration of antisense phosphorothioate olignucleotides to the p65 subunit of NF-κB abrogates experimental colitis in mice. Nat Med 1996; 2: 998-1004.

Neurath MF, Becker C, Barbulescu K. Role of NF-κB in immune and inflammatory responses. Gut 1998; 43: 856-860.

Neurath MF, Fuss I, Schurmann G, Petterson S, Arnold K, Muellr-Lobeck H, Strober W, Herfarth C, Buschenfelde KH. Cytokine gene transcription by NF-kappa B family members in patients with inflammatory bowel disease. Ann N Y Acad Sci 1998; 869: 149-159.

Neurath MF, Fuss I, Strober W. TNBS-colitis. Intern Rev Immunol 2000; 19: 51-62.

Nicklasson M, Bjorkman S, Roth B, Jonsson M, Hoglund P. Stereoselective metabolism of pentoxifylline in vitro and in vivo in humans. Chirality 2002; 14: 643-652.

Nickoloff BJ, Nestle FO. Recent insights into the immunopathogenesis of psoriasis provide new therapeutic opportunities. J Clin Invest 2004; 113(12): 1664-1675.

Niemela O. Collagen breakdown products as markers of fibrosis and cirrhosis. Alcohol Alcohol Suppl 1994; 2: 345-352.

O'Garra A. Cytokines induce the development of functionally heterogeneous T helper cell subsets. Immunity 1998; 8: 275-283.

O'Garra A, Arai N. The molecular basis of T helper 1 and T helper 2 cell differentiation. Trends Cell Biol 2000; 10(12): 542-550.

Ojima Y, Mizuno M, Kuboki Y, Kimori T. In vitro effect of platelet-derived growth factor-BB on collagen synthesis and proliferation of human periodontal ligament cells. Oral Dis 2003; 9(3): 144-151.

O'Neil LA, Green C. Signal transduction pathways activated by the IL-1 receptor family: ancient signaling machinery in mammals, insects, and plants. J Leukoc Biol 1998; 63: 650-657.

O'Neil D, Steidler L. Cytokines, chemokines and growth factors in the pathogenesis and treatment of inflammatory bowel disease. Adv Exp Mol Biol 2003; 520: 252-285.

Oryan A. Role of collagen in soft connective tissue wound healing. Transplant Proc 1995; 27: 2759-2761.

Ostman A, Heldin CH. Involvement of platelet-derived growth factor in disease: development of specific antagonists. Adv Cancer Res 2001; 80: 1-38.

Pages F, Lazar V, Berger A, Danel C, Lebel Binay S, Zinzindohoue F, Desreumeaux P, Cellier C, Thiounn N, Bellet D, Cugnenc PH, Fridman WH. Analysis of interleukin-18, interleukin-1 converting enzyme (ICE) and interleukin-18 related cytokines in Crohn's disease lesions. Eur Cytokine Netw 2001; 12(1): 97-104.

Panja A, Blumberg RS, Balk SP, Mayer L. CD1b is involved in T cell: epithelial cell interactions. J Exp Med 1993; 178: 1115-1119.

Paulukat J, Bosmann M, Nold M, Garkisch S, Kampfer H, Frank S, Raedle J, Zeuzem S, Pfeilschifter J, Muhl H. Expression and release of IL-18 binding protein in response to IFN-γ. J Immunol 2001; 167: 7038-7043.

Pavli P, Maxwell L, Van de Pol E, Doe WF. Distribution of human colonic dendrtitic cells and macrophages. Clin Exp Immunol 1996; 104: 124-132.

Pavli P, Hume DA, Van de Pol E, Doe WF. Dendritic cells: the major antigen presenting cells of the human colonic lamina propria. Immunology 1993; 78: 132-141.

Peterson TC, Williams CN. Depression of peripheral blood monocyte aryl hydrocarbon hydroxylase activity in patients with cirrhosis; possible role of macrophage factors. Hepatology 1987; 7(2): 333-337.

Peterson TC, Isbrucker RA. Fibroproliferation in liver disease: role of monocyte factors. Hepatology 1992; 15: 191-197.

Peterson TC. Pentoxifylline prevents fibrosis in an animal model and inhibits platelet-derived growth factor-driven proliferation of fibroblasts. Hepatology 1993; 17(3): 486-493.

Peterson TC, Isbrucker R, Hooper ML. In vitro effect of platelet-derived growth factor on fibroproliferation and effect of cytokine antagonists. Immunopharmacology 1994; 28: 259-270.

Peterson TC. Inhibition of fibroproliferation by pentoxifylline. Activity of metabolite-1 and lack of role of adenosine receptors. Biochem Pharmacol. 1996; 52(4): 597-602.

Peterson TC, Neumeister M. Effect of pentoxifylline in rat and swine models of hepatic fibrosis: role of fibroproliferation in its mechanism. Immunopharmacology 1996; 31: 183-193.

Peterson TC, Huet PM. Role of PDGF, TGFβ, and TNFα in fibroproliferation stimulated by PBC patient sera. Can J Gastroenterol 1996; 10; 40a, S78.

Peterson TC, Tanton R. Effect of pentoxifylline in collagenous colitis. Can J Gastroenterol 1996; 10: S76.

Peterson TC, Davey K. Effect of acute pentoxifylline treatment in an experimental model of colitis. Aliment Pharmacol Ther 1997; 11(3): 575-580.

Peterson TC, Slyz G, Isbrucker R. The inhibitory effect of ursodeoxycholic acid and pentoxifylline on platelet-derived growth factor-stimulated proliferation is distinct from an effect by cyclic AMP. Immunopharmacology 1998: 39: 181-191.

Peterson TC, Cleary CE, Shaw AM, Malatjalian DA, Veldhuyzen van Zanten SJ. Therapeutic role for bismuth compounds in TNBS-induced colitis in the rat. Dig Dis Sci 2000; 45(3): 466-473.

Peterson TC, Peterson MR, Robertson HA, During M, Dragunow M. Selective down-regulation of c-jun gene expression by pentoxifylline and c-jun antisense interrupts platelet-derived growth factor signaling: pentoxifylline inhibits phosphorylation of c-Jun on serine 73. Mol Pharmacol 2002; 61(6): 1476-1488.

Peterson TC, Peterson MR, Wornell PA, Blanchard MG, Gonzalez FJ. Role of CYP1A2 and CYP2E1 in the pentoxifylline ciprofloxacin drug interaction. Biochem Pharmacol 2004; 68: 395-402.

Peterson MR, Snair J, Peltekian KM, Peterson TC. IL-18 as an indicator of fibrosis in HCV patients. Eur Cytokine Netw 2003a; 14(3): 158.

Peterson TC, Jones J, Tanton RT. IL-18, FSI, and P-II-P in inflammatory bowel disease. Eur Cytokine Netw 2003b; 14(3): 159.

Pifferi G, Perucca E. The cost benefit ratio of enantiomeric drugs. Eur J Drug Metabol Pharmacokinetics 1995, 20(1): 15-25.

Pinzani M. Novel insights into the biology and physiology of the Ito cell. Pharmaocol Ther 1995; 66: 387-412.

Pizarro TT, Michie HM, Bentz M, Woraratanadharm J, Smith Jr MF, Foley E, Moskaluk CA, Bickston, Cominelli F. IL-18, a novel immunoregulatory cytokine, is up-regulated in Crohn's disease: expression and localization in intestinal mucosal

cells. J Immunol 1999; 162: 6829-6835.

Plebani M, Burlina A. Biochemical markers of hepatic fibrosis. Clin Biochem 1991; 24(3): 219-239.

Powell DW, Mifflin RC, Valentich JD, Crowe SE, Saada JI, West AB. Myofibroblasts. II. Intestinal subepithelial myofibroblasts. Am J Physiol Cell Physiol 1999; 277(46): C183-C201.

Preaux A-M, Mallat A, Rosenbaum J, Zafrani E-S, Mauvier P. Pentoxifylline inhibits growth and collagen synthesis of cultured human myofibroblasts-like cells. Hepatology 1997; 26: 315-322.

Prescott SL. New concepts of cytokines in asthma: Is the Th2/Th1 paradigm out the window? J Paediatr Child Health 2003; 39: 575-579.

Prinz M, Hanisch UK. Murine microglial cells produce and respond to interleukin-18. J Neurochem 1999; 72: 2215-2218.

Pucilowska JB, Williams KL, Lund PK. Fibrogeneis IV. Fibrosis and inflammatory bowel disease: cellular mediators and animal models. Am J Physiol Gastrointest Liver Physiol 2000; 279: G653-G659.

Puig-Divi V, Molero X, Salas A, Guarner F, Guarner L, Malagelada JR (1996). Induction of chronic pancreatic disease by trinitrobenzene sulfonic acid infusion into rat pancreatic ducts. Pancreas, 13(4): 417-24.

Raghow R, Thompson JP. Molecular mechanisms of collagen gene expression. Mol Cell Biochem 1989; 86: 5-18.

Rao TS, Curie JL, Shaffer AF, Isakson PC. In vivo characterization of zymosan-induced mouse peritoneal inflammation. J Pharmacol Exp Ther 1994; 269(3): 917-925.

Raoul JM, Verma M, Tan E, Peterson TC. Cytokines as therapeutic targets for the GI manifestations of scleroderma. Can J Gastroenterol 2004; 18(1): 22-24.

Reimold AM, Kim J, Finberg R, Glimcher LH. Decreased immediate inflammatory gene induction in activating transcription factor-2 mutant mice. Int Immunol 2001; 13(2): 241-248.

Reimund JM, Dumont S, Muller CD, Kenney JD, Kedinger M, Baumann R, Poindron P, Duclos B. In vitro effects of oxpentifylline on inflammatory cytokine release in patients with inflammatory bowel disease. Gut 1997; 40(4): 475-480.

Rennick DM, Fort MM. Lessons from genetically engineered animal models. XII. IL-10-deficient (IL-10(-/-)) mice and intestinal inflammation. Am J Physiol Gastrointest

Liver Physiol 2000; 278: G829-G833.

Rice GC, Brown PA, Nelson RJ, et al. Protection from endotoxic shock in mice by pharmacologic inhibition of phosphatidic acid. Proc Natl Acad Sci USA 1994; 91: 3857-3861.

Rieckmann P, Weber F, Gunther A, Martin S, Bitsch A, Brooks A, Kitze B, Weber T, Borner T, Poser S. Pentoxifylline, a phosphodiesterase inhibitor, induces immune deviation in patients with multiple sclerosis. J Neuroimmunol 1996; 64(2): 193-200.

Rieneck K, Diamant M, Haahr PM, Schonharting M, Bendtzen K. In vitro immunomodulatory effects of pentoxifylline. Immunol Lett 1993; 37(2-3): 131-138.

Robinson D, Shibuya K, Mui A, Zonin F, Murphy E, Sana T, Hartley SB, Menon S, Kastelein R, Bazan F, O'Garra A. IGIF does not drive Th1 development but synergizes with IL-12 for interferon-γ production and activates IRAK and NF-κB. Immunity 1997; 7: 571-581.

Rogler G, Andus T. Cytokines in inflammatory bowel disease. World J Surg, 1998; 22: 382-389.

Rogler G; Brand K; Vogl D; Page S; Hofmeister R; Andus T; Kneuchel R; Baeuerle PA; Scholmerich J and Gross V. Nuclear factor κB is activated in macrophages and epithelial cells of inflamed intestinal mucosa. Gastroenterology 1998; 115: 357-369.

Rojkind M, Greenwel P. The Extracellular matrix of the Liver. In: Arias IA, Boyer JL, Fausto N, Jakoby WB, Schachter DA, Shafritz DA (eds). The Liver: biology and pathobiology 3rd edition. New York: Raven Press, 1994: 843-868.

Romagnani S. Th1/Th2 cells. Inflamm Bowel Dis 1999; 5(4): 285-294.

Rothenberg ME, Mishra A, Brandt EB, Hogan SP. Gastrointestinal eosinophils. Immunol Rev 2001; 179: 139-155.

Saiki O, Uda H, Nishimoto N, Miwa T, Mima T, Ogawara T, Azuma N, Katada Y, Sawaki J, Tsutsui H, Matsui K, Meada A, Nakanishi K. Adult Still's disease reflects a Th2 rather than Th1 cytokine profile. Clin Immunol 2004; 112(1): 120-125.

Saito S, Sakai M. Th1/Th2 balance in preeclampsia. J Reprod Immunol 2003; 59(2): 161-173.

Salituro FG, Germann UA, Wilson KP, Bemis GW, Fox T, Su MS. Inhibitors of p38 MAP kinase: therapeutic intervention in cytokine-mediated diseases. Curr Med Chem 1999; 6: 807-823.

Samardzic T, Jankovic V, Stosic-Grujicic S, Popadic D, Trajkovic V.Pentoxifylline inhibits the synthesis and IFN-gamma-inducing activity of IL-18. Clin Exp Immunol 2001; 124(2): 274-281.

Samlaska CP, Winfield EA. Pentoxifylline. J Am Acad Deramtol 1994; 30: 603-621.

Sanai A, Nagata H, Konno A. Extensive interstitial collagen deposition on the basement membrane zone in allergic nasal mucosa. Acta Otolaryngol 1999; 119(4): 473-478.

Sandborn WJ, Hanauer SB. Infliximab in the treatment of Crohn's disease: a users guide for clinicians. Am J Gastroenterol 2002; 97(12): 2962-2972.

Santos J, Yang PC, Soderholm JD, Benjamin M, Perdue MH. Role of mast cells in chronic stress induced colonic epithelial barrier dysfunction in the rat. Gut 2001; 48(5): 630-636.

Sareneva T, Julkunin I, Matikainen S. IFN-α and IL-12 induce IL-18 receptor gene expression in human NK and T cells. J Immunol 2000; 165(4): 1933-1988.

Sartor RB. Therapeutic manipulation of the enteric microflora in inflammatory bowel disease: antibiotics, probiotics, and prebiotics. Gastroenterology 2004; 126(6): 1620-1633.

Satsangi J, PerkesM, Louis E, Hashimoto L, Kato N, Welsh K, Termilliger JD, Lathrop GM, Bell JI, Jewell DP. Two stage genome-wide search in inflammatory bowel disease provides evidence for succeptibility loci on chromosomes 3, 7, and 12. Nat Genet 1996; 14: 199-202.

Savino W, Mendes-da-Cruz DA, Smaniotto S, Silva-Monteiro E, Vilaa-Verde DM. Molecular mechanisms governing thymocyte migration: combined role of chemokines and extracellular matrix. J Leukoc Biol 2004; 75(6): 951-961.

Schieferdecker HL, Ullrich R, Hirseland H, Zeitz M. T cell differentiation antigens on lymphocytes in the human intestinal lamina propria. J Immunol 1992; 149(8): 2816-2822.

Schuppan D, Koda M, Bauer M, Hahn EG. Fibrosis of liver, pancreas, and intestine: common mechanisms and clear targets? Acta Gastroenterol Belg 2000; 63(4): 366-370.

Scribano M, Prantera C. Review article: medical treatment of moderate to severe Crohn's disease. Aliment Pharmacol Ther 2003; 17(Suppl 2): 23-30.

Sherman MA, Kalman D. Initiation and resolution of mucosal inflammation. Immunol Res 2004; 29(1-3): 241-252.

Shin HS, Slattery JT. CYP3A4-mediated oxidation of lisofylline to lisofylline 4,5-diol in human liver microsomes. J Pharm Sci 1998; 87(3): 390-393.

Siegmund B, Fantuzzi G, Rieder F, Gamboni-Robertson F, Lehr H-A, Hartman G, Dinarello CA, Endres S, Eigler A. Neutralization of interleukin-18 reduces severity in murine colitis and intestinal IFN-γ and TNF-α production. Am J Physiol Regulatory Integrative Comp Physiol 2001; 281: R1264-1273.

Siegmund B, Lehr H-A, Fantuzzi C, Dinarello CA. IL-1β-converting enzyme (caspase-1) in intestinal inflammation. PNAS 2001; 98(23): 13249-13245.

Silbiger S, Lei J, Neugarten J. Estradiol suppresses collagen type I synthesis in mesangial cells via activation of activator protein-1. Kidney Int 1999; 55: 1268-1276.

Sivakumar PV, Westrich GM, Kanaly S, Garka K, Born TL, Derry JMJ, Viney JL. Interleukin 18 is a primary mediator of the inflammation associated with dextran sulphate sodium induced colitis: blocking interleukin 18 attenuates intestinal damage. Gut 2002; 50: 812-820.

Slack JL, Parker MI, Bornstein P. Transcriptional repression of the α1(I) collagen gene by Ras is mediated in part by an intronic AP-1 site. J Cell Biochem 1995; 58: 380-392.

Slyz GW, Peterson TC. Pentoxifylline and trapadil do not inhibit PDGF binding to PDGF receptors of human and rat fibroblasts. J Leukoc Biol 1994; 1(Suppl): LB39.

Smith R, Waller E, Doluisio J, Bauza M, Puri S, Ho I, Lassman HB. Pharmacokinetics of orally administered pentoxifylline in humans. J Pharm Sci 1986; 75: 47-52.

Soderholm JD, Yang PC, Ceponis P, Vohra A, Riddell R, Sherman PM, Perdue MH. Chronic stress induces mast cell-dependent bacterial adherence and initiates mucosal inflammation in the rat. Gastroenterology 2002; 123(4): 1099-1108.

Somerville KW, Logan RFA, Edmond M, Langman MJS. Smoking and Crohn's disease. BMJ 1984; 289: 954-956.

Staak K, Prosch S, Stein J, Priemer C, Ewert R, Docke WD, Kruger DH, Volke HD, Reinke P. Pentoxifylline promotes replication of human cytomegalovirus in vivo and in vitro. Blood 1997; 89(10): 3682-3690.

Stagg AJ, Hart AL, Knight SC, Kamm MA. The dendrtitic cell: its role in intestinal inflammation in relationship with gut bacteria. Gut 2003; 52(10): 1522-1529.

Stein RB, Hanauer SB. Comparative tolerability of treatments for inflammatory bowel disease. Drug Saf 2000, 23(5): 429-448.

Stevens C; Walz G; Singaram C; Lipman ML; Zanker B; Muggia A; Antonioli D; Peppercorn MA; Strom TB. Tumor necrosis factor alpha, interleukins 1 beta, and interleukin 6 expression in inflammatory bowel disease. Dig Dis Sci 1992; 37: 818-826.

Stoll S, Jonuliet H, Schmitt E, Muller G, Yamauchi H, Kurimoto M, Knop M, Enk AH. Production of functional IL-18 by different subtypes of human and murine dendritic cells (DC): DC-derived IL-18 enhances IL-12-dependent Th1 development. Eur J Immunol 1998; 28: 3231-3239.

Stoll S, Jonuliet H, Kurimoto M, Saloga J, Tanimoto T, Yamauchi H, Okamura H, Knop M, Enk AH. Production of IL-18 (IFN-gamma-inducing factor) messenger RNA and functional protein by murine keratinocytes. J Immunol 1997; 159: 298-302.

Storkun WJ, Tahara H, Lotze MT. Interleukin-12. In: Thompson AW (ed). The Cytokine Handbook 3rd edition. San Diego, Academic Press: 1998.

Strieter RM, Remick DG, Ward PA, Spengler RN, Lynch JP, Larrick J, Kunkel SL. Cellular and molecular regulation of tumor necrosis factor-alpha production by pentoxifylline. Biochem Biophys Res Comm 1988; 155(3): 1230-1236.

Sturm A, Zeeh J, Sudermann T, Rath H, Gerken G, Dignass A. Lisofylline and lysophospholipids ameliorate experimental colitis in rats. Digestion 2002, 66: 23-29.

Sugawara S, Uehara A, Nochi T, Yamaguchi T, Ueda H, Sugiyama A, Hanzawa K, Kumagi K, Okamura H, Takada H. Neutrophil proteinase-3-mediated induction of bioactive IL-18 secretion by human oral epithelial cells. J Immunol 2001; 167: 6568-6575.

Sugiyama Y, Oshikawa K. Mechanism of sarcoid granuloma formation-participation of cytokines and chemokines. Nippon Rinsho 2002; 60(9): 1728-1733.

Sullivan GW, Carper HT, Novick WJ Jr, Mandell GL. Inhibition of the inflammatory action of interleukin-1 and tumor necrosis factor (alpha) on neutrophil function by pentoxifylline. Infect Immun 1988; 56(7): 1722-1729.

Swantek JL, Cobb MH, Geppert TD. Jun N-terminal kinase/stress-activated protein kinase (JNK/SAPK) is required for lipopolysaccaride stimulation of tumor

necrosis factor alpha (TNF-alpha) translation: glococorticoids inhibit TNF-alpha translation by blocking JNK/SAPK. Mol Cell Biol 1997; 17: 6274-6282.

Sykes AP, Bhogal R, Brampton C, Chander C, Whelan C, Parsons ME, Bird J. The effect of matrix metalloproteinases on colonic inflammation in a trinitrobenzenesulfonic acid rat model of inflammatory bowel disease. Aliment Pharmacol Ther 1999; 13: 1535-1542.

Takagi H, Kanai T, Okazawa A, Kishi Y, Sato T, Takaishi H, Inoue N, Ogata H, Iwao Y, Hoshino K, Takeda K, Akira S, Watanabe M, Ishii H, Hibi T. Contrasting action of IL-12 and IL-18 in the development of dextran sodium sulphate colitis in mice. Scand J Gastroenterol 2003; 38(8): 837-844.

Takanami-Ohnishi Y, Amano S, Kimura S, Asada S, Utani A, Maruyama M, Osada H, Tsunoda H, Irukayama-Tomobe Y, Goto K, Karin M, Sudo T, Kasuya Y. Essential role of p38 mitogen-activated protein kinase in contact hypersensitivity. J Biol Chem 2002; 277(40): 37896-37903.

Tang G, Minemoto Y, Dibling B, Purcell NH, Li Z, Karin M, Lin A. Inhibition of JNK activation through NF-κB target genes. Nature 2001; 414: 313-317.

Tang F, Tang G, Xiang J, Dai Q, Rosner MR, Lin A. The absence of NF-κB-mediated inhibition of c-Jun N-terminal kinase activation contributes to tumor necrosis factor alpha-induced apoptosis. Mol Cell Biol 2002; 22(24): 8571-8579.

Tatsumi Y, Lichtenberger LM. Molecular association of trinitrobenezenesulfonic acid and surface phospholipids in the development of colits in rats. Gastroenterology 1996; 110: 780-789.

Tekeuchi M, Nishikazi Y, Sano O, Ohya T, Ikeda M, Kurimoto M. Immunohistochemical and immuno-electron-microscope detection of interferon-γ-inducing factor ("interleukin-18") in mouse intestinal epithelial cells. Cell Tissue Res 1997; 289: 499-503.

Ten Hove T, Corbaz A, Amitai H, Aloni S, Belzer I, Graber P, Drillenburg P, Van Deventer SJ, Chvatchko Y, Te Velde AA. Blockade of endogenous IL-18 ameliorates TNBS-induced colitis by decreasing local TNF-alpha production in mice. Gastroenterology 2001; 121(6): 1372-1379.

Ten Hove T, Van den Blink B, Pronk I, Drillenburg P, Peppelenbosch MP, Van Deventer SJ. Dichotomal role of inhibition of p38 MAPK with SB203580 in experimental colitis. Gut 2002; 50: 507-512.

Thompson JA, Bianco JA, Benyunes MC, Neubauer MA, Slattery JT, Fefer A. Phase 1b trial of pentoxifylline and ciprofloxacin in patients treated with interleukin-2 and

lymphokine-activated killer cell therapy for metastatic renal carcinoma. Cancer Res 1994; 54: 3436-3441.

Thornton FJ, Barbul A. Healing in the gastrointestinal tract. Surg Clin North Am 1997; 77(3): 549-573.

Tjon JA, Riemann LE. Treatment of intermittent claudication with pentoxifylline and cilostazol. Am J Health Sys Pharm 2001; 58: 485-93.

Togawa J-I, Nagase H, Tanaka K, Inamori M, Umezawa T, Nakajima A, Naito M, Sato S, Saio T, Sekihara H. Lactorferrin reduces colitis in rats via modulation of the immune system and correction of cytokine imbalance. Am J Physiol Gastrointest Liver Physiol 2002; 283: G187-G195.

Torres MI, Garcia-Martin M, Fernandez MI, Nieto N, Gil A, Rios A. Experimental colitis induced by trinitrobenzenesulfonic acid: an untrastuctural and histochemical study. Digest Dis Sci 1999; 44(12); 2523-2529.

Tortora GJ, Grabowski SR. The Digestive System. In: Roesch B, Moore T (eds) Principles of Anatomy and Physiology 8th edition. Harper Collins: New York, NY; 1996: 752-805.

Tsutsui H, Kayagaki N, Kuida K, Nakano H, Hayashi N, Takida K, Matsui K, Kashiwamura S, Hada T, Akira S, Yagita H, Okamura H, Nakanishi K. Caspase-1-independent, Fas/Fas ligand-mediated IL-18 secretion from macrophages causes acute liver injury in mice. Immunity 1999; 11: 359-367.

Tysk C, Lindburg E, Jarnerot G, Floderus-Myrhed B. Ulcerative colitis and Crohn's disease in unselected population of monozygotic and dizygotic twins: a study of heritability and the influence of smoking. Gut 1988; 29: 990-996.

Udagawa N, Horwood NJ, Elliott J, Mackay A, Owens J, Okamura H, Kurimoto M, Chambers TJ, Martin TJ, Gillespie MT. Interleukin-18 (Interferon-gamma-inducing factor) is produced by osteoblasts and acts via granulocyte/macrophage colony-stimulating factor and not via interferon-gamma to inhibit osteoclast formation. J Exp Med 1997; 185: 1005-1012.

Uebelhoer M, Bewig B, Kreipe H, Nowak D, Magnussen H, Barth J. Modulation of fibroblast activity in histiocytosis Xby platelet-derived growth factor. Chest 1995; 107: 701-705.

Ulloa L, Doody J, Massague J. Inhibition of transforming growth factor-β/Smad signaling by the interferon-γ/STAT pathway. Nature 1999; 397: 710-713.

Ulrich D, Noah EM, Burchardt ER, Atkins D, Pallua N. Serum concentration of amino-terminal propeptide of collagen type III procollagen (PIIINP) as a prognostic

marker for skin fibrosis after scar correction in burned patients. Burns 2002; 28(8): 766-771.

Valente EGA, Vernet D, Ferrini MG, Qian A, Rajfer J, Gonzalez-Cadavid NF. L-arginine and phosphodiesterase (PDE) inhibitors counteract fibrosis in the Peyronie's fibrotic plaque and related fibroblast cultures. Nitric Oxide 2003; 9(4): 229-244.

Van Assche G, Geboes K, Rutgeerts P. Medical therapy for Crohn's disease strictures. Inflamm Bowel Dis 2004; 10(1): 55-60.

Van den Blink B, Ten Hove T, Van den Brink GR, Peppelenbosch MP, Van Deventer SJH. From extracellular to intracellular targets, inhibiting MAP kinases in treatment of Crohn's Disease. N Y Acad Sci 2002; 973: 349-358.

Varfolomeev EE, Ashkenazi A. Tumor necrosis factor: an apoptosis JuNKie? Cell 2004; 116: 491-497.

Vervoordeldonk MJ, Tak PP. Cytokines in rheumatoid arthritis. Curr Rheumatol Rep 2002; 4(3): 208-217.

Visser J, Groen H, Klatter F, Rozing J. Timing of pentoxifylline treatment determines its protective effects on diabetes development in the Bio Breeding rat. Eur J Pharmacol 2002; 445: 133-140.

Waetzig GH, Seegert D, Rosenstiel P, Nikolaus S, Schreiber S. p38 mitogen-activated protein kinase is activated and linked to TNF-α signaling in inflammatory bowel disease. J Immunol 2002; 168: 5342-5351.

Waetzig GH, Rosenstiel P, Nikolaus S, Seegert D, Schreiber S. Differential p38 mitogen-activated protein kinase target phosphorylation in responders and non-responders to Infliximab. Gastroenterology 2003; 125(2): 633-634.

Waetzig GH, Shreiber S. Review article: mitogen-activated protein kinases in chronic intestinal inflammation – targeting ancient pathways to treat modern diseases. Aliment Pharmacol Ther 2003; 18: 17-32.

Wallace JL. Glucocorticoid-induced gastric mucosal damage: inhibition of leukotriene, but nor prostaglandin biosynthesis. Prostaglandins 1987; 34(2): 311-323.

Wallace JL, MacNaughton WK, Morris GP, Beck PL. Inhibition of leukotriene synthesis markedly accelerates healing in a rat model of inflammatory bowel disease. Gastroenterology 1989: 96: 29-36.

Wallace JL, Keenan CM, Gale D, Shoupe TS. Exacerbation of experimental colitis by non-steroidal anti-inflammatory drugs is not related to elevated leukotriene B4 synthesis. Gastroenterology 1992; 102: 18-27.

Wallach D, Varfolomeev N, Malinin NL, Goltsev, YV, Kovalenko AV, Boldin MP. Tumor necrosis factor receptor and Fas signaling mechanisms. Annu Rev Immunol 1999; 17: 331-367.

Walsh K, Sata M. Negative regulation of inflammation by Fas ligand expression on the vascular endothelium. Trends Cardiovasc Med 1999; 9(1-2): 34-41.

Wang W, Tam WF, Hughes, Rath S, Sen R. c-Rel is a target of pentoxifylline-mediated inhibition of T lymphocyte activation. Immunity 1997; 6(2): 165-174.

Ward A, Clissold SP. PTX, a review of its pharmacodynamic and pharmacokinetic properties and therapeutic efficacy. Drugs 1987; 34: 50-97.

Weiner HL. Oral tolerance: immune mechanisms of treatment of autoimmune diseases. Immunol Today 1997; 18(7): 335-343.

Windmeier C, Gressner AM. Pharmacological aspects of pentoxifylline with emphasis on its inhibitory actions on hepatic fibrogenesis. Gen Pharmacol 1997; 29(2): 181-196.

Wirtz S, Becker C, Blumberg R, Galle PR, Neurath MF. Treatment of T cell-dependent experimental colitis in SCID mice by local administration of an adenovirus expressing IL-18 antisense mRNA. J Immunol 2002; 168(1): 411-20.

Wisniewski HG, Vilcek J. TSG-6: an IL-1/TNF-inducible protein with anti-inflammatory activity. Cytokine Growth Factor Rev 1997; 8(2): 143-156.

Witte MB, Barbul AB. General principles of wound healing. Surg Clin North Am 1997; 77(3): 509-528.

Wornell PA, Peterson TC. Investigation of the PTX/CIPRO drug interaction in the mouse. Hepatology 1997; 26: 453A.

Wyman TH, Dinarello CA, Banerjee A, Gamboni-Robertson F, Heister AA, England KM, Kehler M, Silliman CC. Physiological levels of interleukin-18 stimulate multiple neutrophil functions through p38 MAP kinase activation. J Leukoc Biol 2002; 72: 401-409.

Xian CJ, Xu X, Mardell CE, Howarth GS, Byard RW, Moore DJ, Meittinen P, Read LC. Site-specific changes in transforming growth factor -α and -β1 expression in colonic mucosa of adolescents with inflammatory bowel disease. Scand J Gastroenterol 1999; 34: 591-600.

Xiong LJ, Luo DD, Zeng LL Li SL. Effect of pentoxifylline of hepatic TGF-beta 1, type I and type III collagen in mice with liver fibrosis due to Schistosoma japonicum infection. Zhongguo Ji Sheng Chong Xue Yu Ji Chong Bing Za Zhi 2002; 20(4): 209-211.

Xiong LJ, Zhu JF, Luo DD, Zen LL, Cai SQ. Effects of pentoxifylline on the hepatic content of TGF-beta 1 and collagen in Schistosoma japonicum mice with liver fibrosis. World J Gastroenterol 2003; 9(1): 152-154.

Xu D, Chan WL, Leung BP, Hunter D, Schuls K, Carter RW, McInnes IB, Robinson JH, Liew FW. Selective expression and functions of interleukin-18 receptor on T helper (Th) type 1 but not Th2 cells. J Exp Med 1998; 188: 1485-1492.

Yamada T, Sartor RB, Marshall S, Specian RD, Grisham MB. Mucosal injury and inflammation in a model of chronic granulomatous colitis in rats. Gastroenterology 1993; 104(3): 759-771.

Yang DD, Conze D, Whitmarsh AJ, Barrett T, Davis RJ, Rincon M, Flavell RA. Differentiation of CD4+ cells to Th1 cells requires MAP kinase JNK2. Immunity 1998; 9: 575-585.

Yoshimoto T, Takeda K, Tanaka T, Ohkusu K, Kashiwamura S, Okamura H, Akira S, Nakanishi K. IL-12 up-regulates IL-18 receptor expression on T cells, Th1 cells, and B cells: synergism with IL-18 for IFN-gamma production. J Immunol 1998; 161: 3400-3407.

Zeroogian JM, Chopra S. Collagenous and lymphocytic colitis. Annu Rev Med 1994; 45: 105-118.

Zhang Y, Chen F. Reactive oxygen species (ROS), troublemakers between nuclear factor-κB (NF-κB) and c-Jun NH2-terminal kinase (JNK). Cancer Res 2004; 64: 1902-1905.

Zhang-Hoover J, Sutton A, van Rooijen N, Stein-Streilein J. A critical role for alveolar macrophages in elicitation of pulmonary immune fibrosis. Immunology 2000; 101(4): 501-511.